

Cover Page



Universiteit Leiden

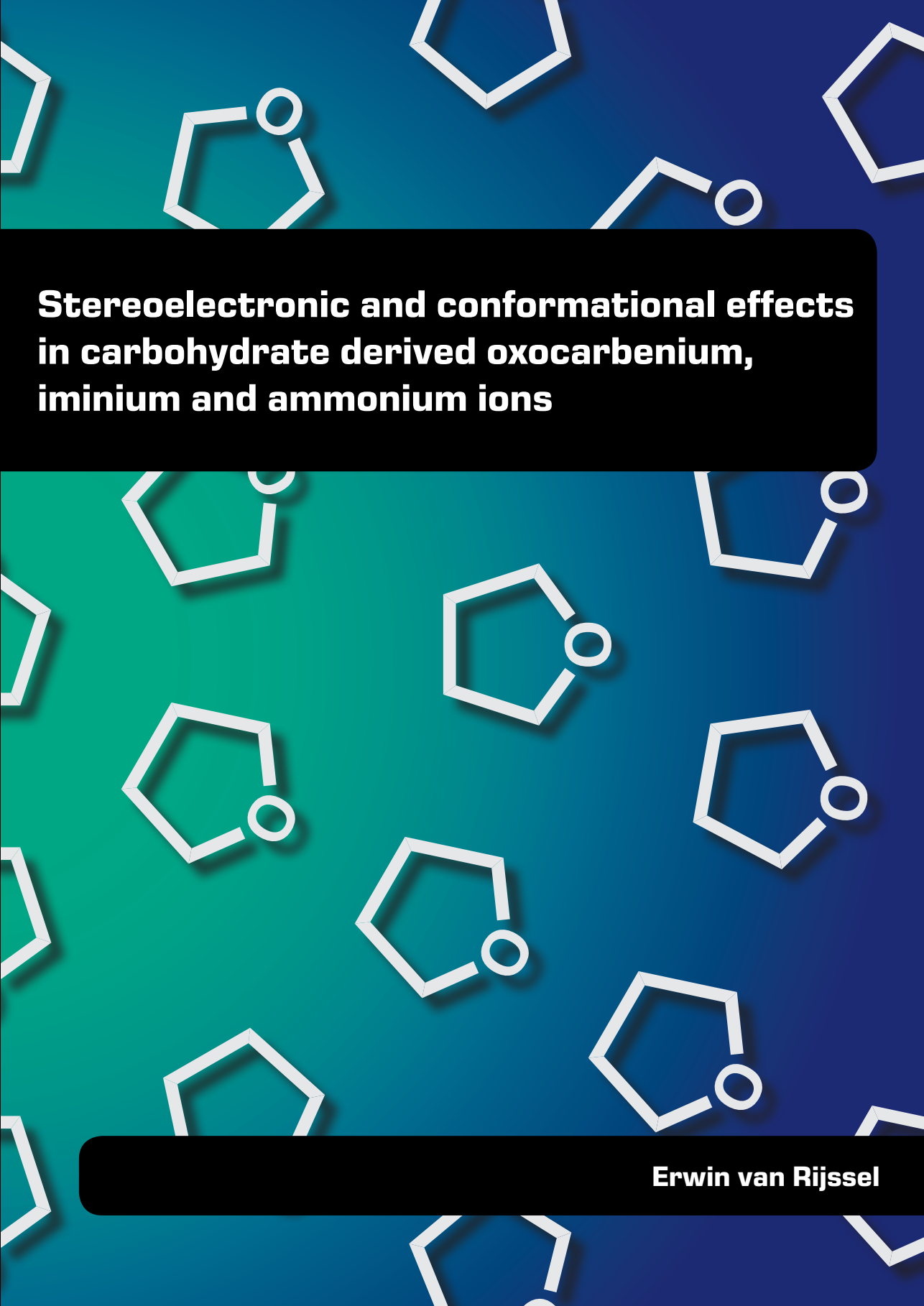


The handle <http://hdl.handle.net/1887/31437> holds various files of this Leiden University dissertation

Author: Rijssel, Erwin Roelof van

Title: Stereoelectronic and conformational effects in carbohydrate derived oxocarbenium, iminium and ammonium ions

Issue Date: 2015-01-14

The background features a repeating pattern of white chemical structures, including five-membered rings with oxygen atoms and other cyclic motifs, set against a gradient background that transitions from dark blue at the top to a lighter teal at the bottom. The structures are rendered in a simple, clean line-art style.

**Stereoelectronic and conformational effects
in carbohydrate derived oxocarbenium,
iminium and ammonium ions**

Erwin van Rijssel

**Stereoelectronic and conformational effects in
carbohydrate derived oxocarbenium, iminium and
ammonium ions**

PROEFSCHRIFT

ter verkrijging van
de graad van Doctor aan de Universiteit Leiden,
op gezag van Rector Magnificus prof. mr. C. J. J. M. Stolker,
volgens besluit van het College voor promoties
te verdedigen op woensdag 14 januari 2015
klokke 16:15 uur

door

Erwin Roelof van Rijssel

Geboren te Haarlemmermeer in 1987

Promotiecommissie

Promotor: Prof. dr. G. A. van der Marel

Co-promotor: Dr. J. D. C. Codée

Overige leden: Prof. dr. H. S. Overkleeft
Prof. dr. K. A. Woerpel
Prof. dr. F. M. Bickelhaupt
Prof. dr. J. Brouwer
Prof. dr. J. Lugtenburg

ISBN/EAN: 978-94-6108-878-9

Geprint door: Gildeprint

Table of Contents

List of Abbreviations	6
Chapter 1	9
General Introduction	
Chapter 2	33
Furanosyl Oxocarbenium Ion Stability and Stereoselectivity	
Chapter 3	61
Stereoselectivity in the Lewis acid mediated reduction of ketofuranosides	
Chapter 4	81
Chiral Pyrroline-Based Ugi-Three-Component Reactions are under Kinetic Control	
Chapter 5	121
A library of lipophilic iminosugars based on all eight stereoisomeric pentofuranosyl iminosugars	
Chapter 6	151
Stereoelectronic substituent effects determine the conformational preferences of mannuronic acid based iminosugar cations	

Chapter 7	167
Summary and future prospects	
Samenvatting	179
List of publications	182
Curriculum Vitae	185
Appendix	187

List of Abbreviations

Ac	acetyl	DMAP	4-dimethylaminopyridine
AMP	5-(adamantane-1-yl-methoxy)pentyl	DMF	dimethylformamide
aq.	aqueous	DMJ	deoxymannojirimycin
Ar	aromatic	DMSO	dimethyl sulfoxide
B3LYP	Becke 3-Parameter, Lee, Yang and Parr	DTBMP	2,6-di- <i>tert</i> -butyl-4-methylpyridine
Bn	benzyl	eq.	molar equivalents
Bu	butyl	E	energy
C	chair	<i>E</i>	envelope
cal	calorie	Et	ethyl
calc.	calculated	FES	Free Energy Surface
cat.	catalytic	<i>g</i>	<i>gauche</i>
COSY	correlation spectroscopy	<i>H</i>	half-chair
C _q	quaternary carbon atom	HR-MS	high-resolution mass spectroscopy
Cy	cyclohexane	HMBC	Heteronuclear multiple-bond correlation spectroscopy
δ	chemical shift (ppm)	HSQC	Heteronuclear Single Quantum Coherence
d	doublet	Hz	Herz
DCM	dichloromethane	IR	infrared
DFT	density function theory	<i>J</i>	coupling constant
DiBAL-H	di-isobutylaluminiumhydride		
DiPEA	<i>N,N</i> -diisopropylethylamine		

m	multiplet	sat.	saturated
M	molar	t	triplet
Me	methyl	<i>t</i>	<i>trans</i>
Ms	methanesulfonyl	<i>T</i>	twist
NIS	<i>N</i> -iodosuccinimide	τ_m	amplitude
NMR	Nuclear Magnet Resonance	TBAI	tetrabutylammonium iodide
NOESY	Nuclear Overhauser effect spectroscopy	<i>t</i> Bu	<i>tert</i> -butyl
Nu	nucleophile	TES	triethylsilane
nPP	5-neopentoxypentyl	Tf	triflyl
obs.	observed	TFA	trifluoromethanesulfonic acid
P	pseudorotational phase angle	THF	tetrahydrofuran
PBP	5-(<i>p</i> -phenylbenzyloxy)pentyl	TLC	thin layer chromatography
PCM	polarizable continuum model	TMS	trimethylsilane
PE	petroleum ether (40-60)	Tol	tolyl
PES	Potential Energy Surface	Tr	trityl
Ph	phenyl	Triflate	trifluoromethanesulfonyl
ppm	parts per million	TS	transition state
q	quartet	TTBP	2,4,6-tri- <i>tert</i> -butylpyrimidine
R_f	retention factor	UV	ultraviolet
s	singlet	ZPE	zero-point energy
S	skew-boat		

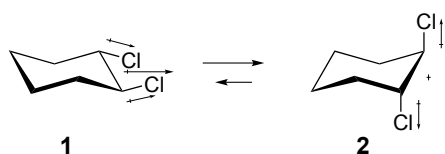
Chapter 1

General Introduction

1.1 Introduction

Electronic effects of functional groups within a molecule control both the 3-dimensional structure and reactivity of the molecule. These electronic effects are dependent on the nature, positioning and configuration of the groups within the molecule, and are therefore called stereoelectronic effects.¹

A basic example of the influence of stereoelectronic effects of substituents in a molecule on its structure can be found with 1,2-*trans* dichlorocyclohexane. When only steric factors are taken into account, this molecule is expected to prefer a chair conformation having both substituents in an equatorial position to minimize unfavorable 1,3-diaxial interactions (Figure 1.1, **1**). However, this molecule also readily adopts the opposite chair conformation placing both chloride substituents in axial position (**2**).²⁻⁴ The conformational preference is dependent on the solvent and shifts to the side of the chair with axial substituent positioning in more apolar solvents. The preference can be explained by the interaction of the dipoles associated with the C-Cl bonds.⁵⁻⁶ In the di-equatorial constellation these dipoles are parallel where they oppose each other in the di-axial situation, which is more favorable.⁷ The reduction of the overall dipole of the molecule is beneficial, especially in apolar solvents, as can be seen in Figure 1.1. In tetrachloromethane the di-axial conformer is favored where the molecule preferentially adopts a di-equatorial conformation in the polar dimethyl sulfoxide.²



Solvent	Equatorial : Axial (%)
CCl ₄	35 : 65
CHCl ₃	52 : 48
DMSO	80 : 20

Figure 1.1 Conformational equilibrium of 1,2-*trans* dichlorocyclohexane.

Stereoelectronic effects also play a decisive role in stabilizing charge in a molecule. For example, the through-space electron donation of substituents with free electron pairs (lone pairs) with proximal positive or partial positive charges can be a strong stabilizing effect.^{1,8-9} This is reflected in the conformational preference of 4-methoxycyclohexanone (Figure 1.2, **3-4**), which prefers to place the methoxy substituent in an axial position (**4**, ⁴C₁).¹⁰⁻¹² Only in the axial position the methoxy group oxygen can donate electron density into the partial positive charge present on the carbonyl carbon.¹³⁻¹⁶ The axial conformer is in equilibrium with the chair that places the methoxy group in an equatorial position (**3**, ¹C₄) which is beneficial for steric reasons.⁷ The stabilizing effect of the electron donation becomes stronger with increasing strength of the positive charge present in the molecule and also depends on the electron density available on the heteroatom substituent.^{15,17} Thus, when a positively charged oxocarbenium ion instead of a polarized carbonyl group is present in the molecule (**5-6**), the equilibrium between the equatorial and the axial

conformers shifts over to the side of the latter as determined using reactions involving this oxocarbenium ion.¹³ The conformer with the axial methoxy substituent benefits from a stronger through-space stabilization thereby overruling the unfavorable steric interactions.

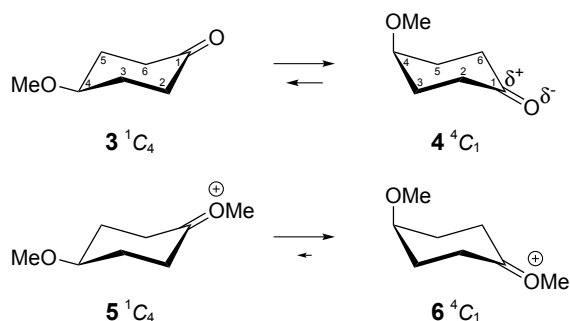


Figure 1.2 Conformational equilibrium of 4-methoxycyclohexanones.

Hyperconjugative effects are stabilizing interactions based on the delocalization of electrons from a filled (bonding) molecular orbital (donor) into an empty or antibonding molecular orbital (acceptor). It is required that the two bonds are properly aligned to allow for overlap between the donating and accepting orbitals.^{1,7} In a saturated system, the two substituents have to take up an antiperiplanar orientation so that the bonding donor orbital is parallel to the antibonding acceptor orbital (Figure 1.3). The strength of the stabilizing effect depends on the degree of overlap and on the type of orbitals involved. σ -Bonds of electron donating substituents (C-H, C-C and especially C-Si) are good donors, the π^* and σ^* orbitals of electron withdrawing substituents (carbonyls, halogens, heteroatoms, etc.) generally form good acceptors and carbocations (empty p-orbitals) are excellent acceptors.^{1,6}

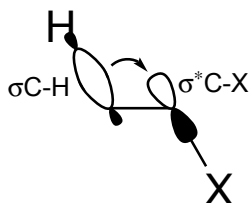
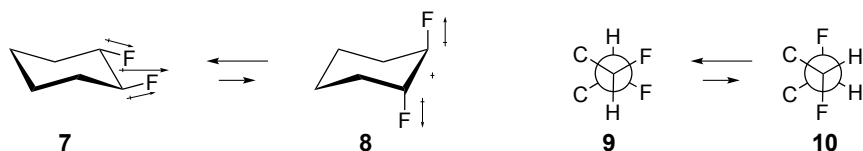


Figure 1.3 Hyperconjugation in saturated systems delocalizes electron density from the σ -bond donor to the σ^* antibonding acceptor orbital. Optimal overlap of the two orbitals occurs when both substituents are placed antiperiplanar to each other.

1,2-*Trans* difluorocyclohexane (**7-8**, Figure 1.4) displays a different conformational behavior than its dichloro counterpart **1-2**. Fluorides are significantly smaller and more

electron withdrawing than chlorides, and based on the dipole interactions outlined above in combination with the smaller steric penalty it could be expected that difluorohexane preferentially takes up a di-axial conformation. However, it is found to favor the diequatorial configuration instead (**7**).² An explanation for this behavior can be found in the hyperconjugative stabilization that is possible in the diequatorial situation.¹ When both substituents are in an equatorial position, a carbon-carbon σ -bond can delocalize its electrons into the C-F σ^* (**9**) stabilizing this conformer.¹ This effect is also referred to as the “gauche effect”.



Solvent	Equatorial : Axial (%)
CCl_4	75 : 25

Figure 1.4 Hyperconjugation causes the small fluorides in 1,2-*trans* difluorocyclohexane to take up a di-axial conformation.

The anomeric effect is defined as the preference of an electron withdrawing substituent at C1 of a carbohydrate pyranoside (the anomeric center) to adopt an axial orientation (See Figure 1.5 and 1.6).^{1,7,9,18} This preference can be explained by a hyperconjugative stabilization arising from the donation of electron density from the lone pair of the ring oxygen into the σ^* (C1-X) antibonding orbital of the aglycon (Figure 1.5 and **13-14**).

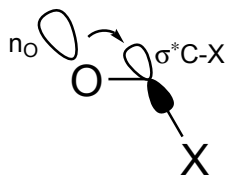


Figure 1.5 Orbital overlap in the stabilizing anomeric effect.

The results of the anomeric effect become clearly visible in a mono-substituted tetrahydropyran. In solution two chair conformers of 2-methoxy tetrahydropyran (Figure 1.6, **11-12**) are in equilibrium, with the chair conformer having the methoxy group positioned axially (**12**) predominating.¹⁸ In case of tri-*O*-benzoyl-1-fluoro- β -D-xylopyranose (**15-16**), the anomeric effect is so strong that it completely shifts the equilibrium between the 4C_1 (**15**) and 1C_4 (**16**) chairs to the sterically highly disfavored all-axial 1C_4 conformation (**16**).¹⁸

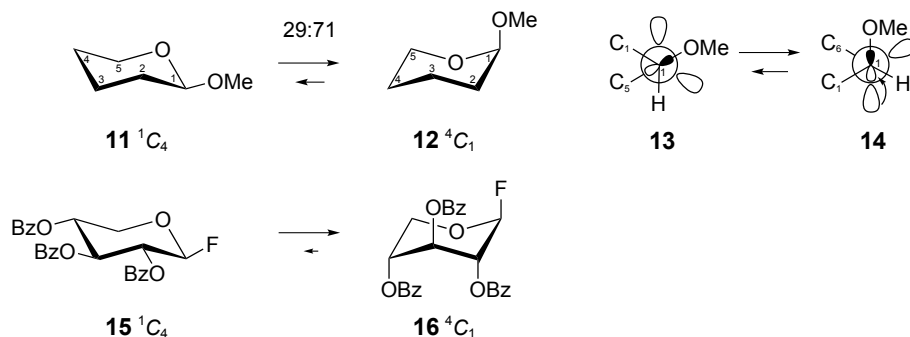


Figure 1.6 The anomeric effect causes 2-methoxy tetrahydropyran to take up a conformation with the methoxy group predominantly positioned axially. 1-Fluoro- β -D-xylopyranose preferentially takes up a 1C_4 chair conformation as a result of the anomeric effect.

1.2 Furanoses

Furanoses are five membered ring carbohydrates, and their chemistry is determined to a large extent by stereoelectronic effects exerted by the ring substituents. This influence becomes clear in reactions taking place at the anomeric center, for example during glycosylation reactions. During a glycosylation, an anomeric leaving group is expelled leading to the development of positive charge at the anomeric center. Because five membered rings can readily adopt a flattened (envelope) structure¹⁹⁻²⁰ this positive charge can be relatively easily accommodated leading to the formation of an oxocarbenium ion, or oxocarbenium ion like species. To account for the stereoselectivity (or lack thereof) it is often hypothesized that glycosylations proceed *via* these intermediates. Woerpel and co-workers have devised a model that takes into account the different conformations of the intermediate oxocarbenium ions to explain the stereochemical outcome of C-furanosylations.^{14,21-26} They proposed a “two conformer” model in which the equilibrium of two oxocarbenium ion conformers, the 3E (**17**) and E_3 (**18**) envelopes, is decisive for the product stereochemistry (Figure 1.7).²¹⁻²³ In case of the 3E envelope, the C3 carbon atom is positioned above the plane formed by the C4-O4-C1-C2, while in the E_3 envelope C3 is below the plane. Attack of a nucleophile on these envelopes can occur from the top or bottom face. When the oxocarbenium ion is approached from the *endo* face, that is on the side of the envelope where the outlying C3 is positioned, it is referred to as “inside attack”, while attack on the other side is termed “outside” (Figure 1.7). The outside attack pathway suffers from an eclipsing interaction of the incoming nucleophile with the axial substituent at C2 in the transition state. It also leads to a product having unfavorable eclipsing C1-C2 interactions. Since an inside attack is devoid of the eclipsing interaction in the transition-state and leads to a product featuring a staggered C1-C2 conformation, this mode of attack is favored. Thus, a reaction on the 3E envelope (**17**) takes place from the

top of the molecule (leading to **19**) and reaction on the E_3 envelope (**18**) takes place on the bottom (to lead to **20**). The equilibrium between the two envelope conformers is defined by stabilizing and destabilizing steric and stereoelectronic effects in the oxocarbenium ions and therefore the stereochemical course of reactions proceeding through these oxocarbenium ions is shaped by the nature of the substituents. It should be noted however that because of their high reactivity and limited lifetime glycosyl oxocarbenium ions have never been spectroscopically detected.

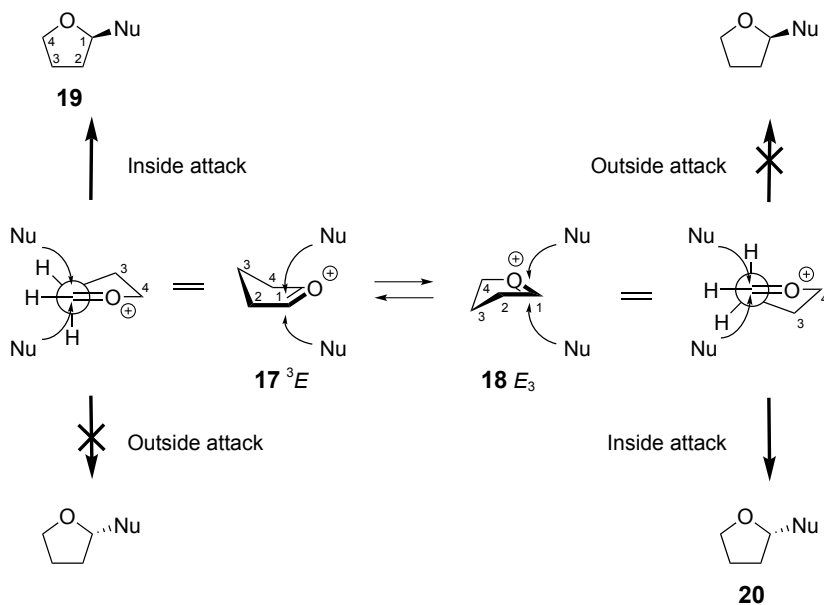


Figure 1.7 The two-conformer model proposed by Woerpel and co-workers. The two furanosyl 3E (**17**) and E_3 (**18**) envelope oxocarbenium ions are preferentially attacked by the incoming nucleophile following an inside trajectory to provide different epimeric products (**19** and **20** respectively).

Pentofuranoses have three (protected) electron withdrawing groups mounted on the ring, being a hydroxyl group at C2 and C3 and a hydroxymethyl at C4. Woerpel and co-workers have determined the effect of each of the individual substituents in reactions using mono-substituted tetrahydrofurans. In the reaction of (*S*)-3-benzyloxy tetrahydrofuranyl acetate (**21**) with allyltrimethylsilane as nucleophile and SnBr_4 as Lewis acidic promoter, the 1,3-*cis* product is obtained with high stereoselectivity (Figure 1.8). This was explained using the equilibrium of the two oxocarbenium ion envelopes **23** and **24** and the inside attack model. If attack on both ions takes place at a comparable rate, the product ratio mirrors the relative stability of the two conformers, and the *cis*-product arises from **24**, where the *trans*-product is formed from **23**. It was reasoned that E_3 oxocarbenium ion **24** is more stable than its E_3 counterpart **23** because of the through-space stabilization of the

pseudoaxial C3-alkoxy lone pair that can donate electron density into the oxocarbenium ion.^{21,24} If the substituent is positioned in a pseudoequatorial position this generates an unfavorable dipole-charge interaction by having the negative terminus directed away from the positive anomeric center.

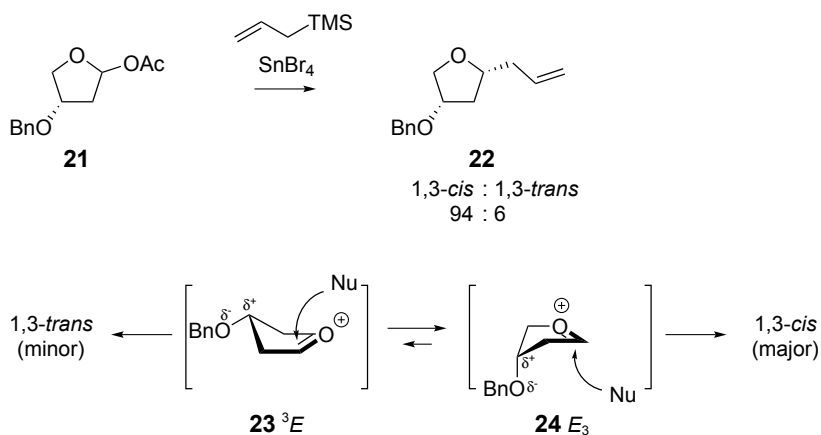


Figure 1.8 The C3 alkoxy substituent can provide through-space stabilization in a pseudoaxial position.

(*R*)-2-benzyloxy tetrahydrofuran acetate (**25**) reacts with allyltrimethylsilane to primarily give 1,2-*cis*-product **26**, originating from the E₃ envelope (Figure 1.9, **28**).²⁴ This envelope is favored over the alternative ³E envelope **27**, because hyperconjugative stabilization of the oxocarbenium ion by the axial C2-H2 bond can only take place in the E₃ envelope. A C2-alkoxy group therefore preferentially takes up a pseudoequatorial position in an oxocarbenium ion for stereoelectronic reasons. This position is also favorable from a steric point of view, minimizing 1,3-diaxial interactions with the ring substituent at C4.

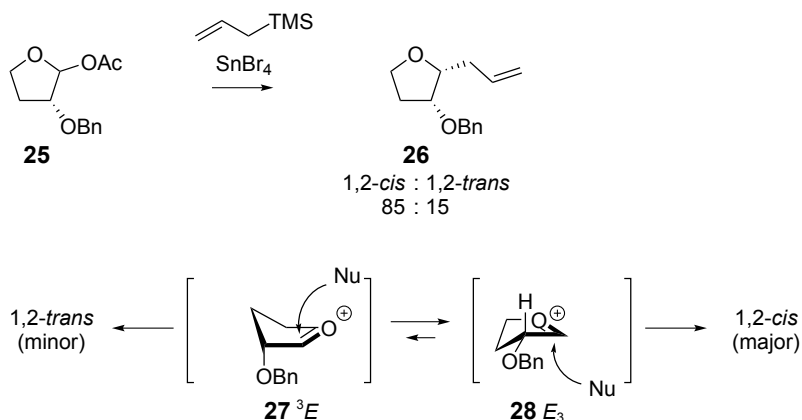


Figure 1.9 The C2 alkoxy substituent is preferentially positioned pseudoequatorially to allow hyperconjugative stabilization of the oxocarbenium ion from the C2-H2 bond.

The (*S*)-4-benzyloxymethyl tetrahydrofuran acetate (**29**) does not have an electron withdrawing substituent directly attached to the furanose ring but has a methylene group in-between the electronegative oxygen and the C4 ring atom. When **29** reacted with allyltrimethylsilane, a mixture of anomers resulted with minimal preference for the 1,4-*trans* product (Figure 1.10).^{24,27} The major product originates from the E_3 envelope (**32**), where the C4 alkoxyethyl group is in a pseudoaxial position. In this position, the C5-oxygen can donate electron density through-space into the electron depleted oxocarbenium ion thereby stabilizing the E_3 conformer. In the 3E envelope (**31**) the C4 substituent takes up a sterically more favorable pseudoequatorial position. The contrasting effects of the through-space interaction and steric preferences makes both envelopes similar in stability, explaining the observed mixture of anomers (**30**).

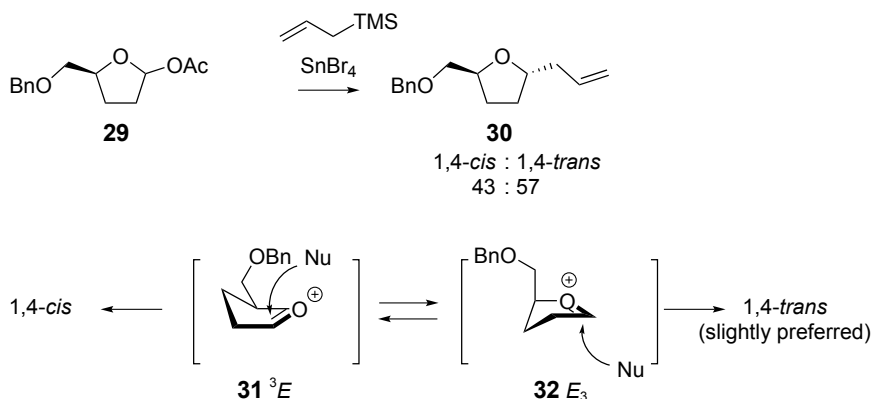


Figure 1.10 The combined effect of stabilizing through-space and destabilizing steric interactions from the C4 alkoxyethyl substituent makes that both envelopes are similar in stability.

When the C2-alkoxy and C3-alkoxy substituents are combined, as in acetates **33** and **37**, the experimental results corroborate the preferences of the individual substituents (Figure 1.11). In 2,3-*cis* dibenzyloxy acetate **33**, both substituents are able to take up their preferred position in the E_3 oxocarbenium ion (**36**). In this conformer the pseudoequatorial C2 substituent has a pseudoaxial C-H bond that is positioned for optimal hyperconjugative stabilization and the pseudoaxial C3 oxygen allows for the most effective through-space stabilization. The product (**34**) ratio reflects the E_3 conformer preference, with the reaction being highly stereoselective for the product originating from this envelope: the 1,2-*cis* product.²⁴ When the two substituent preferences are conflicting, erosion of stereoselectivity is observed. In 2,3-*trans* dibenzyloxy acetate **37**, only one of the two substituents is able to adopt an optimal position for stabilization in either envelope. In the 3E conformer (**39**), the C2 substituent allows for optimal stabilization by placing the C-H in pseudoaxial position. The C3 substituent is in a pseudoequatorial position in this envelope and does not provide any through-space stabilization. In the E_3 envelope (**40**), the pseudoaxial C3 substituent can donate electron density from the C3-oxygen lone pairs into the oxocarbenium ion, but the pseudoequatorial position of H2 does not allow for hyperconjugative stabilization. The reaction of 2,3-*trans* dibenzyloxy acetate with allyltrimethylsilane gives a mixture of products, with a slight preference for the 1,2-*trans* product.²⁴

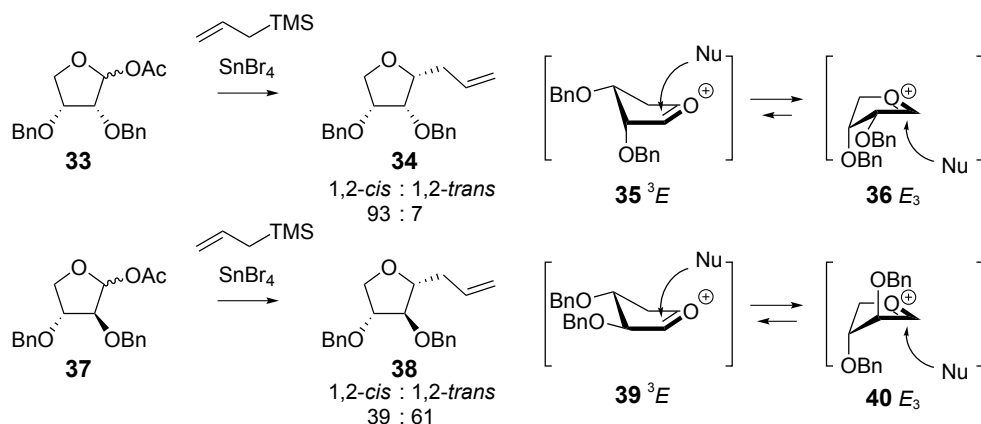


Figure 1.11 The combined effect of both C2 and C3 substituents determine the product ratio.

The situation becomes more complex when a third substituent is present on the furanosyl ring, as in fully functionalized pentofuranoses. Allylation of ribofuranose **41**, the (*S*)-4-benzyloxymethyl analogue of 2,3-*cis*-dibenzyloxy furanose **33**, leads to the 1,2-*cis* product (Figure 1.12).^{24,28-30} This outcome can be explained by invoking the E_3 envelope (**44**) as product forming intermediate. In this envelope the pseudoequatorial C2 alkoxy is

positioned favorably, and the pseudoaxial C3 alkoxy and C4 alkoxymethyl groups allow for optimal stabilization by through-space interactions with the oxocarbenium ion. The E_3 (**43**) places none of the substituents in a favorable position, and is therefore significantly less stable. Performing the nucleophilic substitution with arabinofuranose **45**, the C2 epimer of ribose **41**, lead to a product mixture with a preference for the 1,2-*cis* product.³¹⁻³² This indicates that the major product originates from the 3E conformer (**47**). In this envelope, the only favorably positioned substituent is the pseudoequatorial C2 alkoxy group. The alternative E_3 conformer (**48**) places both the C3 alkoxy and C4 methyleneoxy groups in stabilizing positions. However, in this envelope there is a significant 1,3-diaxial steric clash between the C2 and C4 substituents. The overall energy of this conformer is probably higher than its 3E counterpart shifting the equilibrium to the side of the latter conformer. In all, conformer preferences of furanosyl oxocarbenium ions are a result from the combination of individual substituent stereoelectronic effects and in fully functionalized systems it can be difficult to predict the overall effect.

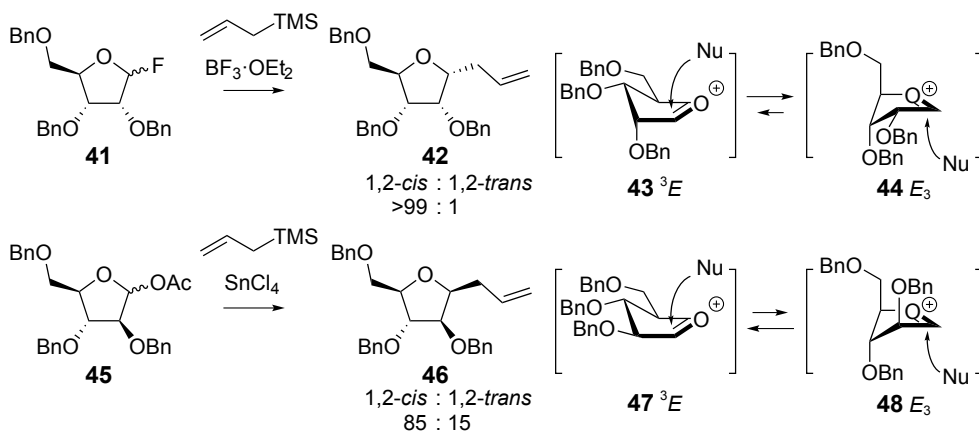


Figure 1.12 C-allylation of D-ribo and D-arabinofuranoses.

In contrast to the above described furanosylations using C-nucleophiles a similar systematic study for O-glycosylations is lacking. A few striking examples are reported that agree with the two conformer model established with C-glycosylations. For example, Mukaiyama and Suda reported that when perbenzylated ribose **49** was activated with tributylphosphine oxide and trifluoromethanesulfonic anhydride and then reacted with cyclohexanol, the 1,2-*cis* linked product was preferentially formed (Figure 1.13).³³ A possible explanation for this stereochemical result can be found in the preference of the intermediate oxocarbenium ion to adopt an E_3 conformation.

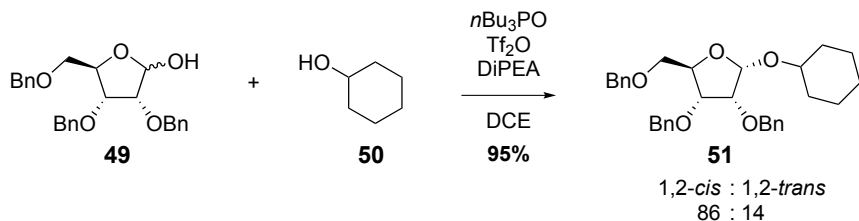


Figure 1.13 An example of a *cis* selective ribofuranosylation.

O-Glycosylation reactions of arabinofuranosyl donors 2'-carboxybenzyl D-arabinofuranoside **52** and thio-L-arabinofuranoside **55** predominantly gave the 1,2-*cis* product isomer **54** and **57**, respectively (Figure 1.14).³⁴⁻³⁸ The stereoselectivities found in these arabinosylation reactions are in line with the selectivity seen for the reaction of a C-nucleophile with arabinose acetate **45**. These results can be accounted for by assuming that nucleophilic attack of glycosyl acceptor **53** and **56** primarily occurs on the ³*E* envelope oxocarbenium ion intermediates to give the 1,2-*cis* linked products. It should be noted however, that *O*-nucleophiles are generally more reactive than C-nucleophiles (such as allyltrimethylsilane) and competing reaction pathways, for example involving the direct S_N2-displacement of anomeric triflates, can lead to different stereochemical results.³⁹⁻⁴⁰

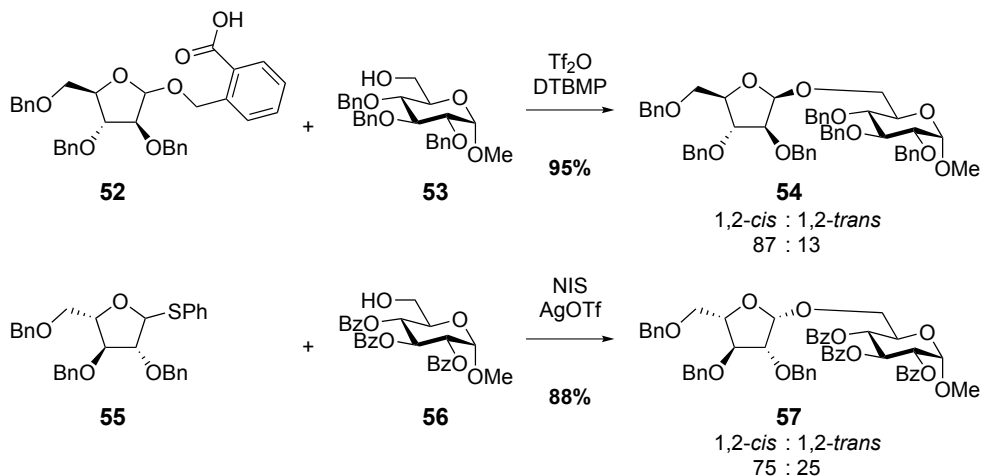


Figure 1.14 Examples of stereoselective arabinofuranosylations.

1.3 Pyranoses

The stereoelectronic substituent effects that play a role in the allylation of pyranoses, six membered ring carbohydrates, have been investigated in detail as well. A two-conformer model similar to the furanosyl system has been proposed to account for the stereoselectivity observed with pyranosides, where the intermediate oxocarbenium ion adopts either a 3H_4 (**58**) or a 4H_3 (**59**) half-chair conformation (Figure 1.15).^{14,41-45} When a nucleophile adds to the half-chairs following an outside attack pathway this leads to an unfavorable skew-boat transition state and product (**62** and **63**). Nucleophilic attack from the inside leads to a chair like transition state and product and is therefore generally more favorable (**60** and **61**).^{9,41-42,46} Therefore, when the oxocarbenium ion adopts a 3H_4 half-chair, inside attack will take place on the top of the molecule while attack on the 4H_3 half-chair proceeds from the bottom face.

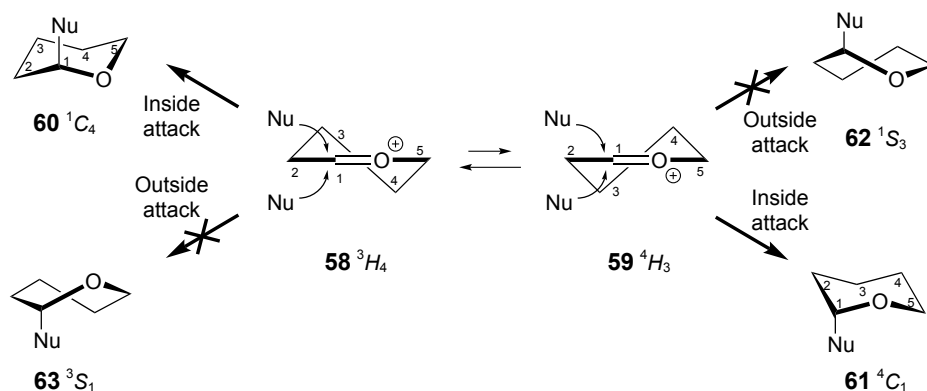


Figure 1.15 The two-conformer model for pyranoses. A nucleophile adds to an oxocarbenium ion half-chair following an inside attack trajectory to lead to the favorable chair product.

To determine the individual substituent preferences in pyranosides, Woerpel and co-workers reacted mono-substituted tetrahydropyranyl acetates with allyltrimethylsilane under the agency of borontrifluoride etherate and determined their product ratios.^{14,41-42,45,47-49} From these results the half-chair preferences were assessed (Figure 1.16). The C2 benzyloxy substituent prefers to be in an equatorial position, placing the C2-H2 bond optimally for hyperconjugative stabilization (Figure 1.16a).⁴² The C3 and C4 benzyloxy substituents both prefer to be positioned axial, to allow for stabilization of the oxocarbenium ion by through-space electron density donation (Figure 1.16b and c).⁴² The C5 benzyloxymethyl group prefers to be in equatorial position, for steric reasons (Figure 1.16d).^{42,49} The preference of the C2-, C3- and C4- alkoxy substituents is in line with those found in the furanosyl oxocarbenium ions. The results of the methyleneoxy functionalized pyranoside and furanoside seem to indicate that there is a difference in the

preference for the C5-pyranosyl and C4-furanosyl methyleneoxy group. In a furanosyl oxocarbenium ion this substituent has a small preference for an axial position, where it prefers an equatorial position in a pyranosyl oxocarbenium ion. It can be reasoned that the axially oriented C5 substituent in the pyranose system leads to an unfavorable steric interactions with the incoming nucleophile,^{45,49} where in the furanosyl system this interaction does not play a role given the inside attack trajectory (see Figure 1.7).

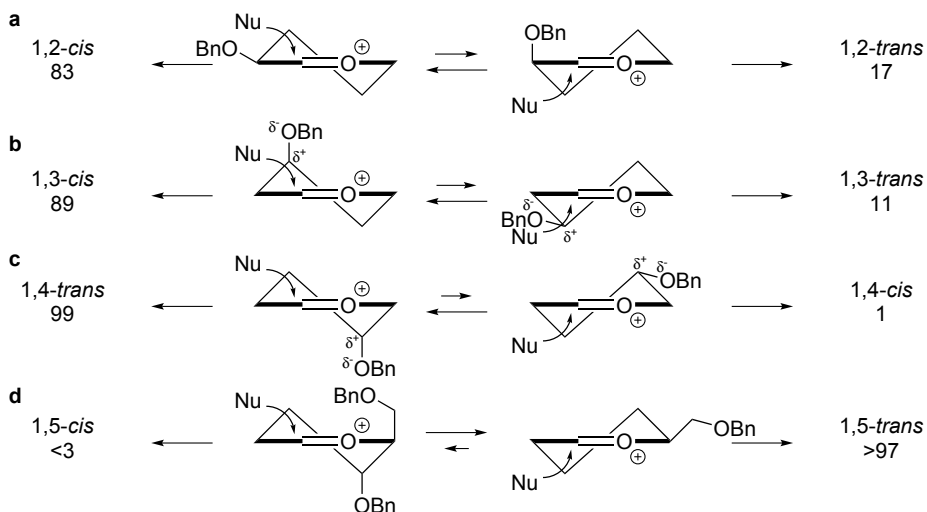


Figure 1.16 Individual substituent preferences in pyranosyl oxocarbenium ions.

In tetrahydropyran systems featuring multiple substituents the substituent preferences can be in line with or opposing each other. If all substituents are configured such that they can all adopt an optimal stabilizing position, this reinforces the half-chair preference (Figure 1.17). For example, the reaction of 1-*O*-acetyl-2,3,4-tri-*O*-benzyl lyxopyranoside **64** with allyltrimethylsilane gives the 1,2-*cis* isomer as major product.⁴⁵ It can be reasoned that the ³H₄ half-chair (**66**) that places the C2, C3 and C4 alkoxides in positions for optimal stabilization, is at the basis of this observed selectivity. The alternative ⁴H₃ half-chair (**67**) does not benefit from any of the substituent stabilizing interactions.

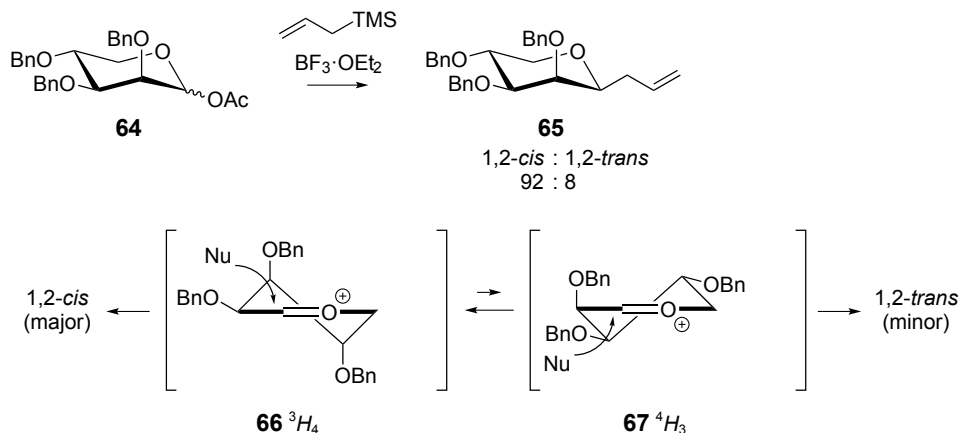


Figure 1.17 Substituent effects on C-allylation of lyxopyranose.

When a C5 alkoxyethyl group is added to the system, as in mannose **68**, the stereochemical course of the reaction alters dramatically. From the reaction shown in Figure 1.18 only the 1,2-*trans* product is isolated and formation of this product can originate from the 4H_3 half-chair oxocarbenium ion intermediate **71**. However when the pair of mannosyl half chair oxocarbenium ions **70** and **71** is analyzed, it becomes apparent that the 3H_4 half-chair **70** should be energetically more favorable because it places three out of four substituents in optimal positions.^{45,50-51} Nucleophilic addition to this oxocarbenium ion should lead to the 1,2-*cis* product. To account for the 1,2-*trans* selectivity observed, Woerpel and co-workers suggested that the developing diaxial interactions between C3, C5 and the incoming nucleophile make this mode of attack too sterically congested. Therefore the nucleophile preferably reacts with the higher energy 4H_3 half-chair oxocarbenium ion, following a Curtin-Hammett kinetic scenario.⁴⁵

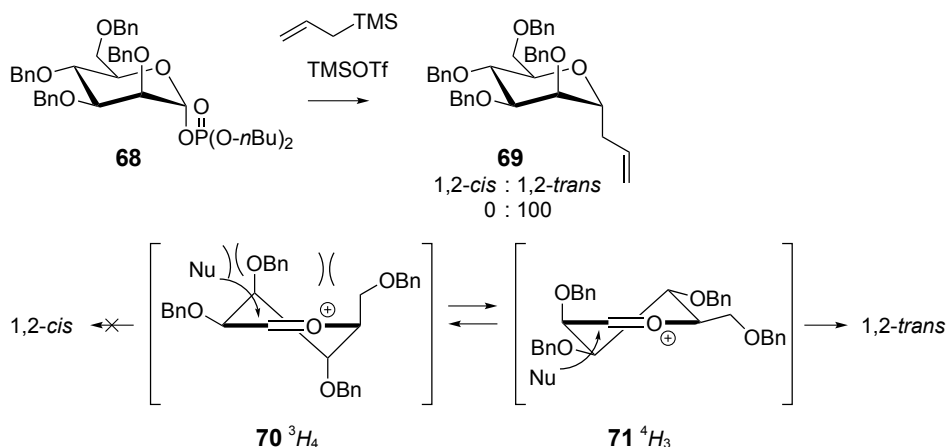


Figure 1.18 Mannopyranosyl C-allylation.

The orientation of the C6 oxygen substituent in hexopyranoses also contributes to the stability of pyranosyl oxocarbenium ion conformers. Rotation around the C6-O6 bond is possible and the interaction of this C6 oxygen substituent with the (partial) positive charge at the anomeric center depends on the orientation of this group, being *trans-gauche*, *gauche-trans* and *gauche-gauche* (See Figure 1.19).⁵²⁻⁵³ Bols and co-workers investigated the influence of the different C5-C6 rotamers on the rate of hydrolysis of dinitrophenyl glycosides (**72-75**). They employed fused bicyclic ring systems to lock the C5-C6 rotamers and found that hydrolysis of the *gg*-rotamer **74** proceeded fastest and the *tg*-rotamer **72** slowest in the series.⁵² The deactivating effect of the conformational lock, imposed on the system by the C4-C6 ring, is reflected by significantly increased hydrolysis rate of unconstrained **75**. The differences in reactivity between the three locked rotamers **72**, **73** and **74** was explained by Bols and co-workers to arise from the different dipole-charge interactions that are developed upon expulsion of the aglycon, with the C6-O6 dipole in **74** emerging as the least destabilizing. The conformational preference of the C5 alkoxymethyl to adopt a *gauche-gauche* configuration has also been observed in dioxocarbenium ions by the group of Woerpel.⁴⁹

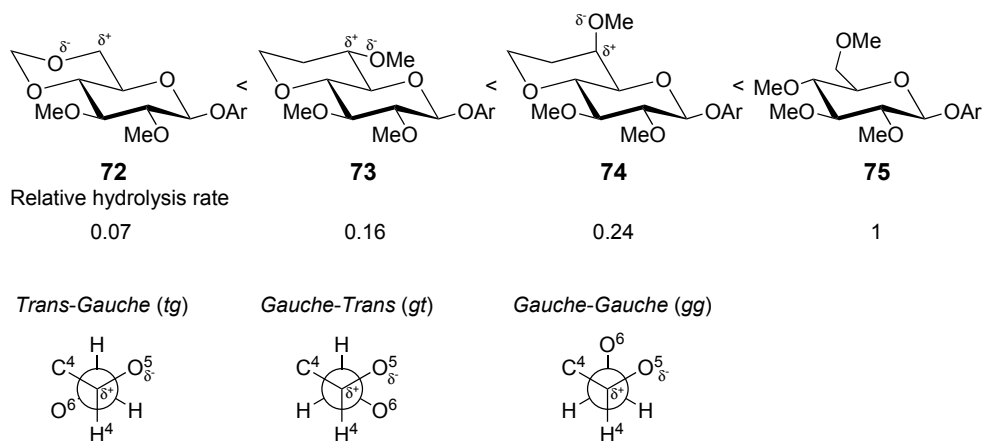


Figure 1.19 Deactivating effect of the conformationally restrained C6 oxygen on the hydrolysis (phosphate buffer in 1,4-dioxane, pH 6.5) of dinitrophenyl glycosides.

The influence of the carbohydrate substitution pattern on the acidic hydrolysis of different α -methyl sugars has long been known.⁵⁴ As displayed in Figure 1.20, the rate of the hydrolysis correlates with the amount of axial substituents, with gulose **78** hydrolyzing more rapidly than galactose **77**, which in turn hydrolyzes more rapidly than glucose **76**.^{14,55-56} The differences in hydrolysis rate can in part be explained with differences in stability of the starting compounds. Considering oxocarbenium ions as intermediates it becomes apparent that the oxocarbenium ion derived from the most reactive epimer,

gulose **78**, can adopt the 4H_3 half chair **79** in which all ring substituents contribute favorably.

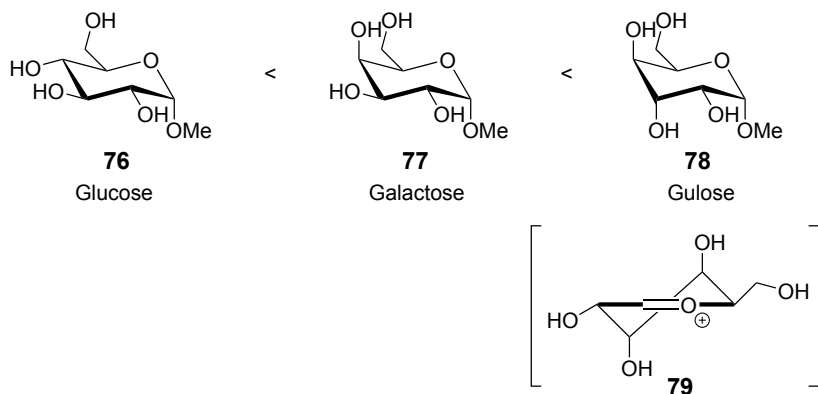


Figure 1.20 The rate of glycoside hydrolysis correlates with the amount of axial substituents.

The relative stability of this oxocarbenium ion has also been used to explain the unusual high 1,2-*cis* selectivity observed in *O*-glycosylations with gulosyl donors. For example, it was shown that gulose donor **80** reacts with glycosyl acceptor **53** in a pre-activation protocol to form 1,2-*cis* as the major product (Figure 1.21).⁵⁷ The *cis* product can originate from the 4H_3 half-chair (**83**) that benefits from optimal substituent stabilization. When this result is compared to the result of the *C*-allylation of mannose donor **69**, described above, it becomes clear that the orientation of the substituent at C5 is of decisive influence.

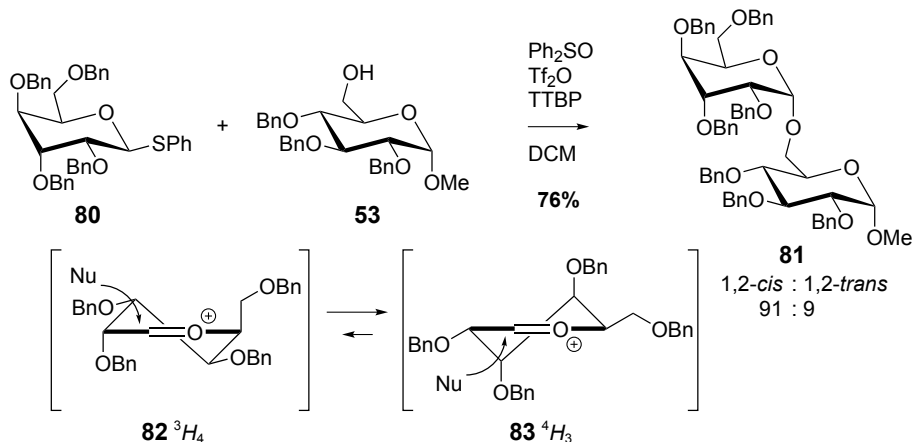


Figure 1.21 Gulose donors react in a pre-activation protocol to form 1,2-*cis* products.

Glycuronic acids are carbohydrates in which the terminal primary alcohol is oxidized to a carboxylic acid. The C5-carboxylic acid ester substituent can have a strong influence on the

reactivity of a pyranoside and generally glycuronic acid esters are less reactive than their “non-oxidized” counterparts in glycosylation reaction, because the electron withdrawing C5 carboxylic acid ester impedes the development of positive charge at the anomeric center during a glycosylation reaction.⁵⁸⁻⁵⁹ Oxidation of mannose however gives a donor with a reactivity that is significantly higher than expected.⁶⁰⁻⁶² Another striking feature of these donors is the fact that they afford primarily the 1,2-*cis* (β) products in glycosylation reactions (Figure 1.22),^{58,60-61,63-65} in contrast to conformationally unbiased mannose donors that give predominantly 1,2-*trans* (α) products as in the case of the *C*-allylation of benzylated mannose acetate **68** described above (see Figure 1.18). The strong 1,2-*cis* selectivity and high reactivity of mannuronic ester donors can be related to the stability of the 3H_4 conformer of the oxocarbenium ion (**84**).⁶⁶ This conformer is stereoelectronically most favored by the positive contribution of the C2, C3 and C4 substituents and the crucial influence of the pseudoaxial C5 carboxylate function. This substituent is less sterically demanding than the alkoxymethyl substituent in mannose and more importantly, the pseudoaxial C5 carboxylate in the 3H_4 conformation allows through-space stabilization of the positive charge at the anomeric center.^{57,62,64} This feature also becomes apparent in the conformation adopted by mannuronic ester anomeric α -triflates. These species are found in a conformational mixture, in which the 1C_4 chair conformation **87** having the anomeric triflate in an equatorial position predominates over the expected 4C_1 chair conformation **86** (**86:87** = 1:1.4).⁶³ It is also of interest to note that the anomeric triflate **86-87** is relatively unstable and decomposes at a relatively low temperature (-40 °C).⁶¹ The increased reactivity of mannuronic ester donors, as also confirmed in a series of competition experiments, corresponds to the relative stability of the oxocarbenium ion.⁶¹ For example, mannuronic acid donor **89** appeared to be more reactive than benzylidene donor **88** and as reactive as perbenzylated mannose donor **90**, one of the most reactive mannosyl donors known to date.⁶⁷

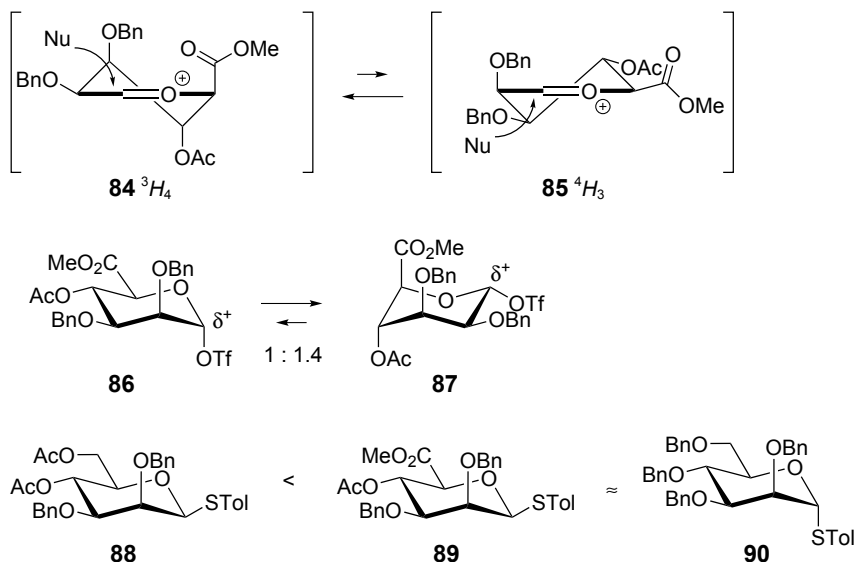


Figure 1.22 Mannuronic acid donors are highly reactive and in contrast to their non-oxidized analogs are highly 1,2-*cis* selective.

The favorable interactions of axially positioned alkoxy substituents on the stability of oxocarbenium ions also becomes apparent in positively charged iminosugars, carbohydrates of which the ring oxygen is replaced by a nitrogen atom. Bols and co-workers determined the pK_a values of a broad range of polyhydroxylated piperidines.^{56,68-71} In the series comprising the iminosugar equivalents of glucose, mannose and galactose (Figure 1.23), it becomes clear that the basicity of the all-equatorial glucose (**91**) is less than that of the iminosugars bearing one axial hydroxyl group. Both mannose (**92**) and galactose (**93**) have a beta hydroxyl substituent configured in axial position and this causes an increase in basicity of 0.8 pK_a units. The difference between an equatorial and axial gamma hydroxyl is smaller as judged from the pK_a difference between **95** and **94** (0.4 pK_a units). Removal of a hydroxyl group leads to an increase of 1.4 pK_a units (compare **91** and **94**). The differences in pK_a indicate that an equatorial hydroxyl is more electron withdrawing than an axial hydroxyl and that the distance of the substituent to the positively charged center also plays a role. To account for the differences between the equatorial and axial epimers, Bols and co-workers reasoned that a ring substituent in equatorial position generates a more unfavorable dipole-charge interaction than the same group in axial position (see Figure 1.24).⁶⁹ In addition, the axial hydroxyl is also positioned properly to allow for through-space stabilization of the cation.

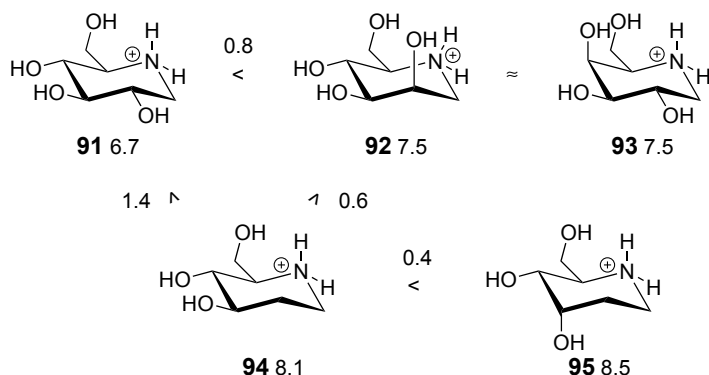


Figure 1.23 The pK_a of ammonium ions **91-95** depends on the configuration of the beta and gamma hydroxyls.

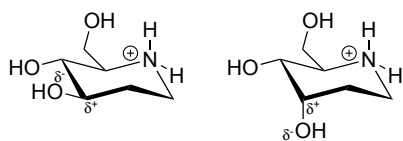


Figure 1.24 Dipole-charge interactions in protonated iminosugars with axially and equatorially oriented hydroxyl groups.

Bols and co-workers also noted that some of the iminosugars change their conformation upon protonation to adopt a more axial-rich conformation.⁶⁹ This behavior can be explained by the more favorable stereoelectronic effects of the axially oriented hydroxyl substituents on the ammonium cation. These are more stabilizing by virtue of through space electron donation and less destabilizing by virtue of the more favorable dipole-charge interaction than their equatorial counterparts. For example, mono-substituted piperidines change their conformational preference under acidic conditions (Figure 1.25).⁷² In a non-protonated state the equilibrium between the 4C_1 and 1C_4 conformers of 3-hydroxypiperidine **96-97** lies to the side of the equatorial conformer. Protonation shifts the equilibrium to the side of the axial isomer (**99** vs **98**). This effect is less pronounced for the gamma hydroxyl analogue (Figure 1.25b), in line with the diminished effect of this substituent on the pK_a value. 4-Hydroxypiperidine (**100-103**) prefers the 4C_1 conformer under both basic and acidic conditions (**100** and **102**), but this preference is less pronounced under acidic conditions.

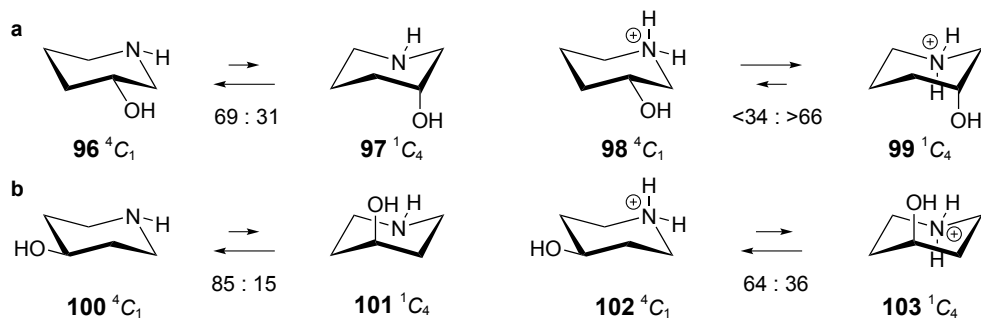


Figure 1.25 Changes in conformational equilibria induced by the protonation of the nitrogen atom.

1.4 Summary and thesis outline

Stereoelectronic effects are decisive in determining the structure and reactivity of molecules. In systems, in which (partial) positive charge is present or develops, the intrinsic destabilizing effects of electron withdrawing substituents, such as alkoxy groups in carbohydrates, can be minimized or even be made stabilizing by correct spatial positioning. This thesis investigates how stereoelectronic effects in carbohydrate based oxocarbenium ions, iminium ions and ammonium ions influences their shape and reactivity, by a combination of computational and experimental methods. **Chapter 2** focuses on detailing the steric and stereoelectronic effects that become apparent in furanosyl oxocarbenium ions of multiply substituted pentoses. Substitution reactions on these oxocarbenium ions all take place to give the 1,2-*cis* addition products with large selectivity, an outcome that can be explained using the conformations of the oxocarbenium ions involved. **Chapter 3** expands the work described in Chapter 2 to furanosyl oxocarbenium ions derived from ketosides featuring different anomeric substituents. **Chapter 4** describes an investigation into the Ugi multi component reaction of iminium ions, derived from the four possible D-pentofuranoses. The stereochemical outcome of this multi component reaction is set in the addition step in which the isocyanide reacts with the iminium ion. Where it is often assumed that Ugi reactions take place under thermodynamic control these results indicate that they in fact are under kinetic control. In **Chapter 5** the construction of a furanose iminosugar library is described from all possible pentofuranosyl iminosugars. **Chapter 6** details how the conformation of mannuronic acid derived iminosugars depends on the pH. Different C5 functionalities (the free acid, the methyl ester and amide) are probed and it is shown that the ester and free acid can flip their conformation, depending on protonation of the endocyclic amine. The last Chapter, **Chapter 7**, summarizes the research described in this Thesis and suggests future research objectives.

References and Notes

- [1] Kirby, A. J., *Oxford Chemistry Primers, Stereoelectronic Effects*, Oxford University Press Inc., **1996**.
- [2] Freitas, M. P.; Rittner, R.; Tormena, C. F.; Abraham, R. J. *Spectrochim. Acta Mol. Biomol. Spectros.* **2005**, *61*, 1771-1776, 10.1016/j.saa.2004.07.007.
- [3] Reeves, L. W.; Stromme, K. O. *Trans. Faraday Soc.* **1961**, *57*, 390-398, 10.1039/tf9615700390.
- [4] Kwestroo, W.; Meijer, F. A.; Havinga, E. *Recl. Trav. Chim. Pays-Bas* **1954**, *73*, 717-736, 10.1002/recl.19540730904.
- [5] Clayden, J.; Greeves, N.; Warren, S.; Wothers, P., *Organic Chemistry*, Oxford University Press, **2000**.
- [6] Smith, M. B.; March, J., *March's Advanced Organic Chemistry*, John Wiley & Sons, Inc., **2007**.
- [7] Carey, F. A.; Sundberg, R. J., *Advanced Organic Chemistry, Part A: Structure and Mechanisms*, Kluwer Academic/Plenum Publishers, **2000**.
- [8] Hosokawa, S.; Kirschbaum, B.; Isobe, M. *Tetrahedron Lett.* **1998**, *39*, 1917-1920, 10.1016/s0040-4039(98)00047-1.
- [9] Deslongchamps, P., *Stereoelectronic Effects in Organic Chemistry*, Pergamon Press, **1983**.
- [10] Stolorow, R. D.; Giants, T. W. *J. Chem. Soc., Chem. Commun.* **1971**, 528-529, 10.1039/c29710000528.
- [11] Baldry, K. W.; Gordon, M. H.; Hafter, R.; Robinson, M. J. T. *Tetrahedron* **1976**, *32*, 2589-2594, 10.1016/0040-4020(76)88032-5.
- [12] Dibble, D. J.; Ziller, J. W.; Woerpel, K. A. *J. Org. Chem.* **2011**, *76*, 7706-7719, 10.1021/jo200950s.
- [13] Baghdasarian, G.; Woerpel, K. A. *J. Org. Chem.* **2006**, *71*, 6851-6858, 10.1021/jo060968z.
- [14] Smith, D. M.; Woerpel, K. A. *Org. Biomol. Chem.* **2006**, *4*, 1195-1201, 10.1039/b600056h.
- [15] Nagao, Y.; Goto, M. *Heterocycles* **1995**, *41*, 883-888, 10.3987/COM-95-7026.
- [16] Gorthey, L. A.; Vairamani, M.; Djerassi, C. *J. Org. Chem.* **1985**, *50*, 4174-4182, 10.1021/jo00222a001.
- [17] Collins, L. J. *Tetrahedron Lett.* **1970**, 1547-1550, 10.1016/S0040-4039(01)98018-9.
- [18] Juaristi, E.; Cuevas, G. *Tetrahedron* **1992**, *48*, 5019-5087, 10.1016/s0040-4020(01)90118-8.
- [19] Taha, H. A.; Richards, M. R.; Lowary, T. L. *Chem. Rev.* **2013**, *113*, 1851-1876, 10.1021/cr300249c.

- [20] Fuchs, B., *Topics in Stereochemistry* **1978**, *10*, 1-94.
- [21] Larsen, C. H.; Ridgway, B. H.; Shaw, J. T.; Woerpel, K. A. *J. Am. Chem. Soc.* **1999**, *121*, 12208-12209, 10.1021/ja993349z.
- [22] Smith, D. M.; Tran, M. B.; Woerpel, K. A. *J. Am. Chem. Soc.* **2003**, *125*, 14149-14152, 10.1021/ja0375176.
- [23] Smith, D. M.; Woerpel, K. A. *Org. Lett.* **2004**, *6*, 2063-2066, 10.1021/ol0492647.
- [24] Larsen, C. H.; Ridgway, B. H.; Shaw, J. T.; Smith, D. M.; Woerpel, K. A. *J. Am. Chem. Soc.* **2005**, *127*, 10879-10884, 10.1021/ja0524043.
- [25] Tran, V. T.; Woerpel, K. A. *J. Org. Chem.* **2013**, *78*, 6609-6621, 10.1021/jo400945j.
- [26] Lavinda, O.; Tran, V. T.; Woerpel, K. A. *Org. Biomol. Chem.* **2014**, *12*, 7083-7091, 10.1039/c4ob01251h.
- [27] Finch, O. C.; Furkert, D. P.; Brimble, M. A. *Tetrahedron* **2014**, *70*, 590-596, 10.1016/j.tet.2013.12.012.
- [28] Araki, Y.; Kobayashi, N.; Ishido, Y.; Nagasawa, J. *Carbohydr. Res.* **1987**, *171*, 125-139, 10.1016/s0008-6215(00)90883-8.
- [29] Tian, Y.; Wu, S. H.; Wei, Z. *Carbohydr. Res.* **2005**, *340*, 235-244, 10.1016/j.carres.2004.11.014.
- [30] Mukaiyama, T.; Shimpuku, T.; Takashima, T.; Kobayashi, S. *Chem. Lett.* **1989**, 145-148, 10.1246/cl.1989.145.
- [31] van Delft, P., **2013**, *Synthetic Studies Towards Oligonucleotide Derivatives and Conjugates*, Ph.D Thesis, Leiden University.
- [32] Doboszewski, B. *Nucleos. Nucleot. Nucl.* **2009**, *28*, 875-901, 10.1080/15257770903306518.
- [33] Mukaiyama, T.; Suda, S. *Chem. Lett.* **1990**, 1143-1146, 10.1246/cl.1990.1143.
- [34] Zhu, X. M.; Kawatkar, S.; Rao, Y.; Boons, G. J. *J. Am. Chem. Soc.* **2006**, *128*, 11948-11957, 10.1021/ja0629817.
- [35] Lee, Y. J.; Lee, K.; Jung, E. H.; Jeon, H. B.; Kim, K. S. *Org. Lett.* **2005**, *7*, 3263-3266, 10.1021/ol0510668.
- [36] Kaeothip, S.; Boons, G. J. *Org. Biomol. Chem.* **2013**, *11*, 5136-5146, 10.1039/c3ob40958a.
- [37] Lee, Y. J.; Lee, B. Y.; Jeon, H. B.; Kim, K. S. *Org. Lett.* **2006**, *8*, 3971-3974, 10.1021/ol061444o.
- [38] Baek, J. Y.; Joo, Y. J.; Kim, K. S. *Tetrahedron Lett.* **2008**, *49*, 4734-4737, 10.1016/j.tetlet.2008.05.118.
- [39] Beaver, M. G.; Woerpel, K. A. *J. Org. Chem.* **2010**, *75*, 1107-1118, 10.1021/jo902222a.
- [40] Moume-Pymbock, M.; Crich, D. *J. Org. Chem.* **2012**, *77*, 8905-8912, 10.1021/jo3011655.

- [41] Romero, J. A. C.; Tabacco, S. A.; Woerpel, K. A. *J. Am. Chem. Soc.* **2000**, *122*, 168-169, 10.1021/ja993366o.
- [42] Ayala, L.; Lucero, C. G.; Romero, J. A. C.; Tabacco, S. A.; Woerpel, K. A. *J. Am. Chem. Soc.* **2003**, *125*, 15521-15528, 10.1021/ja037935a.
- [43] Chamberland, S.; Ziller, J. W.; Woerpel, K. A. *J. Am. Chem. Soc.* **2005**, *127*, 5322-5323, 10.1021/ja050830i.
- [44] Shenoy, S. R.; Woerpel, K. A. *Org. Lett.* **2005**, *7*, 1157-1160, 10.1021/ol0500620.
- [45] Lucero, C. G.; Woerpel, K. A. *J. Org. Chem.* **2006**, *71*, 2641-2647, 10.1021/jo0522963.
- [46] Stevens, R. V.; Lee, A. W. M. *J. Am. Chem. Soc.* **1979**, *101*, 7032-7035, 10.1021/ja00517a042.
- [47] Krumper, J. R.; Salamant, W. A.; Woerpel, K. A. *Org. Lett.* **2008**, *10*, 4907-4910, 10.1021/ol8019956.
- [48] Krumper, J. R.; Salamant, W. A.; Woerpel, K. A. *J. Org. Chem.* **2009**, *74*, 8039-8050, 10.1021/jo901639b.
- [49] Yang, M. T.; Woerpel, K. A. *J. Org. Chem.* **2009**, *74*, 545-553, 10.1021/jo8017846.
- [50] The mannosyl ³H₄ half-chair was calculated to be 3-4 kcal mol⁻¹ lower in energy than the corresponding ⁴H₃ half-chair, see ref 45 and 51.
- [51] Amat, L.; Carbo-Dorca, R. *J. Chem. Inf. Comput. Sci.* **2000**, *40*, 1188-1198, 10.1021/ci0000272.
- [52] Jensen, H. H.; Nordstrom, L. U.; Bols, M. *J. Am. Chem. Soc.* **2004**, *126*, 9205-9213, 10.1021/ja047578j.
- [53] Moume-Pymbock, M.; Furukawa, T.; Mondal, S.; Crich, D. *J. Am. Chem. Soc.* **2013**, *135*, 14249-14255, 10.1021/ja405588x.
- [54] Overend, W. G.; Sequeira, J. S.; Rees, C. W. *J. Chem. Soc.* **1962**, 3429-3439, 10.1039/jr9620003429.
- [55] Bols, M.; Liang, X. F.; Jensen, H. H. *J. Org. Chem.* **2002**, *67*, 8970-8974, 10.1021/jo0205356.
- [56] McDonnell, C.; Lopez, O.; Murphy, P.; Bolanos, J. G. F.; Hazell, R.; Bols, M. *J. Am. Chem. Soc.* **2004**, *126*, 12374-12385, 10.1021/ja04746t.
- [57] Dinkelaar, J.; de Jong, A. R.; van Meer, R.; Somers, M.; Lodder, G.; Overkleeft, H. S.; Codée, J. D. C.; van der Marel, G. A. *J. Org. Chem.* **2009**, *74*, 4982-4991, 10.1021/jo900662v.
- [58] van den Bos, L. J.; Codée, J. D. C.; Litjens, R. E. J. N.; Dinkelaar, J.; Overkleeft, H. S.; van der Marel, G. A. *Eur. J. Org. Chem.* **2007**, 3963-3976, 10.1002/ejoc.200700101.
- [59] Codée, J. D. C.; Christina, A. E.; Walvoort, M. T. C.; Overkleeft, H. S.; Van der Marel, G. A., *Top. Curr. Chem.* **2011**, *301*, 253-289, 10.1007/128_2010_111.

- [60] Codée, J. D. C.; Walvoort, M. T. C.; de Jong, A. R.; Lodder, G.; Overkleef, H. S.; van der Marel, G. A. *J. Carbohydr. Chem.* **2011**, *30*, 438-457, 10.1080/07328303.2011.624284.
- [61] Walvoort, M. T. C.; de Witte, W.; van Dijk, J.; Dinkelaar, J.; Lodder, G.; Overkleef, H. S.; Codée, J. D. C.; van der Marel, G. A. *Org. Lett.* **2011**, *13*, 4360-4363, 10.1021/ol2016862.
- [62] Codée, J. D. C.; van den Bos, L. J.; de Jong, A. R.; Dinkelaar, J.; Lodder, G.; Overkleef, H. S.; van der Marel, G. A. *J. Org. Chem.* **2009**, *74*, 38-47, 10.1021/jo8020192.
- [63] Walvoort, M. T. C.; Lodder, G.; Mazurek, J.; Overkleef, H. S.; Codée, J. D. C.; van der Marel, G. A. *J. Am. Chem. Soc.* **2009**, *131*, 12080-12081, 10.1021/ja905008p.
- [64] Walvoort, M. T. C.; Dinkelaar, J.; van den Bos, L. J.; Lodder, G.; Overkleef, H. S.; Codée, J. D. C.; van der Marel, G. A. *Carbohydr. Res.* **2010**, *345*, 1252-1263, 10.1016/j.carres.2010.02.027.
- [65] Walvoort, M. T. C.; Lodder, G.; Overkleef, H. S.; Codée, J. D. C.; van der Marel, G. A. *J. Org. Chem.* **2010**, *75*, 7990-8002, 10.1021/jo101779v.
- [66] DFT calculations at B3LYP/6-311G** level indicate that the 3H_4 conformer is favored by 5 kcal mol⁻¹ over its 4H_3 counterpart (unpublished results).
- [67] Koeller, K. M.; Wong, C. H. *Chem. Rev.* **2000**, *100*, 4465-4493, 10.1021/cr990297n.
- [68] Jensen, H. H.; Lyngbye, L.; Bols, M. *Angew. Chem. Int. Ed.* **2001**, *40*, 3447-3449, 10.1002/1521-3773(20010917)40:18<3447::aid-anie3447>3.0.co;2-8.
- [69] Jensen, H. H.; Lyngbye, L.; Jensen, A.; Bols, M. *Chem. Eur. J.* **2002**, *8*, 1218-1226, 10.1002/1521-3765(20020301)8:5<1218::aid-chem1218>3.0.co;2-x.
- [70] Pedersen, C. M.; Bols, M. *Tetrahedron* **2005**, *61*, 115-122, 10.1016/j.tet.2004.10.039.
- [71] Jensen, H. H.; Bols, M. *Acc. Chem. Res.* **2006**, *39*, 259-265, 10.1021/ar050189p.
- [72] Terui, Y.; Tori, K. *J. Chem. Soc., Perkin Trans. 2* **1975**, 127-133, 10.1039/p29750000127.

Chapter 2

Furanosyl Oxocarbenium Ion Stability and Stereoselectivity

partly published in
Angewandte Chemie International Edition **2014**, 53, 10381-10385, 10.1002/anie.201405477

2.1 Introduction

Furanoses, five-membered ring carbohydrates, are ubiquitous in nature. They form characteristic motifs in many bacterial and plant oligo- and polysaccharides, while they are absent in mammalian oligosaccharides.¹ Furanose-containing bacterial oligosaccharides are therefore attractive targets to use in vaccine applications and the enzymes involved in

their assembly and degradation are appealing therapeutic targets.² Furanosyl oxocarbenium ions play crucial roles in both the chemistry and biology of glycosyl furanoses. Insight into the structure of such ions is instructive to both the design of mimics to inhibit furanose-processing enzymes,³ and to effect stereoselective transformations at the anomeric center of furanosides. Over the years several examples have been reported on furanosylations of conformationally unbiased furanosyl donors, which bear no apparent stereochemistry-directing functionalities, and proceed with striking stereoselectivity to provide 1,2-*cis* glycosides.⁴⁻¹⁰

To account for the stereochemical outcome of reactions involving substituted tetrahydrofuran oxocarbenium ions as intermediates, Woerpel and co-workers have proposed a two-conformer model, in which the equilibrium between the ³*E* and *E*₃ oxocarbenium ions is decisive (Figure 2.1).¹¹⁻¹⁵ Both envelopes are preferentially attacked on the inside, because this mode of attack leads to a transition state devoid of eclipsing interactions with substituents at C2, and provides a product featuring a favorable staggered C1-C2 conformation.^{11,14} Therefore reaction on the ³*E* conformer occurs on the top face, where the *E*₃ envelope is approached at the bottom face.^{11,14,16} The nature and orientation of the substituents on the tetrahydrofuran ring play an all-important role in determining the stability of the oxocarbenium ion. Alkoxy substituents at the C2-position preferentially adopt a pseudoequatorial position to allow hyperconjugative stabilization of the oxocarbenium ion by the pseudoaxial C2-H2 bond, while a C3-alkoxy substituent can stabilize the electron-depleted anomeric center in a pseudoaxial position. The orientation of an alkyl group at C4 has been reported to be of little influence on the stability of the oxocarbenium ion.¹⁴ This model explains well the stereochemical outcome of the addition of C-nucleophiles, such as allyltrimethylsilane, to monosubstituted tetrahydrofuran cores. For multiple substituted systems, such as genuine furanosyl oxocarbenium ions, the interplay between the ring substituents becomes important and prediction of the energetically most favored oxocarbenium ion envelope is very difficult.

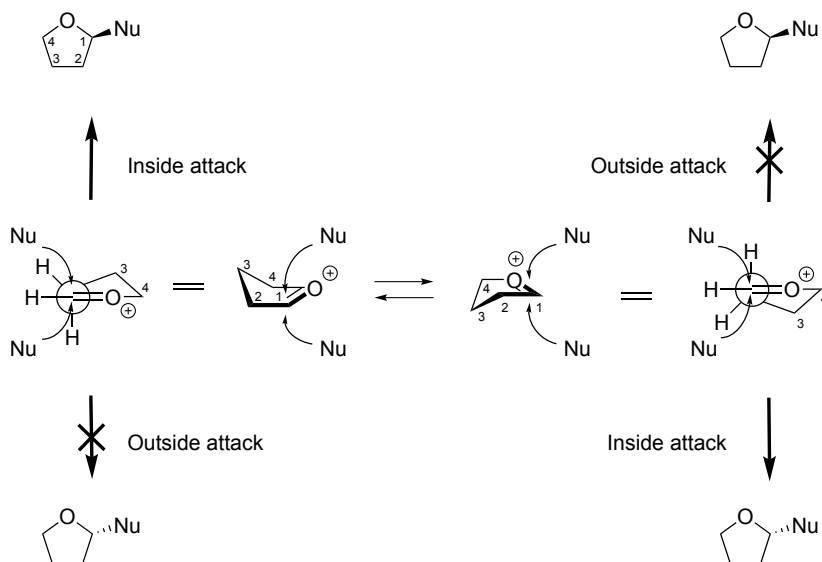


Figure 2.1 The two-conformer model. The two furanosyl 3E and E_3 envelope oxocarbenium ions are preferentially attacked by the incoming nucleophile along an inside trajectory to provide different epimeric products.

This chapter describes a complete survey of the energy landscape of the entire conformational space of the furanosyl oxocarbenium ions for the four possible pentoses, ribose, arabinose, xylose, and lyxose. A clear picture emerges how multiple ring substituents on a furanosyl oxocarbenium ion influence its stability, and therefore its reactivity and stereoselectivity in addition reactions. This study is complemented by a set of substitution reactions to experimentally match the theoretical results.

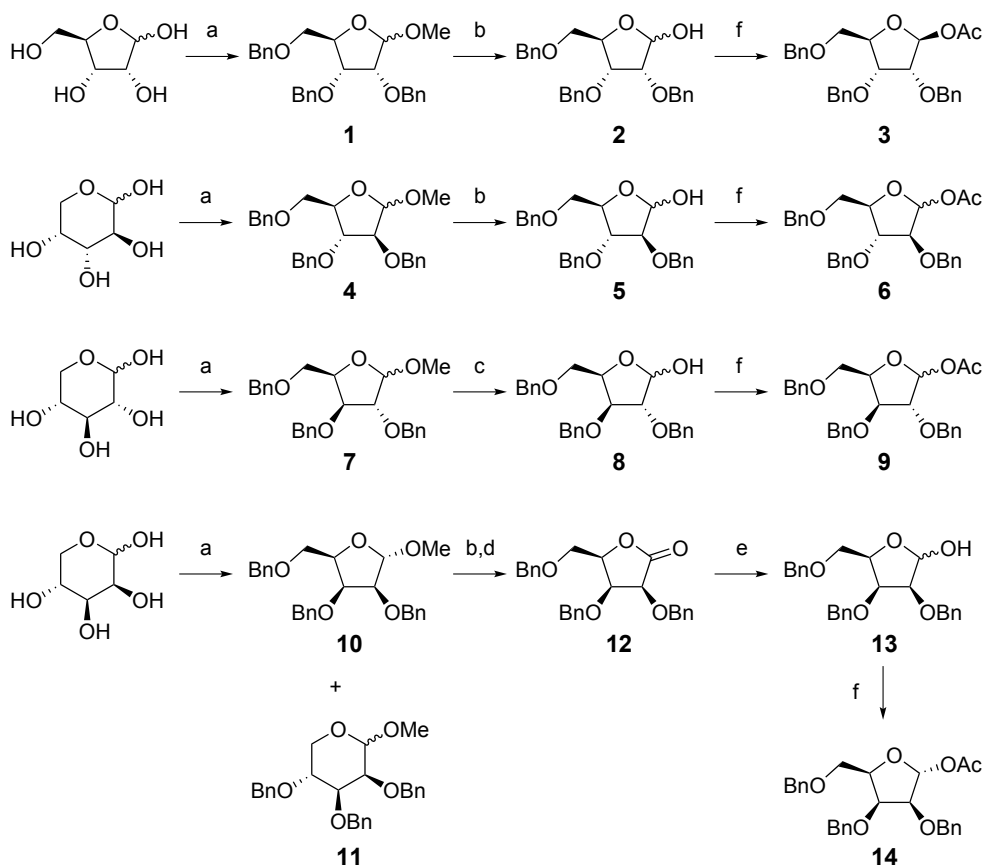
2.2 Results and discussion

Initially the Lewis acid mediated addition of [D]triethylsilane ([D]TES), as model nucleophile, to the four furanosyl acetates 2,3,5-tri-*O*-benzyl-D-ribofuranosyl acetate **3**, 2,3,5-tri-*O*-benzyl-D-arabinofuranosyl acetate **6**, 2,3,5-tri-*O*-benzyl-D-xylofuranosyl acetate **9**, and 2,3,5-tri-*O*-benzyl-D-lyxofuranosyl acetate **14** was investigated (Scheme 2.1). [D]TES was used as a nucleophile because the α - and β -deuterium epimeric products are nearly identical in physical properties, but can be distinguished by ${}^1\text{H}$ NMR spectroscopy, and therefore any isolated sample of the reaction products can be used to reliably determine the α/β product ratio.

The synthesis of the four perbenzylated furanosyl acetates started from the pentoses as depicted in Scheme 2.1. Fischer methylation under kinetic conditions of the pentoses at

room temperature yielded the methyl furanosides that were subsequently benzylated to give the four benzyl protected methyl furanosides **1**, **4**, **7** and **10**. Only in the case of lyxose, pyranose side products (**11**) formed that could not be completely removed. Each of the four benzyl protected methyl furanosides was subjected to an acid catalyzed hydrolysis to yield the corresponding hemi-acetals. To separate the lyxo pyranose side product from **13** the lactols were oxidized. Pure lactone **12** could now be obtained and transformed into **13** by oxidation using a mixture of acetic anhydride and DMSO followed by reduction using DIBAL-H. All four hemi-acetals were acetylated with acetic anhydride in pyridine, yielding perbenzylated β -acetyl ribofuranose (**3**), perbenzylated α/β -acetyl arabinofuranose (**6**), perbenzylated α/β -acetyl xylofuranose (**9**), and perbenzylated α -acetyl lyxofuranose (**14**).

Scheme 2.1 Synthesis of the four furanosyl acetate donors **3,6,9** and **14**.



Reagents and conditions: (a) i) AcCl, MeOH; ii) BnBr, NaH, TBAI, DMF, **1**: 66% over 2 steps, **4**: 68% over 2 steps, **7**: quant. over 2 steps, **10**, **11**: 84% over 2 steps; (b) AcOH, H₂O, 110 °C, **2**: 86%, **5**: 72%; (c) HCl, H₂O, 1,4-dioxane, 90 °C, 77%; (d) Ac₂O, DMSO, 76% over 2 steps; (e) DiBAL-H, DCM, -78 °C, 94%; (f) Ac₂O, pyridine, **3**: 91%, **6**: 94%, **9**: 86%, **14**: quant.

Table 2.1 Results of the substitution reaction of [D]TES with the various furanosides.

Entry	Furanosyl acetate	Product	1,2- <i>cis</i> : 1,2- <i>trans</i> ^[a]	Yield ^[b]
1	 Ribose 3	 15	>98:2	50%
2	 Arabinose 6	 16	>98:2	62%
3	 Xylose 9	 17	85:15	40%
4	 Lyxose 14	 18	>98:2	100%

^[a]Ratio determined by ¹H NMR spectroscopy, stereochemistry was identified using ²J coupling-constants measured from HSQC-HECADE NMR spectra. ^[b]Yield of isolated deuterium-furanosides after column chromatography. The remainders of the mass balance in each entry consist of recovered and hydrolyzed starting materials.

With the four furanosyl acetates in hand, the [D]TES substitution reactions were undertaken. As can be seen in Table 2.1, all furanosyl acetates (**3**, **6**, **9**, **14**) are substituted in a stereoselective manner to provide the 1,2-*cis* products and only xylose **9** delivers a minor amount of the 1,2-*trans* product. Perhaps most striking is the result obtained with lyxose **14**, which features all ring substituents on one side of the ring. Here, the nucleophile attacks the β-face of the molecule with complete stereoselectivity to lead to the counterintuitive all-*cis* product.

The stereoselectivities in the reactions indicate that direct S_N2-type substitution on the (mixtures of) anomeric acetates can be excluded as a major reaction pathway.¹⁷ Also selective substitution reactions on anomeric triflates¹⁸⁻¹⁹ as a major contributing pathway can be excluded because the relative stability of the anomeric triflates cannot be readily reconciled with the experimental results.²⁰ To probe whether the intermediate

oxocarbenium ions can be at the basis of the observed selectivities, the relative energies of the oxocarbenium ions of the different furanosyl epimers were investigated. To this end the energy associated with the complete conformational space of the permethylated furanosyl oxocarbenium ions **19-22** (Figure 2.2a) was calculated using the potential energy surface (PES) scanning method recently introduced by Rhoad, Cagg, and Carver²¹, adapted to correct for solvent and zero-point energy. The conformation of a furanose ring can be defined by a phase angle (P) and puckering amplitude (τ_m) and the complete conformational space of such a ring can be displayed using the pseudorotation circle, which was introduced by Altona and Sundaralingam^{2,22} (Figure 2.2b). The phase angle defines the conformation of the ring, and the puckering amplitude indicates how far out of the median plane the outlying atoms (denoted with super- or subscripts) are positioned. The energies associated with 81 fixed-ring conformers were calculated with Gaussian 03,²³ by employing the B3LYP density functional and the 6-311G** basis set, and corrected for the solvent (CH_2Cl_2) using the polarizable continuum model (PCM) function. The calculated energies were then mapped in the pseudorotational circle to give free-energy surface (FES) maps.²⁴ Because orientation of the C4-C5 bond significantly influences the stability²⁵ of furanosyl rings, the FES of the oxocarbenium ions was scanned for the three individual *gg*, *gt*, and *tg* C4-C5 rotamers (Figure 2.2c). Thus for each furanosyl oxocarbenium ion 243 (3×81) conformers were optimized and the associated energies determined.

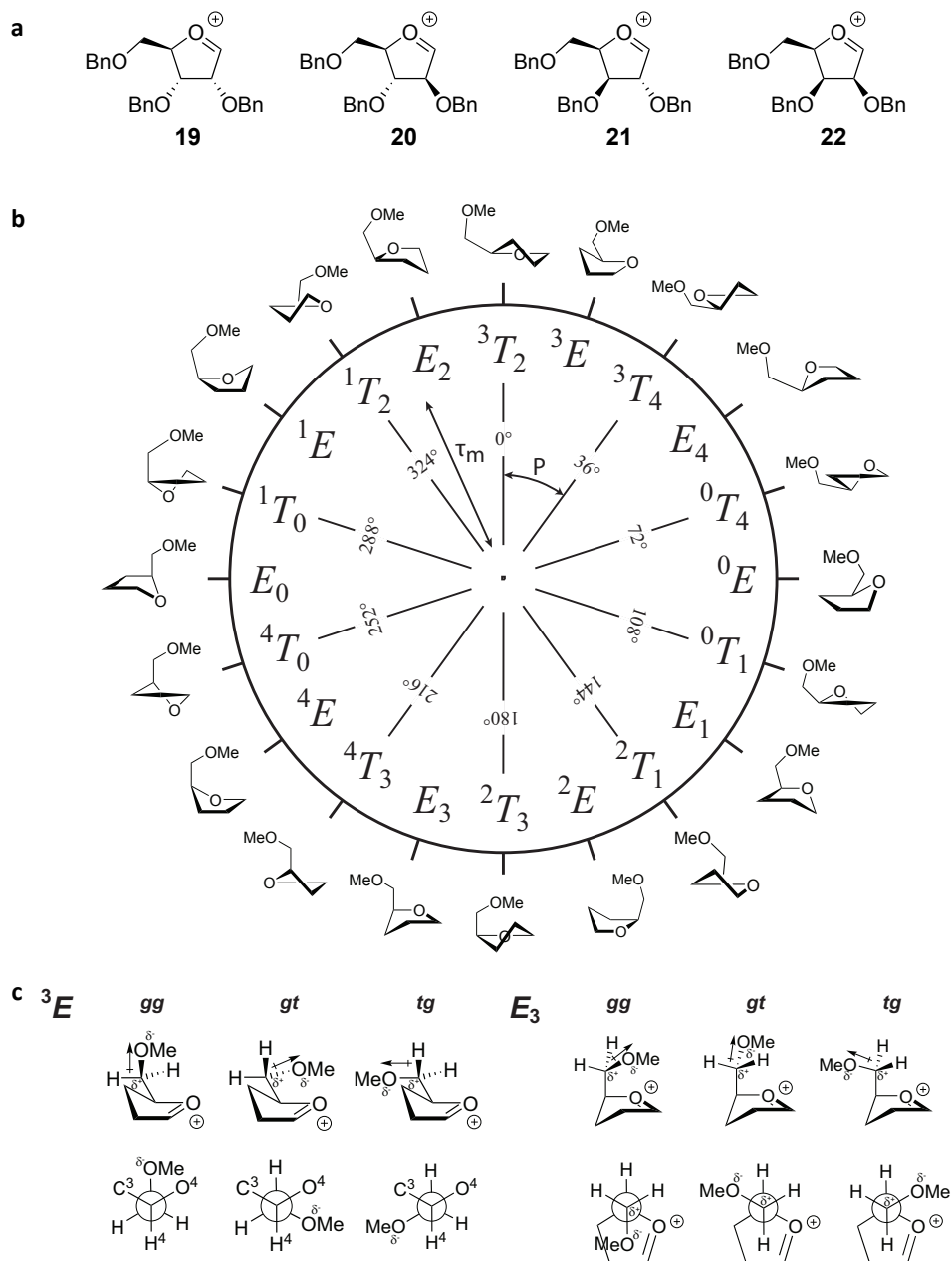


Figure 2.2 a) The investigated furanosyl oxocarbenium ions. b) The pseudorotational circle describing the conformational space a five-membered ring can occupy. The pseudorotational phase angle (P) in combination with the puckering amplitude (τ_m) defines the ring conformation. c) Possible rotamers around the C4-C5 bond in the 3E (left) and E_3 (right) envelope conformers, in which the dipoles of the C5-OMe moieties are indicated.

The ribofuranose FES map

In Figure 2.3a, the FES maps for the three C4-C5 rotamers of the ribofuranosyl oxocarbenium ion **19** are displayed. The combination of the absolute lowest energies of these three conformers in a single picture leads to the global FES map depicted in Figure 2.3d. From the four graphs it becomes apparent that **19** preferentially adopts an E_3 -like structure and that the orientation of the C5-OMe group has a great impact on the stability of the oxocarbenium ion. The *gg* rotamer is significantly more stable than the *gt* structure, which in turn is more favorable than the *tg* conformer. The E_3 *gg* rotamer positions the C5-OMe group above the furanosyl ring to allow through-space stabilization of the oxocarbenium ion. The enhanced stability of the *gt* conformer over its *tg* counterpart can be rationalized by the interaction of the C5-O5 dipole with the positive charge in the oxocarbenium ion ring. As pointed out by Bols and co-workers the interaction of the C5-OMe dipole with the positive charge of the oxocarbenium ion is least favorable in the *tg* conformer (Figure 2.3c).²⁶⁻²⁷ In the most stable E_3 conformation, the C3 and C2 methoxy groups take up a pseudoaxial and pseudoequatorial orientation, respectively, thus lending support to the model devised by Woerpel and co-workers. Notably the E_3 envelope places two out of the three substituents in a pseudoaxial position, which is sterically rather unfavorable.¹⁴ To investigate the steric preference of the system the FES of a ribose-configured 2,3-dimethoxy-4-methylenemethoxy cyclopentene, representing a structural mimic of **19** lacking the positive charge was also calculated. This FES is depicted in Figure 2.4d, and it shows a preference of the noncharged ribo-cyclopentene for the 3E envelope. Thus in the case of the ribofuranosyl oxocarbenium ion the electronic stabilization in the E_3 conformation outweighs the steric preference of the system.

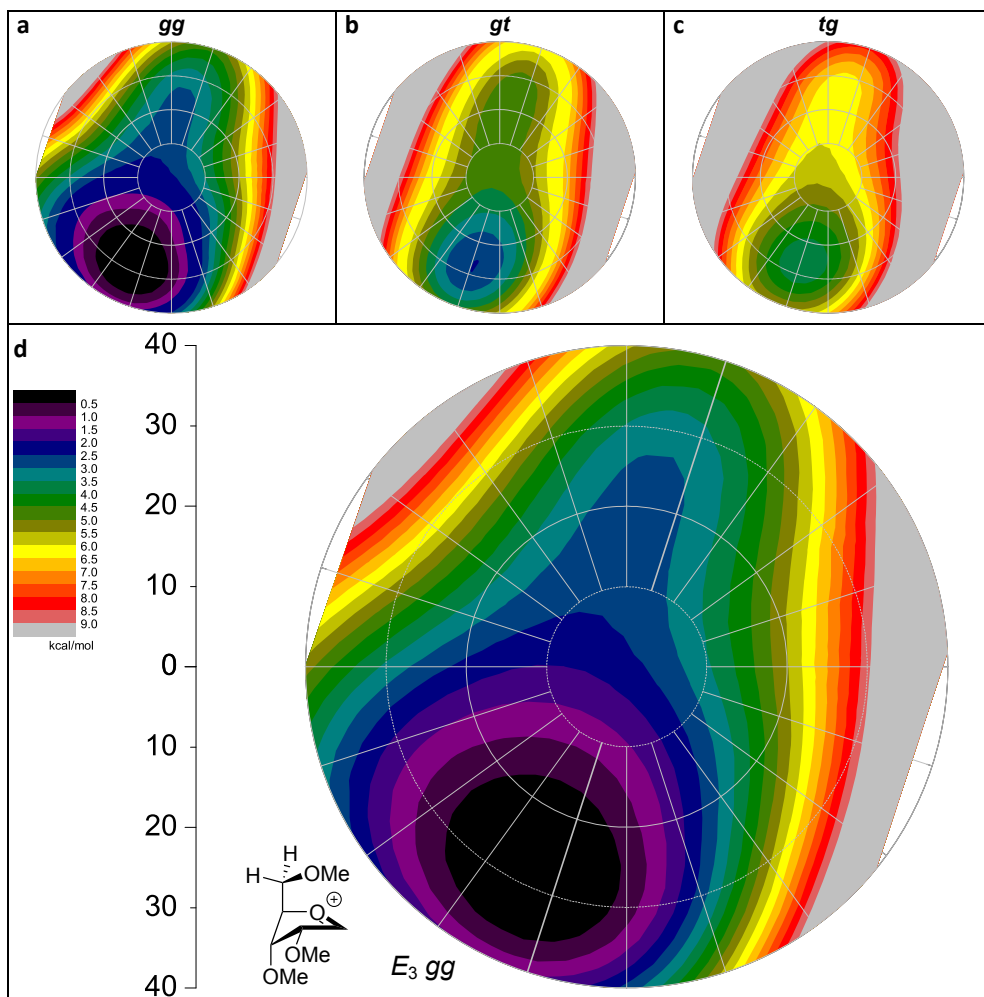


Figure 2.3 The FES maps of ribofuranosyl oxocarbenium ion **19**. a) FES of the *gg* conformer. b) FES of the *gt* conformer. c) FES of the *tg* conformer. d) Global minimal FES of **19** showing the lowest-energy E_3 (*gg*) conformer.

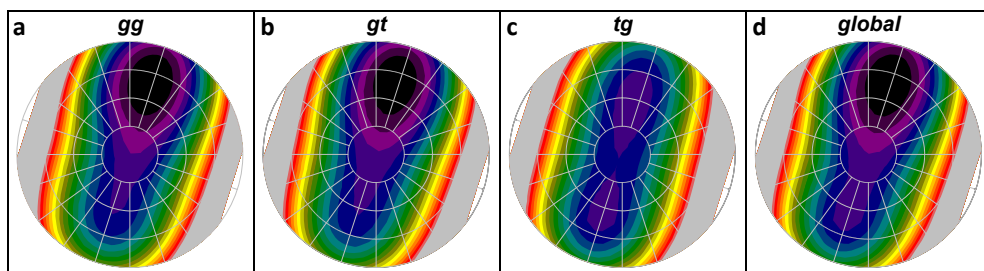


Figure 2.4 The FES maps of ribose configured 2,3-dimethoxy-4-methylenemethoxy cyclopentene. a) FES of the *gg* conformer. b) FES of the *gt* conformer. c) FES of the *tg* conformer. d) Global minimal FES showing the lowest-energy 3E (*gg*) conformer.

With the FES map of **19**, the stereoselectivity in the substitution reaction of [D]TES with **3** can be readily explained. Attack of the nucleophile on the most favorable oxocarbenium ion, that is, the E_3 conformer, on the inside of the envelope explains the selective formation of the 1,2-*cis* product.

The arabinose FES map

The free energy surfaces of arabinofuranosyl oxocarbenium ion **20** are depicted in Figure 2.5, and from these it becomes apparent that this ion is most stable when taking up the 3E conformation. Also in this case the relative stability of the three C5-O5 rotamers decreases going from the *gg* to the *gt* to the *tg* rotamer. Because the C5-OMe group cannot be positioned above the ring in the arabinosyl 3E envelope, this stability trend arises from the different interactions between the C5-OMe dipole with the positive charge of the oxocarbenium ion. This interaction is most favorable for the *gg* C5-OMe, and least favorable for the *tg* conformer, as discussed above (Figure 2.2).²⁶ In addition to the unfavorable dipole-charge interaction of the C5-OMe *tg* conformer, this conformer also suffers from unfavorable steric and electronic interactions of the C5-OMe with the C3 substituent in the 3E envelope. Comparison of the FES maps of the ribofuranosyl and arabinofuranosyl oxocarbenium ions shows not only that the two oxocarbenium ions prefer opposite envelope conformers, but also that the FES of the arabinosyl oxocarbenium ion is more shallow. This outcome indicates that the preference for the arabino 3E envelope is not as strong as the preference for the ribo E_3 envelope, and can be explained by the fact that ribo 3E envelope positions all substituents in an ideal orientation to maximize the stability of the oxocarbenium ion, which is not the case for the arabino 3E envelope. Nonetheless, the preference for the arabino 3E conformer is strong enough to allow a selective substitution reaction as shown by the [D]TES reaction (Table 2.1, entry 2). Only the β -deuterium epimer was isolated in this experiment, the formation of which can be accounted for by inside attack of [D]TES on the 3E oxocarbenium ion.

The map for arabinose configured 2,3-dimethoxy-4-methylenemethoxy cyclopentene in Figure 2.6 shows that this molecule has a stronger preference for the 3E conformer oxocarbenium ion. The all equatorial conformer benefits from placing all substituents in a sterically most favorable position. In the E_3 conformation, the oxocarbenium ion benefits from stereoelectronic stabilization by the pseudoaxial C4, but this effect is absent in the cyclopentene.

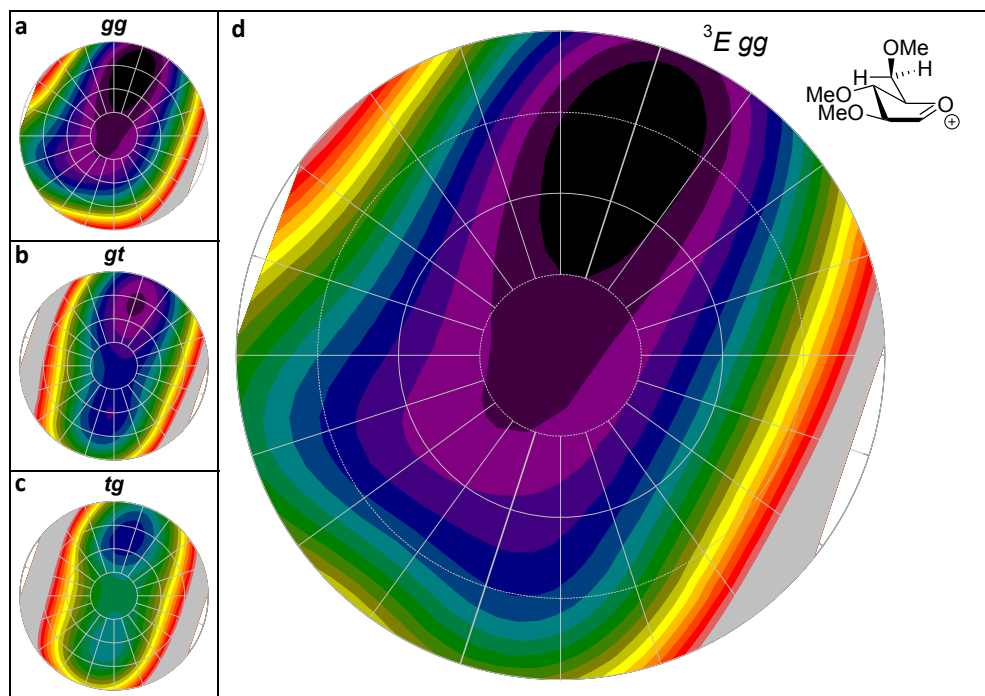


Figure 2.5 The FES maps of arabinofuranosyl oxocarbenium ion **20**. a) FES of the *gg* conformer. b) FES of the *gt* conformer. c) FES of the *tg* conformer. d) Global minimal FES of **20** showing the lowest-energy 3E (*gg*) conformer.

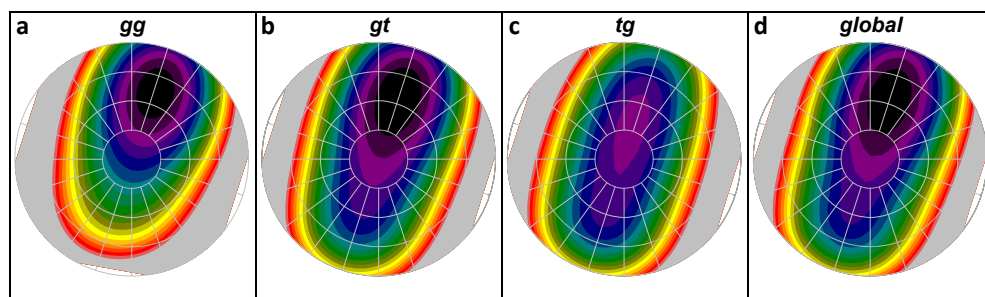


Figure 2.6 The FES maps of arabinose configured 2,3-dimethoxy-4-methylenemethoxy cyclopentene. a) FES of the *gg* conformer. b) FES of the *gt* conformer. c) FES of the *tg* conformer. d) Global minimal FES showing the lowest-energy 3E (*gt*) conformer.

The xylose FES map

The FES maps for the xylofuranosyl oxocarbenium ion **21**, depicted in Figure 2.7, give a different picture than the above described maps of the ribo- and arabino oxocarbenium ions **19** and **20**. Now there are two energy minima, one on the side of the 3E envelope and one on the opposite side, around $P=216^\circ$, thus indicating that a 4T_3 conformer is

energetically most favorable on the southern hemisphere. The two minima have different C4-C5 rotamers which contribute most favorably to the overall oxocarbenium ion energy.

The stability of the 4T_3 *gg* rotamer originates from the stabilizing interaction of the C5-OMe with the underlying oxocarbenium ion. Distortion from the E_3 envelope to the flanking 4T_3 twist structure can be explained by the fact that in these structures there is no stabilizing contribution from the C3-OMe group and in order to maximize stabilization by the C5-OMe group, the furanose ring twists from the E_3 envelope to position this group closer to the oxocarbenium ion. In the 3E envelope, in contrast, the *gg* rotamer suffers from destabilizing steric and dipole interactions with the pseudoaxial C3-OMe. The most stable orientation for the C5-OMe group in the 3E envelope is achieved in the *gt* rotamer, because the *tg* conformer puts the C5-OMe group in an unfavorable antiparallel orientation with respect to the C4-O4 bond (Figure 2.2). The two energy minima found for the xylose furanosyl oxocarbenium ion explain the mixture of products obtained in the [D]TES substitution reaction (Table 2.1, Entry 3), and the 85:15 α/β -ratio fits well with the difference in energy between the two envelope oxocarbenium ions, a difference which the calculations show to be about 1 kcal mol⁻¹.

In Figure 2.8, the FES map for the xylose configured cyclopentene is depicted. The E_3 conformer is the most favored conformer and the *gt* rotamer is favored for both the 3E and E_3 envelopes. This indicates that the electronic stabilization of the oxocarbenium ion in the 4T_3 *gg* rotamer outweighs the steric preference of the C4-substituent.

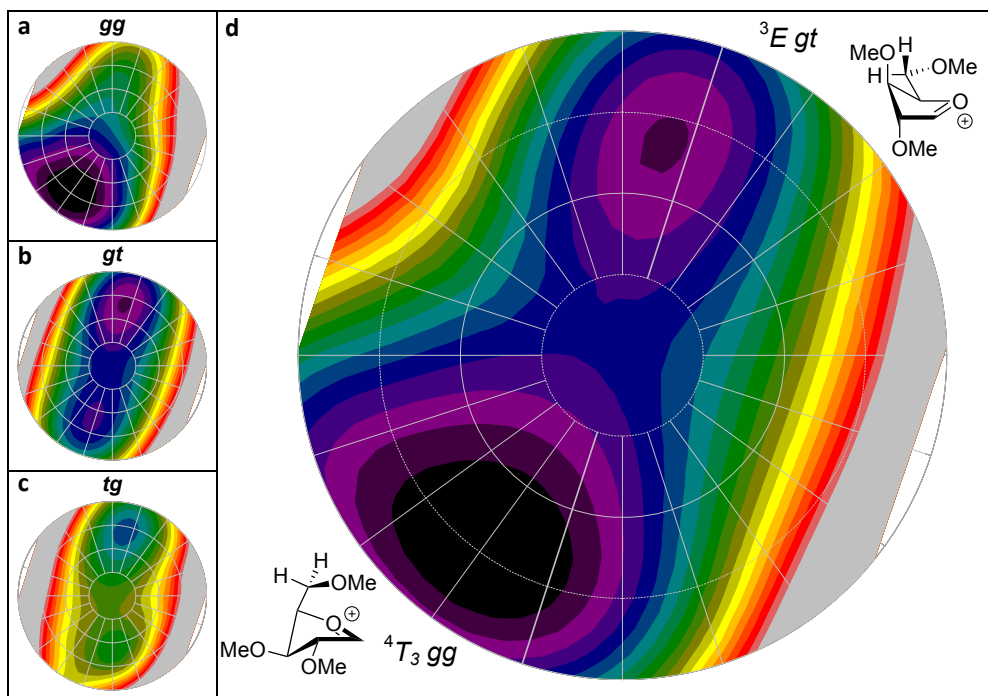


Figure 2.7 The FES maps of xylofuranosyl oxocarbenium ion **21**. a) FES of the *gg* conformer. b) FES of the *gt* conformer. c) FES of the *tg* conformer. d) Global minimal FES of **21** showing the lowest-energy E_3 (*gg*) conformer.

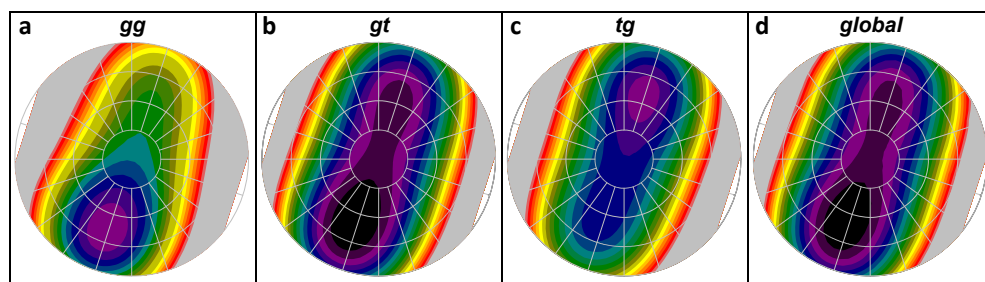


Figure 2.8 The FES maps of xylose configured 2,3-dimethoxy-4-methylenemethoxy cyclopentene. a) FES of the *gg* conformer. b) FES of the *gt* conformer. c) FES of the *tg* conformer. d) Global minimal FES showing the lowest-energy E_3 (*gt*) conformer.

The lyxose FES map

When the lyxofuranosyl acetate **14**, featuring an all-*cis* substituent decoration, is reacted with [D]TES/TMSOTf, the β -deuterium lyxofuranoside **18** is isolated as the sole product (Table 2.1, entry 4). Also in this case the stereoselectivity can be adequately explained by considering the FES of the intermediate oxocarbenium ion **22**, which shows a single, rather deep energy minimum for the 3E conformation (Figure 2.9d). Besides showing the steepest

energy well, the FES of ion **22** also indicates that the ring of the lyxofuranose oxocarbenium ion is the most puckered of the four oxocarbenium ions studied. In the 3E structure, both the C2 and the C3 substituent adopt positions allowing maximum stabilization of the oxocarbenium ion. The C4 group has a pseudoequatorial orientation thereby avoiding steric interactions. In the 3E envelope the C5-OMe group preferentially adopts a *gt* position, because the *gg* rotamer is rather unfavorable due to the destabilizing interaction with the C3-OMe. Inside attack on the 3E envelope oxocarbenium ion leads to the all-*cis* product. When the charge is removed from the lyxose oxocarbenium ion as in the lyxo configured cyclopentene (Figure 2.10), the strong conformer preference disappears.

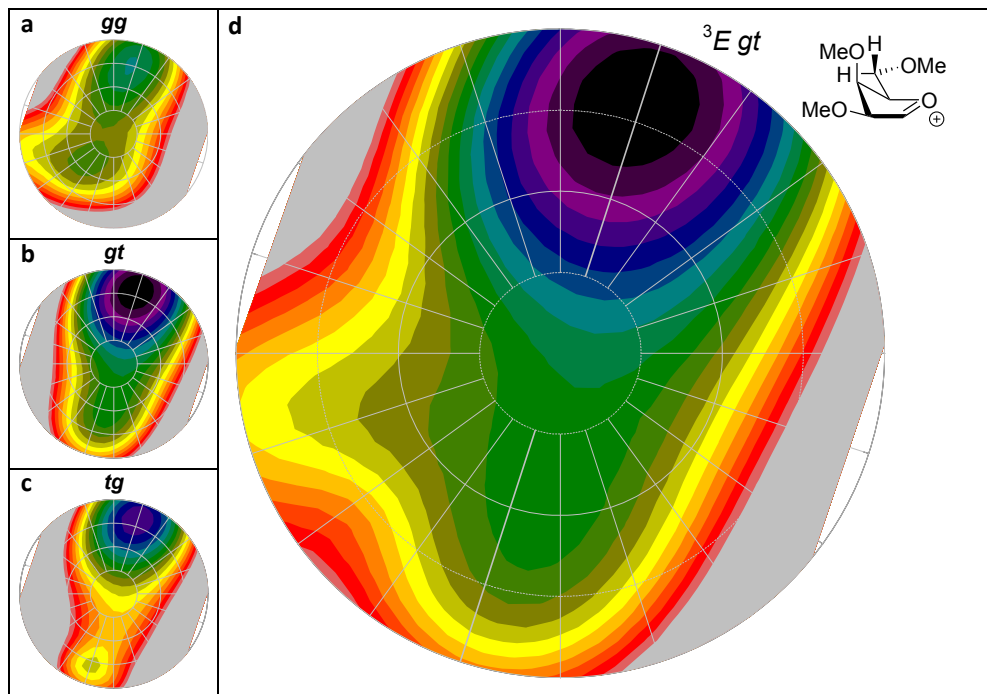


Figure 2.9 The FES maps of lyxofuranosyl oxocarbenium ion **22**. a) FES of the *gg* conformer. b) FES of the *gt* conformer. c) FES of the *tg* conformer. d) Global minimal FES of **22** showing the lowest-energy 3E (*gt*) conformer.

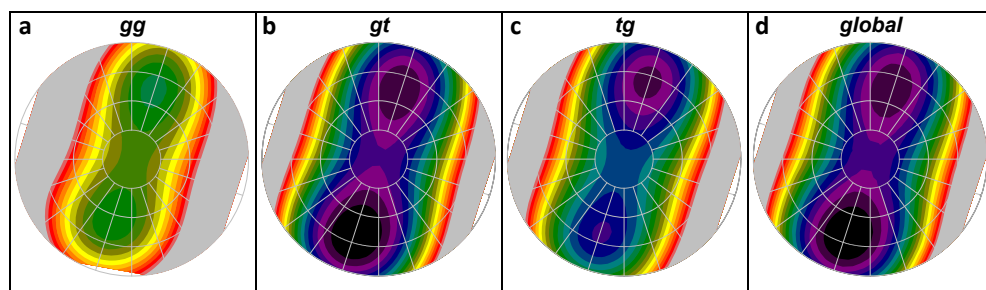


Figure 2.10 The FES maps of lyxose configured 2,3-dimethoxy-4-methylenemethoxy cyclopentene. a) FES of the *gg* conformer. b) FES of the *gt* conformer. c) FES of the *tg* conformer. d) Global minimal FES showing the lowest-energy E_3 (*gt*) conformer.

The obtained results can be summarized to indicate the following ring substituent effects: the stability of the furanosyl oxocarbenium ions benefits from equatorially oriented alkoxy groups at C2, as previously shown by Woerpel and co-workers; a pseudoaxial alkoxy function at C3 leads to a more stable oxocarbenium ion than a C3-alkoxy group in a pseudoequatorial position, corroborating the studies of the Woerpel group and the vast amount of literature data, reporting higher reactivity for glycosides having more axially

oriented substituents^{14,15}; the methylenealkoxy group at C4 significantly adds to the stability of the oxocarbenium ion if steric interactions allow proper positioning. The calculations indicate that the nature of the C4-C5 rotamer is an important factor in determining the stability and that the difference in the ground state energy of the C4-C5 rotamers can be as much as ~ 4 kcal mol⁻¹.

Overall, the calculated FES maps provide a detailed picture of the substituent effects on the stability of furanosyl oxocarbenium ions. Individual stabilizing or destabilizing influences and the interplay between the substituents have become apparent. There is a very good agreement between the calculated lowest-energy furanosyl oxocarbenium ion conformers and the experimental results obtained in the substitution reactions. In a Curtin-Hammett scenario²⁸ the product stereoselectivity solely depends on the relative ground-state energies of the oxocarbenium ions depicted in Figure 2.1, if both conformers react at the same rate. If the more stable conformer reacts more quickly, the product distribution will be even more outspoken, whereas the stereoselectivity erodes (or even inverts) in the case where the more stable conformer reacts slower. During the attack of the nucleophile on the furanosyl ring, interactions will develop between the incoming nucleophile and the furanosyl ring substituents. Rehybridization of the furanosyl ring will alter the mutual interactions of the ring substituents. In the ribose case, a prominent 1,3-diaxial-like interaction will emerge upon inside attack (Figure 2.1) of the nucleophile on the ribosyl E_3 oxocarbenium ion between the nucleophile and the substituent at C3. Where this will be unfavorable from a steric point of view, the lone pairs of O-atom at C3 can help stabilize the development of positive charge on the incoming nucleophile. A similar situation unfolds in the 3E xylo and lyxo case, while inside attack of the nucleophile on the 3E arabino and 4T_3 xylo oxocarbenium ions can occur relatively unhindered. In all, it appears that none of these interactions prevail here as judged from the agreement between the calculated FES maps and the experimental results.²⁹

2.3 Conclusion

The set of substitution experiments, supported by the in-depth quantum mechanical calculations, show that all furanosyl oxocarbenium ions intrinsically react in a 1,2-*cis*-selective manner. These results in turn imply that stereoselective *cis*-glycosylation reactions can be effected if they are persuaded to proceed via the furanosyl oxocarbenium ion as the product-forming intermediate. In combination with glycosylation methodology relying on anchimeric assistance by a suitable neighboring group at the C2 hydroxy, which allows for the reliable installation of 1,2-*trans*-furanosidic linkages, the stereoselective construction of all furanosidic linkages is in theory feasible. It should be noted that given the differences between the nucleophile used in this study and O

nucleophiles, such as typical glycosyl acceptors, transposition of the reaction pathway described here to an *O*-glycosylation event will not be trivial.²⁷ The detailed furanosyl oxocarbenium ion energy maps presented here will also be useful for gaining insight into the reaction mechanisms by which furanose-processing enzymes, such as glycosyl hydrolases and transferases, operate and the FES maps will be valuable in the analysis of conformational itineraries used by furanosyl-processing enzymes.³⁰ This analysis in turn can guide inhibitor design and understanding of inhibitor structure-activity relationships.³¹

Supplementary data

FES maps of mono and di-substituted tetrahydrofuran oxocarbenium ions and the anomeric triflates can be found in the Appendix. The maps of the mono- and di-substituted tetrahydrofuran oxocarbenium ions provide information on the stereoelectronic and steric effects of the individual substituents.

Experimental section

Calculations. In all calculations, methyl ethers were used because of their reduced calculation time over benzyl ethers. All calculations were performed with DFT *ab initio* calculations with the B3LYP model. The starting conformer for the Free Energy Surface (FES) was optimized by starting from a conformer distribution search option included in the Spartan 04³² program in gas phase at 6-31G* as basis set. All generated geometries were optimized with Gaussian 03²³ at 6-311G**, their zero-point energy (ZPE) corrections calculated, and further optimized with incorporated polarizable continuum model (PCM) to correct for solvation in dichloromethane. The geometry with the lowest, ZPE corrected, solvated free energy was selected as the starting point for the FES. Two dihedral angles of the five-membered ring were constrained, namely C4-O4-C1-C2 (τ_0, θ_3) and C1-C2-C3-C4 (τ_2, θ_0), with angles from -40° up to 40° over 9 steps (10° per step) giving a total of 81 conformers and dictating the entire pseudo rotational space within a maximum amplitude (τ_m) of 40° . All other internal coordinates were unconstrained. The geometries were optimized, their ZPE calculated and corrected for solvation with Gaussian 03 at 6-311G**. The FES was visualized as polar contour plot through the Origin 8.5 graphing software by putting the phase angle (P) as θ , the amplitude (τ_m) at r and the energy, corrected for ZPE and optimized in solvent, at the Z-axis. The starting conformer was modified by rotating the O4-C4-C5-O5 dihedral to each of the three staggered conformations (*gauche-gauche* = -65° , *gauche-trans* = 65° , *trans-gauche* = 175°) and then generating the FES through the above mentioned method generating a total of 243 optimized geometries. These three FES maps were graphed individually and in a combined plot by comparing the corrected free energies, and for each point selecting the geometry of lowest energy from the three entities. The geometries of the anomeric triflates were calculated using the same method as applied for finding the starting point of the FES, but using 6-31G* instead of 6-311G** in Gaussian 03 for geometry optimization followed by a single point energy calculation at 6-311G**.

Synthesis

General. All reagents were of commercial grade and used as received. All moisture sensitive reactions were performed under an argon atmosphere. DCM used in the [D]TES reaction was distilled over P_2O_5 and stored on activated 4Å molecular sieves before use. Reactions were performed at room temperature unless stated otherwise and were monitored by TLC analysis with detection by UV (254 nm) and where applicable by spraying

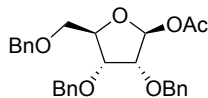
with 20% sulfuric acid in EtOH or with a solution of $(\text{NH}_4)_6\text{Mo}_7\text{O}_{24}\cdot 4\text{H}_2\text{O}$ (25 g/l) and $(\text{NH}_4)_4\text{Ce}(\text{SO}_4)_4\cdot 2\text{H}_2\text{O}$ (10 g/l) in 10% sulfuric acid (aq.) followed by charring at $\sim 150^\circ\text{C}$. Flash column chromatography was performed on silica gel (40–63 μm). ^1H and ^{13}C spectra were recorded on a Bruker AV 400 in CDCl_3 or CD_3OD . Chemical shifts (δ) are given in ppm relative to tetramethylsilane as internal standard (^1H NMR in CDCl_3) or the residual signal of the deuterated solvent. Coupling constants (J) are given in Hz. All ^{13}C spectra are proton decoupled. NMR peak assignments were made using COSY and HSQC experiments. Where applicable NOESY, HMBC and HSQC-HECADE³³ experiments were used to further elucidate the structure. The anomeric product ratios were analysed through integration of proton NMR signals.

2,3,5-Tri-*O*-benzyl-1-*O*-methyl-D-ribofuranose (1). D-Ribose (25 g, 167 mmol) was dissolved in a mixture of acetyl chloride (3.6 ml, 50 mmol) and MeOH (600 ml) and stirred overnight. The reaction mixture was quenched by adjusting the pH to neutral by addition of NaHCO_3 (s, 70 g), the solid was filtered off and the filtrate concentrated under reduced pressure. The crude product was coevaporated twice with toluene before being dissolved in DMF (850 ml). Benzyl bromide (83 ml, 700 mmol) and tetrabutyl ammonium iodide (0.6 g, 1.7 mmol) were added and the mixture was cooled to 0°C . Sodium hydride (28 g, 700 mmol, 60% in mineral oil) was added and the mixture slowly allowed to warm to room temperature where it was stirred overnight. The reaction mixture was concentrated under reduced pressure before being dissolved in Et_2O and subsequently washed with 1M HCl (aq.). The combined aqueous layers were extracted with Et_2O and the organic layers combined before being washed with NaHCO_3 (sat. aq.) and brine. The organic layer was dried over anhydrous MgSO_4 , filtered and concentrated under reduced pressure. The product was purified by flash chromatography (7–19% Et_2O /pentane) yielding an anomeric mixture ($\alpha:\beta$; 1:10) of the title compound (48 g, 111 mmol, 66 % yield). $R_f = 0.30$ (10/90 EtOAc/pentane). β -Anomer: ^1H NMR (400 MHz, CDCl_3) δ 7.39 – 7.23 (m, 15H, CH_{Ar} Bn), 4.92 (s, 1H, C-1), 4.66 (d, $J = 12.1$ Hz, 1H, CHH Bn), 4.61 (d, $J = 11.8$ Hz, 1H, CHH Bn), 4.57 – 4.51 (m, 3H, 3x CHH Bn), 4.44 (d, $J = 11.9$ Hz, 1H, CHH Bn), 4.38 – 4.31 (m, 1H, C-4), 4.02 (dd, $J = 7.0, 4.7$ Hz, 1H, C-3), 3.84 (d, $J = 4.7$ Hz, 1H, C-2), 3.61 (dd, $J = 10.6, 3.7$ Hz, 1H, C-5a), 3.51 (dd, $J = 10.5, 5.7$ Hz, 1H, C-5b), 3.31 (s, 3H, OCH_3). ^{13}C NMR (101 MHz, CDCl_3) δ 138.4, 137.9, 137.9 (C_q Bn), 128.5, 128.4, 128.4, 128.0, 128.0, 127.9, 127.9, 127.7, 127.6 (CH_{Ar} Bn), 106.4 (C-1), 80.5 (C-4), 79.8 (C-2), 78.5 (C-3), 73.2, 72.5, 72.4 (3x CH_2 Bn), 71.4 (C-5), 55.2 (OCH_3). IR (neat): 602, 694, 733, 779, 820, 853, 970, 945, 1026, 1065, 1103, 1206, 1258, 1312, 1360, 1452, 1497, 2862, 2911. HR-MS: $[\text{M}+\text{H}^+]$ Calculated for $\text{C}_{27}\text{H}_{30}\text{O}_5$: 435.21660; found: 435.21686. Analysis data matches literature data.³⁴

2,3,5-Tri-*O*-benzyl-D-ribofuranose (2). 2,3,5-Tri-*O*-benzyl-1-*O*-methyl-D-ribofuranose (1, 42 g, 97 mmol) was dissolved in a mixture of acetic acid (500 ml) and water (125 ml) and refluxed (110°C) overnight. The reaction was allowed to cool down to room temperature before being neutralized with 6M NaOH (aq.) and extracted with EtOAc (3x). The organic layers were combined and washed with NaHCO_3 (sat. aq.) and brine, dried over anhydrous MgSO_4 , filtered and concentrated under reduced pressure. The residue was purified by flash chromatography (27.5%–70% Et_2O /pentane) yielding an anomeric mixture ($\alpha:\beta$; 3:2) of the title compound (35 g, 84 mmol, 86 % yield). $R_f = 0.55$ (25/75 EtOAc/toluene). α -Anomer: ^1H NMR (400 MHz, CDCl_3) δ 7.40 – 7.18 (m, 15H, CH_{Ar} Bn), 5.34 – 5.29 (m, 1H, C-1), 4.72 – 4.38 (m, 6H, 6x CHH Bn), 4.38 – 4.34 (m, 1H, C-4), 4.00 – 3.93 (m, 2H, C-2, C-3), 3.51 – 3.43 (m, 2H, C-5). ^{13}C NMR (101 MHz, CDCl_3) δ 137.9, 137.5, 137.5 (C_q Bn), 128.6, 128.6, 128.5, 128.5, 128.1, 128.0, 128.0, 128.0, 127.9, 127.9, 127.9, 127.8, 127.6 (CH_{Ar} Bn), 96.3 (C-1), 81.1 (C-4), 77.8, 77.7 (C-2, C-3), 73.6, 72.9, 72.5 (3x CH_2 Bn), 70.1 (C-5). β -Anomer: ^1H NMR (400 MHz, CDCl_3) δ 7.39 – 7.20 (m, 15H, CH_{Ar} Bn), 5.31 (s, 1H, C-1), 4.72 – 4.38 (m, 6H, 6x CHH Bn), 4.33 – 4.28 (m, 1H, C-4), 4.20 (dd, $J = 6.8, 4.7$ Hz, 1H, C-3), 3.84 (d, $J = 4.6$ Hz, 1H, C-2), 3.65 (dd, $J = 10.4, 2.9$ Hz, 1H, C-5a), 3.46 – 3.40 (m, 1H, C-5b). ^{13}C NMR (101 MHz, CDCl_3) δ 137.9, 137.8, 137.4 (C_q Bn), 128.6, 128.6, 128.5, 128.5, 128.1, 128.0, 128.0, 128.0, 128.0, 127.9, 127.9, 127.9, 127.8, 127.6 (CH_{Ar} Bn), 100.4 (C-1), 80.8, 80.8 (C-2, C-4), 77.3 (C-3), 73.5, 72.5, 72.3 (3x CH_2 Bn), 69.7 (C-5). IR (neat): 604, 654, 694, 733, 820, 851, 910, 943, 1024, 1074, 1207, 1256, 1314, 1329, 1362, 1398, 1454, 1497,

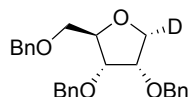
2864, 2922, 3418. HR-MS: $[M+Na]^+$ Calculated for $C_{26}H_{28}O_5$: 443.18290; found: 443.18225. Analysis data matches literature data.³⁴

2,3,5-Tri-O-benzyl-1- β -O-acetyl-D-ribofuranose (3). 2,3,5-Tri-O-benzyl-D-ribofuranose (**2**, 3.5 g, 8.3 mmol) was dissolved in pyridine (13 ml) and added to cooled (0 °C) acetic anhydride (8.6 ml, 92 mmol). The reaction was allowed to continue to stir at room temperature for 4 hours and quenched by pouring it into 1M HCl (aq.) before being diluted with EtOAc. The layers were separated and the organic layer washed with 1M HCl (aq.), $NaHCO_3$ (sat.



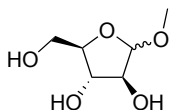
aq.) and brine, dried over anhydrous $MgSO_4$, filtered and concentrated under reduced pressure. The residue was purified by flash chromatography (10-15% EtOAc/pentane) yielding the title compound (3.5 g, 7.6 mmol, 91 % yield). $R_f = 0.75$ (20/80 EtOAc/pentane). 1H NMR (400 MHz, $CDCl_3$) δ 7.41 – 7.25 (m, 15H, CH_{Ar} Bn), 6.20 (s, 1H, C-1), 4.76 (d, $J = 12.1$ Hz, 1H, CHH Bn-2), 4.62 (d, $J = 12.1$ Hz, 1H, CHH Bn-2), 4.58 (d, $J = 12.0$ Hz, 1H, CHH Bn-5), 4.54 (d, $J = 12.0$ Hz, 1H, CHH Bn-3), 4.50 (d, $J = 12.1$ Hz, 1H, CHH Bn-5), 4.42 (d, $J = 11.8$ Hz, 1H, CHH Bn-3), 4.37 (ddd, $J = 7.6, 4.4, 3.1$ Hz, 1H, C-4), 4.14 (dd, $J = 7.8, 4.6$ Hz, 1H, C-3), 3.92 (d, $J = 4.5$ Hz, 1H, C-2), 3.70 (dd, $J = 11.0, 3.1$ Hz, 1H, C-5a), 3.58 (dd, $J = 11.1, 4.4$ Hz, 1H, C-5b), 1.93 (s, 3H, CH_3). ^{13}C NMR (101 MHz, $CDCl_3$) δ 169.9 (C=O), 138.4, 137.7, 137.5 (C_q Bn), 128.5, 128.5, 128.4, 128.2, 128.1, 128.0, 127.9, 127.6, 127.5 (CH_{Ar} Bn), 99.1 (C-1), 81.6 (C-4), 78.8 (C-2), 76.9 (C-3), 73.3 (CH_2 Bn-5), 72.5 (CH_2 Bn-3), 72.2 (CH_2 Bn-2), 69.7 (C-5), 21.3 (CH_3). $[\alpha]_D^{20} = 54^\circ$ (c = 1, $CHCl_3$). IR (neat): 602, 650, 694, 733, 781, 820, 854, 945, 1011, 1043, 1092, 1125, 1217, 1310, 1369, 1454, 1497, 1744, 2864, 2926. HR-MS: $[M+Na]^+$ Calculated for $C_{28}H_{30}O_6$: 485.19346; found: 485.19283. Analysis data is in line with literature data.³⁵

2,3,5-Tri-O-benzyl-1-deoxy-1- α -deutero-D-ribofuranose (15). 2,3,5-Tri-O-benzyl-1- β -O-acetyl-D-ribofuranose (**3**, 93 mg, 0.20 mmol) was coevaporated with toluene (3x), dissolved in DCM (2.7 ml) and cooled to -78 °C. [D]Triethylsilane (64 μ l, 0.4 mmol) was added before slowly adding a solution of trimethylsilyl trifluoromethanesulfonate (47 μ l, 0.26 mmol) in DCM (300 μ l) and the reaction stirred at -78 °C for 3 days. The reaction was quenched by addition of



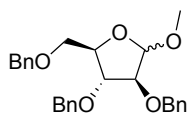
NaH_2PO_4 (sat. aq., 5 ml) and then allowed to warm to room temperature. The suspension was extracted with EtOAc and the combined organic layers washed with $NaHCO_3$ (sat. aq.) and brine, dried over anhydrous $MgSO_4$, filtered and concentrated under reduced pressure. The residue was dissolved in a mixture of sodium methoxide (0.04 mmol) in MeOH (4 ml) and stirred for 5 hours. The reaction was quenched with acetic acid (4 μ l in 400 μ l MeOH) and concentrated. The residue was taken up in EtOAc, washed with $NaHCO_3$ (sat. aq.) and brine, dried over anhydrous $MgSO_4$, filtered and concentrated under reduced pressure. The residue was purified by flash chromatography (3-5% EtOAc/toluene) yielding the title compound (40 mg, 0.10 mmol, 50% yield) as a single diastereomeric product. $R_f = 0.40$ (8/92 EtOAc/toluene). 1H NMR (400 MHz, $CDCl_3$) δ 7.40 – 7.25 (m, 15H, CH_{Ar} Bn), 4.63 (d, $J = 11.9$ Hz, 1H, CHH Bn-2), 4.61 (d, $J = 12.1$ Hz, 1H, CHH Bn-2), 4.58 (d, $J = 12.1$ Hz, 1H, CHH Bn-2), 4.56 (d, $J = 12.2$ Hz, 1H, CHH Bn-5), 4.50 (d, $J = 12.0$ Hz, 1H, CHH Bn-3), 4.49 (d, $J = 12.1$ Hz, 1H, CHH Bn-5), 4.16 (ddd, $J = 6.5, 4.3, 3.3$ Hz, 1H, C-4), 4.02 (t, $J = 4.9$ Hz, 1H, C-2), 3.97 (d, $J = 4.8$ Hz, 1H, C-1), 3.93 (dd, $J = 6.4, 5.0$ Hz, 1H, C-3), 3.62 (dd, $J = 10.7, 3.3$ Hz, 1H, C-5a), 3.51 (dd, $J = 10.7, 4.3$ Hz, 1H, C-5b). ^{13}C NMR (101 MHz, $CDCl_3$) δ 138.3, 138.1, 138.0 (C_q Bn), 128.5, 128.5, 128.5, 128.1, 128.0, 127.9, 127.9, 127.8, 127.7 (CH_{Ar} Bn), 80.5 (C-4), 78.4 (C-3), 76.5 (C-2), 73.5 (CH_2 Bn-5), 72.3 (CH_2 Bn-3), 71.9 (CH_2 Bn-2), 70.4 (t, $J = 23$ Hz, C-1), 70.1 (C-5). $[\alpha]_D^{20} = 52^\circ$ (c = 0.7, $CHCl_3$). IR (neat): 602, 696, 737, 1003, 1026, 1053, 1088, 1130, 1206, 1273, 1312, 1339, 1362, 1454, 1497, 1717, 2860, 2920. HR-MS: $[M+H]^+$ Calculated for $C_{26}H_{27}DO_4$: 406.21231; found: 406.21235.

Methyl-D-arabinofuranose (23). D-Arabinose (30 g, 200 mmol) was dissolved in MeOH (700 ml), acetyl chloride (4.3 ml, 60 mmol) was added and the reaction stirred overnight. The reaction mixture was quenched by adjusting the pH to neutral by addition of $NaHCO_3$ (s), the solid was filtered off and the filtrate concentrated under reduced pressure. The residue was coevaporated with toluene before being purified by flash chromatography (75% EtOAc/Pentane - 20%



MeOH/EtOAc) yielding an anomeric mixture (α : β ; 2:1) of the title compound (35 g, 195 mmol, 98% yield). R_f = 0.65 (2/8 MeOH/DCM). α -Anomer: $^1\text{H NMR}$ (400 MHz, MeOD) δ 4.73 (d, J = 1.6 Hz, 1H, C-1), 3.96 – 3.85 (m, 2H, C-2, C-4), 3.84 – 3.78 (m, 1H, C-3), 3.75 – 3.69 (m, 1H, C-5a), 3.62 (dd, J = 11.9, 5.4 Hz, 1H, C-5b), 3.34 (s, 3H, OCH_3). $^{13}\text{C NMR}$ (101 MHz, MeOD) δ 110.5 (C-1), 85.5 (C-4), 83.4 (C-2), 78.7 (C-3), 63.0 (C-5), 55.2 (OCH_3). β -Anomer: $^1\text{H NMR}$ (400 MHz, MeOD) δ 4.74 (d, J = 4.4 Hz, 1H, C-1), 3.98 – 3.87 (m, 2H, C-2, C-3), 3.80 – 3.74 (m, 1H, C-4), 3.68 (dd, J = 11.6, 3.7 Hz, 1H, C-5a), 3.55 (dd, J = 11.7, 7.1 Hz, 1H, C-5b), 3.41 (s, 3H, OCH_3). $^{13}\text{C NMR}$ (101 MHz, MeOD) δ 104.0 (C-1), 84.4 (C-4), 79.0 (C-2), 76.8 (C-3), 65.5 (C-5), 55.5 (OCH_3). IR (neat): 882, 942, 990, 1002, 1021, 1093, 1191, 1314, 1366, 1415, 1451, 2836, 2923, 3351. HR-MS: $[\text{M}+\text{H}^+]$ Calculated for $\text{C}_6\text{H}_{12}\text{O}_5$: 165.07575; found: 165.07553. Spectroscopic data was identical to literature data.³⁶

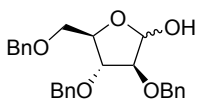
2,3,5-Tri-*O*-benzyl-1-*O*-methyl-*D*-arabinofuranose (4). Methyl-*D*-arabinofuranose (**23**, 33 g, 200 mmol) was



coevaporated twice with toluene before being dissolved in DMF (1 l) and cooled to 0 °C. Benzyl bromide (86 ml, 720 mmol), a catalytic amount of tetrabutyl ammonium iodide (0.7 g, 2 mmol) and sodium hydride (28.8 g, 720 mmol, 60% in mineral oil) were added. The reaction mixture was then allowed to gradually warm to room temperature while

stirring and the reaction continued overnight. The reaction mixture was concentrated under reduced pressure before being taken up in EtOAc/1M HCl (aq.). The layers were separated and the organic layer washed with 1M HCl (aq.). The aqueous layers were combined and extracted with EtOAc. The organic layers were combined and washed with NaHCO_3 (sat. aq.) and brine. The solution was dried over anhydrous MgSO_4 , filtered and concentrated under reduced pressure. The residue was purified by flash chromatography (1-12% Et₂O/pentane) yielding an anomeric mixture (α : β ; 3:1) of the title compound (59 g, 135 mmol, 68 % yield). R_f = 0.30 and 0.45 (10/90 EtOAc/pentane). α -Anomer: $^1\text{H NMR}$ (400 MHz, CDCl_3) δ 7.38 – 7.21 (m, 15H, CH_{Ar} Bn), 4.96 (s, 1H, C-1), 4.59 – 4.50 (m, 4H, 4x CHH Bn), 4.48 (d, J = 12.5 Hz, 1H, CHH Bn), 4.45 (d, J = 12.0 Hz, 1H, CHH Bn), 4.25 – 4.18 (m, 1H, C-4), 3.99 (dd, J = 3.0, 1.1 Hz, 1H, C-2), 3.90 (dd, J = 6.4, 2.8 Hz, 1H, C-3), 3.62 (dd, J = 10.1, 3.5 Hz, 1H, C-5a), 3.58 (dd, J = 10.0, 4.6 Hz, 1H, C-5b), 3.39 (s, 3H, OCH_3). $^{13}\text{C NMR}$ (101 MHz, CDCl_3) δ 138.1, 137.8, 137.5 (3x C_q Bn), 128.5, 128.5, 128.4, 128.4, 128.2, 127.9, 127.9, 127.8, 127.8, 127.7, 127.7 (CH_{Ar} Bn), 107.3 (C-1), 88.1 (C-2), 83.4 (C-3), 81.0 (C-4), 73.4, 72.2, 71.9 (3x CH_2 Bn), 69.8 (C-5), 55.0 (OCH_3). β -Anomer: $^1\text{H NMR}$ (400 MHz, CDCl_3) δ 7.39 – 7.21 (m, 15H, CH_{Ar} Bn), 4.72 (d, J = 4.0 Hz, 1H, C-1), 4.66 – 4.60 (m, 4H, 4x CHH Bn), 4.59 – 4.50 (m, 2H, 2x CHH Bn), 4.16 – 4.03 (m, 3H, C-2, C-3, C-4), 3.57 – 3.52 (m, 1H, C-5a), 3.53 – 3.48 (m, 1H, C-5b), 3.31 (s, 3H, OCH_3). $^{13}\text{C NMR}$ (101 MHz, CDCl_3) δ 138.1, 137.8, 137.6 (3x C_q Bn), 128.5, 128.5, 128.4, 128.4, 128.2, 128.0, 127.9, 127.9, 127.8, 127.8, 127.7, 127.7 (CH_{Ar} Bn), 101.7 (C-1), 84.2 (C-2), 83.3 (C-3), 80.4 (C-4), 73.4, 72.6, 72.6 (3x CH_2 Bn), 72.3 (C-5), 55.0 (OCH_3). IR (neat): 611, 667, 695, 733, 908, 943, 1027, 1047, 1098, 1192, 1207, 1313, 1363, 1453, 1496, 2862, 2906. HR-MS: $[\text{M}+\text{H}^+]$ Calculated for $\text{C}_{27}\text{H}_{30}\text{O}_5$: 435.21660; found: 435.21656. Analytical data matches literature data.³⁷

2,3,5-Tri-*O*-benzyl-*D*-arabinofuranose (5). 2,3,5-Tri-*O*-benzyl-1-*O*-methyl-*D*-arabinofuranose (**4**, 31 g, 70 mmol)

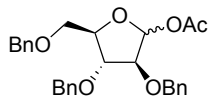


was dissolved in a mixture of acetic acid (360 ml) and water (90 ml). The mixture was refluxed (110 °C) for 3 days. The reaction was quenched by neutralizing the acid with 6M NaOH (aq.) and the aqueous layer extracted thrice with EtOAc. The organic layers were combined and washed with brine, dried over anhydrous MgSO_4 , filtered and

concentrated under reduced pressure. The residue was purified by flash chromatography (10-30% EtOAc/pentane) yielding an anomeric mixture (α : β ; 5:4) of the title compound (21 g, 51 mmol, 72 % yield). R_f = 0.60 (25/75 EtOAc/pentane). α -Anomer: $^1\text{H NMR}$ (400 MHz, CDCl_3) δ 7.38 – 7.24 (m, 15H, CH_{Ar} Bn), 5.39 (d, J = 5.3 Hz, 1H, C-1), 4.67 – 4.42 (m, 7H, 6x CHH Bn, C-4), 3.99 – 3.90 (m, 2H, C-2, C-3), 3.59 (dd, J = 10.0, 5.9 Hz, 1H, C-5a), 3.56 – 3.51 (m, 1H, C-5b), 3.41 (d, J = 7.0 Hz, 1H, OH). $^{13}\text{C NMR}$ (101 MHz, CDCl_3) δ 138.1, 137.4, 137.4 (C_q Bn), 128.6, 128.6, 128.5, 128.5, 128.1, 128.0, 128.0, 127.9, 127.9, 127.9, 127.8, 127.8 (CH_{Ar} Bn), 101.2 (C-1), 86.6 (C-2), 82.8 (C-3), 82.0 (C-4), 73.4, 72.1, 71.8 (3x CH_2 Bn), 70.2 (C-5). β -Anomer: $^1\text{H NMR}$ (400 MHz, CDCl_3) δ 7.38 – 7.24 (m, 15H, CH_{Ar} Bn), 5.32 (dd, J = 9.7, 4.3 Hz, 1H, C-1), 4.65 (d, J = 11.6 Hz, 1H, CHH Bn), 4.62 – 4.42

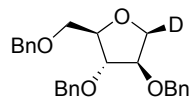
(m, 5H, 5xCHH Bn), 4.16 (t, $J = 4.7$ Hz, 1H, C-3), 4.11 – 4.07 (m, 1H, C-4), 4.01 (t, $J = 4.6$ Hz, 1H, C-2), 3.98 – 3.94 (m, 1H, OH), 3.58 – 3.53 (m, 1H, C-5a), 3.50 (dd, $J = 10.1$, 3.9 Hz, 1H, C-5b). ^{13}C NMR (101 MHz, CDCl_3) δ 137.9, 137.5, 137.4 (C_q Bn), 128.6, 128.6, 128.5, 128.5, 128.1, 128.0, 128.0, 128.0, 127.9, 127.9, 127.9, 127.8, 127.8 (CH_{Ar} Bn), 96.3 (C-1), 84.1 (C-2), 81.9 (C-3), 80.6 (C-4), 73.6, 72.3, 72.1 ($3\times\text{CH}_2$ Bn), 70.6 (C-5). IR (neat): 608, 618, 638, 694, 730, 741, 753, 778, 823, 834, 852, 914, 976, 998, 1021, 1030, 1053, 1081, 1095, 1115, 1140, 1157, 1205, 1216, 1309, 1351, 1366, 1374, 1452, 1452, 1497, 2873, 3030, 3392. HR-MS: $[\text{M}+\text{Na}^+]$ Calculated for $\text{C}_{26}\text{H}_{28}\text{O}_5$: 443.18290; found: 443.18209.

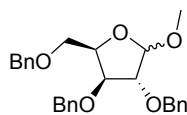
2,3,5-Tri-*O*-benzyl-1-*O*-acetyl-*D*-arabinofuranose (6). 2,3,5-Tri-*O*-benzyl-*D*-arabinofuranose (**5**, 3.2 g, 7.6 mmol) in pyridine (11.5 ml) was added to cooled (0 °C) acetic anhydride (8.0 ml, 85 mmol) and stirred at room temperature for 3 hours. The reaction mixture was poured into 1M HCl (aq.) and diluted with EtOAc, the layers separated and the organic layer washed with 1M HCl (aq.), NaHCO_3 (sat. aq.) and brine. The solution was dried over anhydrous



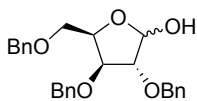
MgSO_4 , filtered and concentrated under reduced pressure. The residue was purified by flash chromatography (10–20% EtOAc/pentane) yielding an anomeric mixture (α : β ; 2:1) of the title compound (3.3 g, 7.1 mmol, 94 % yield). $R_f = 0.8$ (20/80 EtOAc/pentane). α -Anomer: ^1H NMR (400 MHz, CDCl_3) δ 7.39 – 7.21 (m, 15H, CH_{Ar} Bn), 6.25 (s, 1H, C-1), 4.65 – 4.47 (m, 6H, 6xCHH Bn), 4.36 (q, $J = 5.3$ Hz, 1H, C-4), 4.07 (d, $J = 2.2$ Hz, 1H, C-2), 3.98 (dd, $J = 5.7$, 2.2 Hz, 1H, C-3), 3.61 (d, $J = 5.1$ Hz, 2H, C-5), 2.06 (s, 3H, CH_3). ^{13}C NMR (101 MHz, CDCl_3) δ 170.0 (C=O), 138.0, 137.7, 137.3 ($3\times\text{C}_q$ Bn), 128.6, 128.5, 128.5, 128.4, 128.4, 128.0, 128.0, 127.9, 127.8, 127.8, 127.8, 127.7 (CH_{Ar} Bn), 100.6 (C-1), 87.1 (C-2), 83.8 (C-2), 83.4 (C-4), 73.5, 72.2, 72.1 ($3\times\text{CH}_2$ Bn), 69.7 (C-5), 21.3 (CH_3). β -Anomer: ^1H NMR (400 MHz, CDCl_3) δ 7.38 – 7.22 (m, 15H, CH_{Ar} Bn), 6.28 (d, $J = 4.0$ Hz, 1H, C-1), 4.68 (d, $J = 11.8$ Hz, 1H, CHH Bn), 4.65 – 4.47 (m, 5H, 5xCHH Bn), 4.22 – 4.13 (m, 3H, C-2, C-3, C-4), 3.59 – 3.54 (m, 2H, C-5), 1.97 (s, 3H, CH_3). ^{13}C NMR (101 MHz, CDCl_3) δ 170.0 (C=O), 138.1, 137.7, 137.4 ($3\times\text{C}_q$ Bn), 128.6, 128.5, 128.5, 128.4, 128.4, 128.1, 128.0, 128.0, 127.9, 127.8, 127.8, 127.8, 127.7 (CH_{Ar} Bn), 94.4 (C-1), 83.8 (C-4), 81.7, 81.3 (C-2, C-3), 73.3, 73.2, 72.6 ($3\times\text{CH}_2$ Bn), 71.2 (C-5), 21.3 (CH_3). IR (neat): 603, 695, 734, 886, 910, 940, 1006, 1027, 1047, 1090, 1227, 1364, 1454, 1734, 1748, 2865, 2926, 3031. HR-MS: $[\text{M}+\text{Na}^+]$ Calculated for $\text{C}_{28}\text{H}_{30}\text{O}_6$: 485.19346; found: 485.19274.

2,3,5-Tri-*O*-benzyl-1-deoxy-1- β -deutero-*D*-arabinofuranose (16). 2,3,5-Tri-*O*-benzyl-1-*O*-acetyl-*D*-arabinofuranose (**6**, 93 mg, 0.20 mmol) was coevaporated with toluene (3x), dissolved in DCM (2.7 ml) and cooled to -78 °C. $[\text{D}]$ Triethylsilane (64 μl , 0.4 mmol) was added before slowly adding a solution of trimethylsilyl trifluoromethanesulfonate (47 μl , 0.26 mmol) in DCM (300 μl) and the reaction stirred at -78 °C for 1 week. The reaction was quenched by addition of NaHCO_3 (sat. aq., 5 ml) and then allowed to warm to room temperature. The suspension was extracted with EtOAc and the combined organic layers washed with NaHCO_3 (sat. aq.) and brine, dried over anhydrous MgSO_4 , filtered and concentrated under reduced pressure. The residue was dissolved in a mixture of sodium methoxide (0.04 mmol) in MeOH (4 ml) and stirred for 5 hours. The reaction was quenched with acetic acid (4 μl in 400 μl MeOH) and concentrated. The residue was taken up in EtOAc, washed with NaHCO_3 (sat. aq.) and brine, dried over anhydrous MgSO_4 , filtered and concentrated under reduced pressure. The residue was purified by flash chromatography (1.5–3% EtOAc/toluene) yielding the title compound (51 mg, 0.13 mmol, 63 % yield) as a single diastereomeric product. $R_f = 0.70$ (20/80 EtOAc/pentane). ^1H NMR (400 MHz, CDCl_3) δ 7.36 – 7.24 (m, 15H, CH_{Ar} Bn), 4.58 (d, $J = 12.1$ Hz, 1H, CHH Bn-5), 4.54 (d, $J = 12.1$ Hz, 1H, CHH Bn-5), 4.53 (s, 2H, 2xCHH Bn-3), 4.48 (d, $J = 12.0$ Hz, 1H, CHH Bn-2), 4.44 (d, $J = 11.9$ Hz, 1H, CHH Bn-2), 4.09 – 4.04 (m, 2H, C-2, C-4), 3.96 (dd, $J = 3.9$, 1.6 Hz, 1H, C-3), 3.92 (d, $J = 4.4$ Hz, 1H, C-1), 3.62 (dd, $J = 10.0$, 6.1 Hz, 1H, C-5a), 3.57 (dd, $J = 10.0$, 5.7 Hz, 1H, C-5b). ^{13}C NMR (101 MHz, CDCl_3) δ 138.3, 137.9 (C_q Bn), 128.6, 128.5, 127.9, 127.9, 127.9, 127.8, 127.7 (CH_{Ar} Bn), 84.6 (C-3), 83.3 (C-2), 82.8 (C-4), 73.5 (CH_2 Bn-5), 71.8 (CH_2 Bn-3), 71.3 (t, $J = 23$ Hz, C-1), 71.3 (CH_2 Bn-2), 70.5 (C-5). $[\alpha]_D^{20} = -1^\circ$ ($c = 1$, CHCl_3). IR (neat): 667, 694, 733, 908, 969, 1002, 1024, 1071, 1088, 1206, 1363, 1453, 1496, 2862, 2919, 3031. HR-MS: $[\text{M}+\text{H}^+]$ Calculated for $\text{C}_{26}\text{H}_{27}\text{DO}_4$: 406.21231; found: 406.21218.



2,3,5-Tri-O-benzyl-1-O-methyl-D-xylofuranose (7).

α -D-Xylose (30 g, 200 mmol) was dissolved MeOH (700 ml), acetyl chloride (4.3 ml, 60 mmol) was added to the reaction and the mixture stirred overnight. The reaction mixture was quenched by adjusting the pH to neutral by addition of NaHCO_3 (s, 90g), the solid was filtered off and the filtrate concentrated under reduced pressure. The residue was coevaporated twice with toluene before being dissolved in DMF (1 ml) and cooled to 0 °C. Benzyl bromide (143 ml, 1.2 mol), a catalytic amount of tetrabutylammonium iodide (0.7 g, 2 mmol) and sodium hydride (48 g, 1.2 mol, 60% in mineral oil) were added to the mixture. After 1 hour of stirring at 0 °C, the mixture was allowed to gradually warm up to room temperature and stirred overnight. The reaction mixture was concentrated under reduced pressure before being taken up in Et_2O and washed with 1M HCl (aq.). The combined aqueous layers were extracted with Et_2O and the organic layers then combined before being washed with NaHCO_3 (sat. aq.) and brine. The solution was dried over anhydrous MgSO_4 , filtered and concentrated under reduced pressure. The residue was purified by flash chromatography (2.5%-30% Et_2O /pentane) yielding an anomeric mixture (α : β : 7:8) of the title compound (87 g, 200 mmol, quant.). R_f = 0.35 and 0.45 (10/90 EtOAc /pentane). α -Anomer: ^1H NMR (400 MHz, CDCl_3) δ 7.38 – 7.21 (m, 15H, CH_{Ar} Bn), 4.81 (d, J = 4.3 Hz, 1H, C-1), 4.69 – 4.47 (m, 6H, 6x CHH Bn), 4.42 – 4.36 (m, 1H, C-4), 4.31 (dd, J = 7.2, 6.0 Hz, 1H, C-3), 4.02 (dd, J = 6.0, 4.3 Hz, 1H, C-2), 3.70 (dd, J = 10.5, 3.6 Hz, 1H, C-5a), 3.59 (dd, J = 10.6, 6.7 Hz, 1H, C-5b), 3.40 (s, 3H, OCH_3). ^{13}C NMR (101 MHz, CDCl_3) δ 138.3, 138.2, 137.8 (C_q Bn), 128.6, 128.5, 128.4, 128.4, 128.2, 128.0, 128.0, 127.9, 127.9, 127.8, 127.7, 127.7, 127.7 (CH_{Ar} Bn), 100.6 (C-1), 84.0 (C-2), 81.6 (C-3), 76.0 (C-4), 73.6, 72.7, 72.0 (3x CH_2 Bn), 69.5 (C-5), 55.4 (OCH_3). β -Anomer: ^1H NMR (400 MHz, CDCl_3) δ 7.39 – 7.21 (m, 15H, CH_{Ar} Bn), 4.91 (d, J = 1.5 Hz, 1H, C-1), 4.69 – 4.47 (m, 6H, 6x CHH Bn), 4.49-4.41 (m, 1H, C-4), 4.05 (dd, J = 5.9, 2.6 Hz, 1H, C-3), 3.97 (dd, J = 2.6, 1.5 Hz, 1H, C-2), 3.78 (dd, J = 10.2, 4.9 Hz, 1H, C-5a), 3.72 (dd, J = 10.3, 7.0 Hz, 1H, C-5b), 3.40 (s, 3H, OCH_3). ^{13}C NMR (101 MHz, CDCl_3) δ 138.4, 137.8, 137.6 (C_q Bn), 128.6, 128.5, 128.4, 128.4, 128.2, 128.0, 128.0, 127.9, 127.9, 127.8, 127.7, 127.7, 127.7 (CH_{Ar} Bn), 108.3 (C-1), 86.9 (C-2), 81.5 (C-3), 80.2 (C-4), 73.5, 72.7, 72.3 (3x CH_2 Bn), 69.8 (C-5), 55.8 (OCH_3). IR (neat): 605, 695, 732, 889, 908, 953, 1001, 1026, 1056, 1081, 1097, 1194, 1206, 1340, 1363, 1453, 2865, 2915, 3030. HR-MS: $[\text{M}+\text{H}^+]$ Calculated for $\text{C}_{27}\text{H}_{30}\text{O}_5$: 435.21660; found: 435.21677.

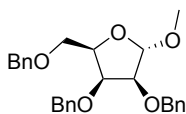
2,3,5-Tri-O-benzyl-D-xylofuranose (8).

2,3,5-Tri-O-benzyl-1-O-methyl-D-xylofuranose (7, 35 g, 81 mmol) was dissolved in 1,4-dioxane (280 ml) before addition of aqueous HCl (4M, 280 ml) and the mixture was heated (90 °C) for a total of 2,5 hours. The mixture was cooled down and quenched by pouring the mixture into a NaHCO_3 solution (sat. aq.) and extracting the mixture with EtOAc . The combined organic layers were washed with brine, dried over anhydrous MgSO_4 , filtered and concentrated under reduced pressure. The residue was purified by flash chromatography (15-40% Et_2O /pentane) yielding an anomeric mixture (α : β : 1:2) of the title compound (26 g, 62 mmol, 77 % yield). R_f = 0.30 (20/80 EtOAc /pentane). α -Anomer: ^1H NMR (400 MHz, CDCl_3) δ 7.39 – 7.21 (m, 15H, CH_{Ar} Bn), 5.47 (d, J = 4.2 Hz, 1H, C-1), 4.64 – 4.43 (m, 6H, 6x CHH Bn), 4.43 – 4.34 (m, 1H, C-4), 4.03 (dd, J = 4.5, 2.3 Hz, 1H, C-3), 3.93 (dd, J = 4.2, 2.3 Hz, 1H, C-2), 3.73 – 3.69 (m, 1H, C-5a), 3.66 (dd, J = 9.9, 5.8 Hz, 1H, C-5b). ^{13}C NMR (101 MHz, CDCl_3) δ 138.2, 137.8, 136.9 (C_q Bn), 128.7, 128.6, 128.6, 128.6, 128.4, 128.4, 128.1, 128.0, 128.0, 127.9, 127.9, 127.8, 127.7 (CH_{Ar} Bn), 96.3 (C-1), 81.3 (C-3), 81.1 (C-2), 77.4 (C-4), 73.6, 73.1, 72.4 (3x CH_2 Bn), 68.4 (C-5). β -Anomer: ^1H NMR (400 MHz, CDCl_3) δ 7.39 – 7.21 (m, 15H, CH_{Ar}), 5.25 (s, 1H, C-1), 4.65 – 4.43 (m, 6H, 6x CHH Bn), 4.42 – 4.35 (m, 1H, C-4), 4.10 (dd, J = 5.5, 3.1 Hz, 1H, C-3), 4.00 (d, J = 3.0 Hz, 1H, C-2), 3.75 (dd, J = 10.0, 5.0 Hz, 1H, C-5a), 3.73 – 3.69 (m, 1H, C-5b). ^{13}C NMR (101 MHz, CDCl_3) δ 137.6, 137.5, 137.4 (C_q Bn), 128.7, 128.6, 128.6, 128.6, 128.4, 128.4, 128.1, 128.0, 128.0, 128.0, 127.9, 127.9, 127.9, 127.8, 127.7 (CH_{Ar} Bn), 101.8 (C-1), 86.7 (C-2), 81.4 (C-3), 79.9 (C-4), 73.8, 72.7, 71.9 (3x CH_2 Bn), 68.8 (C-5). IR (neat): 604, 694, 733, 779, 920, 845, 908, 941, 1026, 1053, 1207, 1350, 1366, 1454, 1497, 2864, 2920, 3421. HR-MS: $[\text{M}+\text{Na}^+]$ Calculated for $\text{C}_{26}\text{H}_{28}\text{O}_5$: 443.18290; found: 443.18216.

2,3,5-Tri-*O*-benzyl-1-*O*-acetyl-*D*-xylofuranose (9). 2,3,5-Tri-*O*-benzyl-*D*-xylofuranose (**8**, 4.2 g, 10 mmol) was dissolved in pyridine (15 ml) and slowly added to cooled (0 °C) acetic anhydride (10 ml, 106 mmol). The mixture was then stirred at room temperature for 4 hours. The mixture was poured into 1M HCl (aq.) and diluted with EtOAc. The two layers were separated and the organic layer washed with 1M HCl (aq.), NaHCO₃ (sat. aq.) and brine. The solution was dried over anhydrous MgSO₄, filtered and concentrated under reduced pressure. The residue was purified by flash chromatography (10-20% EtOAc/pentane) yielding an anomeric mixture (α:β; 1:3) of the title compound (4.2 g, 8.6 mmol, 86 % yield). *R*_f = 0.60 (20/80 EtOAc/pentane). α-Anomer: ¹H NMR (400 MHz, CDCl₃) δ 7.39 – 7.22 (m, 15H, CH_{Ar} Bn), 6.35 (d, *J* = 4.2 Hz, 1H, C-1), 4.66 – 4.45 (m, 7H, 6xCHH Bn, C-4), 4.29 – 4.24 (t, *J* = 6.2, 1H, C-3), 4.21 (dd, *J* = 5.7, 4.3 Hz, 1H, C-2), 3.72 (dd, *J* = 10.4, 4.2 Hz, 1H, C-5a), 3.61 (dd, *J* = 10.6, 5.9 Hz, 1H, C-5b), 2.07 (s, 3H, CH₃). ¹³C NMR (101 MHz, CDCl₃) δ 170.2 (C=O), 138.3, 137.8, 137.5 (C_q Bn), 128.6, 128.5, 128.4, 128.1, 128.1, 128.1, 127.9, 127.9, 127.8, 127.8, 127.7, 127.7, 127.6, 127.6 (CH_{Ar} Bn), 94.3 (C-1), 83.4 (C-2), 80.9 (C-3), 78.2 (C-4), 73.6, 73.3, 72.8 (3xCH₂ Bn), 68.9 (C-5), 21.3 (CH₃). β-Anomer: ¹H NMR (400 MHz, CDCl₃) δ 7.41 – 7.20 (m, 15H, CH_{Ar} Bn), 6.18 (s, 1H, C-1), 4.67 – 4.49 (m, 6H, 5xCHH Bn, C-4), 4.46 (d, *J* = 12.1 Hz, 1H, CHH Bn), 4.10 – 4.04 (m, 2H, C-2, C-3), 3.82 (dd, *J* = 10.2, 5.4 Hz, 1H, C-5a), 3.74 (dd, *J* = 10.3, 6.6 Hz, 1H, C-5b), 2.02 (s, 3H, CH₃). ¹³C NMR (101 MHz, CDCl₃) δ 170.2 (C=O), 138.3, 137.8, 137.4 (C_q Bn), 128.6, 128.5, 128.4, 128.1, 128.1, 127.9, 127.9, 127.8, 127.8, 127.7, 127.7, 127.6, 127.6 (CH_{Ar} Bn), 100.6 (C-1), 85.2 (C-3), 82.2 (C-4), 81.1 (C-2), 73.5, 72.2, 72.1 (3xCH₂ Bn), 68.9 (C-5), 21.4 (CH₃). IR (neat): 602, 696, 733, 781, 820, 845, 914, 945, 1007, 1090, 1231, 1371, 1454, 1497, 1744, 2864, 2926. HR-MS: [M+Na⁺] Calculated for C₂₈H₃₀O₆: 485.19346; found: 485.19274.

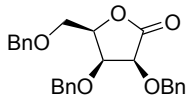
2,3,5-Tri-*O*-benzyl-1-deoxy-α/β-deutero-*D*-xylofuranose (17). 2,3,5-Tri-*O*-benzyl-1-*O*-acetyl-*D*-xylofuranose (**9**, 93 mg, 0.2 mmol) was coevaporated with toluene (3x), dissolved in DCM (2.7 ml) and cooled to -78 °C. [D]Triethylsilane (64 μl, 0.4 mmol) was added before slowly adding a solution of trimethylsilyl trifluoromethanesulfonate (47 μl, 0.26 mmol) in DCM (300 μl) and the reaction stirred at -78 °C for 1 week. The reaction was quenched by addition of NaHCO₃ (sat.aq., 5 ml) and then allowed to warm to room temperature. The suspension was extracted with EtOAc and the combined organic layers washed with NaHCO₃ (sat. aq.) and brine, dried over anhydrous MgSO₄, filtered and concentrated under reduced pressure. The residue was dissolved in a mixture of sodium methoxide (0.04 mmol) in MeOH (4 ml) and stirred for 5 hours. The reaction was quenched with acetic acid (4 μl in 400 μl MeOH) and concentrated. The residue was taken up in EtOAc, washed with NaHCO₃ (sat. aq.) and brine, dried over anhydrous MgSO₄, filtered and concentrated under reduced pressure. The residue was purified by flash chromatography (2-3.5% EtOAc/toluene) yielding an anomeric mixture (α:β; 85:15) of the title compound (32 mg, 0.08 mmol, 40 % yield). *R*_f = 0.70 (20/80 EtOAc/pentane). ¹H NMR (400 MHz, CDCl₃) α-Anomer: δ 4.14 (d, *J* = 5.0 Hz, 1H). β-Anomer: δ 3.80 (d, *J* = 2.4 Hz, 1H). Both: δ 7.39 – 7.25 (m, 15H, CH_{Ar} Bn), 4.62 (d, *J* = 12.0 Hz, 1H, CHH-Bn-5), 4.57 (d, *J* = 12.1 Hz, 1H, CHH Bn-3), 4.52 (d, *J* = 12.0 Hz, 1H, CHH Bn-5), 4.53 – 4.46 (m, 1H, CHH Bn-3), 4.47 (s, 2H, 2xCHH Bn-2), 4.24 (ddd, *J* = 6.5, 5.5, 3.9 Hz, 1H, C-4), 4.08 (dd, *J* = 5.0, 1.2 Hz, 1H, C-2), 4.02 (dd, *J* = 3.9, 1.2 Hz, 1H, C-3), 3.76 (dd, *J* = 10.0, 5.5 Hz, 1H, C-5a), 3.71 (dd, *J* = 10.0, 6.6 Hz, 1H, C-5b). ¹³C NMR (101 MHz, CDCl₃) δ 138.4, 138.0, 137.8 (C_q Bn), 128.6, 128.6, 128.5, 128.0, 127.9, 127.7, 127.7 (CH_{Ar} Bn), 82.2 (C-2), 82.1 (C-3), 79.7 (C-4), 73.6 (CH₂ Bn-5), 72.1 (CH₂ Bn-3), 71.5 (CH₂ Bn-2), 71.4 (t, *J* = 23 Hz, C-1), 68.5 (C-5). IR (neat): 602, 694, 733, 814, 908, 966, 1026, 1072, 1206, 1348, 1454, 1497, 2857, 2920. HR-MS: [M+H⁺] Calculated for C₂₆H₂₇DO₄: 406.21231; found: 406.21209.

2,3,5-Tri-*O*-benzyl-α-1-*O*-methyl-*D*-lyxofuranose (10). *D*-Lyxose (25 g, 167 mmol) was dissolved in MeOH (430 ml), a solution of acetyl chloride (2.5 ml, 35 mmol) in MeOH (130 ml) added and the reaction mixture stirred overnight. The reaction was quenched by adjusting the pH of the reaction mixture to ~7 by addition of 3M NaOH (aq.) before being concentrated and coevaporated with toluene (4x). The crude product was dissolved in DMF (850 ml) and



cooled down (0 °C). Benzyl bromide (83 ml, 700 mmol), a catalytic amount of tetrabutylammonium iodide and sodium hydride (28 g, 700 mmol, 60% in mineral oil) were added and the reaction allowed to slowly warm to room temperature whilst stirring. After the reaction was stirred overnight, the mixture was concentrated under reduced pressure, the mixture taken up in a mixture of EtOAc/1M HCl (aq.) and the layers separated. The organic layer was washed with 1M HCl (aq.), with NaHCO₃ (sat. aq.) and brine, dried over anhydrous MgSO₄, filtered and concentrated under reduced pressure. The residue was purified by flash chromatography (2-20% Et₂O/pentane) yielding the title compound (61 g, 140 mmol, 84 % yield) with a minor fraction of its pyranose side product. *R*_f = 0.30 (10/90 EtOAc/pentane). ¹H NMR (400 MHz, CDCl₃) δ 7.41 – 7.23 (m, 15H, CH_{Ar} Bn), 5.02 (d, *J* = 2.3 Hz, 1H, C-1), 4.70 – 4.57 (m, 3H, CHH Bn), 4.58 (d, *J* = 12.1 Hz, 1H, CHH Bn), 4.52 (d, *J* = 12.0 Hz, 1H, CHH Bn), 4.50 (d, *J* = 12.0 Hz, 1H, CHH Bn), 4.39 – 4.31 (m, 1H, C-4), 4.19 (t, *J* = 5.0 Hz, 1H, C-3), 3.88 (dd, *J* = 4.6, 2.4 Hz, 1H, C-2), 3.80 – 3.72 (m, 2H, C-5), 3.36 (s, 3H, OCH₃). ¹³C NMR (101 MHz, CDCl₃) δ 138.3, 138.2, 137.9 (C_q Bn), 128.5, 128.4, 128.0, 127.8, 127.8, 127.8, 127.7 (CH_{Ar} Bn), 106.4 (C-1), 82.5 (C-2), 78.3 (C-4), 77.9 (C-3), 73.5, 73.3, 72.6 (3xCH₂ Bn), 69.8 (C-5), 55.7 (OCH₃). [α]_D²⁰ = 10° (c = 0.8, CHCl₃). IR (neat): 604, 650, 694, 733, 808, 920, 851, 910, 968, 1026, 1047, 1099, 1206, 1271, 1314, 1346, 1362, 1452, 1497, 1722, 2913. HR-MS: [M+H]⁺ Calculated for C₂₇H₃₀O₅: 435.21660; found: 435.21665. Spectroscopic data was identical to literature data.³⁸

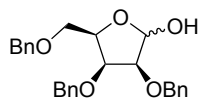
2,3,5-Tri-*O*-benzyl-*D*-lyxofuranolactone (12). 2,3,5-Tri-*O*-benzyl-α-1-*O*-methyl-*D*-lyxofuranose (**10**, 25 g, 58



mmol) was dissolved in acetic acid (300 ml) and H₂O (75 ml). The mixture was refluxed (110 °C) overnight and allowed to cool down before being neutralized with 6M NaOH and extracted with EtOAc. The organic layers were combined and washed with NaHCO₃ (sat. aq.) and brine. The organic layer was dried over anhydrous MgSO₄, filtered and

concentrated under reduced pressure. The residue was purified by flash chromatography (25-75% Et₂O/pentane) yielding 2,3,5-Tri-*O*-benzyl-*D*-lyxofuranose (18 g, 44 mmol, 76 % yield) with minor fractions of its pyranose isomer (*R*_f = 0.40, 25/75 EtOAc/pentane) which was used without any further identification in the next step. The hemiacetal was dissolved in dimethyl sulfoxide (350 ml) and acetic anhydride (230 ml) was added. The mixture was stirred overnight and diluted with Et₂O, washed twice with H₂O, twice with NaHCO₃ (sat. aq.) and once with brine. The organic layer was dried over anhydrous MgSO₄, filtered and concentrated under reduced pressure. The residue was crystallized from methanol yielding the pure title compound (14 g, 33 mmol, 76 % yield). *R*_f = 0.55 (25/75 EtOAc/pentane). ¹H NMR (400 MHz, CDCl₃) δ 7.42 – 7.24 (m, 15H, CH_{Ar} Bn), 4.98 (d, *J* = 12.1 Hz, 1H, CHH Bn-2), 4.85 (d, *J* = 11.7 Hz, 1H, CHH Bn-3), 4.79 (d, *J* = 12.1 Hz, 1H, CHH Bn-2), 4.56 (d, *J* = 11.2 Hz, 1H, CHH Bn-3), 4.48 (d, *J* = 11.8 Hz, 1H, CHH Bn-5a), 4.48 (d, *J* = 11.8 Hz, 1H, CHH Bn-5b), 4.44 (dt, *J* = 6.1, 3.1 Hz, 1H, C-4), 4.22 (dd, *J* = 4.5, 3.2 Hz, 1H, C-3), 4.19 (d, *J* = 4.6 Hz, 1H, C-2), 3.79 (d, *J* = 6.1 Hz, 2H, C-5). ¹³C NMR (101 MHz, CDCl₃) δ 173.2 (C=O), 137.6, 137.5, 136.9 (C_q Bn), 128.7, 128.6, 128.5, 128.3, 128.1, 128.1, 128.0, 128.0, 127.9 (CH_{Ar} Bn), 78.5 (C-4), 76.2 (C-2), 75.1 (C-3), 73.8 (CH₂ Bn-5), 73.7 (CH₂ Bn-3), 72.7 (CH₂ Bn-2), 67.6 (C-5). [α]_D²⁰ = -26° (c = 1, CHCl₃). IR (neat): 611, 644, 662, 692, 725, 779, 827, 880, 891, 910, 953, 993, 1024, 1053, 1078, 1103, 1132, 1159, 1198, 1213, 1267, 1344, 1360, 1410, 1452, 1497, 1802, 2876, 2916, 3028. HR-MS: [M+Na]⁺ Calculated for C₂₆H₂₆O₅: 441.16725; found: 441.16651.

2,3,5-Tri-*O*-benzyl-*D*-lyxofuranose (13). 2,3,5-Tri-*O*-benzyl-*D*-lyxofuranolactone (**12**, 2.1 g, 5 mmol) was dissolved

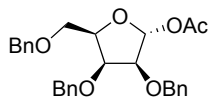


in DCM (25 ml) and cooled to -78 °C. Diisobutylaluminum hydride (7 ml, 7 mmol, 1M in hexanes) was added slowly over 10-15 minutes and the reaction mixture kept at -78 °C for 1 hour. Methanol (2 ml) was added dropwise to quench the reaction and the solution allowed to warm to room temperature. The solution was diluted with DCM

and washed with potassium sodium tartrate (1M aq.). The solution was dried over anhydrous MgSO₄, filtered and concentrated under reduced pressure. The product was purified by flash chromatography (30-40% EtOAc/pentane) yielding an anomeric mixture (α:β; 1:4) of the title compound (2.0 g, 4.7 mmol, 94 % yield). *R*_f = 0.15 (20/80 EtOAc/pentane). α-Anomer: ¹H NMR (400 MHz, CDCl₃) δ 7.39 – 7.23 (m, 15H, CH_{Ar} Bn), 5.49 (d, *J* = 2.7 Hz, 1H, C-1), 4.68 (d, *J* = 12.0 Hz, 1H, CHH Bn), 4.66 (d, *J* = 12.0 Hz, 1H, CHH Bn), 4.62 – 4.47 (m, 4H, 4xCHH Bn),

4.47 – 4.42 (m, 1H, C-4), 4.21 (t, $J = 4.9$ Hz, 1H, C-3), 3.92 – 3.85 (m, 1H, C-2), 3.76 – 3.73 (m, 2H, C-5). ^{13}C NMR (101 MHz, CDCl_3) δ 138.2, 138.1, 137.9 (C_q Bn), 128.6, 128.5, 128.5, 128.4, 128.4, 128.0, 128.0, 127.9, 127.9, 127.8, 127.8, 127.7, 127.6 (CH_{Ar} Bn), 100.1 (C-1), 83.4 (C-2), 78.4 (C-4), 77.9 (C-3), 73.5, 73.3, 72.5 ($3\times\text{CH}_2$ -Bn), 69.8 (C-5). β -Anomer: ^1H NMR (400 MHz, CDCl_3) δ 7.39 – 7.23 (m, 15H, CH_{Ar} Bn), 5.25 (dd, $J = 12.1$, 4.4 Hz, 1H, C-1), 4.84 (d, $J = 11.3$ Hz, 1H, CHH Bn), 4.73 (d, $J = 11.7$ Hz, 1H, CHH Bn), 4.64 – 4.46 (m, 4H, $4\times\text{CHH}$ Bn), 4.28 (d, $J = 12.2$ Hz, 1H, OH), 4.15 – 4.06 (m, 2H, C-3, C-4), 3.91 – 3.87 (m, 1H, C-2), 3.81 (dd, $J = 9.5$, 6.6 Hz, 1H, C-5a), 3.69 (dd, $J = 9.5$, 5.5 Hz, 1H, C-5b). ^{13}C NMR (101 MHz, CDCl_3) δ 138.0, 137.7, 137.5 (C_q Bn), 128.6, 128.5, 128.5, 128.4, 128.4, 128.0, 128.0, 127.9, 127.8 (CH_{Ar} Bn), 95.6 (C-1), 79.3 (C-2), 78.2, 77.4 (C-3, C-4), 74.4, 73.7, 72.0 ($3\times\text{CH}_2$ Bn), 69.3 (C-5). IR (neat): 602, 648, 694, 733, 820, 849, 885, 910, 947, 1026, 1045, 1078, 1146, 1207, 1308, 1346, 1454, 1497, 2866, 2922, 3418. HR-MS: $[\text{M}+\text{H}^+]$ Calculated for $\text{C}_{26}\text{H}_{28}\text{O}_5$: 421.20095; found: 421.20090.

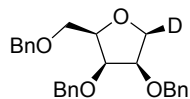
2,3,5-Tri-*O*-benzyl-1- α -*O*-acetyl-D-lyxofuranose (14). 2,3,5-Tri-*O*-benzyl-D-lyxofuranose (**13**, 2.3 g, 5.5 mmol) was



dissolved in pyridine (8 ml) and cooled (0 °C). Acetic anhydride (5.7 ml, 60 mmol) was added and the reaction allowed to stir at room temperature for 5 hours. The mixture was then poured into a solution of 1M HCl (aq.) and extracted with EtOAc. The organic phase was washed twice with 1M HCl (aq.), NaHCO_3 (sat. aq.) and brine

before being dried over anhydrous MgSO_4 , filtered and concentrated under reduced pressure. The residue was purified by flash chromatography (15-22.5% EtOAc/pentane) yielding the title compound (2.6 g, 5.5 mmol, quantitative) as a single diastereomer. $R_f = 0.45$ (20/80 EtOAc/pentane). ^1H NMR (400 MHz, CDCl_3) δ 7.37 – 7.25 (m, 15H, CH_{Ar} Bn), 6.29 (d, $J = 2.2$ Hz, 1H, C-1), 4.68 (d, $J = 12.1$ Hz, 1H, CHH Bn), 4.66 (d, $J = 11.9$ Hz, 1H, CHH Bn), 4.60 (d, $J = 12.1$ Hz, 1H, CHH Bn), 4.59 (d, $J = 11.9$ Hz, 1H, CHH Bn), 4.52 (d, $J = 11.8$ Hz, 1H, CHH Bn), 4.50 (d, $J = 11.9$ Hz, 1H, CHH Bn), 4.48 – 4.42 (m, 1H, C-4), 4.22 (t, $J = 5.2$ Hz, 1H, C-3), 3.99 (dd, $J = 4.7$, 2.2 Hz, 1H, C-2), 3.82 (dd, $J = 10.3$, 4.9 Hz, 1H, C-5a), 3.75 (dd, $J = 10.3$, 7.0 Hz, 1H, C-5b), 2.03 (s, 3H, CH_3). ^{13}C NMR (101 MHz, CDCl_3) δ 169.9 (C=O), 138.2, 137.9, 137.5 (C_q Bn), 128.5, 128.5, 128.4, 128.0, 127.9, 127.9, 127.7, 127.7 (CH_{Ar} Bn), 99.3 (C-1), 81.4 (C-4), 79.9 (C-2), 77.0 (C-3), 73.5, 73.2, 72.5 ($3\times\text{CH}_2$ Bn), 69.4 (C-5), 21.3 (CH_3). $[\alpha]_D^{20} = 15^\circ$ (c = 1, CHCl_3). IR (neat): 602, 694, 733, 820, 851, 907, 945, 1009, 1053, 1090, 1552, 1227, 1369, 1454, 1497, 1744, 2866. HR-MS: $[\text{M}+\text{Na}^+]$ Calculated for $\text{C}_{28}\text{H}_{30}\text{O}_6$: 485.19346; found: 485.19270.

2,3,5-Tri-*O*-benzyl-1-deoxy-1- β -deutero-D-lyxofuranose (18). 2,3,5-Tri-*O*-benzyl-1- α -*O*-acetyl-D-lyxofuranose



(**14**, 93 mg, 0.2 mmol) was coevaporated with toluene (3x), dissolved in DCM (2.7 ml) and cooled to -78 °C. $[\text{D}]\text{Triethylsilane}$ (64 μl , 0.4 mmol) was added before slowly adding a solution of trimethylsilyl trifluoromethanesulfonate (47 μl , 0.26 mmol) in DCM (300 μl) and the reaction stirred at -78 °C for 1 week. The reaction was quenched by addition of

NaHCO_3 (sat. aq., 5 ml) and allowed to warm to room temperature. The suspension was extracted thrice with EtOAc and the combined organic layers washed with NaHCO_3 (sat. aq.) and brine, dried over anhydrous MgSO_4 , filtered and concentrated under reduced pressure. The residue was purified by flash chromatography (2-4.5% EtOAc/toluene) yielding the title compound (88 mg, 0.2 mmol, quantitative) as a single diastereomer. $R_f = 0.45$ (10/90 EtOAc/toluene). ^1H NMR (400 MHz, CDCl_3) δ 7.37 – 7.23 (m, 15H, CH_{Ar} Bn), 4.75 (d, $J = 11.9$ Hz, 1H, CHH Bn-3), 4.63 – 4.52 (m, 4H, $2\times\text{CHH}$ Bn-2, CHH Bn-3, CHH Bn-5), 4.50 (d, $J = 11.9$ Hz, 1H, CHH Bn-5), 4.21 – 4.15 (m, 1H, C-4), 4.12 – 4.05 (m, 2H, C-2, C-3), 3.88 (d, $J = 5.6$ Hz, 1H, C-1), 3.77 (dd, $J = 10.5$, 5.4 Hz, 1H, C-5a), 3.73 (dd, $J = 10.5$, 7.4 Hz, 1H, C-5b). ^{13}C NMR (101 MHz, CDCl_3) δ 138.4, 138.3, 138.0 (C_q Bn), 128.5, 128.4, 128.4, 127.9, 127.8, 127.8, 127.7, 127.6 (CH_{Ar} Bn), 79.0 (C-4), 78.5 (C-2), 77.8 (C-3), 73.5 (CH_2 Bn-5), 73.3 (CH_2 Bn-3), 72.3 (CH_2 Bn-2), 69.5 (C-5), 68.9 (t, $J = 23$ Hz, C-1). $[\alpha]_D^{20} = -9^\circ$ (c = 1, CHCl_3). IR (neat): 608, 635, 694, 733, 808, 849, 910, 1026, 1059, 1074, 1148, 1207, 1260, 1346, 1452, 1497, 2860, 2920. HR-MS: $[\text{M}+\text{H}^+]$ Calculated for $\text{C}_{26}\text{H}_{27}\text{DO}_4$: 406.21231; found: 406.21219.

References and notes

- [1] Richards, M. R.; Lowary, T. L. *ChemBiochem* **2009**, *10*, 1920-1938, 10.1002/cbic.200900208.
- [2] Taha, H. A.; Richards, M. R.; Lowary, T. L. *Chem. Rev.* **2013**, *113*, 1851-1876, 10.1021/cr300249c.
- [3] Schramm, V. L. *ACS Chem. Biol.* **2013**, *8*, 71-81, 10.1021/cb300631k.
- [4] Yin, H. F.; D'Souza, F. W.; Lowary, T. L. *J. Org. Chem.* **2002**, *67*, 892-903, 10.1021/jo010910e.
- [5] Joe, M.; Sun, D.; Taha, H.; Completo, G. C.; Croudace, J. E.; Lammas, D. A.; Besra, G. S.; Lowary, T. L. *J. Am. Chem. Soc.* **2006**, *128*, 5059-5072, 10.1021/ja057373q.
- [6] Lee, Y. J.; Lee, K.; Jung, E. H.; Jeon, H. B.; Kim, K. S. *Org. Lett.* **2005**, *7*, 3263-3266, 10.1021/ol0510668.
- [7] Baek, J. Y.; Joo, Y. J.; Kim, K. S. *Tetrahedron Lett.* **2008**, *49*, 4734-4737, 10.1016/j.tetlet.2008.05.118.
- [8] Mukaiyama, T.; Suda, S. *Chem. Lett.* **1990**, 1143-1146, 10.1246/cl.1990.1143.
- [9] Czernecki, S.; Ville, G. *J. Org. Chem.* **1989**, *54*, 610-612, 10.1021/jo00264a020.
- [10] Sollogoub, M.; Fox, K. R.; Powers, V. E. C.; Brown, T. *Tetrahedron Lett.* **2002**, *43*, 3121-3123, 10.1016/s0040-4039(02)00481-1.
- [11] Larsen, C. H.; Ridgway, B. H.; Shaw, J. T.; Woerpel, K. A. *J. Am. Chem. Soc.* **1999**, *121*, 12208-12209, 10.1021/ja993349z.
- [12] Smith, D. M.; Tran, M. B.; Woerpel, K. A. *J. Am. Chem. Soc.* **2003**, *125*, 14149-14152, 10.1021/ja0375176.
- [13] Smith, D. M.; Woerpel, K. A. *Org. Lett.* **2004**, *6*, 2063-2066, 10.1021/ol0492647.
- [14] Larsen, C. H.; Ridgway, B. H.; Shaw, J. T.; Smith, D. M.; Woerpel, K. A. *J. Am. Chem. Soc.* **2005**, *127*, 10879-10884, 10.1021/ja0524043.
- [15] Smith, D. M.; Woerpel, K. A. *Org. Biomol. Chem.* **2006**, *4*, 1195-1201, 10.1039/b600056h.
- [16] Zhu, X. M.; Kawatkar, S.; Rao, Y.; Boons, G. J. *J. Am. Chem. Soc.* **2006**, *128*, 11948-11957, 10.1021/ja0629817.
- [17] Krumper, J. R.; Salamant, W. A.; Woerpel, K. A. *Org. Lett.* **2008**, *10*, 4907-4910, 10.1021/ol8019956.
- [18] Huang, M.; Garrett, G. E.; Birlirakis, N.; Bohe, L.; Pratt, D. A.; Crich, D. *Nat. Chem.* **2012**, *4*, 663-667, 10.1038/nchem.1404.
- [19] Crich, D. *Acc. Chem. Res.* **2010**, *43*, 1144-1153, 10.1021/ar100035r.

- [20] The relative stability of the anomeric triflates was calculated using B3LYP/6-311G**//B3LYP/6-31G*. Relative energy of *cis* to *trans*; ribose: +1.0 kcal mol⁻¹; arabinose: +0.1 kcal mol⁻¹; xylose: +0.6 kcal mol⁻¹, lyxose: +1.0 kcal mol⁻¹. See appendix for FES maps of the triflates.
- [21] Rhoad, J. S.; Cagg, B. A.; Carver, P. W. *J. Phys. Chem. A* **2010**, *114*, 5180-5186, 10.1021/jp9100448.
- [22] Altona, C.; Sundaralingan, M. *J. Am. Chem. Soc.* **1972**, *94*, 8205-8212, 10.1021/ja00778a043.
- [23] Gaussian 03 (Revision E.01), Frisch, M. J. *et al.*, Gaussian, Inc. **2004**.
- [24] Kim, Y.; Mohrig, J. R.; Truhlar, D. G. *J. Am. Chem. Soc.* **2010**, *132*, 11071-11082, 10.1021/ja101104q.
- [25] Houseknecht, J. B.; Lowary, T. L.; Hadad, C. M. *J. Phys. Chem. A* **2003**, *107*, 5763-5777, 10.1021/jp027716w.
- [26] Jensen, H. H.; Nordstrom, L. U.; Bols, M. *J. Am. Chem. Soc.* **2004**, *126*, 9205-9213, 10.1021/ja047578j.
- [27] Moume-Pymbock, M.; Crich, D. *J. Org. Chem.* **2012**, *77*, 8905-8912, 10.1021/jo3011655.
- [28] Seeman, J. I. *Chem. Rev.* **1983**, *83*, 83-134, 10.1021/cr00054a001.
- [29] Calculations to determine the transition states of S_N1 reactions on glycosyl oxocarbenium ions are notoriously difficult because these require the use of counterions, both on the side of the electrophile and the nucleophile, to prevent the barrierless formation of noncharged species. See for example: Ref 27; Whitfield, D. M. *Adv. Carbohydr. Chem. Biochem.* **2009**, *62*, 83-159, 10.1016/s0065-2318(09)00004-3.
- [30] Davies, G. J.; Planas, A.; Rovira, C. *Acc. Chem. Res.* **2012**, *45*, 308-316, 10.1021/ar2001765.
- [31] Zhang, Y.; Luo, M. K.; Schramm, V. L. *J. Am. Chem. Soc.* **2009**, *131*, 4685-4694, 10.1021/ja808346y.
- [32] Spartan '04, Kong, J. *et al.*, Wavefunction Inc. **2004**.
- [33] Daranas, A. H.; Napolitano, J. G.; Gavin, J. A.; Garcia, C.; Norte, M.; Fernandez, J. J. *Chem. Eur. J.* **2011**, *17*, 6338-6347, 10.1002/chem.201100412.
- [34] Xu, G. X.; Moeller, K. D. *Org. Lett.* **2010**, *12*, 2590-2593, 10.1021/ol100800u.
- [35] Mukaiyama, T.; Kobayashi, S. *Carbohydr. Res.* **1987**, *171*, 81-87, 10.1016/s0008-6215(00)90880-2.
- [36] Barry, C. S.; Backus, K. M.; Barry, C. E.; Davis, B. G. *J. Am. Chem. Soc.* **2011**, *133*, 13232-13235, 10.1021/ja204249p.

- [37] van der Klein, P. A. M.; de Nooy, A. E. J.; van der Marel, G. A.; van Boom, J. H. *Synthesis* **1991**, 347-349, 10.1055/s-1991-26461.
- [38] Kawana, M.; Kuzuhara, H.; Emoto, S. *Bull. Chem. Soc. Jpn.* **1981**, *54*, 1492-1504, 10.1246/bcsj.54.1492.

Chapter 3

Stereoselectivity in the Lewis acid mediated reduction of ketofuranosides

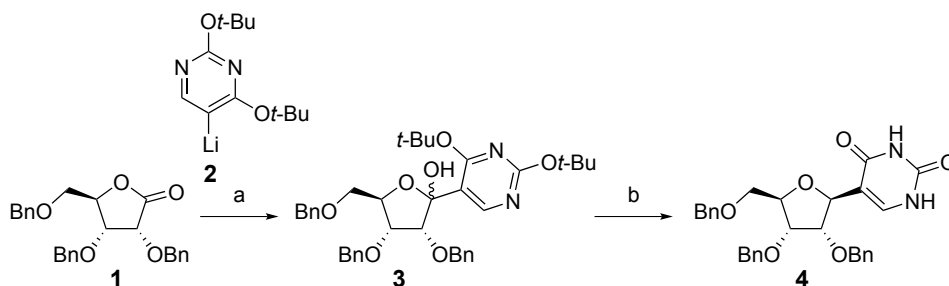
3.1 Introduction

C-glycosides are carbohydrates of which the aglycon is attached to the anomeric center through a carbon atom. Examples of naturally occurring C-glycosides are pseudouridine,¹⁻⁴ a C-nucleoside and the C-arylglycoside dapagliflozin.⁵ These structures are close mimics of naturally occurring *O*- and *N*-glycosides, but are metabolically more stable, by virtue of the

stable carbon-carbon bond that connects the aglycon to the carbohydrate ring.¹⁻² As a result, many of these C-glycosides have appealing biological properties, ranging from antibiotic and antiviral activity to anticancer activity.^{1-3,6-7} For example, the C-glycoside analogue of the naturally occurring O-glycoside phlorizin, dapagliflozin, is currently being used for the treatment of type 2 diabetes.⁵

A commonly used method to synthesize C-glycosides entails the reaction of a glycosyl lactone with an alkyl or aryl nucleophile to give an intermediate glycosyl hemi-ketal that can be reduced under Lewis acidic conditions to provide the target compounds.^{1-2,8-15} In this process a new stereogenic center is created and control over the stereochemical course of the reaction is required to enable a productive and effective overall transformation. Several examples of this strategy have been reported in literature.^{1-2,8-15} Of note is the reduction of perbenzylated ribofuranose ketosides to provide the beta-linked products in a highly stereoselective fashion.¹⁵⁻¹⁶ Scheme 3.1 depicts a synthesis of pseudouridine that builds on the stereoselective reduction of perbenzylated riboketosides.¹⁷ Reaction of perbenzylated ribonolactone **1** with lithiated pyrimidine **2** gave the intermediate hemi-ketal **3** that was reduced with triethylsilane (TES) using $\text{BF}_3 \cdot \text{OEt}_2$ as the Lewis acid. After complete removal of the *tert*-butyl protecting groups with trifluoroacetic acid (TFA) the desired 1,2-*trans* compound **4** was obtained as a single anomer. The stereoselectivity in the reduction is striking because the nucleophile comes in *cis* with respect to the substituent at C2.

Scheme 3.1 The diastereoselective synthesis of protected pseudouridine.



Reagents and conditions: (a) **2**, THF, -78 °C to -55 °C, 58%; (b) i) TES, $\text{BF}_3 \cdot \text{OEt}_2$, DCM, -78 °C to -10 °C; ii) TFA, -5 °C, 68% over 2 steps.

An explanation for the striking stereoselectivity can be found in the nature of the reactive intermediate in the reaction: the furanosyl oxocarbenium ion. In Chapter 2, a method to establish the relative stability of completely decorated furanosyl oxocarbenium ions is described. A complete survey of the energy landscape of the entire conformational space for the four possible pentoses (ribose, arabinose, xylose and lyxose) provided a clear

picture how the three ring substituents on the furanosyl oxocarbenium ion affect the stability, and therefore the reactivity in addition reactions. Given the enhanced stability of tertiary cations over their secondary counterparts it is likely that ketofuranosyl oxocarbenium ions are involved in the reduction of the C-furanosides described above. To investigate how the substituent at the anomeric center of ketofuranoses influences the stability of the corresponding oxocarbenium ions and the nucleophilic additions to these, this Chapter describes the reduction of the methyl and phenyl C-furanoses of all four possible pentoses (Figure 3.1). The conformational energy landscape of the intermediate oxocarbenium ions has been mapped to correlate the experimental outcome of the reduction reactions.

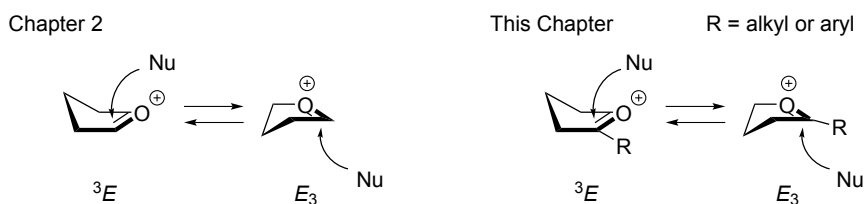
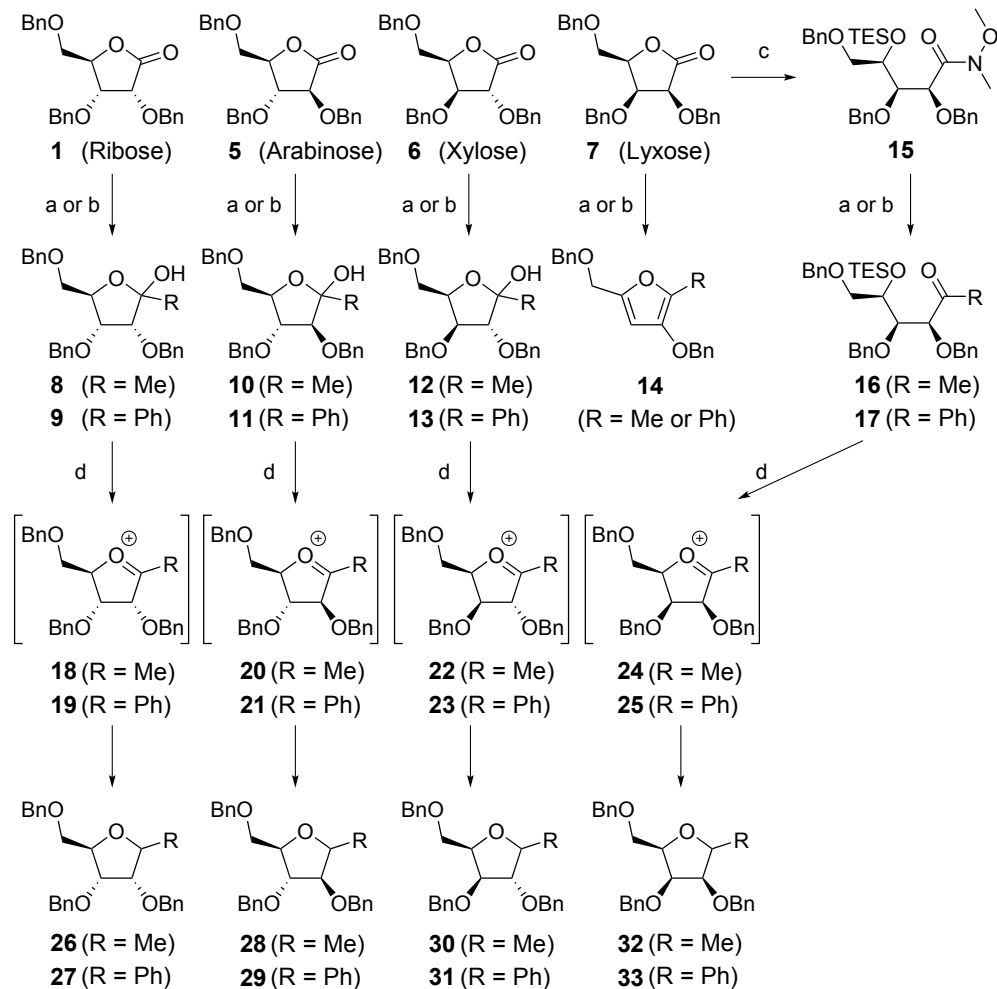


Figure 3.1 In chapter 2 furanosyl oxocarbenium ions were studied, this chapter investigates on ketofuranosyl oxocarbenium ions.

3.2 Results and discussion

The synthesis of the furanosyl lactols used in this study and the Lewis acid mediated reductions are depicted in Scheme 3.2. The ribose, arabinose and xylose derived perbenzylated methyl- and phenyl ketofuranose starting materials were prepared from the perbenzylated lactones. Ribonolactone **1**, arabinolactone **5** and xylonolactone **6** were reacted with methyl lithium or phenyl lithium to yield the methyl- and phenyl ketofuranoses that were directly used in the reduction step. Subjecting perbenzylated lyxonolactone **7** to methyl- or phenyl lithium did not yield the desired ketofuranoses but instead furan **14** was isolated as a result of a double β -elimination sequence. Because furan formation could not be suppressed it was decided to generate the lyxose oxocarbenium ions *in situ* in the projected reduction reactions from their linear precursors **16** and **17**. These were synthesized from Weinreb amide **15** that was generated from lactone **7** using *N,O*-dimethylhydroxylamine and trimethylaluminium. Reaction of the Weinreb amide **15** with methyl- or phenyl lithium delivered the open chain ketones of which the alcohol functions were capped as triethyl silyl ether.

Scheme 3.2 Synthesis of the perbenzylated ribo-, arabino, and xylofuranosyl hemi-ketals, the lyxose configured ketones and their ensuing reduction reactions.



Reagents and conditions: (a) MeLi, THF, $-78\text{ }^{\circ}\text{C}$, **8**: 77%, **10**: 86%, **12**: 93%, **16**: 72%; (b) PhLi, THF, $-78\text{ }^{\circ}\text{C}$, **9**: 48%, **11**: 70%, **13**: 91%, **17**: 60%; (c) i) *N,O*-dimethylhydroxylamine HCl, AlMe₃, THF, $0\text{ }^{\circ}\text{C}$; ii) TES-Cl, imidazole, THF, $0\text{ }^{\circ}\text{C}$, 73% over 2 steps; (d) TES, BF₃·OEt₂, DCM, $-78\text{ }^{\circ}\text{C}$ (see Table 3.1).

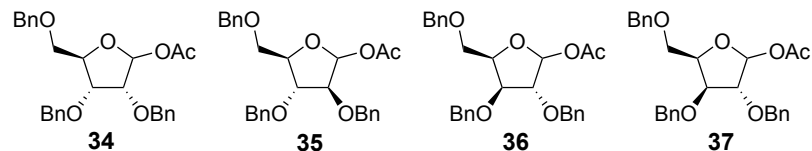


Figure 3.2 Reference aldose furanosyl donors from Chapter 2.

Table 3.1 Results of the Lewis acid mediated reduction.

Furanosyl donor	Product	1,2- <i>trans</i> : 1,2- <i>cis</i> ^[a,b]	Yield ^[c]
Reaction conditions a R = H 			
Reaction conditions b R = Me or Ph 			
Ribose			
R = H: 34	R = D: 38	R = D: 2:>98	50%
R = Me: 8	R = Me: 26	R = Me: >98:2	64%
R = Ph: 9	R = Ph: 27	R = Ph: >98:2	78%
Arabinose			
R = H: 35	R = D: 39	R = D: 2:>98	62%
R = Me: 10	R = Me: 28	R = Me: >98:2	83%
R = Ph: 11	R = Ph: 29	R = Ph: 85:15	65%
Xylose			
R = H: 36	R = D: 40	R = D: 15:85	40%
R = Me: 12	R = Me: 30	R = Me: 85:15	87%
R = Ph: 13	R = Ph: 31	R = Ph: 75:25	79%
Lyxose			
R = H: 37	R = D: 41	R = D: 2:>98	100%
R = Me: 16	R = Me: 32	R = Me: >98:2	44%
R = Ph: 17	R = Ph: 33	R = Ph: >98:2	60%

^[a]Ratio determined by ¹H NMR spectroscopy, stereochemistry was identified using ²J coupling-constants measured from HSQC-HECADE NMR spectra. ^[b]Addition of [D]TES to aldoses affords the *cis* product (reaction conditions **a**) while addition of TES in ketoses (reaction conditions **b**) gives the *trans* product (*cis* addition). ^[c]Yield of isolated furanosides after column chromatography.

The six ketofuranoses **8-13** and two linear chain lyxose-derived ketones **16** and **17** were subjected to a Lewis acid mediated reduction protocol using triethylsilane as reducing agent and boron trifluoride diethyletherate as Lewis acid in dichloromethane at -78 °C. The results of these reactions are summarized in Table 3.1, in combination with the results obtained in the experiments of the corresponding aldoses (in which furanosyl acetates were treated with [D]TES and TMSOTf, see Chapter 2). As can be seen in all cases preferentially the 1,2-*trans* C-furanosides were formed, corresponding to an attack of the hydride *cis* with respect to the substituent at C2. These results closely resemble those obtained for the aldoses **34-37**. In the case of ribose and lyxose, the reactions were completely stereoselective and the products were obtained as a single diastereomer, independent of the substituent on the anomeric position. In the arabinose series, both the

aldose **35** and methyl ketofuranose **10** yielded a single product, where the reduction of phenyl ketofuranose **11** proceeded with diminished stereopreference. The *xylo*-aldofuranose **36** and *xylo*-methyl ketofuranose **12** reacted with a similar preference for the 1,2-*cis* products,⁹ where the phenyl ketofuranose **13** again displayed the least stereoselectivity.

To account for the stereoselectivity observed in the reduction of the ketofuranoses and assess the influence of the substituent on the anomeric position on the intermediate oxocarbenium ions, the energy landscapes of the permethylated ketofuranosyl oxocarbenium ions **43-44**, **46-47**, **49-50**, and **52-53** (Figure 3.3) were calculated. To this extent the free energy surface (FES) mapping method was used, introduced by Rhoad et al.¹⁸ and adapted to interrogate the aldofuranosyl oxocarbenium ions as described in Chapter 2. In this method, the energy associated with the complete conformational space is calculated, and mapped on a spherical graph, the pseudorotational circle (see Chapter 2, figure 2.2b).¹⁹ Each conformation is described here by a phase angle (P), that defines the shape of the ring and the puckering amplitude (τ_m), that indicates how far out of the median plane the outlying atoms are positioned. The energy of 81 fixed ring conformers were calculated with Gaussian 03,²⁰ by employing the B3LYP density functional and the 6-311G** basis set, and these were corrected for the solvent (CH_2Cl_2) using the polarizable continuum model (PCM) function. Because rotation of the C4-C5 bond significantly influences the stability of the furanosyl oxocarbenium ions as described in Chapter 2, the FES of the oxocarbenium ions was scanned for the three individual *gg*, *gt* and *tg* C4-C5 rotamers (Chapter 2, figure 2.2c). Thus for each furanosyl oxocarbenium ion 243 (3x81) conformers were optimized and the associated energies determined.

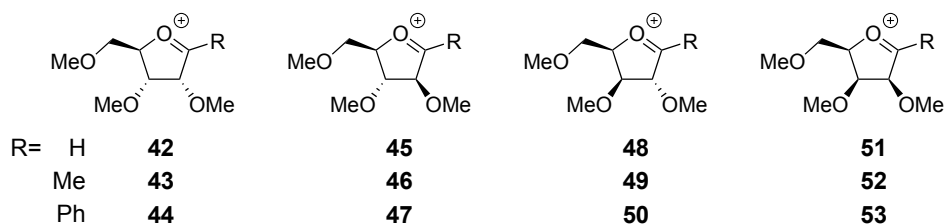


Figure 3.3 The investigated furanosyl oxocarbenium ions.

Ribose

In Figure 3.4, the oxocarbenium ion FES maps for the ribofuranosyl (**42**), methyl ribofuranosyl (**43**) and phenyl ribofuranosyl (**44**) oxocarbenium ions are graphed vertically over the different rows. In the columns, the *gg*, *gt*, *tg* and the global lowest FES maps are displayed from left to right. The global FES map is a combination of the absolute lowest energies of the *gg*, *gt* and *tg* in a single picture. From these maps it becomes clear that the ribofuranosyl E_3 oxocarbenium ion is highly preferred, independent of the nature of the anomeric substituent.²¹ In the E_3 oxocarbenium ions the C2 and C3 methoxy groups adopt a pseudoequatorial and pseudoaxial position respectively, maximizing the stabilizing effect on the oxocarbenium ion. In all oxocarbenium ions the C4-C5 *gg* rotamer is more stable than its *gt* counterpart, which in turn is preferred over the *tg* conformer. Small differences can be observed for the maps of the different anomeric substituents. The energy maps of the methyl furanosyl oxocarbenium ion conformers are somewhat steeper than the map of its unsubstituted ribofuranosyl oxocarbenium ion congener. The phenyl ribofuranosyl oxocarbenium ion maps on the other hand show a decreased energy difference between the 3E *gg* and E_3 *gg* conformer. The energy difference is large enough (~ 2.7 kcal mol⁻¹) to account for the selectivity in the reaction.

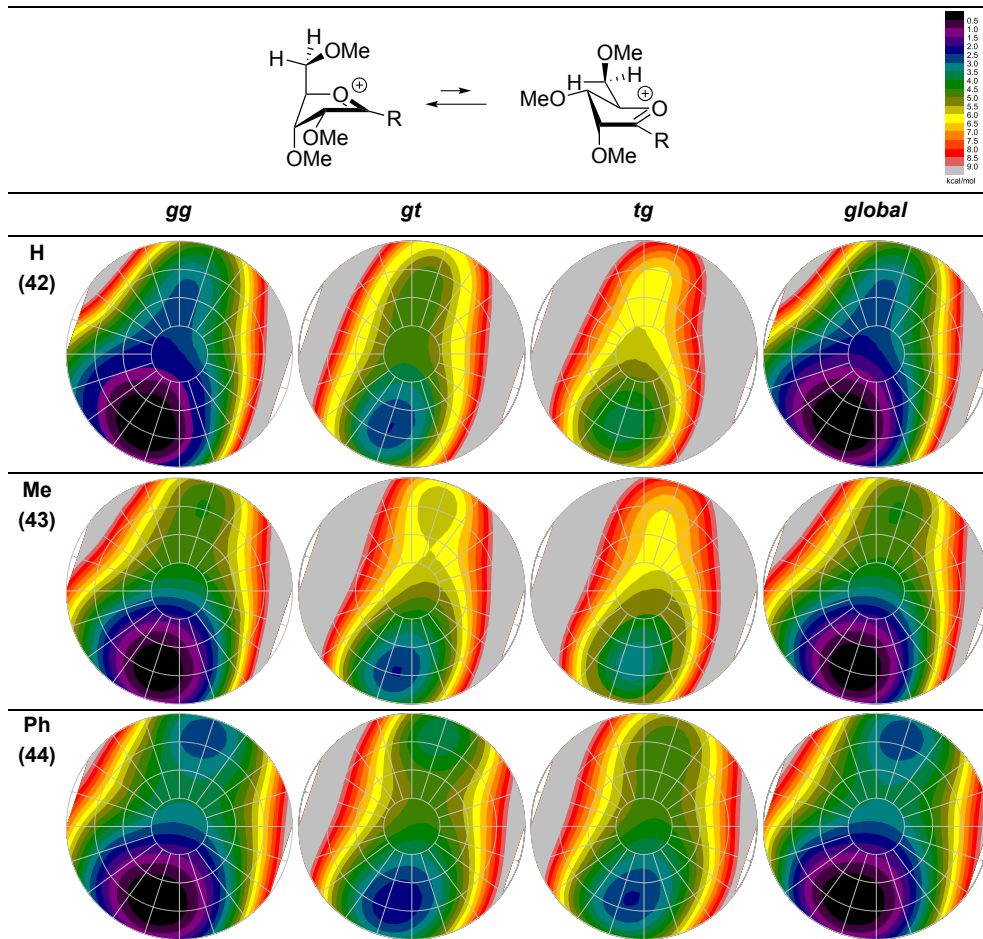


Figure 3.4 The *gg*, *gt*, *tg* and global FES maps of the ribofuranosyl oxocarbenium ions, mapped for the aldose (42), methyl ketose (43) and phenyl ketose (44).

A closer look at the structures associated with the energies in the FES maps of the methyl ketofuranose, shows that the methyl substituent is placed in an eclipsed conformation with respect to the plane of the oxocarbenium ion [C=O⁺] function (Figure 3.5a). This is surprising because the hyperconjugative stabilization of the carbocation would be most effective if the anomeric methyl group would position a proton perpendicular to the C=O⁺ plane. To investigate this unexpected conformational finding, the energy associated with rotation of the methyl substituent around the C1-methyl bond was profiled. As can be seen in Figure 3.5c the eclipsed conformation is most stable where the perpendicular structure ($\phi = 90^\circ$) is 0.4 kcal mol⁻¹ higher in energy. This parallels the energy profile for the position of a methyl substituent next to an (uncharged) carbonyl group²² so apparently steric factors overrule the electronic preferences also in the furanosyl oxocarbenium ion case at hand. Indeed, if the methyl group would have provided a significant stabilization to

the oxocarbenium ion, the overall difference in energy between the different furanose ring conformers would be expected to be somewhat smaller, resulting in a more shallow FES. An analogous analysis for the phenyl ketofuranose reveals that the phenyl substituent is positioned parallel to the $C=O^+$ plane (Figure 3.5b) to allow for effective conjugative stabilization of the positive charge. In the E_3 conformation, this planar constellation does lead to an unfavorable 1,3-allyl interaction between the phenyl ring and the substituent on C2 (Figure 3.5d). This allyl strain can destabilize the E_3 conformer, thereby decreasing the energy difference with the 3E conformers, leading to flattening of the FES map for the phenyl keto furanosides.

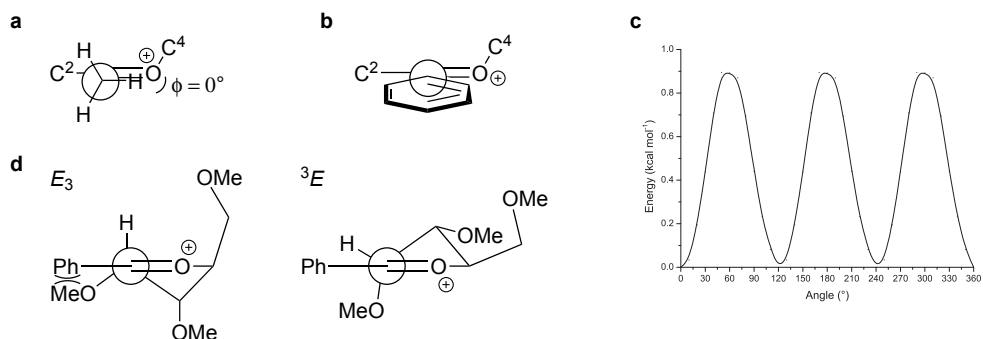


Figure 3.5 Conformation of the anomeric substituents relative to the oxocarbenium ion for a) methyl and b) phenyl. c) Rotation energy profile of the anomeric methyl substituent for the ribofuranosyl oxocarbenium ion. d) Steric interaction for phenyl substituted oxocarbenium ions, the figure reveals an unfavorable 1,3-allyl strain in the E_3 conformer.

The oxocarbenium ion FES maps for the non-substituted ($R = H$), the methyl- and phenyl substituted ribofuranosyl oxocarbenium ions show that a single envelope is preferred for all three furanoses, *i.e.* the 3E conformer. Inside attack of the nucleophile (TES) on this oxocarbenium ion conformer, leads to the formation of 1,2-*cis* products, providing an explanation for the stereoselectivity observed in the reaction of **34**, **8** and **9**.

Arabinose

The FES maps of the arabinofuranosyl oxocarbenium ions **46** and **47** are displayed next to those of arabinofuranosyl oxocarbenium ion **45** in Figure 3.6. From the global FES maps it becomes clear that the arabinosyl oxocarbenium ions preferentially take up an 3E conformation. The individual C4-C5 rotamer maps reveal that the *gg* conformers are the most stable. As with the arabino-aldose, the conformational preference of the arabinoketose oxocarbenium ions is less profound than the preference of the corresponding ribo-oxocarbenium ions. This can be accounted for by the fact that the C2 and C3 substituents cannot simultaneously adopt a most favorable orientation in either of

the envelope structures. In line with the FES maps for the different ribofuranosyl oxocarbenium ions, the FES maps for the methyl substituted arabinofuranose are somewhat steeper than the aldose while the maps for the phenyl substituted arabinofuranose are somewhat less steep. The global FES maps of the arabinofuranosyl oxocarbenium ions do not show a distinct two conformer model, instead they show a gradual increase in energy for the conformers around the ${}^3E - E_3$ axis (from 18° to 198°). From the flattened phenyl ketose oxocarbenium ion FES, one can expect an erosion of stereoselectivity in reactions involving this species. This is confirmed in the experiments: the *arabino* aldose and methyl ketofuranose both provide a single product upon reduction, where arabino phenyl ketofuranose gives an anomeric mixture with the major 1,2-*trans* product originating from a 3E oxocarbenium ion.

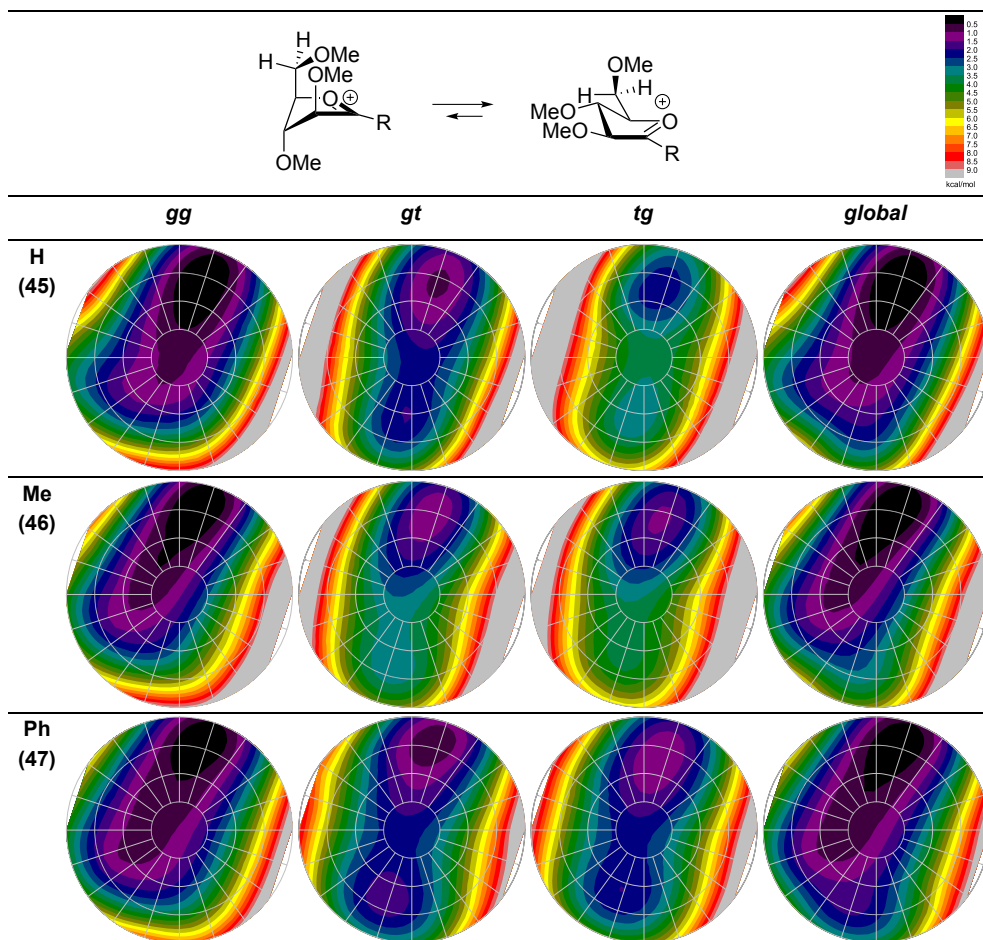


Figure 3.6 The *gg*, *gt*, *tg* and global FES maps of the arabinofuranosyl oxocarbenium ions, mapped for the aldose (45), methyl ketose (46) and phenyl ketose (47).

Xylose

The reductions of the xylofuranosides proceed with the least selectivity of the studied furanoses. The global xylofuranose oxocarbenium ion FES maps (Figure 3.7) show two energy minima, accounting for the formation of two anomers in the experiments. The major oxocarbenium ion conformer in the ketofuranoses is the *gg* E_3 envelope, where the minor 3E conformer places the C5 methoxy group in a *gt* position. In the aldose, the lowest energy conformation proved to be the 4T_3 , a structure that slightly deviates from the 3E - E_3 axis. This conformation optimally positions the C5-OMe over the furanosyl ring providing most stabilization. In the ketoxylofuranosyl FES maps, this effect is not observed. In line with the ribo- and arabino-case, the energy difference between the E_3 and 3E oxocarbenium ions for the methyl ketofuranose is somewhat larger than the difference observed in the aldofuranose and somewhat diminished for the phenyl furanosyl oxocarbenium ion. The larger energy difference between the E_3 and 3E methyl xylofuranosyl oxocarbenium ions is not reflected in the experimental results. Over the methyl ketofuranose, the phenyl ketose shows increased preference towards the 3E envelope, while still maintaining the E_3 as the major conformer but decreasing the energy difference between the two envelopes. The more shallow FES map for the phenyl xylofuranosyl oxocarbenium ion is reflected in the diminished stereoselectivity observed in the reduction of phenyl ketoside **13**.

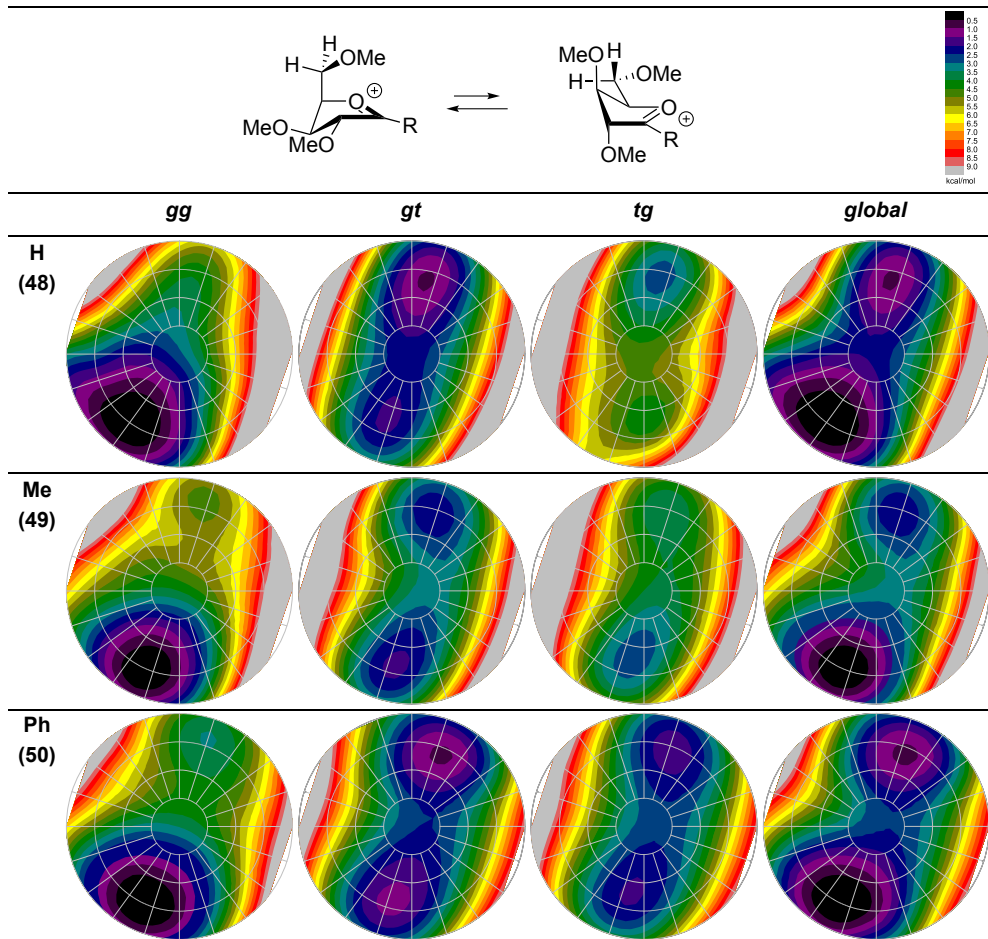


Figure 3.7 The *gg*, *gt*, *tg* and global FES maps of the xylofuranosyl oxocarbenium ions, mapped for the aldose (48), methyl ketose (49) and phenyl ketose (50).

Lyxose

In Figure 3.8, the FES maps for the lyxofuranosyl oxocarbenium ions are mapped for the aldose (51), methyl ketose (52) and phenyl ketose (53). Chapter 2 described the strong preference for the ³*E* lyxofuranosyl oxocarbenium ion envelope and the associated remarkable stereoselectivity in additions on this intermediate (*cis* with respect to *all* ring substituents). This strong conformational preference is maintained in the ketofuranosyl oxocarbenium ions as shown in the global FES maps. In the ³*E* oxocarbenium ion, lyxofuranose places the C2 substituent in the preferred pseudoequatorial position and the C3 substituent in a pseudoaxial position to allow stabilization of the positive charge at the anomeric position. The individual C4-C5 rotamer FES maps show a pseudoequatorial C5 *gt*, avoiding a sterically and electronically unfavorable interaction with the axial C3

substituent. Inside attack on the lyxofuranosyl 3E oxocarbenium ion leads to the all-*cis* addition product in both the aldose and ketoses.

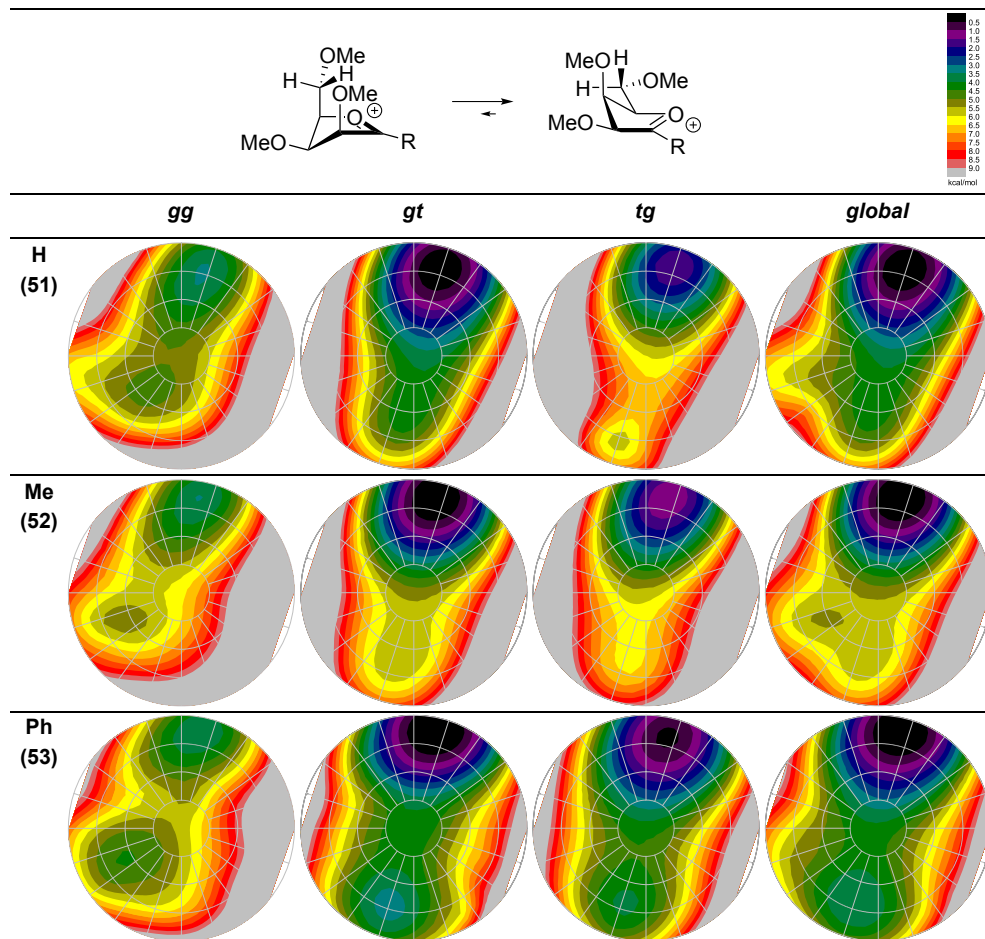


Figure 3.8 The *gg*, *gt*, *tg* and global FES maps of the lyxofuranosyl oxocarbenium ions, mapped for the aldose (**51**), methyl ketose (**52**) and phenyl ketose (**53**).

3.3 Conclusion

Overall it can be concluded that the nature of the anomeric substituent on the studied furanosides has a small effect on the stereoselectivity of the studied reduction reactions. The detailed calculations show that the energy differences between the various oxocarbenium ion conformers are mostly maintained, independent of the nature of the anomeric appendage. Small changes are observed for the methyl/phenyl ketoses with respect to the aldoses. The anomeric methyl substituent makes the preference for one of the two envelopes stronger, where the phenyl substituent leads to smaller energy

differences. This latter effect can be partially attributed to the destabilizing 1,3-allyl strain between the anomeric phenyl ring positioned parallel to the C=O⁺ plane and the pseudoequatorial C2 substituent. Also the general conjugative stabilization of the oxocarbenium by the phenyl ring can lead to diminished relative energies for the different oxocarbenium ion conformers. The differences in energy between the different oxocarbenium ions provide a reliable prediction for the stereoselectivity of reactions on these intermediates using the inside attack model. Notably, substitution reactions at the anomeric center of all furanosides proceed with great stereoselectivity to provide the 1,2-*cis* addition products, independent of the substitution pattern on the carbohydrate ring and the anomeric center.

Experimental section

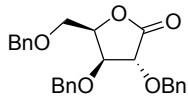
Calculations. In all calculations, methyl ethers were used because of their reduced calculation costs over benzyl ethers. All calculations were performed with DFT *ab initio* calculations with the B3LYP model. The starting conformer for the Free Energy Surface (FES) was optimized by starting from a conformer distribution search option included in the Spartan 04²³ program in gas phase at 6-31G* as basis set. All generated geometries were optimized with Gaussian 03²⁰ at 6-311G**, their zero-point energy (ZPE) corrections calculated, and further optimized with incorporated polarizable continuum model (PCM) to correct for solvation in dichloromethane. The geometry with the lowest, ZPE corrected, solvated free energy was selected as the starting point for the FES. Two dihedral angles of the five-membered ring were constrained, namely C4-O4-C1-C2 (τ_0, θ_3) and C1-C2-C3-C4 (τ_2, θ_0), with angles from -40° up to 40° over 9 steps (10° per step) giving a total of 81 conformers and dictating the entire pseudo rotational space within a maximum amplitude (τ_m) of 40°. All other internal coordinates were unconstrained. The geometries were optimized, their ZPE calculated and corrected for solvation with Gaussian 03 at 6-311G** as above. The FES was visualized as polar contour plot through the Origin 8.5 graphing software by putting the phase angle (P) as θ , the amplitude (τ_m) at r and the energy, corrected for ZPE and optimized in solvent, at the Z-axis. To interrogate all rotamers of the C5 substituent, the starting conformer was modified by rotating the O4-C4-C5-O5 dihedral to each of the three staggered configurations (gauche-gauche = -65°, gauche-trans = 65°, trans-gauche = 175°) and then generating the FES through the above mentioned method generating a total of 243 optimized geometries. These three FESs were graphed individually and in a combined plot by comparing the corrected free energies, and for each point selecting the geometry of lowest energy from the three entities.

Synthesis

General. The Lewis acid mediated reductions of arabinofuranosyl and ribofuranosyl ketoses have been published earlier by van Delft.¹⁷ Chemicals were purchased from Acros Organics and Sigma Aldrich and used as received. All non-commercially available starting materials were synthesized in Chapter 2. THF (Biosolve) was distilled over LiAlH₄ and dichloromethane (Biosolve, amylene stabilized) was distilled over P₂O₅ before being treated and stored over activated 4 Å molecular sieves. All reactions were performed at ambient temperature under an argon atmosphere unless stated otherwise. Reactions were monitored by TLC on Kieselgel 60 F254 (Merck). Compounds were visualized by using UV light (254 nm) or applying a solution of (NH₄)₆Mo₇O₂₄·4 H₂O 25 g/L, (NH₄)₄Ce(SO₄)₄·2 H₂O 10 g/L, 10% H₂SO₄ in H₂O followed by charring (+/- 150 °C). ¹H- and ¹³C-NMR spectra were recorded on a Bruker AV-400 instrument. Chemical shifts (δ) of ¹H and ¹³C spectra are relative to

tetramethylsilane. NMR peak assignments were made using COSY and HSQC experiments, where applicable NOESY and HSQC-HECADE²⁴ experiments were used to determine the stereochemical configuration.

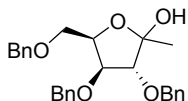
2,3,5-Tri-O-benzyl-D-xylo-1,4-lactone (6). 2,3,5-Tri-O-benzyl-D-xylofuranose (6.9 g, 16.4 mmol) was dissolved



in DMSO (25 ml, 345 mmol). Ac₂O (16 ml, 172 mmol) was added and the reaction was stirred at room temperature for 44 hours after which TLC analysis indicated full conversion. The reaction mixture was quenched with ice water, extracted with Et₂O, the organic layer washed with H₂O and brine, dried over MgSO₄, filtered and concentrated.

The residue was purified by silica gel column chromatography (7.5%-12.5% EtOAc/petroleum ether) to provide the title compound (6.5 g, 15.5 mmol, 95 % yield) as a white solid which was recrystallized from MeOH to provide an analytical sample. *R*_f = 0.80 (25/75 EtOAc/petroleum ether). ¹H NMR (400 MHz, CDCl₃) δ 7.44 – 7.17 (m, 15H, CH_{Ar} Bn), 5.04 (d, *J* = 11.5 Hz, 1H, CHH Bn), 4.69 (d, *J* = 11.4 Hz, 1H, CHH Bn), 4.65 (d, *J* = 11.9 Hz, 1H, CHH Bn), 4.60 – 4.48 (m, 5H, C-4, C-2, 3xCHH Bn), 4.36 (t, *J* = 7.1 Hz, 1H, C-2), 3.76 (dd, *J* = 10.9, 2.8 Hz, 1H, C-5a), 3.70 (dd, *J* = 10.9, 3.2 Hz, 1H, C-5b). ¹³C NMR (101 MHz, CDCl₃) δ 173.4 (C=O), 137.7, 137.4, 137.2 (C_q Bn), 128.6, 128.6, 128.5, 128.4, 128.2, 128.2, 127.8, 127.8, 127.7 (CH_{Ar} Bn), 79.5 (C-3), 77.4 (C-2, C-4), 73.7, 72.8, 72.7 (3xCH₂ Bn), 67.2 (C-5). [α]_D²⁰ = 91.9° (c = 1, CHCl₃). IR (neat): 608, 625, 646, 671, 698, 743, 799, 835, 864, 912, 930, 972, 993, 1024, 1070, 1088, 1105, 1128, 1188, 1213, 1242, 1285, 1344, 1377, 1393, 1454, 1466, 1497, 1732, 1769, 2872, 2909. HR-MS: [M+H]⁺ Calculated for C₂₆H₂₆O₅: 419.18530; found 419.18545.

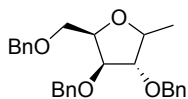
2,3,5-tri-O-benzyl-1-methyl-D-xylofuranose (12). 2,3,5-Tri-O-benzyl-D-xylo-1,4-lactone (6, 252 mg, 0.60



mmol), three times coevaporated with toluene, was dissolved in anhydrous THF (2.5 ml) and cooled to -78 °C. Methyl lithium (0.41 ml, 0.66 mmol, 1.6 M in Et₂O) was added slowly. After 3 hours TLC analysis indicated full conversion. The reaction was quenched by addition of NH₄Cl (2.5 ml, sat. aq.), and the mixture was allowed to warm to room

temperature. The suspension was extracted 3 times with EtOAc and the combined organic layers washed with brine, dried over MgSO₄, filtered and concentrated. The residue was purified by silica gel column chromatography (20%-30% EtOAc/pentane) to provide the title compound (243 mg, 0.56 mmol, 93 % yield) as colorless oil which was used directly in the next step. *R*_f = 0.55 (25/75 EtOAc/pentane).

2,3,5-Tri-O-benzyl-1-deoxy-α/β-1-methyl-D-xylofuranose (30). 2,3,5-tri-O-benzyl-1-methyl-D-xylofuranose (12,

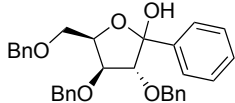


242 mg, 0.56 mmol) three times coevaporated with toluene, was dissolved in anhydrous DCM (7.2 ml) and cooled to -78 °C. Triethylsilane (116 μl, 0.73 mmol) was added before drop wise addition of BF₃·OEt₂ (92 μl, 0.73 mmol). The reaction was stirred for 6 days at -78 °C after which TLC analysis indicated near full conversion, the reaction was

quenched with NaHCO₃ (8 ml, sat. aq.), warmed to room temperature and the suspension extracted with EtOAc (3x). The combined organic layers were washed with H₂O and brine, dried over MgSO₄, filtered and concentrated. The residue was purified by silica gel column chromatography (8%-12% EtOAc/pentane) to provide an anomeric mixture (α/β = 15:85) of the title compound (203 mg, 0.49 mmol, 87 % yield) as a colorless oil. *R*_f = 0.80 (20/80 EtOAc/Petroleum ether). β-Anomer: ¹H NMR (400 MHz, CDCl₃) δ 7.39 – 7.21 (m, 15H, CH_{Ar} Bn), 4.63 (d, *J* = 12.0 Hz, 1H, CHH Bn), 4.56 (d, *J* = 12.1 Hz, 1H, CHH Bn), 4.54 – 4.43 (m, 4H, 4xCHH Bn), 4.18 (ddd, *J* = 6.5, 5.3, 4.1 Hz, 1H, C-4), 3.99 – 3.91 (m, 2H, C-1, C-3), 3.81 – 3.76 (m, 1H, C-5a), 3.73 (dd, *J* = 10.0, 6.5 Hz, 1H, C-5b), 3.65 (dd, *J* = 4.1, 1.3 Hz, 1H, C-2), 1.35 (d, *J* = 6.5 Hz, 3H, CH₃). ¹³C NMR (101 MHz, CDCl₃) δ 138.3, 138.1, 137.9 (3xC_q Bn), 128.6, 128.5, 128.5, 128.4, 128.0, 127.9, 127.9, 127.9, 127.8, 127.7, 127.7, 127.6 (CH_{Ar} Bn), 88.7 (C-2), 83.5 (C-3), 80.1 (C-4), 79.9 (C-1), 73.6, 71.8, 71.8 (3xCH₂ Bn), 68.6 (C-5), 19.9 (CH₃). α-Anomer: ¹H NMR (400 MHz, CDCl₃) δ 7.39 – 7.21 (m, 15H, CH_{Ar} Bn), 4.62 (d, *J* = 12.1 Hz, 1H, CHH Bn), 4.57 – 4.44 (m, 5H, 5xCHH Bn), 4.40 – 4.34 (m, 1H, C-4), 4.32 – 4.25 (m, 1H, C-1), 4.04 (dd, *J* = 4.3, 1.3 Hz, 1H, C-3), 3.78 (dd, *J* = 9.9, 5.3 Hz, 1H, C-2), 3.73 – 3.64 (m, 2H, C-5), 1.27 (d, *J* = 7.0 Hz, 3H, CH₃). ¹³C NMR (101 MHz, CDCl₃) δ 138.4, 138.2, 138.1 (3xC_q Bn), 128.6, 128.4, 128.0, 127.9, 127.9, 127.9, 127.8, 127.7, 127.7, 127.6 (CH_{Ar} Bn), 82.7 (C-2), 82.1 (C-3), 78.5 (C-4), 76.2 (C-1), 73.5,

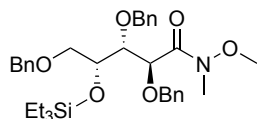
72.4, 72.0 (3xCH₂ Bn), 68.7 (C-5), 14.6 (CH₃). IR (neat): 606, 640, 673, 696, 733, 799, 849, 910, 930, 970, 993, 1026, 1069, 1088, 1190, 1206, 1312, 1344, 1393, 1454, 1497, 1771, 2862, 2913. HR-MS: [M+H⁺] Calculated for C₂₇H₃₀O₄: 419.22169; found: 419.22142.

2,3,5-tri-*O*-benzyl-1-phenyl-*D*-xylofuranose (13). Bromobenzene (76 μ l, 0.70 mmol) was dissolved in THF (1.5 ml) and cooled to -78 $^{\circ}$ C. *n*-Butyl lithium (0.45 ml, 0.70 mmol, 1.6 M in hexanes) was added slowly and the mixture was stirred for 30 minutes. Three times with toluene coevaporated 2,3,5-Tri-*O*-benzyl-*D*-xylono-1,4-lactone (**6**, 230 mg, 0.55 mmol) in anhydrous THF (1.5 ml) was added drop wise. After 2 hours TLC analysis indicated full conversion, the reaction was quenched with NH₄Cl (3 ml, sat. aq.), and the suspension extracted with EtOAc. The organic layer was washed with H₂O and brine, dried over MgSO₄, filtered and concentrated. The residue was purified by silica gel column chromatography (10%-14% EtOAc/pentane) to provide the title compound (250 mg, 0.50 mmol, 91 % yield) as a colorless oil which was used directly in the next step. *R*_f = 0.55 (20/80 EtOAc/pentane).



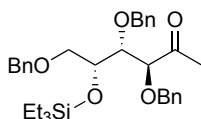
2,3,5-Tri-*O*-benzyl-1-deoxy- α/β -1-phenyl-*D*-xylofuranose (31). 2,3,5-tri-*O*-benzyl-1-phenyl-*D*-xylofuranose (**13**, 238 mg, 0.48 mmol), three times coevaporated with toluene, was dissolved in anhydrous DCM (6.9 ml) and cooled to -78 $^{\circ}$ C. Triethylsilane (103 μ l, 0.65 mmol) was added followed by drop wise addition of BF₃·OEt₂ (82 μ l, 0.65 mmol). After 3 days of stirring at this temperature, TLC analysis indicated full conversion. The reaction was quenched with NaHCO₃ (7 ml, sat. aq.), allowed to warm to room temperature and the suspension extracted with EtOAc (3x). The combined organic layers were washed with H₂O and brine, dried over MgSO₄, filtered and concentrated. The residue was purified by silica gel column chromatography (6-8% EtOAc/pentane) to provide an anomeric mixture (α/β = 25:75) of the title compound (183 mg, 0.38 mmol, 79% yield) as a colorless oil. *R*_f = 0.76 (20/80 EtOAc/petroleum ether). β -Anomer: ¹H NMR (400 MHz, CDCl₃) δ 7.49 – 7.11 (m, 20H, CH_{Ar} Ph, CH_{Ar} Bn), 4.85 (d, *J* = 4.0 Hz, 1H, C-1), 4.67 – 4.39 (m, 6H, 6xCHH Bn), 4.40 – 4.35 (m, 1H, C-4), 4.09 – 4.05 (m, 1H, C-3), 3.99 (dd, *J* = 4.1, 1.4 Hz, 1H, C-2), 3.92 (dd, *J* = 10.0, 5.3 Hz, 1H, C-5a), 3.87 (dd, *J* = 9.9, 6.2 Hz, 1H, C-5b). ¹³C NMR (101 MHz, CDCl₃) δ 140.7 (C_q Ph), 138.3, 138.0, 137.7 (C_q Bn), 128.5, 128.5, 128.4, 128.4, 128.3, 127.9, 127.9, 127.8, 127.7, 127.7, 127.6, 127.5, 127.5, 126.7 (CH_{Ar} Ph, CH_{Ar} Bn), 89.6 (C-2), 86.1 (C-1), 83.3 (C-3), 80.7 (C-4), 73.6, 72.0, 71.5 (3xCH₂ Bn), 68.4 (C-5). α -Anomer: ¹H NMR (400 MHz, CDCl₃) δ 7.44 – 7.13 (m, 18H, CH_{Ar} Ph, CH_{Ar} Bn), 6.93 – 6.86 (m, 2H, CH_{Ar} Ph), 5.21 (d, *J* = 3.5 Hz, 1H, C-1), 4.67 – 4.60 (m, 1H, C-4), 4.59 – 4.39 (m, 4H, 4xCHH Bn), 4.13 (dd, *J* = 4.0, 1.2 Hz, 1H, C-2), 4.10 (d, *J* = 12.3 Hz, 1H, CHH Bn), 4.04 – 4.00 (m, 1H, CHH Bn), 3.96 – 3.93 (m, 1H, C-3), 3.84 – 3.75 (m, 2H, C-5). ¹³C NMR (101 MHz, CDCl₃) δ 140.7 (C_q Ph), 138.4, 138.0, 137.8 (C_q Bn), 128.5, 128.5, 128.4, 128.4, 128.4, 128.3, 127.9, 127.9, 127.8, 127.6, 127.5, 127.5 (CH_{Ar} Ph, CH_{Ar} Bn), 83.2 (C-3), 82.8 (C-2), 82.5 (C-1), 73.5, 72.5, 72.1 (3xCH₂ Bn), 68.6 (C-5). IR (neat): 604, 646, 694, 731, 887, 908, 951, 986, 1003, 1026, 1067, 1206, 1252, 1308, 1358, 1452, 1495, 2860, 2918, 3028. HR-MS: [M+H⁺] Calculated for C₃₂H₃₂O₄: 481.23734; found: 481.23748.

2,3,5-Tri-*O*-benzyl-4-*O*-triethylsilyl-*D*-lyxonic *N,O*-dimethyl hydroxylamide (15). *N,O*-dimethylhydroxylamine-HCl (506 mg, 5.2 mmol), three times coevaporated with toluene, was dissolved in anhydrous THF (8 ml) and cooled to 0 $^{\circ}$ C. AlMe₃ (2M in toluene, 2.4 ml, 4.8 mmol) was added slowly and stirred for 30 minutes. 2,3,5-Tri-*O*-benzyl-*D*-lyxono-1,4-lactone (**7**, 1.0 g, 2.40 mmol) in anhydrous THF (8 ml) was slowly added, stirred for 5 minutes and allowed to warm to room temperature. After 1.5 hours, TLC analysis indicated full conversion. The reaction was quenched using EtOAc and the mixture washed with potassium sodium tartrate (sat. aq.), the aqueous layer was extracted with EtOAc and the combined organic layers washed with brine, dried over MgSO₄, filtered and concentrated. The crude 2,3,5-tri-*O*-benzyl-*D*-lyxonic *N,O*-dimethyl hydroxylamide, three times coevaporated with toluene, was put under argon, dissolved in



anhydrous THF (12 ml) and cooled to 0 °C. Imidazole (245 mg, 3.6 mmol) was added followed by drop wise addition of triethylchlorosilane (1.0 ml, 6.0 mmol) and the mixture stirred for 5 minutes at 0 °C after which the mixture was allowed to warm to room temperature. After overnight stirring, TLC analysis indicated full conversion and the reaction was quenched with NaHCO₃ (sat. aq.). The suspension was extracted with Et₂O and the combined organic layers were washed with brine, the combined aqueous layers were extracted with Et₂O and the combined organic layers dried over MgSO₄, filtered and concentrated. The residue was purified by silica gel column chromatography (14%-16% EtOAc/pentane) to provide the title compound (1.0 g, 1.8 mmol, 73%) as a colorless oil. *R*_F = 0.60 (20/80 EtOAc/pentane). ¹H NMR (400 MHz, CDCl₃) δ 7.38 – 7.17 (m, 15H, CH_{Ar} Bn), 4.88 (d, *J* = 8.8 Hz, 1H, C-2), 4.56 – 4.43 (m, 5H, CHH Bn), 4.40 (d, *J* = 11.9 Hz, 1H, 5xCHH Bn), 4.25 – 4.18 (m, 1H, C-4), 3.95 (dd, *J* = 8.8, 2.2 Hz, 1H, C-3), 3.61 – 3.46 (m, 5H, CH₃N, C-5), 3.13 (s, 3H, CH₃O), 0.92 (t, *J* = 7.9 Hz, 9H, 3xCH₃ TES), 0.67 – 0.49 (m, 6H, 3xCH₂ TES). ¹³C NMR (101 MHz, CDCl₃) δ 172.3 (C=O), 138.7, 138.2, 137.7 (C_q Bn), 128.4, 128.3, 128.2, 127.8, 127.8, 127.6, 127.5 (CH_{Ar} Bn), 80.0 (C-3), 74.9, 73.3 (2xCH₂ Bn), 72.7 (C-2), 71.8 (CH₂ Bn), 71.6 (C-5), 70.8 (C-4), 61.7 (NCH₃), 32.1 (OCH₃), 7.1 (CH₃ TES), 5.4 (CH₂ TES). IR (neat): 613, 694, 731, 787, 956, 999, 1076, 1090, 1142, 1238, 1454, 1663, 2874, 2951. [α]²⁰_D: -3.1 (*c* = 1, CHCl₃). HRMS: [M+H]⁺ Calculated for C₃₄H₄₇NO₆Si: 594.32454; found: 594.32451.

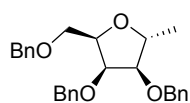
2,3,5-Tri-*O*-benzyl-4-*O*-triethylsilyl-1-methyl-*D*-lyxose (16). 2,3,5-Tri-*O*-benzyl-4-*O*-triethylsilyl-*D*-lyxonic *N,O*-



dimethyl hydroxylamide (**15**, 416 mg, 0.7 mmol), three times coevaporated with toluene, was dissolved in anhydrous THF (4 ml) and cooled to -78 °C. Methyl lithium (0.70 ml, 1.12 mmol, 1.6 M in Et₂O) was added drop wise. After 5 hours of stirring at this temperature, TLC analysis indicated complete conversion. The reaction was quenched with NH₄Cl (sat. aq.), the suspension extracted with Et₂O, the organic layer

washed with water, the combined aqueous layers extracted with Et₂O, the combined organic layers were washed with brine, dried over MgSO₄, filtered and concentrated. The residue was purified by silica gel column chromatography (4%-5% EtOAc/pentane) yielding the title compound (278 mg, 0.51 mmol, 72% yield) as a colorless oil. *R*_F = 0.7 (10/90 EtOAc/pentane). ¹H NMR (400 MHz, CDCl₃) δ 7.36 – 7.23 (m, 15H, CH_{Ar} Bn), 4.64 (d, *J* = 11.7 Hz, 1H, CHH Bn), 4.60 (d, *J* = 11.7 Hz, 1H, CHH Bn), 4.55 (d, *J* = 11.9 Hz, 1H, CHH Bn), 4.51 (d, *J* = 12.4 Hz, 1H, CHH Bn), 4.48 (d, *J* = 12.1 Hz, 1H, CHH Bn), 4.44 (d, *J* = 12.0 Hz, 1H, CHH Bn), 4.11 – 4.07 (m, 1H, C-4), 4.07 (d, *J* = 3.7 Hz, 1H, C-2), 3.94 (dd, *J* = 5.6, 3.7 Hz, 1H, C-3), 3.68 (dd, *J* = 10.3, 3.7 Hz, 1H, C-5a), 3.64 (dd, *J* = 10.3, 5.6 Hz, 1H, C-5b), 2.17 (s, 3H, COCH₃), 0.89 (t, *J* = 7.9 Hz, 9H, CH₃ TES), 0.61 – 0.48 (m, 6H, CH₂ TES). ¹³C NMR (101 MHz, CDCl₃) δ 210.0 (C=O), 138.3, 138.3, 137.7 (C_q Bn), 128.5, 128.4, 127.9, 127.8, 127.7, 127.6 (CH_{Ar} Bn), 84.6 (C-2), 81.8 (C-3), 73.6, 73.3, 72.9 (3xCH₂ Bn), 72.6 (C-4), 72.3 (C-5), 27.9 (C=OCH₃), 7.0 (CH₃ TES), 4.9 (CH₂ TES). IR (neat): 606, 694, 731, 783, 908, 980, 1003, 1026, 1074, 1088, 1207, 1283, 1350, 1414, 1454, 1715, 2874, 2911, 2951. [α]²⁰_D: 0.8 (*c* = 1, CHCl₃). HRMS: [M+H]⁺ Calculated for C₃₃H₄₄O₅Si: 549.30308; found: 549.30337.

2,3,5-Tri-*O*-benzyl-1-deoxy-α-1-methyl-*D*-lyxofuranose (32). 2,3,5-Tri-*O*-benzyl-4-*O*-triethylsilyl-1-methyl-*D*-

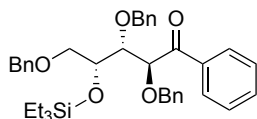


lyxose (**16**, 137 mg, 0.25 mmol), three times coevaporated with toluene, was dissolved in anhydrous DCM (3.1 ml) and cooled to -78 °C. Triethylsilane (52 μl, 0.33 mmol) was added before drop wise addition of BF₃·OEt₂ (82 μl, 0.65 mmol). After 1 week of stirring at this temperature TLC analysis showed partial conversion, with the remainder still

being the starting material. The reaction was quenched with NaHCO₃ (sat. aq.), allowed to warm to room temperature and extracted with Et₂O, the organic layer was washed with water and brine, the combined aqueous layers extracted with Et₂O, the combined organic layers dried over MgSO₄, filtered and concentrated. The residue was purified by silica gel column chromatography (8-13% EtOAc/pentane) yielding the title compound (46 mg, 0.11 mmol, 44% yield) as a single diastereomer. *R*_F = 0.55 (20/80 EtOAc/pentane). ¹H NMR (400 MHz, CDCl₃) δ 7.37 – 7.24 (m, 15H, CH_{Ar} Bn), 4.72 (d, *J* = 11.8 Hz, 1H, CHH Bn), 4.64 – 4.56 (m, 3H, 3xCHH Bn), 4.50 (d, *J* = 11.9 Hz, 1H, CHH Bn), 4.47 (d, *J* = 12.0 Hz, 1H, CHH Bn), 4.27 – 4.21 (m, 1H, C-4), 4.19 – 4.11 (m, 1H, C-1), 4.08 (t, *J* = 4.2 Hz, 1H, C-4), 3.74 (dd, *J* = 9.8, 5.8 Hz, 1H, C-5a), 3.67 (dd, *J* = 9.7, 6.7 Hz, 1H, C-5b), 3.55

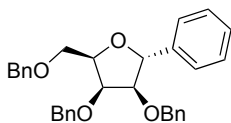
(dd, $J = 7.7, 4.2$ Hz, 1H, C-2), 1.24 (d, $J = 6.3$ Hz, 3H, CH_3). ^{13}C NMR (101 MHz, CDCl_3) δ 138.5, 138.3, 138.0 (C_q Bn), 128.5, 128.4, 128.4, 128.0, 127.9, 127.9, 127.8, 127.7, 127.7 (CH_{Ar} Bn), 85.1 (C-2), 78.6 (C-4), 77.2 (C-3), 75.6 (C-1), 73.6, 73.5, 72.7 (CH_2 Bn), 69.1 (C-5), 19.4 (CH_3). $[\alpha]_D^{20} = 26.6^\circ$ ($c = 1.1$, CHCl_3). IR (neat): 696, 735, 810, 845, 914, 932, 1003, 1026, 1061, 1086, 1146, 1206, 1273, 1312, 1344, 1366, 1452, 1497, 1722, 2866, 2924, 2968. HR-MS: $[\text{M}+\text{H}^+]$ Calculated for $\text{C}_{27}\text{H}_{30}\text{O}_4$: 419.22169; found: 419.22149.

2,3,5-Tri-*O*-benzyl-4-*O*-triethylsilyl-1-phenyl-*D*-lyxose (17).



Bromobenzene (76 μl , 0.72 mmol) was dissolved in anhydrous THF (1 ml) and cooled to -78°C . *n*-Butyl lithium (0.45 ml, 0.72 mmol, 1.6 M in hexanes) was added drop wise and the mixture was stirred at this temperature for 30 minutes. 2,3,5-Tri-*O*-benzyl-4-*O*-triethylsilyl-*D*-lyxonic *N,O*-dimethyl hydroxylamide (**15**, 342 mg, 0.58 mmol), three times coevaporated with toluene, in dry THF (4 ml) was added slowly and the reaction mixture stirred for 18 hours. TLC analysis indicated full consumption of the starting material and the reaction was quenched with NH_4Cl (sat. aq.), the suspension was extracted with Et_2O , the organic layer was washed with water and brine, the combined aqueous layers were extracted with Et_2O , the combined organic layers dried over MgSO_4 , filtered and concentrated. The residue was purified by silica gel column chromatography (4%-7% EtOAc /pentane) to provide the title compound (210 mg, 0.34 mmol, 60% yield) as a colorless oil. $R_f = 0.80$ (10/90 EtOAc /pentane). ^1H NMR (400 MHz, CDCl_3) δ 8.06 – 7.98 (m, 2H, *m*- CH_{Ar} Ph), 7.53 – 7.45 (m, 1H, *p*- CH_{Ar} Ph), 7.39 – 7.33 (m, 2H, *o*- CH_{Ar} Ph), 7.32 – 7.21 (m, 10H, CH_{Ar} Bn), 7.16 – 7.09 (m, 3H, CH_{Ar} Bn), 6.95 – 6.89 (m, 2H, CH_{Ar} Bn), 5.14 (d, $J = 7.4$ Hz, 1H, C-2), 4.56 (d, $J = 11.2$ Hz, 1H, CHH Bn), 4.45 (d, $J = 12.0$ Hz, 1H, CHH Bn), 4.42 – 4.34 (m, 3H, $3\times\text{CHH}$ Bn), 4.29 (d, $J = 11.4$ Hz, 1H, CHH Bn), 4.27 – 4.20 (m, 1H, C-4), 4.04 (dd, $J = 7.4, 3.1$ Hz, 1H, C-3), 3.59 – 3.50 (m, 2H, C-5), 0.91 (t, $J = 7.9$ Hz, 9H, CH_3 TES), 0.63 – 0.52 (m, 6H, CH_2 TES). ^{13}C NMR (101 MHz, CDCl_3) δ 200.4 (C=O), 138.1, 137.8, 137.5, 137.1 (C_q Ph, C_q Bn), 133.2 (*p*- CH_{Ar} Ph), 129.0 (*m*- CH_{Ar} Ph), 128.4, 128.3, 128.1, 128.0, 127.8, 127.8, 127.6, 127.4 (CH_{Ar} Bn, *o*- CH_{Ar} Ph), 80.9 (C-3), 79.7 (C-2), 74.2, 73.2, 72.0 (CH_2 Bn), 71.7 (C-4), 71.5 (C-5), 7.1 (CH_3 TES), 5.2 (CH_2 TES). IR (neat): 652, 694, 735, 802, 824, 845, 812, 1001, 1026, 1070, 1090, 1177, 1207, 1248, 1269, 1315, 1362, 1395, 1452, 1688, 1722, 2874, 2951. $[\alpha]_D^{20}$: 3.2 ($c = 1$, CHCl_3). HRMS: $[\text{M}+\text{H}^+]$ Calculated for $\text{C}_{38}\text{H}_{46}\text{O}_5\text{Si}$: 611.31873; found: 611.31904.

2,3,5-Tri-*O*-benzyl-1-deoxy- α -1-phenyl-*D*-lyxofuranose (33).



2,3,5-Tri-*O*-benzyl-4-*O*-triethylsilyl-1-phenyl-*D*-lyxose (**17**, 70 mg, 0.12 mmol), three times coevaporated with toluene, was dissolved in anhydrous DCM (1.4 ml) and cooled to -78°C . Triethylsilane (24 μl , 0.15 mmol) was added before drop wise addition of $\text{BF}_3\cdot\text{OEt}_2$ (38 μl , 0.30 mmol). After 1 week of stirring at this temperature TLC analysis showed partial conversion, with the remainder still being the starting material. The reaction was quenched NaHCO_3 (sat. aq.), the suspension was extracted with Et_2O , the organic layer was washed with water and brine, the combined aqueous layers were extracted with Et_2O , the combined organic layers were dried over MgSO_4 , filtered and concentrated. The residue was purified by silica gel column chromatography (8-10% EtOAc /pentane) yielding the title compound (43 mg, 0.09 mmol, 77 % yield) as a single diastereomer. $R_f = 0.60$ (10/90 EtOAc /pentane). ^1H NMR (400 MHz, CDCl_3) δ 7.40 – 7.21 (m, 18H, CH_{Ar} Bn, CH_{Ar} Ph), 7.18 – 7.09 (m, 2H, $2\times\text{CH}_{Ar}$ Ph), 5.05 (d, $J = 7.7$ Hz, 1H, C-2), 4.79 (d, $J = 11.8$ Hz, 1H, CHH Bn), 4.63 (d, $J = 11.7$ Hz, 1H, CHH Bn), 4.61 (d, $J = 11.9$ Hz, 1H, CHH Bn), 4.53 (d, $J = 11.9$ Hz, 1H, CHH Bn), 4.50 – 4.42 (m, 2H, C-4, CHH Bn), 4.40 (d, $J = 12.1$ Hz, 1H, CHH Bn), 4.17 (t, $J = 4.1$ Hz, 1H, C-3), 3.91 – 3.83 (m, 2H, C-2, C-5a), 3.78 (dd, $J = 9.8, 6.4$ Hz, 1H, C-5b). ^{13}C NMR (101 MHz, CDCl_3) δ 141.1 (C_q Ph), 138.4, 138.3, 137.8 (C_q Bn), 128.5, 128.5, 128.5, 128.4, 127.8, 127.7, 127.6, 126.2 (CH_{Ar} Ph, CH_{Ar} Bn), 86.2 (C-2), 81.3 (C-1), 79.6 (C-4), 77.5 (C-3), 73.7, 73.6, 72.6 (CH_2 Bn), 69.2 (C-5). $[\alpha]_D^{20} = 25.8^\circ$ ($c = 1$, CHCl_3). IR (neat): 652, 694, 729, 752, 833, 887, 920, 961, 984, 1007, 1026, 1053, 1084, 1101, 1144, 1159, 1204, 1360, 1452, 1493, 2859, 2884, 2899, 2949, 3030. HR-MS: $[\text{M}+\text{H}^+]$ Calculated for $\text{C}_{32}\text{H}_{32}\text{O}_4$: 481.23734; found: 481.23746.

References and notes

- [1] Wu, Q. P.; Simons, C. *Synthesis* **2004**, 1533-1553, 10.1055/s-2004-829106.
- [2] Stambasky, J.; Hocek, M.; Kocovsky, P. *Chem. Rev.* **2009**, *109*, 6729-6764, 10.1021/cr9002165.
- [3] Wellington, K. W.; Benner, S. A. *Nucleos. Nucleot. Nucl.* **2006**, *25*, 1309-1333, 10.1080/15257770600917013.
- [4] Charette, M.; Gray, M. W. *IUBMB Life* **2000**, *49*, 341-351, 10.1080/152165400410182.
- [5] Meng, W.; Ellsworth, B. A.; Nirschl, A. A.; McCann, P. J.; Patel, M.; Girotra, R. N.; Wu, G.; Sher, P. M.; Morrison, E. P.; Biller, S. A.; Zahler, R.; Deshpande, P. P.; Pullockaran, A.; Hagan, D. L.; Morgan, N.; Taylor, J. R.; Obermeier, M. T.; Humphreys, W. G.; Khanna, A.; Discenza, L.; Robertson, J. G.; Wang, A.; Hang, S.; Wetterau, J. R.; Janovitz, E. B.; Flint, O. P.; Whaley, J. M.; Washburn, W. N. *J. Med. Chem.* **2008**, *51*, 1145-1149, 10.1021/jm701272q.
- [6] Roy-Burman, S.; Roy-Burman, P.; Visser, D. W. *Cancer Res.* **1968**, *28*, 1605-1610.
- [7] Hosoya, T.; Takashiro, E.; Matsumoto, T.; Suzuki, K. *J. Am. Chem. Soc.* **1994**, *116*, 1004-1015, 10.1021/ja00082a023.
- [8] Cortezano-Arellano, O.; Melendez-Becerra, C. A.; Cortes, F.; Sartillo-Piscil, F.; Cordero-Vargas, A. *Carbohydr. Res.* **2014**, *393*, 51-59, 10.1016/j.carres.2014.04.005.
- [9] Calzada, E.; Clarke, C. A.; Roussinbouchard, C.; Wightman, R. H. *J. Chem. Soc., Perkin Trans. 1* **1995**, 517-518, 10.1039/p19950000517.
- [10] Liu, W. M.; Wise, D. S.; Townsend, L. B. *J. Org. Chem.* **2001**, *66*, 4783-4786, 10.1021/jo001555f.
- [11] Centrone, C. A.; Lowary, T. L. *J. Org. Chem.* **2002**, *67*, 8862-8870, 10.1021/jo026247r.
- [12] Sollogoub, M.; Fox, K. R.; Powers, V. E. C.; Brown, T. *Tetrahedron Lett.* **2002**, *43*, 3121-3123, 10.1016/s0040-4039(02)00481-1.
- [13] Terauchi, M.; Abe, H.; Matsuda, A.; Shuto, S. *Org. Lett.* **2004**, *6*, 3751-3754, 10.1021/ol048525+.
- [14] Peifer, M.; Berger, R.; Shurtleff, V. W.; Conrad, J. C.; MacMillan, D. W. C. *J. Am. Chem. Soc.* **2014**, *136*, 5900-5903, 10.1021/ja502205q.
- [15] Metobo, S. E.; Xu, J.; Saunders, O. L.; Butler, T.; Aktoudianakis, E.; Cho, A.; Kim, C. U. *Tetrahedron Lett.* **2012**, *53*, 484-486, 10.1016/j.tetlet.2011.11.055.
- [16] Hernández, A. R.; Kool, E. T. *Org. Lett.* **2011**, *13*, 676-679, 10.1021/ol102915f.
- [17] van Delft, P., **2013**, *Synthetic Studies Towards Oligonucleotide Derivatives and Conjugates*, Ph.D Thesis, Leiden University.

- [18] Rhoad, J. S.; Cagg, B. A.; Carver, P. W. *J. Phys. Chem. A* **2010**, *114*, 5180-5186, 10.1021/jp9100448.
- [19] Altona, C.; Sundaralingan, M. *J. Am. Chem. Soc.* **1972**, *94*, 8205-8212, 10.1021/ja00778a043.
- [20] Gaussian 03 (Revision E.01), Frisch, M. J. *et al.*, Gaussian, Inc. **2004**.
- [21] The graphs of the ribofuranosyl, methyl ribofuranosyl and phenyl ribo-furanosyl oxocarbenium ions have not been normalized with respect to each other, and can therefore not be compared to each other.
- [22] Allinger, N. L.; Hirsch, J. A.; Miller, M. A.; Tyminski, I. J. *J. Am. Chem. Soc.* **1969**, *91*, 337-343, 10.1021/ja01030a022.
- [23] Spartan '04, Kong, J. *et al.*, Wavefunction Inc. **2004**.
- [24] Daranas, A. H.; Napolitano, J. G.; Gavin, J. A.; Garcia, C.; Norte, M.; Fernandez, J. J. *Chem. Eur. J.* **2011**, *17*, 6338-6347, 10.1002/chem.201100412.

Chapter 4

Chiral Pyrroline-Based Ugi-Three-Component Reactions Are Under Kinetic Control

partly published in
Organic Letters **2013**, *15*, 3026-3029, 10.1021/ol4012053

4.1 Introduction

The Ugi reaction is one of the most widely used multicomponent reactions and has found extensive application in the generation of structural diversity in diverse compound libraries.¹⁻³ In the classic Ugi four-component reaction, an aldehyde, an amine, a carboxylic acid, and an isocyanide are combined to form a diamide motif. In this event, the aldehyde

is condensed with the amine to generate an imine (**3**, Figure 4.1a). This species is protonated by the carboxylic acid component to provide an iminium ion (**4**), which is attacked by the isocyanide to generate a nitrilium ion (**5**). This cation is intercepted by the carboxylate to form an intermediate imidate (**6**). Mumm rearrangement of this imidate leads to the final Ugi product (**7**).⁴ In the closely related Ugi-three-component reaction, preformed imines are made to react with an isocyanide and a carboxylic acid. As a result of an Ugi multicomponent reaction, a new chiral center is formed between the two newly created amide functions and it is often assumed that the stereoselectivity in the reaction is determined by the irreversible Mumm rearrangement, which terminates the series of preceding equilibria.¹⁻⁵

Chiral carbohydrate-derived azidoaldehydes (exemplified by pentose derived 4-azidoaldehyde **8**) have been explored to generate cyclic imines as a starting point for an ensuing Ugi three-component reaction process (see Figure 4.1b-c).⁶⁻⁹ During the course of these investigations it was observed that some of these reactions proceeded with excellent stereoselectivity while others provided diastereomeric products with little or no selectivity.¹⁰⁻¹⁶ For example, the D-lyxo configured pyrroline (**12**) gave after Ugi reaction with a variety of isocyanides and carboxylates exclusively the all-*cis* pyrrolidines, whereas the D-arabino configured pyrroline (**13**) provided the 1,2-*cis*- and 1,2-*trans*-products in almost equal amounts.^{9,17} The stereochemical course of these reactions is obviously guided by the configuration of the starting imine, but is not easily explained by considering the Mumm rearrangement as the stereoselectivity determining step. Would this be true, then formation of the thermodynamically more stable product would be expected. This chapter describes experimental and computational studies on the Ugi three-component reaction of all four possible 4-deoxy-4-azido-D-pentose derived pyrrolines **12-15**. The results indicate that the stereoselectivity of these Ugi multicomponent reactions is based on kinetic control and is determined at the stage of attack of the isocyanide at the iminium ion.

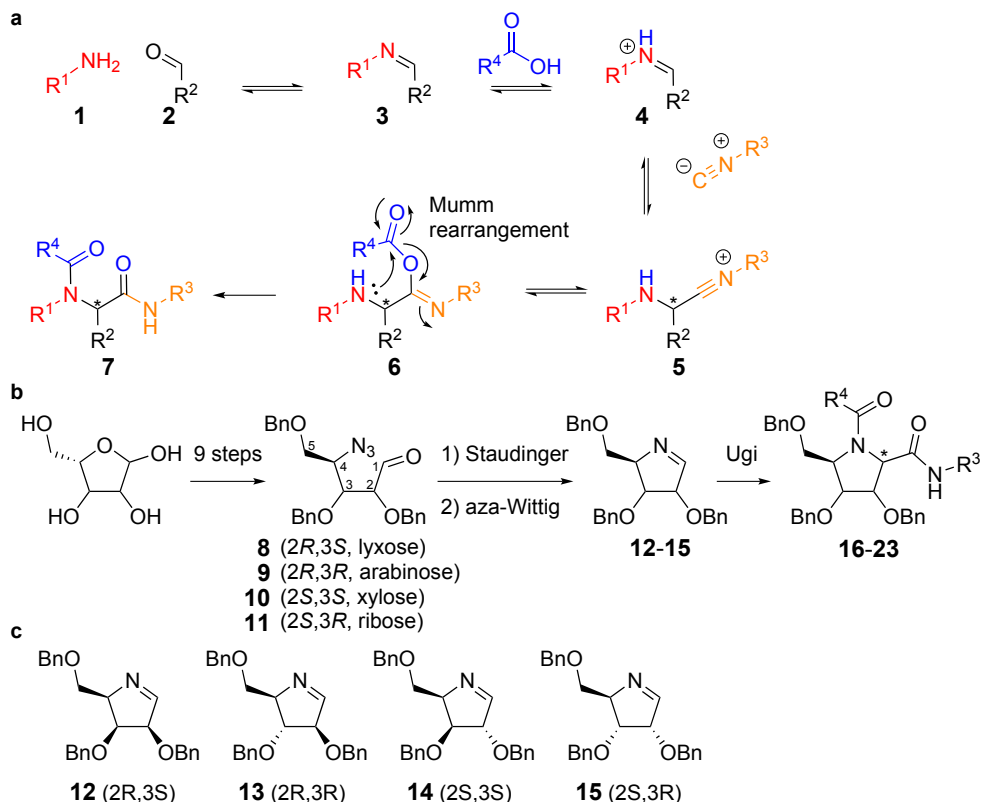
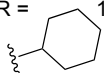
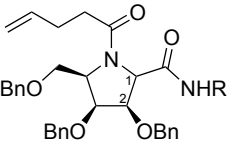
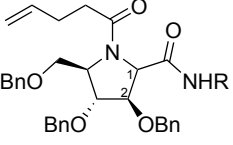
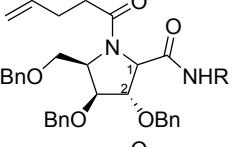
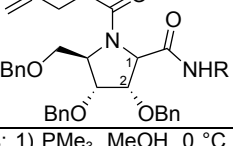


Figure 4.1 a) The Ugi multi-component reaction. b) The Ugi reaction on a preformed pyrroline, generated from a D-pentose derived 4-azido aldehyde, through a Staudinger-aza-Wittig reaction. c) the four investigated pentofuranosyl imines.

4.2 Results and discussion

The four diastereomeric pentose-derived azidoaldehydes used in this study, **8** (D-lyxo), **9** (D-arabino), **10** (D-xylo), and **11** (D-ribo), and corresponding imines (**12-15**) are depicted in Figure 4.1. Table 4.1 shows the results of the Ugi reaction of these imines with either *tert*-butyl isocyanide or cyclohexyl isocyanide and pent-4-enoic acid. To fully establish the stereochemistry of the newly formed stereocenters in products **16-23**, the pentenoyl groups, which give rise to rotameric product mixtures, were removed by iodine mediated hydrolysis (Table 4.2). The structures of the resulting products (**24-31**) were unambiguously established with ^1H and ^{13}C NMR spectroscopy.

Table 4.1 Products of the Ugi reaction on D-pentose derived pyrrolidines **12-15**.^[a]

azido-aldehyde	imine	Ugi product	R =  1,2- <i>cis</i> :1,2- <i>trans</i> ^[b] yield ^[c]	R =  1,2- <i>cis</i> :1,2- <i>trans</i> ^[b] yield ^[c]
8	12		>98:2 (16a) (16b) 55%	>98:2 (17a) (17b) 60%
9	13		58:42 (18a) (18b) 50%	54:46 (19a) (19b) 61%
10	14		43:57 (20a) (20b) 39%	45:55 (21a) (21b) 37%
11	15		>98:2 (22a) (22b) 49%	>98:2 (23a) (23a) 51%

^[a]Reaction conditions: 1) PMe_3 , MeOH, 0 °C 2) pent-4-enoic acid, RNC, MeOH, 0 °C. ^[b]Product ratios are determined by ^1H NMR at 393K to allow free rotation around the newly formed tertiary amide bond. Stereochemistry was assessed using NOESY NMR spectra of the individual deacylated products. ^[c]Yield of isolated furanosides after column chromatography.¹⁸

Table 4.2 Iodine mediated hydrolysis of the 4-pentenoyl group.

R=	Lyxose		Arabinose		Xylose		Ribose	
	tBu (16a)	Cy (17a)	tBu (18a,18b)	Cy (19a,19b)	tBu (20a,20b)	Cy (21a,21b)	tBu (22a)	Cy (23a)
<i>cis</i>	(24) 78%	(25) 71%	(26a) 52%	(27a) 85%	(28a) 75%	(29a) 51%	(30) 44%	(31) 29%
<i>trans</i>			(26b) 60%	(27b) 80%	(28b) 89%	(29b) 60%		

Reaction conditions: I_2 , THF, H_2O .

The Ugi three-component reaction on lyxo-configured imine **12** proceeded with excellent 1,2-*cis* stereoselectivity to provide the all-*cis*-linked pyrrolidines **16a** and **17a**, in line with previous observations. A similar stereochemical outcome is observed for the ribo-configured imine **15**, with only the 1,2-*cis* pyrrolidines **22a** and **23a** formed. In contrast, Ugi three-component reaction on the arabino- and xylo-configured imines (**13** and **14**) proceeded with virtually no stereoselectivity. The stereochemical outcome of the Ugi

reaction cannot be rationalized through appreciation of the steric interactions in products **16-23**. For example, unfavorable 1,2-*cis* interactions would already be manifest in the imidate intermediates (**6**), thereby eliminating the Mumm rearrangement as the step governing the stereochemical outcome of the reaction. Rather, the parallels between the stereochemical course of C-allylation reactions on furanosyl oxocarbenium ions as reported by Woerpel and co-workers¹⁹⁻²⁰ and those described in Chapter 2 and the stereochemical outcome of the Ugi three-component reactions described here, become apparent. Woerpel and coworkers proposed a model to account for the stereoselectivity observed in C-allylation reactions of furanosides based on the conformational preferences of the intermediate oxocarbenium ions. They reasoned that the orientational preferences of the ring substituents dictate the relative stabilities of the oxocarbenium ion envelope conformers and this was confirmed by calculations in Chapter 2. Alkoxy substituents at C2 and C3 preferentially take up an equatorial and axial position, respectively (as in **33a**, see Figure 4.2). The C4 alkyl substituent does not have a strong preference for either orientation but can play an important role in combination with the other ring substituents through mutual steric interactions (see Chapter 2). Nucleophiles would then approach the intermediate envelope oxocarbenium ions preferentially from the “inside” (the side of the envelope *syn* to the carbon atom which lies out of the envelope plane) to avoid developing eclipsing interactions with the neighboring ring substituent. A final contributing factor is the steric interaction between the substituents and the incoming nucleophile. When these conformational preferences are translated to the iminium ions at hand it becomes clear that the D-lyxo iminium ion preferentially adopts an ³*E*-conformation (**35a** Figure 4.2), allowing the C2 and C3 substituents to take up a preferred orientation. Inside attack on this iminium ion leads to the all *cis*-product. In the same vein, the D-ribo iminium ion prefers the *E*₃-envelope and inside attack on this conformer accounts for the formation of the 1,2-*cis* products. For the D-arabino and the D-xylo iminium ions the substituent preferences are conflicting, resulting in a mixture of iminium ion conformers of comparable stability and thereby leading to a mixture of diastereomeric products.

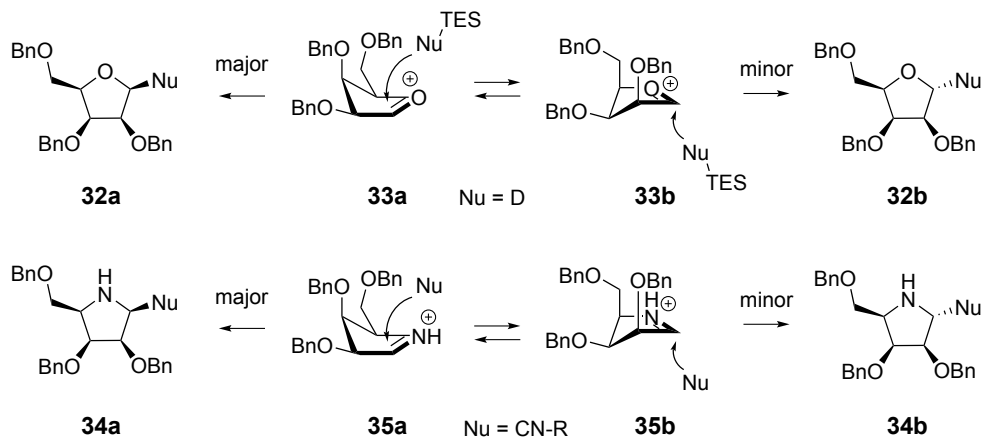


Figure 4.2 D-Lyxose oxocarbenium conformers **33a** and **33b** attacked by [D]triethylsilane and D-lyxo configured iminium ion conformers **35a** and **35b** attacked by an isocyanide.

To gain more insight into the course of the Ugi reactions on pentose derived pyrrolines, a quantum mechanical DFT study²¹⁻²² was performed, in which the relative energies of the intermediates through which the reaction passes were calculated for all four diastereomeric imines, starting from either envelope conformer. The calculations were performed at the B3LYP/6-31G* level with inclusion of the solvent (methanol) through a Polarized Continuum Model and employed methyl substituted imines, methyl isocyanide, and acetic acid as reaction partners.²³ Energies of the individual reactants were added to the energies of the protonated imines and the nitrilium species in order to compare relative energies. In addition, transition states were calculated for the attack of the isocyanide on the protonated imines.

Figure 4.3 (top) shows the reaction pathway energy diagram of the D-lyxo configured imine **12** starting at the protonated imine (**36**). The pathway shows two exothermic steps, one, the formation of the imidate (**39**) from the nitrilium ion (**38**) and, the other, the Mumm rearrangement, proceeding through a cyclic intermediate²⁴ (**40**) that is higher in energy than the preceding imidate.²⁵ The large drop in energy in going from the nitrilium ion to the imidate indicates that the addition of the carboxylate to the nitrilium ion is essentially nonreversible. Therefore the stereochemistry of the Ugi reaction is determined before this event. The calculations provide support for the two conformer hypothesis, described above. Two low energy envelope conformations were found for the D-lyxo iminium ion (**36a** and **36b**), of which the ³E-envelope ion (**36a**) is the one lower in energy. This conformer places the C2 and C3 substituents in favorable positions while steric interactions between the C2 and C4 substituent are minimal in this structure. Notably, the difference in energies between the conformers is larger in the two transition states (**37a**

and **37b**) in which the isocyanide attacks the iminium ions than in the starting envelope conformers **36a** and **36b**. This contrasts the perception that steric interactions between the axially oriented C3 substituent and the incoming nucleophile make transition state **37a** less favorable. A close inspection of transition state **37a** for the attack on the methyl isocyanide on the 3E iminium ion reveals that the C3 substituent actually approaches the incoming nucleophile. A possible explanation for this approach is the electrostatic stabilization of the positive charge that develops on the isocyanide carbon atom by the C3 oxygen substituent while the addition progresses.²⁶⁻²⁷ Figure 4.3 (middle) depicts the course of the addition and shows the ${}^3E \rightarrow {}^3T_2^\ddagger \rightarrow E_2$ reaction trajectory in which the stabilizing interaction of the C3-substituent and the incoming nucleophile becomes clear. The calculated difference in energy between the two transition states ($\Delta\Delta E^\ddagger = 2.5 \text{ kcal mol}^{-1}$; 1,2-*cis*:1,2-*trans*, **37a**:**37b** = 98:2) corroborates the observed stereoselectivity in the Ugi reaction of imine **12** (experimental 1,2-*cis*:1,2-*trans* = >98:2).

The Free Energy Surface (FES) maps, introduced in Chapter 2, for D-lyxo configured imine **36** (Figure 4.3 bottom) corroborates the finding of two low energy conformers **36a** and **36b**. The energy difference between these 3E and E_3 envelopes obtained with the initial conformer search (Scheme 4.3 top) and the FES maps (Figure 4.3 bottom) is consistent (1.8 vs 1.9 kcal mol⁻¹). In both envelopes, the *gt* rotamer is lowest in energy as steric repulsions are avoided that are present in the *gg* rotamer (description of the rotamers can be found in Chapter 2).

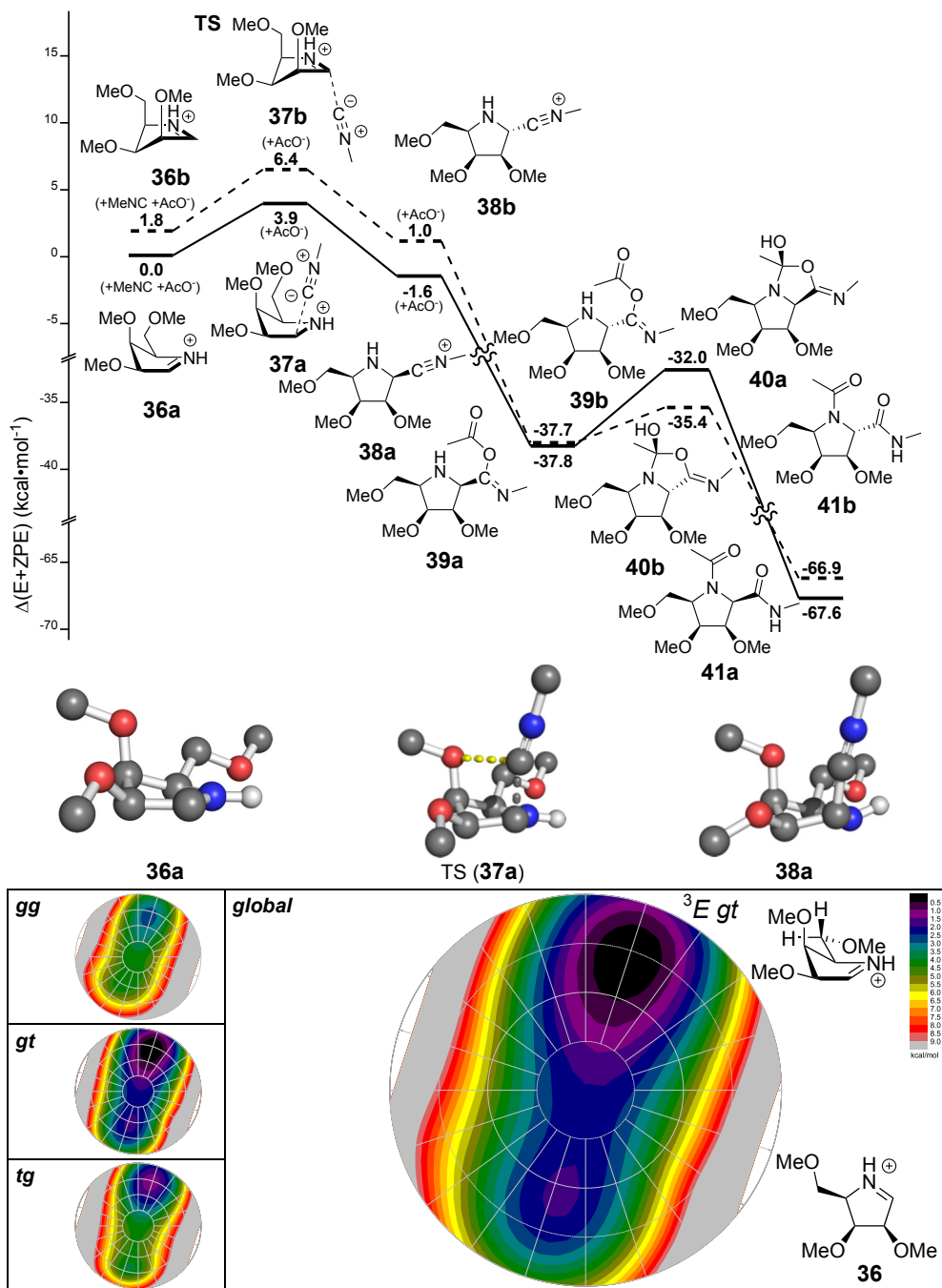


Figure 4.3 Top: Energy diagram of the Ugi reaction on the d-lyxo configured imine starting at the iminium ion. Energies are given relative to the combined energy of the ³*E* iminium ion (36a) and its reaction partners. Middle: Optimized structures of the d-lyxo ³*E* iminium ion (36a), the transition state (37a) of the attack of the isocyanide on this ion and the resulting nitrilium ion (38a). Bottom: FES map of d-lyxo configured iminium ion 36.

The other three imine stereoisomers show similar energy diagrams (see Figure 4.6-4.6 top), indicating that the reaction pathways of the Ugi reactions of these imines are comparable to the one described for the D-lyxo imine.²⁸ The relative energies of the iminium ion envelope conformers, the transition states of the corresponding isocyanide additions, and the resulting nitrilium ions are summarized in Table 4.3. Although the overall reaction pathways are similar there are important differences to note. For both the D-arabino and D-xylo configured iminium ions, the energy difference between the transition states of the isocyanide additions is smaller than the difference in energy between the starting envelope conformers. Also here the stabilizing interaction of the axially oriented C3-substituent with the nucleophile becomes apparent. For example, while the D-xylo configured E_3 iminium ion is favored over its 3E counterpart by 1 kcal mol⁻¹, the transition state originating from the latter ion is slightly lower in energy than the transition state derived from the former. The D-ribo Ugi reaction energy profile parallels that of its D-lyxo congener. The difference in energy between the two isocyanide addition transition states is larger than the energy difference between the parent iminium ion envelopes leading to the selective formation of the 1,2-*cis*-nitrilium ion and subsequently the 1,2-*cis*-Ugi product. The calculated energy differences between the transition states nicely match the experimental stereoselectivities for the four diastereomeric imines as summarized in Table 4.3. Finally, the calculations confirm that the relative stabilities of the Ugi products cannot account for the observed selectivities.

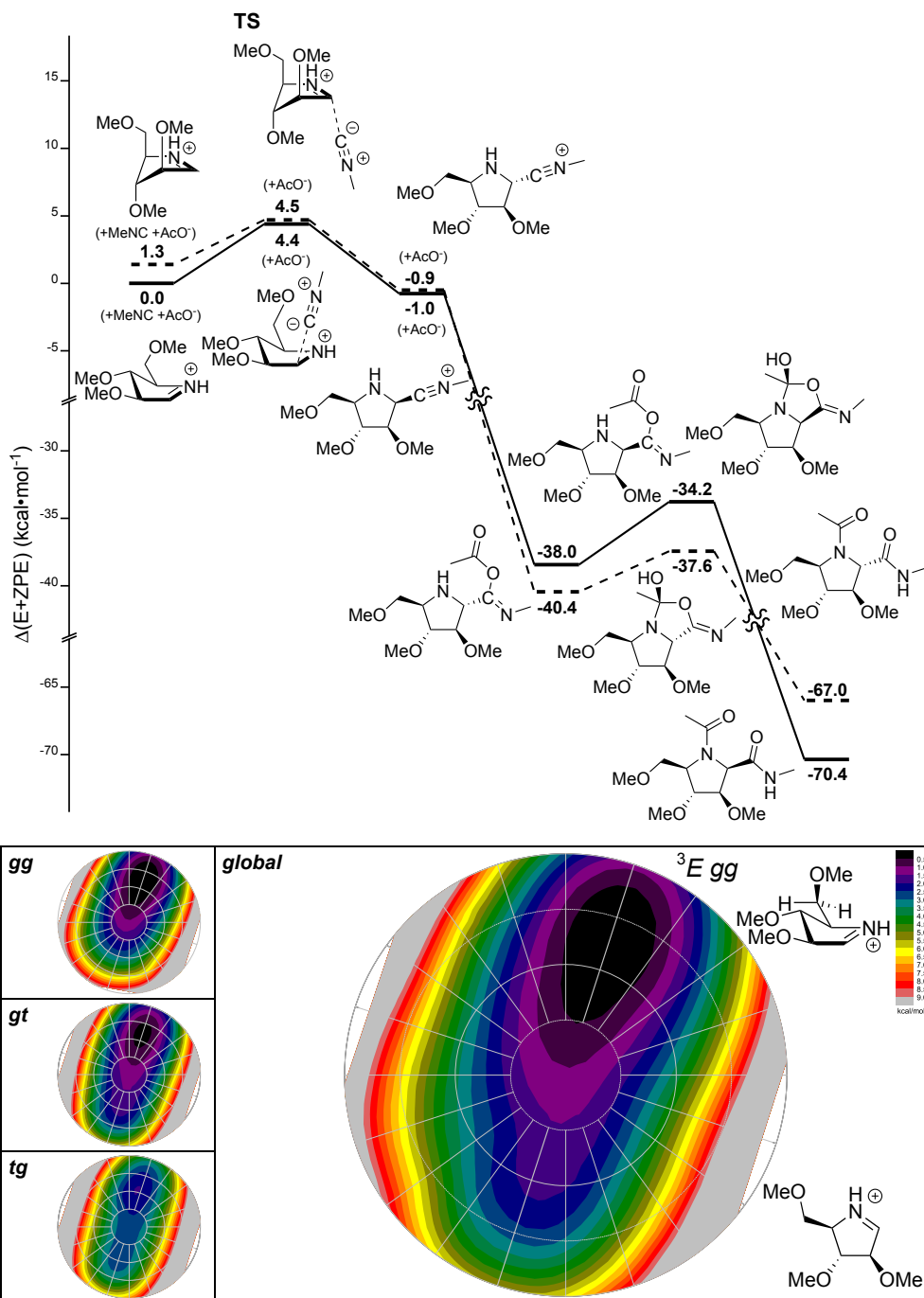


Figure 4.4 Top: Energy diagram of the Ugi reaction on the D-arabino configured imine. Energies are given relative to the combined energy of the 3E iminium ion and its reaction partners. Bottom: FES map of D-arabino configured iminium ion.

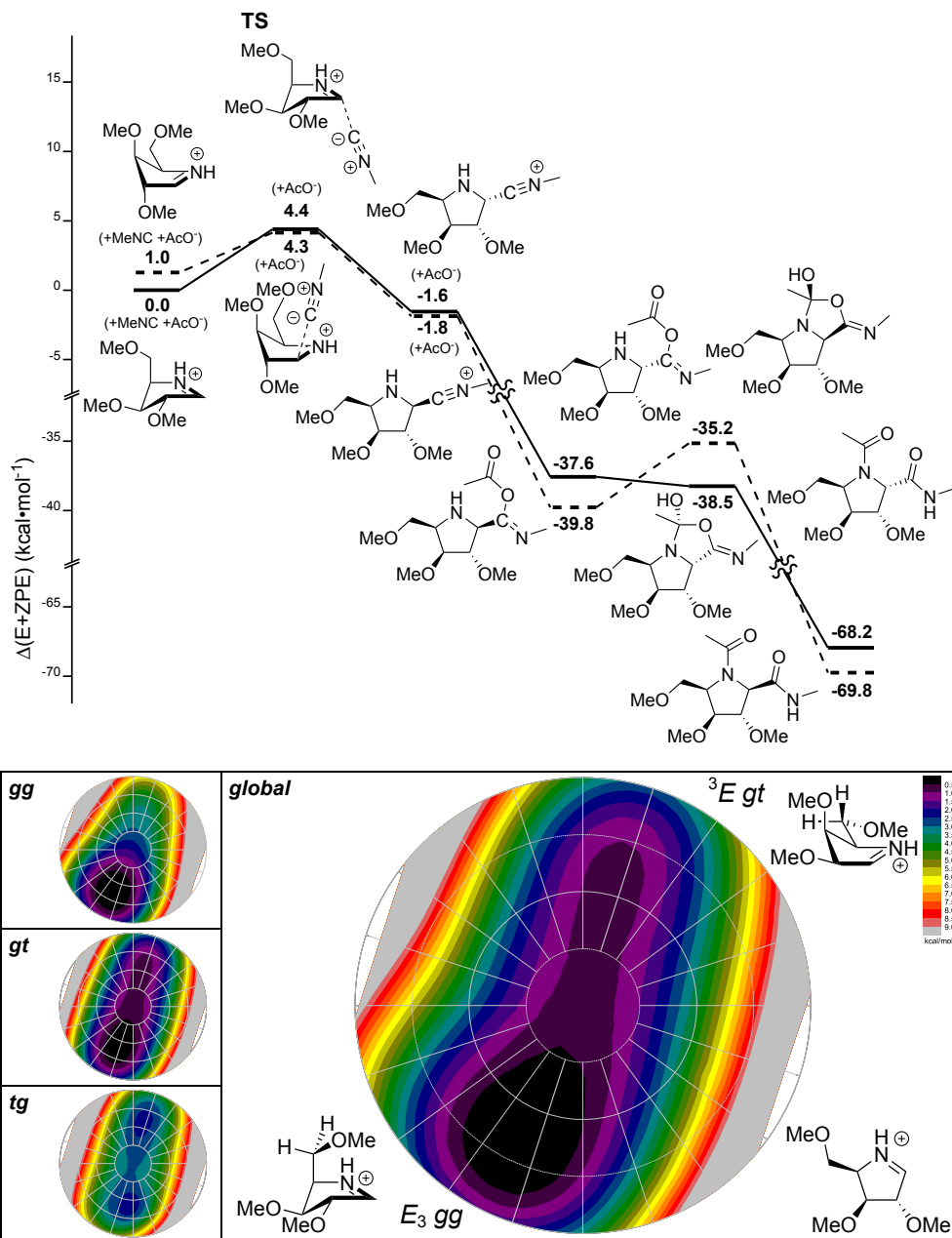


Figure 4.5 Top: Energy diagram of the Ugi reaction on the D-xylo configured imine. Energies are given relative to the combined energy of the E_3 iminium ion and its reaction partners. Bottom: FES map of D-xylo configured iminium ion.

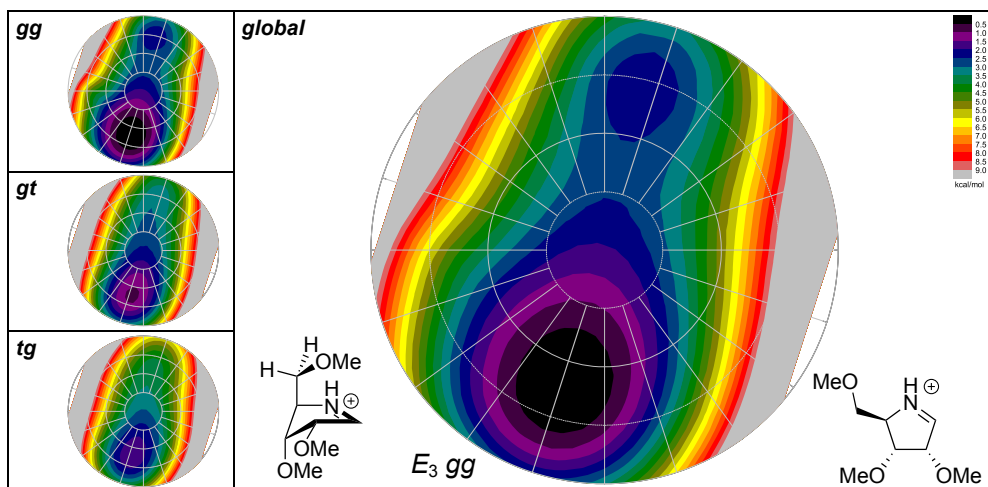
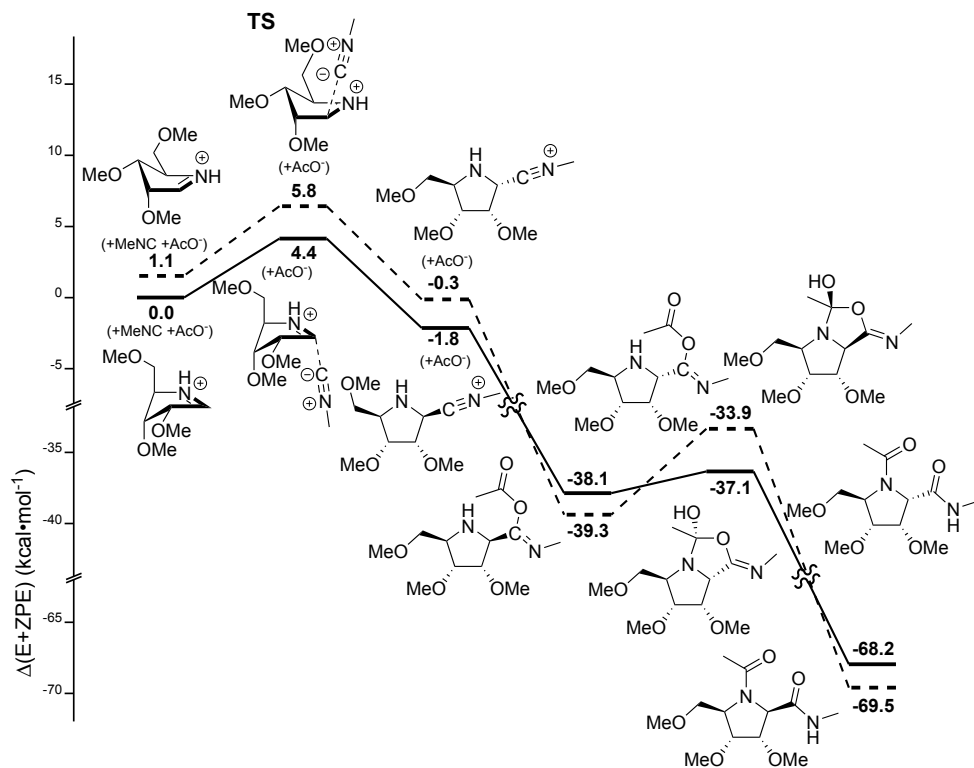


Figure 4.6 Top: Energy diagram of the Ugi reaction on the D-ribo configured imine. Energies are given relative to the combined energy of the E_3 iminium ion and its reaction partners. Bottom: FES map of D-ribo configured iminium ion.

Table 4.3 Relative energies of iminium ion conformers, transition states, nitrilium ions and theoretical product ratios.

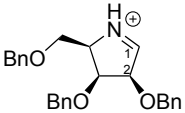
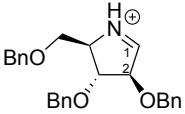
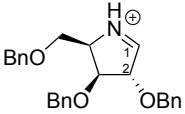
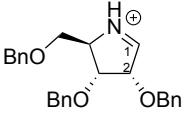
starting iminium ions	products	iminium ions (kcal mol ⁻¹)	TSs (kcal mol ⁻¹)	nitrilium ions (kcal mol ⁻¹)
<i>Lyxo</i>	1,2- <i>cis</i> (16a)	<i>E</i> ₃ : 0.0	<i>E</i> ₃ : 3.9	-1.6
	1,2- <i>trans</i> (16b)	³ <i>E</i> : 1.8	³ <i>E</i> : 5.4	1.0
			$\Delta\Delta E^\ddagger = 2.5$	(16a:16b = 98:2)
<i>Arabino</i>	1,2- <i>cis</i> (18a)	³ <i>E</i> : 0.0	³ <i>E</i> : 4.4	-1.0
	1,2- <i>trans</i> (18b)	<i>E</i> ₃ : 1.3	<i>E</i> ₃ : 4.5	-0.9
			$\Delta\Delta E^\ddagger = -0.1$	(18a:18b = 55:45)
<i>Xylo</i>	1,2- <i>cis</i> (20a)	<i>E</i> ₃ : 0.0	<i>E</i> ₃ : 4.4	-1.6
	1,2- <i>trans</i> (20b)	³ <i>E</i> : 1.0	³ <i>E</i> : 4.3	-1.8
			$\Delta\Delta E^\ddagger = 0.1$	(20a:20b = 45:55)
<i>Ribo</i>	1,2- <i>cis</i> (22a)	<i>E</i> ₃ : 0.0	<i>E</i> ₃ : 4.4	-1.8
	1,2- <i>trans</i> (22b)	³ <i>E</i> : 1.1	³ <i>E</i> : 5.8	-0.3
			$\Delta\Delta E^\ddagger = 1.4$	(22a:22b = 91:9)

Figure 4.6-4.6 bottom give the FES maps for the *D*-arabino, *D*-xylo and *D*-ribo configured iminium ions, respectively. The maps support the energy differences of the envelope conformers of these isomers that were found by the initial conformer search, starting from the ³*E* and *E*₃ envelopes. The largest deviation is seen for the *D*-ribose configured iminium ion, where the energy difference has increased from 1.1 kcal mol⁻¹ in the initial conformer search to 2.3 kcal mol⁻¹ in the FES map. This may be accounted for by the more thorough interrogation of the conformer space and/or the use of a larger basis set in the FES map method (6-31G* vs 6-311G**). The energy differences between the two envelopes were found to increase in the transition states. Therefore this energy difference may well explain why the Ugi reaction for the ribo configured imine gave only a single product. When the iminium ion FES maps are compared with the aldoses FES maps described in Chapter 2, it becomes clear that stabilizing stereoelectronic interactions play a smaller role. The arabino iminium ion and the aldose oxocarbenium ion FES map are comparable but the iminium ion has a greater preference for ³*E* because the *E*₃ conformer is less stabilized by stereoelectronic interactions. The xylo iminium ion FES map shows that the iminium ion preferentially takes up an *E*₃ envelope and that the iminium ion FES map is more shallow than the oxocarbenium ion map, indicating that the iminium ions are

overall more stable and the relative differences smaller. The conformer preference of the ribo iminium ion for the E_3 envelope has decreased in comparison with the ribosyl oxocarbenium ion, suggesting that the iminium ions in methanol requires less stabilizing interactions.

4.3 Conclusion

The experimental results supported by the calculational data reported here show that the diastereoselectivity of the Ugi three-component reaction using pentose derived pyrrolines is determined in the transition state of the isocyanide addition step to the iminium ion and that these reactions therefore proceed under kinetic control. This stands in contrast to the classic mechanistic view that the Ugi reaction proceeds through a series of equilibrium reactions before ending with the irreversible Mumm rearrangement in the thermodynamically favored product. For the pyrrolines studied here, the conformation of the iminium ion intermediates, in combination with the stabilizing effect of an axially positioned C3 ether on the developing positive charge in the incoming nucleophile, is the deciding factor in the stereochemical course of the isocyanide addition reaction. It might well be that the kinetic scenario described here is not only valid for the pyrrolines used in this study but also of importance for many other Ugi reactions and other multicomponent reaction featuring isocyanides. The results therefore may help in the development of predictive models for diastereoselective Ugi-type multicomponent reactions, which would have considerable impact in library design for drug discovery and development.

Experimental section

Calculations. For all calculations, the benzyl ethers were replaced by methyl ethers and methyl isocyanide and acetic acid were used as reaction partners. To find the lowest energy conformation of the starting iminium ions, the intermediate nitrilium ions, the imidate intermediates, the bicyclic Mumm rearrangement intermediates and the final products the following calculations were performed. First, the conformer distribution option included in the Spartan '04 program²⁹ was used to find a set of initial gas-phase geometries. For the iminium ions, the nitrilium ions (both *1,2-cis* and *1,2-trans*) and the final products (both *1,2-cis* and *1,2-trans*) the conformer distribution search was performed using DFT calculations at the B3LYP/6-31G* level. For the imidates, both the *E*- and *Z*-amides of the *1,2-cis* and *1,2-trans* epimers were evaluated using semi-empirical calculations at the AM1 level. Also for the bicyclic intermediates of the Mumm rearrangements, all isomers (*1,2-cis/1,2-trans*, *E/Z* amide configuration and *R/S* alcohol configuration) were subjected to the conformer distribution search using semi-empirical calculations at the AM1 level. After the semi empirical AM1 calculations a DFT calculation at the B3LYP/6-31G* level was done on the set of isomers. Next, the geometry of a selected set of the lowest energy conformers was optimized in Gaussian 03³⁰ at the B3LYP/6-31G* level and zero point energy corrections for these were calculated. For the iminium ions two conformers were optimized, for the nitrilium ions 6-8 geometries were optimized, for the imidates 18-20 structures were optimized, for the bicyclic Mumm rearrangement intermediates 24-27 structures were optimized and for the final products 6-7 structures were optimized. In the case where calculations for the iminium ion conformers converged to a single envelope, a

partial structural optimization with geometrical constraints was done to find the energy of the alternative envelope. Finally, the solvent (methanol) effect was incorporated using the polarizable continuum model (PCM) and after inclusion of the unscaled gas-phase zero-point energies, the energies of the conformers were determined. The energies of all reaction components were added up to establish the total energy.

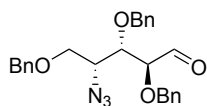
The transition states for the addition of the isocyanide to the different iminium ions were found through the Bery optimization algorithm, which was started after placing the methyl isocyanide in the vicinity (1.75-1.85 Å) of the electrophilic iminium ion. The found structures were checked for the absence of imaginary frequencies and the presence of only one imaginary frequency for the transition states. Intrinsic reaction coordinate (IRC) calculations were performed to verify that each transition state indeed connected the reactants and products.

FES maps were calculated according to the procedure described in Chapter 2.

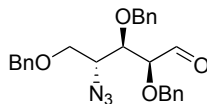
Synthesis

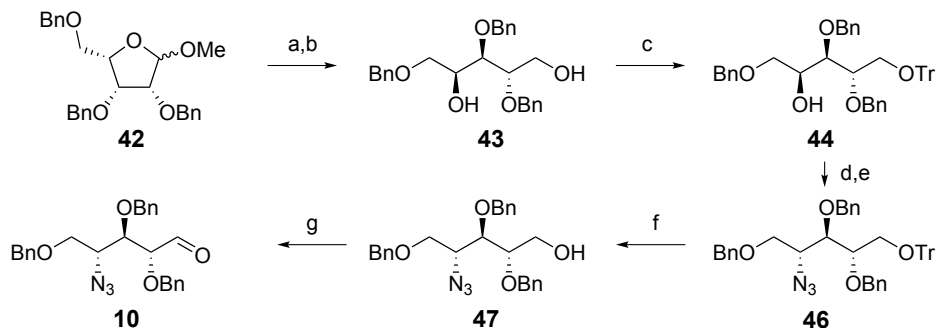
General. All reagents were of commercial grade and used as received. All moisture sensitive reactions were performed under an argon atmosphere. Methanol used in the SAWU-3CR was distilled from magnesium (5 g/L)/molecular iodine (0.5 g/L) and stored on activated 3 Å molecular sieves under argon. Reactions were performed at room temperature unless stated otherwise and were monitored by TLC analysis with detection by UV (254 nm) and where applicable by spraying with 20% sulfuric acid in EtOH or with a solution of $(\text{NH}_4)_6\text{Mo}_7\text{O}_{24}\cdot 4\text{H}_2\text{O}$ (25 g/l) and $(\text{NH}_4)_4\text{Ce}(\text{SO}_4)_4\cdot 2\text{H}_2\text{O}$ (10 g/l) in 10% sulfuric acid (aq.) followed by charring at ~150 °C. Flash column chromatography was performed on silica gel (40-63 μm). ^1H and ^{13}C NMR spectra were recorded on a Bruker AV 750 or Bruker AV 400 in CDCl_3 , CD_3OD , CD_3CN or C_6D_6 . Chemical shifts (δ) are given in ppm relative to tetramethylsilane as internal standard (^1H NMR in CDCl_3) or the residual signal of the deuterated solvent. Coupling constants (J) are given in Hz. All ^{13}C NMR spectra are proton decoupled. NMR peak assignments were made using COSY and HSQC experiments. Where applicable NOESY and HMBC experiments were used to further elucidate the structure.

2,3,5-Tri-*O*-benzyl-4-deoxy-4-azido-D-lyxose (8). 2,3,5-Tri-*O*-benzyl-4-deoxy-4-azido-D-lyxose (**8**) was prepared as described by Bongler *et al.*⁹



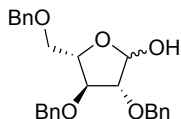
2,3,5-Tri-*O*-benzyl-4-deoxy-4-azido-D-arabinose (9). 2,3,5-Tri-*O*-benzyl-4-deoxy-4-azido-D-arabinose (**9**) was prepared as described by Bongler *et al.*⁹



Scheme 4.1 Synthesis of 2,3,5-Tri-*O*-benzyl-4-deoxy-4-azido-D-xylose (**10**).

Reagents and conditions: (a) NaBH₄, EtOH, 85%; (b) TrCl, Et₃N, DMAP, DCM, 88%; (c) MsCl, pyridine, 4 °C, 96%; (d) NaN₃, 15-crown-5, Bu₄NHSO₄, DMF, 100 °C, 90%; (e) *p*-TsOH, CHCl₃, MeOH, 85%; (f) Dess-Martin periodinane, DCM, 4 °C, 66%.

2,3,5-Tri-*O*-benzyl-L-arabinofuranose (42) 2,3,5-Tri-*O*-benzyl-L-arabinofuranose (**42**) was synthesized as its enantiomer (compound **5**) described in Chapter 2.

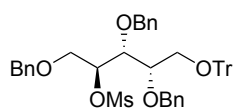


2,3,5-Tri-*O*-benzyl-L-arabinitol (43). To a cooled solution (0 °C) of 2,3,5-Tri-*O*-benzyl-L-arabinofuranose (**42**, 20 g, 48 mmol) in EtOH (500 ml) was added sodium borohydride (4.2 g, 111 mmol). After stirring for 5 hours at room temperature, TLC analysis showed complete conversion of the starting material into a lower running product. The pH of the reaction mixture was adjusted to pH 4-5 by the addition of acetic acid and the resulting mixture was concentrated, taken up in EtOAc and washed consecutively with 1 M HCl (aq.), NaHCO₃ (sat. aq.), and brine. The organic layer was dried (anhydrous MgSO₄), filtered and concentrated. The residue was purified by silica gel column chromatography (30-60% EtOAc/PE) yielding the title compound (17 g, 41 mmol, 85 % yield) as a turbid syrup. *R*_f = 0.6 (1/1; EtOAc/PE). ¹H NMR (400 MHz, CDCl₃) δ 7.35 – 7.18 (m, 15H, CH_{Ar}), 4.61 (d, *J* = 11.6 Hz, 1H, CHH Bn), 4.57 (d, *J* = 12.2 Hz, 2H, 2xCHH Bn), 4.53 (d, *J* = 11.1 Hz, 1H, CHH Bn), 4.50 (d, *J* = 11.0 Hz, 1H, CHH Bn), 4.47 (d, *J* = 11.8 Hz, 1H, CHH Bn), 3.99 (q, *J* = 5.1 Hz, 1H, C-4), 3.79 – 3.66 (m, 4H, C-1, C-2, C-3), 3.65 – 3.57 (m, 2H, C-5), 3.07 (bs, 1H, OH), 2.89 (bs, 1H, OH). ¹³C NMR (101 MHz, CDCl₃) δ 138.0, 137.9 (3x C_q Bn), 128.4, 128.4, 128.1, 128.1, 127.9, 127.8, 127.8 (CH_{Ar} Bn), 79.5 (C-2), 78.4 (C-3), 73.7, 73.4, 72.8 (3x CH₂ Bn), 71.1 (C-5), 70.5 (C-4), 61.3 (C-1). [α]_D²⁰: -2.7° (*c* = 1, CHCl₃). IR (neat): 698, 737, 1003, 1028, 1072, 1092, 1209, 1321, 1352, 1396, 1454, 1715, 2338, 2868, 3030, 3310, 3372, 3447, 3482. HR-MS: [M+H]⁺ Calculated for C₂₆H₃₀O₅: 423.21660; found: 423.21658.

2,3,5-Tri-*O*-benzyl-1-*O*-trityl-L-arabinitol (44). 2,3,5-Tri-*O*-benzyl-L-arabinitol (**43**, 17 g, 41 mmol) was dissolved in DCM (300 ml). To this solution was added Et₃N (12 ml, 85 mmol), triphenylmethyl chloride (16 g, 57 mmol) and DMAP (0.60 g, 4.7 mmol). The reaction mixture was stirred overnight after which the reaction was quenched by addition of MeOH (3.5 ml). The mixture was concentrated under reduced pressure, the residue taken up in EtOAc and washed with 0.1 M HCl (aq.), NaHCO₃ (sat. aq.) and brine. The organic phase was dried using anhydrous MgSO₄, filtered and concentrated under reduced pressure. The residue was purified by silica gel column chromatography (50% Ether/PE) yielding 2,3,5-Tri-*O*-benzyl-1-*O*-trityl-L-arabinitol (25 g, 37 mmol, 88 %

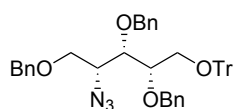
yield). $R_f = 0.7$ (1/3; EtOAc/PE). $^1\text{H NMR}$ (400 MHz, CDCl_3) δ 7.46 – 7.38 (d, $J = 6.9$ Hz, 6H, CH_{Ar} Tr), 7.31 – 7.14 (m, 22H, CH_{Ar} Bn, CH_{Ar} Tr), 7.07 – 7.02 (m, 2H, CH_{Ar}), 4.68 (d, $J = 11.6$ Hz, 1H, CHH Bn), 4.55 (d, $J = 11.7$ Hz, 1H, CHH Bn), 4.48 – 4.38 (m, 4H, CHH Bn), 3.99 – 3.92 (m, 2H, C-2, C-4), 3.78 (dd, $J = 7.3$, 3.1 Hz, 1H, C-3), 3.56 (dd, $J = 9.8$, 3.6 Hz, 1H, C-5a), 3.52 (dd, $J = 10.0$, 5.3 Hz, 1H-C-5b), 3.48 (dd, $J = 9.8$, 6.0 Hz, 1H, C-1a), 3.34 (dd, $J = 9.7$, 5.8 Hz, 1H, C-1b). 2.80 (d, $J = 5.4$ Hz, 1H, OH), $^{13}\text{C NMR}$ (101 MHz, CDCl_3) δ 143.9 (3x C_q Tr), 138.1, 138.0 (3x C_q), 128.6, 128.4, 128.3, 128.3, 128.1, 128.1, 127.8, 127.8, 127.6, 127.5, 127.0 (CH_{Ar} Tr, CH_{Ar} Bn), 87.0 (C_q Tr), 78.1 (C-2), 77.9 (C-3), 73.8, 73.3, 73.1 (3x CH_2 Bn), 71.2 (C-5), 70.1 (C-4), 63.1 (C-1). $[\alpha]_{\text{D}}^{20}$: -1.7° ($c = 1$, CHCl_3). IR (neat): 619, 633, 648, 696, 746, 899, 988, 1001, 1028, 1070, 1153, 1182, 1215, 1321, 1393, 1449, 1491, 1599, 2320, 2868, 3030, 3061. HR-MS: $[\text{M}+\text{Na}^+]$ Calculated for $\text{C}_{45}\text{H}_{44}\text{O}_5$: 687.30810; found: 687.30799.

2,3,5-Tri-*O*-benzyl-4-*O*-methanesulfonyl-1-*O*-trityl-L-arabinitol (45). 2,3,5-Tri-*O*-benzyl-1-*O*-trityl-L-arabinitol (**44**,



44, 21 g, 32 mmol) was coevaporated twice with toluene, dissolved in pyridine (70 ml) and cooled to 0 °C. Methanesulfonyl chloride (6.4 ml, 82 mmol) was added and the solution stirred for 22 hours at 4 °C. The reaction mixture was quenched by addition of methanol (15 ml) and then concentrated under reduced pressure. The residue was taken up in EtOAc and subsequently washed with 0.1 M HCl (aq.), NaHCO_3 (sat. aq.) and brine. The organic phase was dried over anhydrous MgSO_4 , filtered and concentrated under reduced pressure. The crude product was purified by flash chromatography (70% Toluene/PE - 5% EtOAc/Toluene) yielding 2,3,5-Tri-*O*-benzyl-4-*O*-methanesulfonyl-1-*O*-trityl-L-arabinitol (23 g, 32 mmol, 96 % yield) as a slightly yellow highly viscous oil. $R_f = 0.6$ (1/9; EtOAc/toluene). $^1\text{H NMR}$ (400 MHz, CDCl_3) δ 7.42 (d, $J = 7.1$ Hz, 6H, CH_{Ar} Tr), 7.32 – 7.18 (m, 22H, CH_{Ar} Bn, CH_{Ar} Tr), 7.17 – 7.11 (m, 2H, CH_{Ar}), 4.95 (ddd, $J = 7.6$, 3.9, 3.0 Hz, 1H, C-4), 4.62 (d, $J = 11.3$ Hz, 1H, CHH Bn-3), 4.58 (d, $J = 11.4$ Hz, 1H, CHH Bn-2), 4.51 (d, $J = 11.3$ Hz, 1H, CHH Bn-3), 4.51 (d, $J = 11.3$ Hz, 1H, CHH Bn-2), 4.41 (d, $J = 11.8$ Hz, 1H, CHH Bn-5), 4.37 (d, $J = 11.8$ Hz, 1H, CHH Bn-5), 4.07 (t, $J = 3.9$ Hz, 1H, C-3), 3.81 (dd, $J = 11.3$, 3.0 Hz, 1H, C-5a), 3.74 – 3.66 (m, 2H, C-2, C-5b), 3.35 (dd, $J = 10.1$, 5.2 Hz, 1H), 3.29 (dd, $J = 10.1$, 5.7 Hz, 1H), 2.86 (s, 3H, CH_3 Ms). $^{13}\text{C NMR}$ (101 MHz, CDCl_3) δ 143.8 (3x C_q Tr), 138.1, 137.7, 137.7 (3x C_q Bn), 128.7, 128.5, 128.4, 128.3, 128.3, 128.0, 127.9, 127.8, 127.8, 127.8, 127.2 (CH_{Ar} Tr, CH_{Ar}), 87.3 (C_q Tr), 82.5 (C-4), 79.4 (C-3), 78.6 (C-2), 74.8 (CH_2 Bn-3), 73.3 (CH_2 Bn-2, CH_2 Bn-5), 69.1 (C-5), 63.1 (C-1), 38.5 (CH_3 Ms). $[\alpha]_{\text{D}}^{20}$: -7.5° ($c = 1$, CHCl_3). IR (neat): 633, 696, 745, 810, 845, 912, 968, 1001, 1028, 1074, 1090, 1155, 1175, 1217, 1356, 1449, 1491, 2876, 2934, 3030. HR-MS: $[\text{M}+\text{Na}^+]$ Calculated for $\text{C}_{46}\text{H}_{46}\text{O}_5$: 765.28565; found: 765.28558.

2,3,5-Tri-*O*-benzyl-4-deoxy-4-azido-1-*O*-trityl-D-xylitol (46). 2,3,5-Tri-*O*-benzyl-4-*O*-methanesulfonyl-1-*O*-trityl-L-

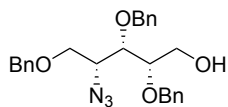


arabinitol (**45**, 23 g, 32 mmol) was coevaporated twice with toluene and dissolved in DMF (200 ml). Sodium azide (13 g, 200 mmol), 15-crown-5 (1.3 ml, 6.7 mmol) and tetrabutylammonium hydrogen sulfate (2.3 g, 6.7 mmol). The resulting suspension was stirred at 100 °C for 5 days until TLC showed complete conversion

into a higher running product. The reaction mixture was concentrated under reduced pressure, taken up in EtOAc and subsequently washed with water. The aqueous layer was extracted with EtOAc and the combined organic layers washed with water, NaHCO_3 (sat. aq.) and brine. The organic layer was dried over anhydrous MgSO_4 , filtered and concentrated under reduced pressure. The residue was purified by flash chromatography (2%-10% EtOAc/PE) yielding 2,3,5-Tri-*O*-benzyl-4-deoxy-4-azido-1-*O*-trityl-D-xylitol (20 g, 28 mmol, 90 % yield). $R_f = 0.7$ (1/9; EtOAc/toluene). $^1\text{H NMR}$ (400 MHz, CDCl_3) δ 7.45 (d, $J = 7.0$ Hz, 6H, CH_{Ar} Tr), 7.31 – 7.14 (m, 24H, 15x CH_{Ar} Bn, 9x CH_{Ar} Tr), 4.71 (d, $J = 11.3$ Hz, 1H, CHH Bn), 4.65 (d, $J = 11.6$ Hz, 1H, CHH Bn), 4.61 (d, $J = 11.4$ Hz, 1H, CHH Bn), 4.46 (d, $J = 11.6$ Hz, 1H, CHH Bn), 4.39 (d, $J = 12.1$ Hz, 1H, CHH Bn), 4.35 (d, $J = 12.0$ Hz, 1H, CHH Bn), 3.96 (dd, $J = 5.7$, 4.4 Hz, 1H, C-3), 3.76 (q, $J = 4.6$ Hz, 1H, C-2), 3.58 – 3.53 (m, 1H, C-4), 3.54 – 3.38 (m, 3H, C-5, C-1a), 3.22 (dd, $J = 10.3$, 4.6 Hz, 1H, C-1b). $^{13}\text{C NMR}$ (101 MHz, CDCl_3) δ 143.8 (3x C_q Tr), 138.2, 138.1, 137.8 (3x C_q Bn), 128.7, 128.6, 128.4, 128.4, 128.3, 128.1, 127.9, 127.7, 127.6, 127.1 (CH_{Ar}), 86.9 (C_q Tr), 79.2 (C-2), 78.3 (C-3), 75.0 (CH_2 Bn), 73.1 (CH_2 Bn), 72.8 (CH_2 Bn), 69.4 (C-5), 62.6 (C-1), 61.3 (C-4). $[\alpha]_{\text{D}}^{20}$: 6.6° ($c = 1$, CHCl_3). IR (neat):

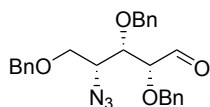
633 696, 746, 804, 918, 970, 1001, 1028, 1092, 1173, 1217, 1342, 1358, 1396, 1449, 1491, 2874, 2924, 3030, 3061. HR-MS: $[M+Na]^+$ Calculated for $C_{45}H_{44}N_3O_4$: 712.31458; found: 712.31442.

2,3,5-Tri-*O*-benzyl-4-deoxy-4-azido-D-xylitol (47). 2,3,5-Tri-*O*-benzyl-4-deoxy-4-azido-1-*O*-trityl-D-xylitol (**46**, 19 g,

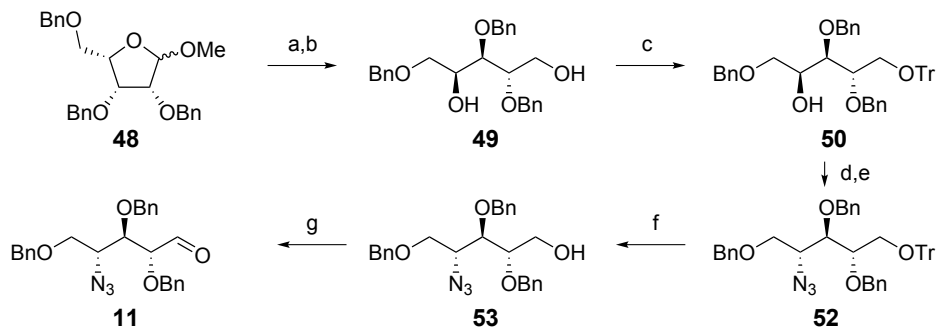


28 mmol) was dissolved in chloroform (125 ml) and MeOH (125 ml) and a catalytic amount of *p*-toluenesulfonic acid monohydrate (250 mg, 1.3 mmol) was added. The reaction mixture was stirred for 3 hours after which it was diluted with DCM and washed with $NaHCO_3$ (sat. aq.) and brine. The solution was then dried over anhydrous $MgSO_4$, filtered and concentrated under reduced pressure. The crude product was purified by flash chromatography (20%-30% EtOAc/PE) yielding 2,3,5-Tri-*O*-benzyl-4-deoxy-4-azido-D-xylitol (11 g, 24 mmol, 85 % yield) as a colorless liquid. R_f = 0.35 (1/9; EtOAc/toluene). 1H NMR (400 MHz, $CDCl_3$) δ 7.37 – 7.19 (m, 15H, CH_{Ar} Bn), 4.71 (d, J = 11.5 Hz, 1H, CHH Bn), 4.59 (d, J = 11.7 Hz, 1H, CHH Bn), 4.57 (d, J = 11.2 Hz, 1H, CHH Bn), 4.54 (d, J = 11.4 Hz, 1H, CHH Bn), 4.45 (d, J = 12 Hz, 1H, CHH Bn), 4.59 (d, J = 11.9 Hz, 1H, CHH Bn), 3.81 – 3.72 (m, 2H, C-1, C-3), 3.71 – 3.61 (m, 3H, C-4, C-2, C-1), 3.61 – 3.51 (m, 2H, C-5), 2.27 (bs, 1H, OH). ^{13}C NMR (101 MHz, $CDCl_3$) δ 138.0, 137.8, 137.6 (3x C_q Bn), 128.5, 128.4, 128.1, 128.0, 127.9, 127.8, 127.8, 126.9 (CH_{Ar} Bn), 79.8 (C-2), 78.1 (C-3), 74.6, 73.3, 72.9 (3x CH_2 Bn), 69.5 (C-5), 61.3 (C-1), 60.8 (C-4). $[\alpha]_D^{20}$: -7.1° (c = 1, $CHCl_3$). IR (neat): 696, 735, 820, 847, 881, 910, 957, 993, 1028, 1059, 1088, 1101, 1207, 1269, 1319, 1342, 1358, 1393, 1454, 1497, 1535, 1722, 2097, 2326, 2868, 2926, 3030, 3063, 3503. HR-MS: $[M+H]^+$ Calculated for $C_{26}H_{29}N_3O_4$: 448.22308; found: 448.22323.

2,3,5-Tri-*O*-benzyl-4-deoxy-4-azido-D-xylose (10). 2,3,5-Tri-*O*-benzyl-4-deoxy-4-azido-D-xylitol (**47**, 224 mg, 0.50

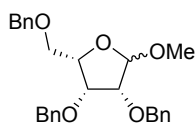


mmol) was dissolved in DCM (10 ml) and cooled to 0 °C. Dess-Martin periodinane (318 mg, 0.75 mmol) was added and the reaction mixture stirred overnight at 0-4 °C. A mixture of 10% $NaHCO_3$ (aq.)/1M $Na_2S_2O_3$ (aq. 1/1 v/v, 25 ml) was added and the solution stirred vigorously for 30 minutes. The organic layer was separated and washed with $NaHCO_3$ (sat. aq.) and brine. The organic layer was dried over anhydrous $MgSO_4$ and concentrated under reduced pressure. The residue was purified by flash chromatography (5-13% EtOAc/PE) yielding 2,3,5-Tri-*O*-benzyl-4-deoxy-4-azido-D-xylose (147 mg, 0.33 mmol, 66 % yield) which was used immediately in the SAWU reaction. R_f = 0.6 (1/9; EtOAc/toluene). 1H NMR (400 MHz, $CDCl_3$) δ 9.73 (s, 1H, C-1), 7.37 – 7.19 (m, 15H, CH_{Ar} Bn), 4.71 (d, J = 11.8 Hz, 1H, CHH Bn), 4.58 (d, J = 11.6 Hz, 1H, CHH Bn), 4.55 (d, J = 11.6 Hz, 1H, CHH Bn), 4.48 – 4.37 (m, 3H, 3x CHH Bn), 3.94 – 3.84 (m, 2H, C-2, C-3), 3.86 – 3.81 (m, 1H, C-4), 3.55 – 3.47 (m, 2H, C-5). ^{13}C NMR (101 MHz, $CDCl_3$) δ 201.2 (C-1), 137.3, 136.9, 136.6 (C_q Bn), 128.5, 128.3, 128.2, 128.1, 128.0, 127.8, 127.7 (CH_{Ar} Bn), 81.3 (C-2), 78.3 (C-3), 73.9, 73.2, 73.1 (3x CH_2 Bn), 68.8 (C-5), 60.5 (C-4). $[\alpha]_D^{20}$: -7.5° (c = 1, $CHCl_3$). IR (neat): 696, 735, 822, 849, 912, 1003, 1026, 1070, 1090, 1207, 1267, 1314, 1348, 1362, 1396, 1454, 1728, 2099, 2866, 2924, 3030. HR-MS: $[M+H]^+$ Calculated for $C_{26}H_{27}N_3O_4$: 446.20743; found: 446.20745.

Scheme 4.2 Synthesis of 2,3,5-Tri-*O*-benzyl-4-deoxy-4-azido-D-ribose (**11**).

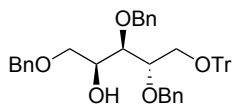
Reagents and conditions: (a) H_2SO_4 , AcOH, H_2O , 100 °C; (b) NaBH_4 , EtOH, 48% (2 steps); (c) TrCl , Et_3N , DMAP, DCM, 44%; (d) MsCl , pyridine, 4 °C, 75%; (e) NaN_3 , 15-crown-5, Bu_4NHSO_4 , DMF, 100 °C, 76%; (f) *p*-TsOH, CHCl_3 , MeOH, 84%; (g) Dess-Martin periodinane, DCM, 4 °C, 84%.

2,3,5-Tri-*O*-benzyl-1-*O*-methyl-L-lyxofuranose (48). 2,3,5-Tri-*O*-benzyl-1-*O*-methyl-L-lyxofuranose (**48**) was prepared as its enantiomer (compound **10**) described in Chapter 2.



2,3,5-Tri-*O*-benzyl-L-lyxitol (49). To a solution of acetic acid (290 ml) and aq. 3 M sulphuric acid (77 ml, 232 mmol) was added 2,3,5-Tri-*O*-benzyl-1-*O*-methyl-L-lyxofuranose (**48**, 21.4 g, 39 mmol, 80% pure). The mixture was heated to 100 °C for 1 hour and then cooled to ambient temperature. The solution was neutralized with NaHCO_3 (sat. aq.) and then extracted with DCM (3x). The combined organic layers were washed with water and brine, dried over anhydrous MgSO_4 and concentrated under reduced pressure. The product was purified by flash chromatography (40-100% Ether/PE) yielding the hydrolyzed product. To a cooled solution (0 °C) of the hydrolyzed furanose in EtOH (310 ml) was added sodium borohydride (2.3 g, 61 mmol). After 5h of stirring at room temperature, the pH of the reaction mixture was adjusted to pH 4-5 by the addition of acetic acid. The resulting mixture was then concentrated, taken up in EtOAc and washed consecutively with 1 M HCl (aq.), NaHCO_3 (sat. aq.), and brine. The organic layer was dried over anhydrous MgSO_4 , filtered and concentrated. The residue was purified by silica gel column chromatography (20-40% EtOAc/PE) yielding 2,3,5-Tri-*O*-benzyl-L-lyxitol (5.3 g, 12.6 mmol, 48 % yield) as a highly viscous syrup consisting of a mixture of products resulting from the reduction of the furanose and pyranose isomers of L-lyxofuranose (55% of the desired furanose product). $R_f = 0.6$ (40/60; EtOAc/PE). ^1H NMR (400 MHz, CDCl_3) δ 7.36 – 7.22 (m, 15H, CH_{Ar} Bn), 4.75 – 4.40 (m, 6H, $3\times\text{CH}_2$ Bn), 4.00 (dt, $J = 6.0, 2.1$ Hz, 1H, C-4), 3.88 – 3.65 (m, 4H, C-1, C-2, C-3), 3.52 (dd, $J = 9.4, 6.1$ Hz, 1H, C-5a), 3.45 (dd, $J = 9.5, 6.1$ Hz, 1H, C-5b), 2.81 (s, 1H, OH), 2.57 (s, 1H, OH). ^{13}C NMR (101 MHz, CDCl_3) δ 137.9, 137.9 ($3\times\text{C}_q$ Bn), 128.5, 128.5, 128.5, 128.4, 128.3, 128.3, 128.0, 127.9, 127.9, 127.8 (CH_{Ar} Bn), 79.6 (C-2), 77.0 (C-3), 74.3, 73.4, 72.4 ($3\times\text{CH}_2$ Bn), 71.3 (C-5), 69.7 (C-4), 60.5 (C-1). $[\alpha]_D^{20}$: 16° (c = 1, CHCl_3). IR (neat): 608, 698, 737, 912, 1028, 1063, 1094, 1209, 1244, 1327, 1391, 1454, 1732, 2872, 3030, 3333, 3366, 3456. HR-MS: $[\text{M}+\text{H}^+]$ Calculated for $\text{C}_{26}\text{H}_{30}\text{O}_5$: 423.21660; found: 423.21658. Spectroscopic data matched literature data.³¹

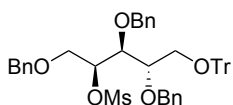
2,3,5-Tri-*O*-benzyl-1-*O*-trityl-L-lyxitol (50). 2,3,5-Tri-*O*-benzyl-L-lyxitol (**49**, 5.3 g, 12.6 mmol) was dissolved in



DCM (126 ml). To this solution was added Et₃N (7.1 ml, 51 mmol), triphenylmethyl chloride (10.6 g, 38 mmol) and DMAP (0.50 g, 3.8 mmol). The reaction mixture was stirred for 6 days after which the reaction was quenched with MeOH (8 ml) and the mixture was concentrated under reduced pressure. The residue was taken up in

EtOAc and washed with 1 M HCl (aq.), NaHCO₃ (sat. aq.) and brine. The organic phase was dried over anhydrous MgSO₄, filtered and concentrated under reduced pressure. The residue was purified by silica gel column chromatography (15-25% Ether/PE) yielding 2,3,5-Tri-*O*-benzyl-1-*O*-trityl-L-lyxitol (3.7 g, 5.6 mmol, 44 % yield). *R*_f = 0.4 (25/75; EtOAc/PE). ¹H NMR (400 MHz, CDCl₃) δ 7.48 (d, *J* = 6.5 Hz, 6H, CH_{Ar} Tr), 7.36 (m, 2H, CH_{Ar}), 7.33 – 7.14 (m, 20H, CH_{Ar} Bn, CH_{Ar} Tr), 7.01 – 6.96 (m, 2H, CH_{Ar} Tr), 4.73 (d, *J* = 11.3 Hz, 1H, CHH Bn), 4.56 (d, *J* = 11.4 Hz, 1H, CHH Bn), 4.50 (d, *J* = 12.0 Hz, 1H, CHH Bn), 4.47 – 4.39 (m, 2H, 2xCHH Bn), 4.36 (d, *J* = 11.0 Hz, 1H, CHH Bn), 4.12 (m, 1H, C-4), 3.92 (dd, *J* = 7.1, 2.2 Hz, 1H, C-3), 3.83 (m, 1H, C-2), 3.58 – 3.47 (m, 3H, C-1a, C-5), 3.29 (dd, *J* = 10.3, 4.6 Hz, 1H, C-1b), 2.76 (d, *J* = 6.9 Hz, 1H, OH). ¹³C NMR (101 MHz, CDCl₃) δ 143.9 (3xC_q Tr), 138.1, 138.1, 137.8 (3xC_q Bn), 128.7, 128.4, 128.4, 128.2, 127.9, 127.8, 127.7, 127.6, 127.0 (CH_{Ar} Bn, CH_{Ar} Tr), 86.7 (C_q Tr), 78.5 (C-2), 77.0 (C-3), 73.7, 73.3, 72.9 (3xCH₂ Bn), 71.2 (C-5), 69.5 (C-4), 62.7 (C-1). [α]_D²⁰: 18.6° (c = 1, CHCl₃). IR (neat): 633, 696, 746, 901, 1001, 1028, 1051, 1072, 1090, 1155, 1215, 1327, 1393, 1449, 1491, 2868, 2924, 3030, 3061. HR-MS: [M+Na⁺] Calculated for C₄₅H₄₄O₅: 687.30810; found: 687.30789.

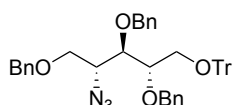
2,3,5-Tri-*O*-benzyl-4-*O*-methanesulfonyl-1-*O*-trityl-L-lyxitol (51). 2,3,5-Tri-*O*-benzyl-1-*O*-trityl-L-lyxitol (**50**, 3.7 g,



5.6 mmol) was dissolved in pyridine (15 ml) and cooled to 0 °C. Methanesulfonyl chloride (1.1 ml, 14 mmol) was added and the solution stirred overnight at 4 °C. TLC analysis of the reaction showed complete conversion into a higher running spot. The reaction mixture was quenched by addition of methanol (4 ml) and then

concentrated under reduced pressure. The residue was taken up in EtOAc and washed with 1 M HCl (aq.), NaHCO₃ (sat. aq.) and brine. The organic phase was dried over anhydrous MgSO₄, filtered and concentrated under reduced pressure. The crude product was purified by flash chromatography (70% Toluene/PE - 3% EtOAc/Toluene) yielding 2,3,5-Tri-*O*-benzyl-4-*O*-methanesulfonyl-1-*O*-trityl-L-lyxitol (3.8 g, 4.2 mmol, 75 % yield) as a highly viscous syrup. *R*_f = 0.75 (10/90; EtOAc/Toluene). ¹H NMR (400 MHz, CDCl₃) δ 7.49 – 7.40 (m, 6H, CH_{Ar} Tr), 7.38 – 7.10 (m, 22H, CH_{Ar} Tr, CH_{Ar} Bn), 7.02 (dd, *J* = 6.6, 2.9 Hz, 2H, CH_{Ar} Tr), 5.24 (ddd, *J* = 7.0, 3.9, 3.7 Hz, 1H, C-4), 4.69 (d, *J* = 10.9 Hz, 1H, CHH Bn), 4.63 (d, *J* = 10.9 Hz, 1H, CHH Bn), 4.54 – 4.46 (m, 2H, 2xCHH Bn), 4.45 – 4.35 (m, 2H, CHH Bn), 4.08 (dd, *J* = 7.0, 3.7 Hz, 1H, C-3), 3.80 (ddd, *J* = 7.0, 4.1, 3.2 Hz, 1H, C-2), 3.74 (dd, *J* = 10.8, 7.0 Hz, 1H, C-5a), 3.65 (dd, *J* = 10.4, 3.2 Hz, 1H, C-1a), 3.58 (dd, *J* = 10.8, 3.9 Hz, 1H, C-5b), 3.27 (dd, *J* = 10.4, 4.1 Hz, 1H, C-1b), 2.87 (s, 3H, CH₃ Ms). ¹³C NMR (101 MHz, CDCl₃) δ 143.9 (C_q Tr), 138.2, 137.7, 137.5 (C_q Bn), 128.8, 128.6, 128.4, 128.3, 128.3, 128.0, 127.9, 127.8, 127.7, 127.1 (CH_{Ar}), 87.0 (C_q Tr), 80.8 (C-4), 77.8 (C-2), 77.0 (C-3), 74.5, 73.4, 72.3 (3xCH₂ Bn), 69.8 (C-5), 61.7 (C-1), 38.7 (CH₃ Ms). [α]_D²⁰: 6.6° (c = 1, CHCl₃). IR (neat): 633, 696, 746, 804, 918, 970, 1001, 1028, 1092, 1173, 1217, 1342, 1358, 1396, 1449, 1491, 2874, 2924, 3030, 3061. HR-MS: [M+Na⁺] Calculated for C₄₆H₄₆O₅S: 765.28565; found: 765.28570.

2,3,5-Tri-*O*-benzyl-4-deoxy-4-azido-1-*O*-trityl-D-ribitol (52). 2,3,5-Tri-*O*-benzyl-4-*O*-methanesulfonyl-1-*O*-trityl-L-

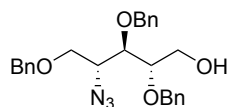


lyxitol (**51**, 3.8 g, 5.1 mmol) was coevaporated twice with toluene and then dissolved in DMF (40 ml). Sodium azide (2.1 g, 33 mmol), 15-crown-5 (0.2 ml, 1.1 mmol) and tetrabutylammonium hydrogen sulphate (0.37 g, 1.1 mmol) were added and the resulting suspension was stirred at 100 °C for 2 days. The mixture

was diluted with EtOAc and washed with water. The aqueous layer was extracted with EtOAc and subsequently the layers were combined and washed with water, NaHCO₃ (sat. aq.) and brine. The organic layer was dried over anhydrous MgSO₄, filtered and concentrated under reduced pressure. The residue was purified by flash chromatography (5-6% EtOAc/PE) yielding 2,3,5-Tri-*O*-benzyl-4-deoxy-4-azido-1-*O*-trityl-D-ribitol (2.7 g, 3.9 mmol, 76 % yield). *R*_f = 0.85 (5/95; EtOAc/Toluene). ¹H NMR (400 MHz, CDCl₃) δ 7.49 – 7.42 (m, 6H, CH_{Ar} Tr), 7.34

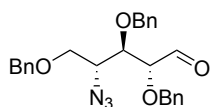
– 7.16 (m, 2H, CH_{Ar} Bn, CH_{Ar} Tr), 7.05 – 6.99 (m, 2H, CH_{Ar} Bn), 4.71 (d, $J = 11.4$ Hz, 1H, CHH Bn), 4.56 (d, $J = 10.9$ Hz, 1H, CHH Bn), 4.50 – 4.37 (m, 4H, 4x CHH Bn), 4.00 – 3.95 (m, 1H, C-4), 3.90 (dd, $J = 6.6, 4.2$ Hz, 1H, C-3), 3.74 – 3.68 (m, 1H, C-2), 3.63 (d, $J = 5.6$ Hz, 2H, C-5), 3.53 (dd, $J = 10.3, 3.0$ Hz, 1H, C-1a), 3.28 (dd, $J = 10.3, 4.7$ Hz, 1H, C-1b). ^{13}C NMR (101 MHz, $CDCl_3$) δ 144.0 (C_q Tr), 138.1, 138.0, 137.8 (3x C_q Bn), 128.8, 128.5, 128.3, 128.1, 128.0, 127.9, 127.7, 127.7, 127.1 (CH_{Ar}), 86.7 (C_q Tr), 78.5 (C-3), 78.3 (C-2), 74.0, 73.3, 72.5 (3x CH_2 Bn), 69.9 (C-5), 62.6 (C-1), 62.5 (C-4). $[\alpha]^{20}_D$: 11.3° ($c = 1$, $CHCl_3$). IR (neat): 633, 696, 746, 899, 1001, 1018, 1028, 1076, 1090, 1153, 1215, 1265, 1325, 1366, 1391, 1449, 1491, 2095, 2868, 2924, 3030, 3061. HR-MS: $[M+Na]^+$ Calculated for $C_{45}H_{43}N_3O_4$: 712.31458; found: 712.31438.

2,3,5-Tri-*O*-benzyl-4-deoxy-4-azido-D-ribitol (53). 2,3,5-Tri-*O*-benzyl-4-deoxy-4-azido-1-*O*-trityl-D-ribitol (**52**, 2.6

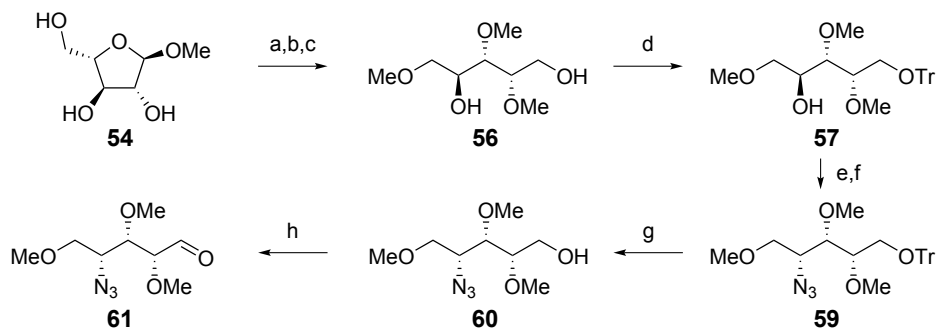


g, 3.8 mmol) was dissolved in chloroform (20 ml) and MeOH (20 ml) and a catalytic amount of *p*-toluenesulfonic acid monohydrate (0.05 g, 0.28 mmol) was added. The reaction mixture was stirred for 6h after which it was diluted with DCM and washed with $NaHCO_3$ (sat. aq.) and brine. The solution was then dried over anhydrous $MgSO_4$, filtered and concentrated under reduced pressure. The crude product was purified by flash chromatography (15%-20% EtOAc/PE) yielding 2,3,5-Tri-*O*-benzyl-4-deoxy-4-azido-D-ribitol (1.4 g, 3.2 mmol, 84 % yield). $R_f = 0.15$ (5/95; EtOAc/Toluene). 1H NMR (400 MHz, $CDCl_3$) δ 7.35 – 7.20 (m, 15H, CH_{Ar}), 4.68 – 4.58 (m, 2H, 2x CHH Bn), 4.56 (d, $J = 11.5$ Hz, 1H, CHH Bn), 4.47 (d, $J = 11.5$ Hz, 2H, 2x CHH Bn), 4.43 (d, $J = 11.9$ Hz, 1H, CHH Bn), 3.93 – 3.88 (m, 1H, C-4), 3.81 – 3.68 (m, 3H, C-1, C-3), 3.67 – 3.56 (m, 3H, C-2, C-5), 2.30 (bs, 1H, OH). ^{13}C NMR (101 MHz, $CDCl_3$) δ 137.6 (C_q Bn), 128.5, 128.5, 128.4, 128.1, 128.0, 127.9, 127.7, 127.7 (CH_{Ar}), 78.6 (C-2), 78.1 (C-3), 74.1, 73.3, 71.9 (3x CH_2 Bn), 69.7 (C-5), 62.3 (C-4), 60.4 (C-1). $[\alpha]^{20}_D$: -11.5° ($c = 1$, $CHCl_3$). IR (neat): 604, 696, 735, 822, 849, 880, 910, 1001, 1028, 1069, 1092, 1207, 1267, 1315, 1366, 1391, 1454, 1497, 1726, 2095, 2868, 2914, 3030. HR-MS: $[M+H]^+$ Calculated for $C_{26}H_{29}N_3O_4$: 448.22308; found: 448.22316.

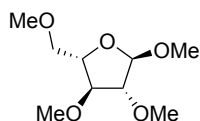
2,3,5-Tri-*O*-benzyl-4-deoxy-4-azido-D-ribose (11). 2,3,5-Tri-*O*-benzyl-4-deoxy-4-azido-D-ribitol (**53**, 224 mg, 0.5



mmol) was dissolved in DCM (10 ml) and cooled to 0 °C. Dess-Martin periodinane (424 mg, 1.0 mmol) was added and the reaction mixture stirred overnight at 0-4 °C. The reaction mixture was quenched by addition of a mixture of 10% $NaHCO_3$ (aq.)/1M $Na_2S_2O_3$ (aq. 1/1 v/v, 25 ml) and stirred for 30 minutes. The organic layer was separated and washed with $NaHCO_3$ (sat. aq.) and brine. The organic layer was dried over anhydrous $MgSO_4$, filtered and concentrated under reduced pressure. The residue was purified by flash chromatography (13% EtOAc/PE) yielding 2,3,5-Tri-*O*-benzyl-4-deoxy-4-azido-D-ribose (188 mg, 0.42 mmol, 84 % yield). $R_f = 0.6$ (10/90; EtOAc/Toluene). 1H NMR (400 MHz, $CDCl_3$) δ 9.65 (d, $J = 1.1$ Hz, 1H, C-1), 7.37 – 7.26 (m, 14H, CH_{Ar} Bn), 7.22 – 7.18 (m, 2H, CH_{Ar} Bn), 4.75 (d, $J = 12.0$ Hz, 1H, CHH Bn), 4.69 (d, $J = 12.0$ Hz, 1H, CHH Bn), 4.58 – 4.52 (m, 2H, 2x CHH Bn), 4.49 (d, $J = 11.9$ Hz, 1H, CHH Bn), 4.45 (d, $J = 11.4$ Hz, 1H, CHH Bn), 4.06 (dd, $J = 2.2, 1.1$ Hz, 1H, C-2), 3.89 – 3.81 (m, 2H, C-3, C-4), 3.79 (dd, $J = 10.0, 2.4$ Hz, 1H, C-5a), 3.64 (dd, $J = 10.1, 5.6$ Hz, 1H, C-5b). ^{13}C NMR (101 MHz, $CDCl_3$) δ 201.2 (C-1), 137.7, 137.1, 137.0 (C_q Bn), 128.5, 128.4, 128.1, 128.0, 127.8, 127.7 (C_q Bn), 82.2 (C-2), 79.7 (C-3), 73.3, 73.3, 73.0 (3x CH_2 Bn), 69.5 (C-5), 60.1 (C-4). $[\alpha]^{20}_D$: 13.7° ($c = 1$, $CHCl_3$). IR (neat): 698, 735, 750, 1028, 1088, 1105, 1260, 1271, 1317, 1364, 1454, 1730, 2100, 2860, 2938. HR-MS: $[M+NH_4]^+$ Calculated for $C_{26}H_{27}N_3O_4$: 463.23398; found: 463.23415.

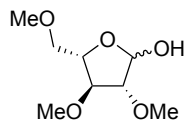
Scheme 4.3 Synthesis of 2,3,5-Tri-*O*-methyl-4-deoxy-4-azido-D-xylose (**61**)

Reagents and conditions: (a) NaH, MeI, DMF, 80%; (b) HCl, H₂O, 1,4-dioxane, 100 °C, 70%; (c) NaBH₄, EtOH, 95%; (d) TrCl, Et₃N, DMAP, DCM, 90%; (e) MsCl, pyridine, 4 °C, 96%; (f) NaN₃, 15-crown-5, Bu₄NHSO₄, DMF, 100 °C, 80%; (g) *p*-TsOH, chloroform, MeOH, 90%, (h) Dess-Martin periodinane, DCM, 4 °C, 88%.

1,2,3,5-Tetra-*O*-methyl- α -L-arabinofuranose (54**).**

Methyl- α -L-arabinofuranose was synthesized as described in *Org. Lett.* **2013**, *15*, 3026-3029, 10.1021/ol4012053. Methyl- α -L-arabinofuranose (10.4 g, 63 mmol) was dissolved in DMF (320 ml) and cooled to 0 °C. Sodium hydride (15 g, 380 mmol) was added and the reaction stirred for 5 minutes before dropwise addition of iodomethane (24 ml, 380 mmol). The reaction mixture was then slowly allowed to warm to room temperature and stirred overnight. After overnight stirring, TLC analysis

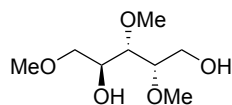
indicated complete conversion. The reaction was quenched with cold water and extracted with DCM. The combined organic layers were washed with 1M HCl (aq.), NaHCO₃ (sat. aq.) and brine. The solution was dried over anhydrous MgSO₄, filtered and concentrated under reduced pressure. The crude product was purified by flash chromatography (3-20% EtOAc/PE) yielding 1,2,3,5-Tetra-*O*-methyl- α -L-arabinofuranose (11 g, 51 mmol, 80 % yield). *R*_f = 0.4 (25/75; EtOAc/PE). ¹H NMR (400 MHz, CDCl₃) δ 4.92 (s, 1H, C-1), 4.14 – 4.08 (m, 1H, C-4), 3.70 (d, *J* = 1.7 Hz, 1H, C-2), 3.62 – 3.51 (m, 3H, C-3, C-5), 3.42 (s, 3H, OCH₃), 3.42 (s, 3H, OCH₃), 3.41 (s, 3H, OCH₃), 3.40 (s, 3H, OCH₃). ¹³C NMR (101 MHz, CDCl₃) δ 106.8 (C-1), 89.5 (C-2), 86.0 (C-3), 81.0 (C-4), 73.0 (C-5), 59.5, 58.2, 57.6, 55.0 (4xOCH₃). [α]_D²⁰: -191.8° (*c* = 1, CHCl₃). IR (neat): 941, 1011, 1057, 1105, 1188, 1315, 1367, 1452, 2828, 2911, 2930, 2988. HR-MS: [M+NH₄⁺] Calculated for C₉H₁₈O₅: 224.14925; found: 224.14939.

2,3,5-Tri-*O*-methyl-L-arabinofuranose (55**).**

1,2,3,5-Tetra-*O*-methyl- α -L-arabinofuranose (**54**, 8.3 g, 40 mmol) in 1,4-dioxane (140 ml) and 4M aq. HCl (140 ml) was refluxed for 4 hours. The mixture was cooled to rt, neutralized with Et₃N and concentrated under reduced pressure. The crude product was purified by flash chromatography (100% Ether) yielding 2,3,5-Tri-*O*-methyl-L-arabinofuranose (5.4 g, 28 mmol, 70 % yield). *R*_f = 0.25 (50/50; EtOAc/PE). α -Anomer

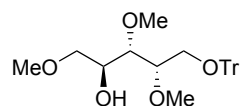
¹H NMR (400 MHz, CDCl₃) δ 5.36 (d, *J* = 6.0 Hz, 1H, C-1), 4.34 – 4.28 (m, 1H, C-4), 3.74 (d, *J* = 2.0 Hz, 1H, C-2), 3.71 (s, 1H, OH), 3.61 (dd, *J* = 4.4, 1.8 Hz, 1H, C-3), 3.51 (d, *J* = 5.7 Hz, 2H, C-5), 3.43 (s, 3H, OCH₃), 3.42 (s, 3H, OCH₃), 3.40 (s, 3H, OCH₃). ¹³C NMR (101 MHz, CDCl₃) δ 100.5 (C-1), 88.6 (C-2), 85.3 (C-3), 81.3 (C-4), 73.0 (C-5), 59.3, 57.9, 57.5 (3xOCH₃). β -Anomer ¹H NMR (400 MHz, CDCl₃) δ 5.32 (dd, *J* = 9.3, 4.4 Hz, 1H, C-1), 4.11 (d, *J* = 9.3 Hz, 1H, OH), 4.01 (q, *J* = 4.3 Hz, 1H, C-4), 3.84 (t, *J* = 4.9 Hz, 1H, C-3), 3.75 (m, 1H, C-2), 3.55 – 3.52 (m, 2H, C-5), 3.47 (s, 3H, OCH₃), 3.44 (s, 3H, OCH₃), 3.42 (s, 3H, OCH₃). ¹³C NMR (101 MHz, CDCl₃) δ 95.9 (C-1), 86.2 (C-2), 83.8 (C-3), 80.4 (C-4), 73.7 (C-5), 59.3, 58.0, 57.8 (3xOCH₃). IR (neat): 924, 974, 1057, 1094, 1111, 1190, 1346, 1452, 1638, 2830, 2901, 2932, 2984, 3364, 3397. HR-MS: [M+H⁺] Calculated for C₈H₁₆O₅: 193.10705; found: 193.10684.

2,3,5-Tri-*O*-methyl-L-arabinitol (56). To a cooled solution (0 °C) of 2,3,5-Tri-*O*-methyl-L-arabinofuranose (**55**, 5.3 g, 28 mmol) in EtOH (130 ml) was added sodium borohydride (2.4 g, 64 mmol).



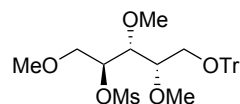
After 4 hours at room temperature, TLC analysis showed complete conversion of the starting material into a lower running product and the pH of the reaction mixture was adjusted to pH 4-5 by the addition of acetic acid. The resulting mixture was concentrated and consecutively purified by flash chromatography (75% EtOAc/PE - 20% MeOH/EtOAc) yielding 2,3,5-Tri-*O*-methyl-L-arabinitol (5.1 g, 26 mmol, 95 % yield). $R_f = 0.10$ (75/25; EtOAc/PE). $^1\text{H NMR}$ (400 MHz, CDCl_3) δ 3.93 (ddd, $J = 7.2, 5.1, 4.0$ Hz, 1H, C-4), 3.84 (dd, $J = 11.7, 5.2$ Hz, 1H, C-1a), 3.79 (dd, $J = 11.7, 4.9$ Hz, 1H, C-1b), 3.60 – 3.53 (m, 3H, C-5, C-2), 3.51 (s, 3H, 2- OCH_3), 3.47 (s, 3H, 3- OCH_3), 3.41 (s, 3H, 5- OCH_3), 3.40 (dd, $J = 7.3, 3.4$ Hz, 1H, C-3). $^{13}\text{C NMR}$ (101 MHz, CDCl_3) δ 81.1 (C-2), 80.7 (C-3), 73.5 (C-5), 70.0 (C-4), 61.2 (C-1), 59.8 (3- OCH_3), 59.1 (5- OCH_3), 58.7 (2- OCH_3). $[\alpha]_D^{20}$: -1.6° ($c = 1, \text{CHCl}_3$). IR (neat): 989, 1043, 1096, 1234, 1454, 1641, 1715, 2830, 2934, 3321. HR-MS: $[\text{M}+\text{H}^+]$ Calculated for $\text{C}_8\text{H}_{18}\text{O}_5$: 195.12270; found: 195.12286.

2,3,5-Tri-*O*-methyl-1-*O*-trityl-L-arabinitol (57). 2,3,5-Tri-*O*-methyl-L-arabinitol (**56**, 5.1 g, 26 mmol) was dissolved in DCM (180 ml). To this solution was added Et_3N (8 ml, 57 mmol), triphenylmethyl chloride (10.6 g, 38 mmol) and DMAP (0.3 g, 2.8 mmol). The reaction mixture was stirred overnight after which the reaction was quenched by addition of MeOH (2.5 ml). The mixture was concentrated under reduced pressure, the residue taken up

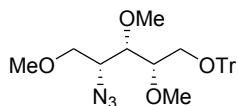


in EtOAc and washed with 0.1 M HCl (aq.), NaHCO_3 (sat. aq.) and brine. The combined aqueous layers were combined and extracted with EtOAc. The combined organic layers were then dried using anhydrous MgSO_4 , filtered and concentrated under reduced pressure. The residue was purified by silica gel column chromatography (20-80% Ether/PE) yielding 2,3,5-Tri-*O*-methyl-1-*O*-trityl-L-arabinitol (11 g, 25 mmol, 96 % yield). $R_f = 0.75$ (EtOAc). $^1\text{H NMR}$ (400 MHz, CDCl_3) δ 7.46 (d, $J = 7.8$ Hz, 6H, CH_{Ar} Tr), 7.30 (t, $J = 7.5$ Hz, 6H, CH_{Ar} Tr), 7.24 (d, $J = 8.3$ Hz, 3H, CH_{Ar} Tr), 3.91 – 3.83 (m, 1H, C-4), 3.63 (ddd, $J = 6.1, 6.0, 1.9$ Hz, 1H, C-2), 3.56 – 3.43 (m, 3H, C-1a, C-5), 3.44 (s, 3H, 2- OCH_3), 3.39 (s, 3H, 5- OCH_3), 3.35 (dd, $J = 7.4, 1.9$ Hz, 1H, C-3), 3.26 (s, 3H, 3- OCH_3), 3.23 (dd, $J = 9.6, 6.5$ Hz, 1H, C-1b), 2.75 (d, $J = 3.5$ Hz, 1H, OH). $^{13}\text{C NMR}$ (101 MHz, CDCl_3) δ 144.1 (C_q Tr), 128.8, 128.0, 127.2 ($3\times\text{CH}_{\text{Ar}}$), 87.2 (C_q Tr), 80.2 (C-3), 80.0 (C-2), 73.7 (C-5), 69.8 (C-4), 62.6 (C-1), 60.1 (3- OCH_3), 59.4 (2- OCH_3), 59.2 (5- OCH_3). $[\alpha]_D^{20}$: 9.8° ($c = 1, \text{CHCl}_3$). IR (neat): 633, 650, 704, 746, 843, 880, 899, 932, 993, 1001, 1032, 1076, 1088, 1186, 1219, 1321, 1366, 1449, 1491, 1597, 2828, 2893, 2930, 2978. HR-MS: $[\text{M}+\text{Na}^+]$ Calculated for $\text{C}_{27}\text{H}_{32}\text{O}_5$: 459.21420; found: 459.21393.

2,3,5-Tri-*O*-methyl-4-*O*-methanesulfonyl-1-*O*-trityl-L-arabinitol (58). 2,3,5-Tri-*O*-methyl-1-*O*-trityl-L-arabinitol

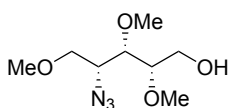


(**57**, 13 g, 30 mmol) was coevaporated twice with toluene, dissolved in pyridine (66 ml) and cooled to 0 °C. Methanesulfonyl chloride (6 ml, 78 mmol) was added and the solution stirred for 18 hours while allowing the solution to slowly warm to room temperature. The reaction mixture was quenched by addition of methanol (15 ml) and then concentrated under reduced pressure. The residue was taken up in EtOAc and washed with 0.1 M HCl (aq.), NaHCO_3 (sat. aq.) and brine. The organic phase was dried over anhydrous MgSO_4 , filtered and concentrated under reduced pressure. The crude product was purified by flash chromatography (15-50% EtOAc/PE) yielding 2,3,5-Tri-*O*-methyl-4-*O*-methanesulfonyl-1-*O*-trityl-L-arabinitol (15 g, 29 mmol, 90 % yield). $R_f = 0.80$ (70/30 EtOAc/PE). $^1\text{H NMR}$ (400 MHz, CDCl_3) δ 7.45 (d, $J = 7.5$ Hz, 6H, CH_{Ar} Tr), 7.31 (t, $J = 7.5$ Hz, 6H, CH_{Ar} Tr), 7.25 (d, $J = 6.6$ Hz, 3H, CH_{Ar} Tr), 4.91 (ddd, $J = 6.2, 6.2, 2.5$ Hz, 1H, C-4), 3.75 (dd, $J = 11.4, 2.5$ Hz, 1H, C-5a), 3.68 – 3.61 (m, 2H, C-3, C-5b), 3.48 – 3.39 (m, 2H, C-1a, C-2), 3.36 (s, 3H, OCH_3), 3.36 (s, 3H, OCH_3), 3.32 (s, 3H, OCH_3), 3.25 – 3.16 (m, 1H, C-1b), 3.07 (s, 3H, CH_3 Ms). $^{13}\text{C NMR}$ (101 MHz, CDCl_3) δ 143.9 (C_q Tr), 128.8, 128.0, 127.3 ($3\times\text{CH}_{\text{Ar}}$ Tr), 87.4 (C_q Tr), 80.9 (C-4), 80.1 (C-3), 79.1 (C-2), 71.4 (C-5), 61.6 (C-1), 61.2, 59.0, 59.0 ($3\times\text{OCH}_3$), 38.8 (CH_3 Ms). $[\alpha]_D^{20}$: -0.4° ($c = 1, \text{CHCl}_3$). IR (neat): 708, 748, 766, 918, 968, 1001, 1032, 1090, 1144, 1153, 1175, 1219, 1354, 1449, 1491, 2832, 2886, 2932, 3055. HR-MS: $[\text{M}+\text{Na}^+]$ Calculated for $\text{C}_{28}\text{H}_{34}\text{O}_7\text{S}$: 537.19175; found: 537.19154.

2,3,5-Tri-*O*-methyl-4-deoxy-4-azido-1-*O*-trityl-D-xylitol (59).

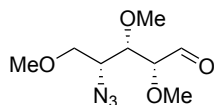
L-arabinitol (**58**, 16 g, 30 mmol) was dissolved in DMF (150 ml). Sodium azide (13 g, 200 mmol), 15-crown-5 (1.3 ml, 6.5 mmol) and tetrabutylammonium hydrogen sulfate (2.2 g, 6.5 mmol). The resulting suspension was stirred at 100 °C for 4 days.

The reaction mixture was concentrated under reduced pressure, then taken up in EtOAc and washed with water. The aqueous layer was extracted with EtOAc and the combined organic layers washed with water, NaHCO₃ (sat. aq.) and brine. The organic layer was dried over anhydrous MgSO₄, filtered and concentrated under reduced pressure yielding the crude product. The residue was purified by flash chromatography (5% EtOAc/PE) yielding 2,3,5-Tri-*O*-methyl-4-deoxy-4-azido-1-*O*-trityl-D-xylitol (11 g, 24 mmol, 80 % yield). $R_f = 0.80$ (70/30 EtOAc/PE). $R_f = 0.75$ (30/70 EtOAc/PE). ¹H NMR (400 MHz, CDCl₃) δ 7.49 – 7.43 (m, 6H, CH_{Ar} Tr), 7.34 – 7.27 (m, 6H, CH_{Ar}), 7.27 – 7.21 (m, 3H, CH_{Ar}), 3.62 (ddd, $J = 6.7, 5.4, 4.1$ Hz, 1H, C-4), 3.56 (dd, $J = 10.1, 4.0$ Hz, 1H, C-5a), 3.54 – 3.51 (m, 1H, C-3), 3.47 (dd, $J = 10.0, 6.8$ Hz, 1H, C-5b), 3.45 (s, 3H, OCH₃), 3.38 (s, 3H, OCH₃), 3.37 (s, 3H, OCH₃), 3.36 – 3.31 (m, 2H, C-1a, C-2), 3.28 – 3.18 (m, 1H, C-1b). ¹³C NMR (101 MHz, CDCl₃) δ 143.9 (C_q Tr), 128.7, 128.0, 127.2 (3xCH_{Ar} Tr), 87.1 (C_q Tr), 80.8, 80.7 (C-2, C-3), 72.2 (C-5), 61.8 (C-4), 61.7 (C-1), 61.0, 59.2, 58.7 (3xOCH₃). $[\alpha]_D^{20}$: 7.3° (c = 1, CHCl₃). IR (neat): 633, 704, 746, 764, 899, 926, 1001, 1032, 1076, 1111, 1198, 1221, 1267, 1449, 1491, 2093, 2828, 2893, 2928, 2980. HR-MS: [M+Na⁺] Calculated for C₂₇H₃₁N₃O₄: 484.22068; found: 484.22021.

2,3,5-Tri-*O*-methyl-4-deoxy-4-azido-D-xylitol (60).

2,3,5-Tri-*O*-methyl-4-deoxy-4-azido-1-*O*-trityl-D-xylitol (**59**, 11 g, 24 mmol) was dissolved in chloroform (75 ml) and MeOH (75 ml) and a catalytic amount of *p*-toluenesulfonic acid monohydrate (250 mg, 1.3 mmol) was added. The reaction mixture was stirred for 3 hours after which the mixture was neutralized with Et₃N and concentrated under reduced pressure. The crude product

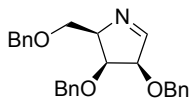
was purified by flash chromatography (15-80% EtOAc/PE) yielding 2,3,5-Tri-*O*-methyl-4-deoxy-4-azido-D-xylitol (4.8 g, 22 mmol, 90 % yield). $R_f = 0.10$ (70/30 EtOAc/PE). ¹H NMR (400 MHz, CDCl₃) δ 3.86 (dd, $J = 11.9, 4.1$ Hz, 1H, C-1a), 3.72 – 3.66 (m, 2H, C-1b, C-4), 3.66 – 3.57 (m, 2H, C-5), 3.54 (s, 3H, 3-OCH₃), 3.48 (s, 3H, 2-OCH₃), 3.47 – 3.42 (m, 2H, C-2, C-3), 3.41 (s, 3H, 5-OCH₃), 2.18 (s, 1H, OH). ¹³C NMR (101 MHz, CDCl₃) δ 81.3 (C-2), 81.0 (C-3), 72.0 (C-5), 61.2 (C-4), 61.0 (C-1), 60.8 (3-OCH₃), 59.2 (5-OCH₃), 58.6 (2-OCH₃). $[\alpha]_D^{20}$: -9.0° (c = 1, CHCl₃). IR (neat): 677, 735, 941, 914, 989, 1055, 1078, 1096, 1196, 1269, 1323, 1462, 2093, 2832, 2897, 2932, 2980, 3354, 3402. HR-MS: [M+H⁺] Calculated for C₈H₁₇N₃O₄: 220.12918; found: 220.12921.

2,3,5-Tri-*O*-methyl-4-deoxy-4-azido-D-xylose (61).

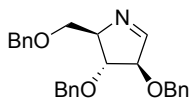
2,3,5-Tri-*O*-methyl-4-deoxy-4-azido-D-xylitol (**60**, 110 mg, 0.50 mmol) was dissolved in DCM (10 ml) and cooled to 0 °C. Dess-Martin periodinane (424 mg, 1.0 mmol) was added and the reaction mixture stirred overnight at 0-4 °C. A mixture of 10% NaHCO₃ (aq.)/1M Na₂S₂O₃ (aq. 1/1 v/v, 25 ml) was added and the solution stirred vigorously for 30 minutes. The organic layer was separated and

washed with NaHCO₃ (sat. aq.) and brine. The organic layer was dried over anhydrous MgSO₄, filtered and concentrated under reduced pressure. The residue was purified by flash chromatography (20-30% EtOAc/PE) yielding 2,3,5-Tri-*O*-methyl-4-deoxy-4-azido-D-xylose (96 mg, 0.44 mmol, 88 % yield) which was used immediately in the SAWU reaction. $R_f = 0.50$ (40/60 EtOAc/PE). ¹H NMR (400 MHz, CDCl₃) δ 9.83 (d, $J = 1.0$ Hz, 1H, C-1), 3.84 – 3.80 (m, 1H, C-4), 3.79 (dd, $J = 4.2, 1.1$ Hz, 1H, C-2), 3.73 (dd, $J = 4.9, 4.3$ Hz, 1H, C-3), 3.62 (dd, $J = 10.1, 4.7$ Hz, 1H, C-5a), 3.56 (dd, $J = 10.2, 6.5$ Hz, 1H, C-5b), 3.53 (s, 3H, OCH₃), 3.50 (s, 3H, OCH₃), 3.40 (s, 3H, OCH₃). ¹³C NMR (101 MHz, CDCl₃) δ 202.1 (C-1), 84.2 (C-2), 81.1 (C-3), 71.6 (C-5), 60.7 (C-4), 60.2, 59.3, 59.2 (3xOCH₃). $[\alpha]_D^{20}$: 47.1° (c = 1, CHCl₃). IR (neat): 851, 916, 954, 1002, 1029, 1092, 1196, 1269, 1315, 1339, 1458, 1730, 2097, 2833, 2897, 2933, 2987. HR-MS: [M+H⁺] Calculated for C₈H₁₅N₃O₄: 218.11353; found: 218.11350.

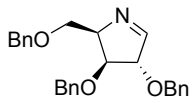
2,3,5-Tri-*O*-benzyl-4-deoxy-4-amino-D-lyxose (12). Trimethylphosphine (1M in toluene, 0.80 ml, 0.80 mmol) was added to a cooled (0 °C), with toluene coevaporated solution of 2,3,5-Tri-*O*-benzyl-4-deoxy-4-azido-D-lyxose (**8**, 179 mg, 0.40 mmol) in anhydrous MeOH (2 ml). The reaction mixture was stirred for 1 hour at 0 °C. Subsequently, the mixture was concentrated before coevaporation with toluene (3x under high vacuum) yielding the crude cyclic imine. $R_f = 0.25$ (25/75 EtOAc/Toluene). $^1\text{H NMR}$ (400 MHz, CDCl_3) δ 7.69 (d, $J = 2.4$ Hz, 1H, C-1), 7.41 – 7.05 (m, 15H, CH_A Bn), 4.70 (d, $J = 12.0$ Hz, 1H, CHH Bn), 4.69 (d, $J = 11.7$ Hz, 1H, CHH Bn), 4.65 – 4.53 (m, 4H, 4x CHH Bn), 4.37 (d, $J = 4.9$ Hz, 1H, C-2), 4.27 – 4.17 (m, 1H, C-3), 4.01 – 3.85 (m, 3H, C-4, C-5). $^{13}\text{C NMR}$ (101 MHz, CDCl_3) δ 167.3 (C-1), 138.2, 138.2, 137.5 (3x C_q Bn), 128.5, 128.4, 128.3, 128.0, 127.9, 127.9, 127.8, 127.7, 127.6 (CH_A Bn), 85.9 (C-2), 78.0 (C-3), 73.8 (CH_2 Bn), 73.6 (C-4), 73.5, 73.0 (2x CH_2 Bn), 68.8 (C-5). IR (neat): 698, 737, 1028, 1096, 1207, 1362, 1454, 1684, 2866, 2926, 3028. HR-MS: $[\text{M}+\text{H}^+]$ Calculated for $\text{C}_{26}\text{H}_{27}\text{NO}_3$: 402.20637; found: 402.20640. Spectroscopic data matched literature data.⁹



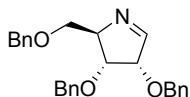
2,3,5-Tri-*O*-benzyl-4-deoxy-4-amino-D-arabinose (13). Trimethylphosphine (1M in toluene, 0.87 ml, 0.87 mmol) was added to a cooled (0 °C) and, with toluene, coevaporated solution of 2,3,5-Tri-*O*-benzyl-4-deoxy-4-azido-D-arabinose (**9**, 193 mg, 0.43 mmol) in anhydrous MeOH (2.2 ml). The reaction mixture was stirred for 1 hour at 0 °C. Subsequently, the mixture was concentrated before coevaporation with toluene (3x under high vacuum) yielding the crude cyclic imine. $R_f = 0.30$ (10/90 EtOAc/Toluene). $^1\text{H NMR}$ (400 MHz, CDCl_3) δ 7.61 (d, $J = 2.3$ Hz, 1H, C-1), 7.39 – 7.26 (m, 15H, CH_A Bn), 4.64 – 4.51 (m, 7H, C-2, 6x CHH Bn), 4.19 – 4.14 (m, 1H, C-4), 4.11 (t, $J = 3.8$ Hz, 1H, C-3), 3.76 (dd, $J = 9.8, 4.6$ Hz, 1H, C-5a), 3.55 (dd, $J = 9.8, 6.3$ Hz, 1H, C-5b). $^{13}\text{C NMR}$ (101 MHz, CDCl_3) δ 166.0 (C-1), 138.1, 137.9, 137.5 (3x C_q Bn), 128.6, 128.4, 128.4, 128.1, 128.0, 127.9, 127.8, 127.7, 127.6 (CH_A Bn), 90.7 (C-2), 84.4 (C-3), 76.8 (C-4), 73.3, 72.3, 72.0 (3x CH_2 Bn), 71.0 (C-5). IR (neat): 608, 696, 735, 847, 910, 959, 1003, 1028, 1074, 1096, 1206, 1250, 1267, 1312, 1341, 1362, 1454, 1497, 2860, 3030, 3063. HR-MS: $[\text{M}+\text{H}^+]$ Calculated for $\text{C}_{26}\text{H}_{27}\text{NO}_3$: 402.20637; found: 402.20595. Spectroscopic data matched literature data.⁹



2,3,5-Tri-*O*-benzyl-4-deoxy-4-amino-D-xylose (14). Trimethylphosphine (1M in toluene, 0.66 ml, 0.66 mmol) was added to a cooled (0 °C) and, with toluene, coevaporated solution of 2,3,5-Tri-*O*-benzyl-4-deoxy-4-azido-D-xylose (**10**, 147 mg, 0.33 mmol) in anhydrous MeOH (1.7 ml). The reaction mixture was stirred for 1 hour at 0 °C. Subsequently, the mixture was concentrated before coevaporation with toluene (3x under high vacuum) yielding the crude cyclic imine. $R_f = 0.30$ (25/75 EtOAc/Toluene). $^1\text{H NMR}$ (400 MHz, CDCl_3) δ 7.67 (d, $J = 1.5$ Hz, 1H, C-1), 7.39 – 7.18 (m, 15H), 4.68 – 4.45 (m, 7H, C-2, 6x CHH Bn), 4.39 – 4.31 (m, 1H, C-4), 4.17 (dd, $J = 6.4, 4.7$ Hz, 1H, C-3), 3.80 – 3.72 (m, 2H, C-5). $^{13}\text{C NMR}$ (101 MHz, CDCl_3) δ 167.2 (C-1), 138.5, 138.0, 137.7 (3x C_q Bn), 128.6, 128.5, 128.4, 128.3, 128.1, 127.9, 127.8, 127.7, 127.6, 127.5 (CH_A Bn), 88.5 (C-2), 83.1 (C-3), 73.4, 72.7 (2x CH_2 Bn), 72.6 (C-4), 72.5 (CH_2 Bn), 67.9 (C-5). IR (neat): 696, 735, 1003, 1028, 1076, 1098, 1206, 1364, 1454, 1498, 2859, 2922. HR-MS: $[\text{M}+\text{H}^+]$ Calculated for $\text{C}_{26}\text{H}_{27}\text{NO}_3$: 402.20637; found: 402.20596.

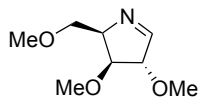


2,3,5-Tri-*O*-benzyl-4-deoxy-4-amino-D-ribose (15). Trimethylphosphine (1M in toluene, 0.84 ml, 0.84 mmol) was added to a cooled (0 °C) and, with toluene, coevaporated solution of 2,3,5-Tri-*O*-benzyl-4-deoxy-4-azido-D-ribose (**11**, 0.19 g, 0.42 mmol) in anhydrous MeOH (2.1 ml). The reaction mixture was stirred for 1 hour at 0 °C. Subsequently, the mixture was concentrated before coevaporation with toluene (3x under high vacuum) yielding the crude cyclic imine. $R_f = 0.30$ (25/75 EtOAc/Toluene). $^1\text{H NMR}$ (400 MHz, CDCl_3) δ 7.65 (d, $J = 1.6$ Hz, 1H, C-1), 7.37 – 7.12 (m, 15H, CH_A Bn), 4.69 (d, $J = 11.7$ Hz, 1H, CHH Bn), 4.66 – 4.39 (m, 6H, C-2, 5x CHH Bn), 4.39 – 4.35 (m, 1H, C-4), 4.02 (dd, $J = 6.0, 2.0$ Hz, 1H, C-3), 3.67 (dd, $J = 9.7, 3.6$ Hz, 1H, C-5a), 3.57 (dd, $J = 9.7, 4.2$ Hz, 1H, C-5b). $^{13}\text{C NMR}$ (101 MHz, CDCl_3) δ 167.2 (C-1), 137.8, 137.7, 137.5 (C_q Bn), 128.3, 128.2, 127.9, 127.9, 127.8, 127.6, 127.5, 127.3 (CH_A Bn), 83.5 (C-2), 77.4 (C-4), 76.5 (C-3), 73.1, 72.7, 71.7 (3x CH_2 Bn), 69.5 (C-5). IR (neat): 696, 735, 912,

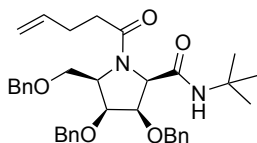


1001, 1026, 1098, 1175, 1207, 1260, 1310, 1362, 1684, 1744, 2860, 3030, 3063. HR-MS: $[M+NH_4^+]$ Calculated for $C_{26}H_{27}NO_3$: 402.20637; found: 402.20614.

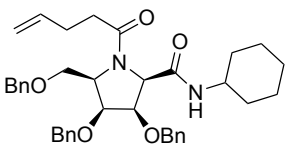
2,3,5-Tri-*O*-methyl-4-deoxy-4-amino-D-xylofuranose (62). Trimethylphosphine (1M in toluene, 0.88 ml, 0.88 mmol) was added to a cooled (0 °C) and, with toluene, coevaporated solution of 2,3,5-Tri-*O*-methyl-4-deoxy-4-azido-D-xylose (**61**, 96 mg, 0.44 mmol) in anhydrous MeOH (2.2 ml). The reaction mixture was stirred for 1 hour at 0 °C. Subsequently, the mixture was concentrated before coevaporation with toluene (3x under high vacuum) yielding the crude cyclic imine. R_f = 0.20 (50/50 EtOAc/PE). 1H NMR (400 MHz, $CDCl_3$) δ 7.74 (d, J = 1.3 Hz, 1H, C-1), 4.37 (d, J = 4.4 Hz, 1H, C-2), 4.34 – 4.26 (m, 1H, C-4), 3.86 (dd, J = 6.5, 4.7 Hz, 1H, C-3), 3.64 (dd, J = 10.0, 4.4 Hz, 1H, C-5a), 3.59 (dd, J = 10.2, 4.8 Hz, 1H, C-5b), 3.49 (s, 3H, CH_3 Me), 3.44 (s, 3H, CH_3 Me), 3.36 (s, 3H, CH_3 Me). ^{13}C NMR (101 MHz, $CDCl_3$) δ 166.6 (C-1), 89.9 (C-2), 84.9 (C-3), 72.2 (C-4), 70.0 (C-5), 59.2, 58.5, 57.8 (3xOCH₃). IR (neat): 322, 338, 390, 419, 492, 530, 632, 862, 948, 1104, 1195, 1226, 1299, 1456, 1646, 1950, 2006, 2102, 2334, 2362, 2831, 2926, 3300. HR-MS: $[M+H^+]$ Calculated for $C_8H_{15}NO_3$: 174.11247; found: 174.11256.



***N*-(*tert*-butyl) [*N*-(pent-4-enoyl)-2,5-dideoxy-2,5-imino]-3,4,6-tri-*O*-benzyl-D-galacto-hexonamide (16a).** Crude 2,3,5-Tri-*O*-benzyl-4-deoxy-4-amino-D-lyxose (**12**, 0.20 mmol) was dissolved in anhydrous MeOH (0.7 ml) and cooled to 0 °C. Next, pent-4-enoic acid (82 μ l, 0.8 mmol) and *tert*-butyl isocyanide (28 μ l, 0.25 mmol) were successively added and the reaction mixture was stirred overnight at 0-4 °C. $NaHCO_3$ (sat. aq.) was added to the mixture before allowing it to warm to room temperature while stirring. Ethyl acetate was added to the mixture and the organic phase was washed with $NaHCO_3$ (sat. aq.) and brine. The organic phase was dried over anhydrous $MgSO_4$, concentrated under reduced pressure and the product was isolated by silica gel chromatography (20-40% EtOAc/toluene) yielding the title compound as a single stereoisomer in 55% yield (64 mg, 0.11 mmol). R_f = 0.35 (40/60 EtOAc/toluene). 5:4 Mixture of rotamers; major rotamer: 1H NMR (400 MHz, $CDCl_3$) δ 7.41 – 7.22 (m, 15H, CH_{Ar}), 5.96 (s, 1H, NH), 5.89 – 5.68 (m, 1H, =CH), 5.07 – 4.86 (m, 2H, =CH₂), 4.76 (d, J = 11.9 Hz, 1H, CHH Bn), 4.72 – 4.61 (m, 1H, CHH Bn), 4.59 – 4.47 (m, 4H, C-2, 3xCHH Bn), 4.47 – 4.38 (m, 2H, C-3, CHH Bn), 4.37 – 4.28 (m, 1H, C-5), 4.17 – 4.09 (m, 1H, C-6a), 3.89 – 3.79 (m, 2H, C-4, C-6b), 2.92 – 2.76 (m, 1H, CHHCH pentenyl), 2.46 – 2.24 (m, 3H, CHHCH pentenyl, CH_2CO pentenyl), 1.20 (s, 9H, 3xCH₃ *t*-butyl). ^{13}C NMR (101 MHz, $CDCl_3$) δ 173.8 (NC=O pentenyl), 167.0 (NH(C=O)-2), 138.4, 137.9, 137.8 (C_q Bn), 137.4 (=CH pentenyl), 128.6, 128.5, 128.3, 128.3, 128.3, 128.2, 128.0, 128.0, 127.9, 127.9, 127.8, 127.7, 127.6, 127.6, 127.5 (CH_{Ar} Bn), 115.2 (=CH₂ pentenyl), 78.8 (C-4), 76.8 (C-3), 74.9, 73.8, 72.4 (3xCH₂ Bn), 69.8 (C-6), 65.0 (C-2), 58.9 (C-5), 50.9 (C_q *t*-butyl), 33.4 (CH₂CH pentenyl), 29.0 (CH₂CO pentenyl), 28.6 (CH₃ *t*-butyl). $[\alpha]_D^{20}$: 10.8° (c = 1, $CHCl_3$). IR (neat): 604, 615, 656, 696, 735, 822, 843, 912, 955, 1003, 1026, 1059, 1098, 1142, 1177, 1213, 1250, 1285, 1308, 1364, 1395, 1404, 1454, 1497, 1524, 1658, 2870, 2926, 2965, 3030, 3063, 3329. HR-MS: $[M+H^+]$ Calculated for $C_{36}H_{44}N_2O_5$: 585.33230; found: 585.33214. Spectroscopic data matched literature data.⁹

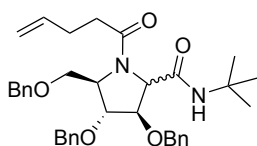


***N*-(cyclohexyl) [*N*-(pent-4-enoyl)-2,5-dideoxy-2,5-imino]-3,4,6-tri-*O*-benzyl-D-galacto-hexonamide (17a).** Crude 2,3,5-Tri-*O*-benzyl-4-deoxy-4-amino-D-lyxose (**12**, 0.20 mmol) was dissolved in anhydrous MeOH (0.7 ml) and cooled to 0 °C. Next, pent-4-enoic acid (82 μ l, 0.80 mmol) and cyclohexyl isocyanide (31 μ l, 0.25 mmol) were successively added and the reaction mixture was stirred overnight at 0-4 °C. $NaHCO_3$ (sat. aq.) was added to the mixture before allowing it to warm to room temperature while stirring. Ethyl acetate was added to the mixture and the organic phase was washed with $NaHCO_3$ (sat. aq.) and brine. The organic phase was dried over anhydrous $MgSO_4$, concentrated under reduced pressure and the product was isolated by silica gel chromatography (20-50% EtOAc/toluene) yielding the title compound as a single stereoisomer in 60% yield (73 mg, 0.12 mmol). R_f = 0.25 (40/60 EtOAc/toluene). 1:1



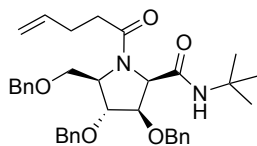
Mixture of rotamers; major rotamer: ^1H NMR (400 MHz, CDCl_3) δ 7.39 – 7.22 (m, 15H, CH_{Ar} Bn), 6.08 (d, $J = 7.8$ Hz, 1H, NH), 5.86 – 5.71 (m, 1H, =CH pentenyl), 5.07 – 4.89 (m, 2H, =CH₂ pentenyl), 4.72 – 4.61 (m, 3H, C-2, 2xCHH Bn-3), 4.60 – 4.41 (m, 4H, C-3, 2xCHH Bn-4, 2xCHH Bn-3), 4.40 – 4.31 (m, 1H, C-5), 4.21 – 4.11 (m, 1H, C-6a), 3.91 – 3.78 (m, 2H, C-4, C-6b), 3.76 – 3.66 (m, 1H, CH Cy), 2.43 – 2.25 (m, 4H, CH₂CH pentenyl, CH₂CO pentenyl), 1.78 – 1.38 (m, 6H, 3xCH₂ Cy), 1.24 – 0.52 (m, 4H, 2xCH₂ Cy). ^{13}C NMR (101 MHz, CDCl_3) δ 173.7 (NC=O pentenyl), 166.8 (NHC(O)-1), 138.3, 137.9, 137.8 (3xC_q Tr), 137.4 (=CH pentenyl), 128.6, 128.5, 128.5, 128.4, 128.3, 128.2, 128.1, 128.0, 127.9, 127.6, 127.6 (CH_{Ar} Bn), 115.2 (=CH₂ pentenyl), 78.9 (C-4), 76.8 (C-3), 74.9 (CH₂ Bn-3), 73.7 (CH₂ Bn-6), 72.4 (CH₂ Bn-4), 69.6 (C-6), 64.5 (C-2), 58.7 (C-5), 47.7 (CH Cy), 33.4 (CH₂CH pentenyl), 32.6, 32.5 (2xCH Cy), 29.0 (CH₂CO), 25.5, 24.8, 24.6 (3xCH₂ Cy). $[\alpha]^{20}_{\text{D}}$: 8.2° (c = 1, CHCl_3). IR (neat): 627, 696, 735, 820, 845, 891, 912, 959, 1003, 1028, 1067, 1101, 1144, 1211, 1256, 1275, 1308, 1352, 1406, 1452, 1497, 1526, 1655, 2853, 2928, 3030, 3063, 3292. HR-MS: $[\text{M}+\text{H}^+]$ Calculated for $\text{C}_{38}\text{H}_{46}\text{N}_2\text{O}_5$: 611.34795; found: 611.34803. Spectroscopic data matched literature data.⁹

***N*-(*tert*-butyl) [*N*-(pent-4-enoyl)-2,5-dideoxy-2,5-imino]-3,4,6-tri-*O*-benzyl-*D*-gluco/*D*-manno-hexonamide (18).**



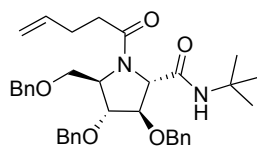
Crude 2,3,5-Tri-*O*-benzyl-4-deoxy-4-amino-*D*-arabinose (**13**, 0.22 mmol) was dissolved in anhydrous MeOH (0.7 ml) and cooled to 0 °C. Next, pent-4-enoic acid (89 μl , 0.87 mmol) and *tert*-butyl isocyanide (31 μl , 0.27 mmol) were successively added and the reaction mixture was stirred overnight at 0–4 °C. NaHCO_3 (sat. aq.) was added to the mixture before allowing it to warm to room temperature while stirring. Ethyl acetate was added to the mixture and the organic phase was washed with NaHCO_3 (sat. aq.) and brine. The organic phase was dried over anhydrous MgSO_4 , concentrated under reduced pressure and the product was isolated by silica gel chromatography (5–15% EtOAc/toluene; 2,3-*trans*-isomer **18b**: 5% EtOAc/toluene, 2,3-*cis*-isomer **18a** 5–15% EtOAc/toluene) yielding a separable 2,3-*cis*:2,3-*trans* mixture with a ratio of 58:42 in 50% combined yield (64 mg, 0.11 mmol) as a light yellow oil.

***N*-(*tert*-butyl) [*N*-(pent-4-enoyl)-2,5-dideoxy-2,5-imino]-3,4,6-tri-*O*-benzyl-*D*-gluco-hexonamide (18a).** $R_f = 0.40$



(25/75 EtOAc/toluene). 5:1 Mixture of rotamers; major rotamer: ^1H NMR (400 MHz, CDCl_3) δ 7.40 – 7.12 (m, 15H, CH_{Ar}), 5.83 (m, 1H, =CH pentenyl), 5.09 – 4.96 (m, 2H, =CH₂ pentenyl), 4.92 (d, $J = 11.2$ Hz, 1H, CHH Bn), 4.64 (d, $J = 11.6$ Hz, 1H, CHH Bn), 4.59 – 4.39 (m, 5H, C-2, 4xCHH Bn), 4.27 – 4.14 (m, 3H, C-3, C-4, C-6a), 3.95 – 3.88 (m, 1H, C-5), 3.48 (dd, $J = 9.7$, 2.4 Hz, 1H, C-6b), 2.46 – 2.33 (m, 3H, CH₂CH pentenyl, CHHCO pentenyl), 2.32 – 2.23 (m, 1H, CHHCO pentenyl), 1.30 (s, 9H, 3xCH₃ *t*-butyl). ^{13}C NMR (101 MHz, CDCl_3) δ 173.6 (NC=O pentenyl), 168.2 (NHC(O)-1), 137.8, 137.7, 137.5 (3xC_q Bn), 137.1 (=CH pentenyl), 128.6, 128.6, 128.4, 128.1, 128.1, 127.9, 127.9 (CH_{Ar}), 115.5 (=CH₂ pentenyl), 82.3 (C-3), 79.6 (C-4), 73.3, 72.8, 72.7 (CH₂ Bn), 65.8 (C-6), 64.4 (C-2), 60.5 (C-5), 51.3 (C_q *t*-butyl), 33.5 (CH₂CO pentenyl), 28.7 (CH₂CH pentenyl), 28.7 (3xCH₃ *t*-butyl). $[\alpha]^{20}_{\text{D}}$: -29.7° (c = 1, CHCl_3). IR (neat): 608, 696, 735, 820, 845, 912, 1001, 1026, 1074, 1094, 1206, 1225, 1248, 1287, 1304, 1329, 1364, 1393, 1454, 1497, 1541, 1661, 1866, 2918, 2963, 3030, 3065, 3327. HR-MS: $[\text{M}+\text{H}^+]$ Calculated for $\text{C}_{36}\text{H}_{44}\text{N}_2\text{O}_5$: 585.33230; found: 585.33233. Spectroscopic data matched literature data.⁹

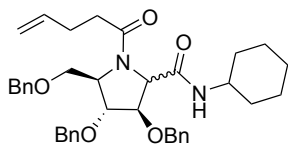
***N*-(*tert*-butyl) [*N*-(pent-4-enoyl)-2,5-dideoxy-2,5-imino]-3,4,6-tri-*O*-benzyl-*D*-manno-hexonamide (18b).** $R_f =$



0.45 (25/75 EtOAc/toluene). 7:2 Mixture of rotamers; major rotamer: ^1H NMR (400 MHz, CDCl_3) δ 7.40 – 7.19 (m, 15H, CH_{Ar}), 5.95 (s, 1H, NH), 5.88 – 5.70 (m, 1H, =CH pentenyl), 5.07 – 4.90 (m, 2H, =CH₂ pentenyl), 4.70 – 4.54 (m, 3H, C-5, 2xCHH Bn), 4.54 – 4.41 (m, 4H, 4xCHH Bn), 4.26 (s, 1H, C-2), 4.22 (s, 1H, C-3), 4.15 (s, 1H, C-4), 3.97 (dd, $J = 8.8$, 4.4 Hz, 1H, C-6), 3.48 (dd, $J = 10.5$, 9.0 Hz, 1H, C-6), 2.42 – 2.32 (m, 2H, CH₂CH pentenyl), 2.32 – 2.22 (m, 2H, CH₂CO pentenyl), 1.08 (s, 9H, 3xCH₃ *t*-butyl). ^{13}C NMR (101 MHz, CDCl_3) δ 173.0 (NC=O pentenyl), 169.1 (NHC(O)-1), 138.4, 137.1 (2xC_q Bn), 137.0 (=CH pentenyl), 136.9 (C_q Bn), 128.6, 128.5, 128.3, 128.0, 127.7, 127.7, 127.7 (CH_{Ar}), 115.7 (=CH₂ pentenyl), 86.1 (C-4), 81.0 (C-3), 73.2, 71.8, 71.6 (3xCH₂ Bn), 69.8 (C-2), 66.6 (C-6), 63.9 (C-5), 51.4 (C_q *t*-butyl), 34.0 (CH₂CO pentenyl), 28.8 (CH₂CH

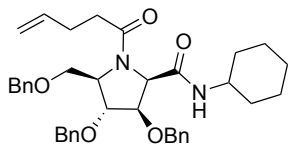
pentenyl), 28.2 (3xCH₃ *t*-butyl). [α]²⁰_D: -26.7° (c = 1, CHCl₃). IR (neat): 698, 735, 800, 912, 1001, 1028, 1076, 1096, 1206, 1225, 1254, 1281, 1298, 1314, 1364, 1400, 1454, 1497, 1528, 1655, 1678, 2857, 1868, 2922, 2961, 3030, 3065. HR-MS: [M+H]⁺ Calculated for C₃₆H₄₄N₂O₅: 585.33230; found: 585.33243. Spectroscopic data matched literature data.⁹

***N*-(cyclohexyl) [N-(pent-4-enoyl)-2,5-dideoxy-2,5-imino]-3,4,6-tri-*O*-benzyl-D-gluco/D-manno-hexonamide (19).**



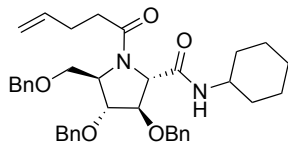
Crude 2,3,5-Tri-*O*-benzyl-4-deoxy-4-amino-D-arabinose (**13**, 0.22 mmol) was dissolved in anhydrous MeOH (0.7 ml) and cooled to 0 °C. Next, pent-4-enoic acid (89 μ l, 0.87 mmol) and cyclohexyl isocyanide (34 μ l, 0.27 mmol) were successively added and the reaction mixture was stirred overnight at 0-4 °C. NaHCO₃ (sat. aq.) was added to the mixture before allowing it to warm to room temperature while stirring. Ethyl acetate was added to the mixture and the organic phase was washed with NaHCO₃ (sat. aq.) and brine. The organic phase was dried over anhydrous MgSO₄, concentrated under reduced pressure and the product was isolated by silica gel chromatography (5-15% EtOAc/toluene; 2,3-*trans*-isomer **19b**: 5-6% EtOAc/toluene, 2,3-*cis*-isomer **19a** 6-15% EtOAc/toluene) yielding a separable 2,3-*cis*:2,3-*trans* mixture with a ratio of 54:46 in 61% combined yield (81 mg, 0.13 mmol) as a light yellow oil.

***N*-(cyclohexyl) [N-(pent-4-enoyl)-2,5-dideoxy-2,5-imino]-3,4,6-tri-*O*-benzyl-D-gluco-hexonamide (19a).** R_f = 0.35

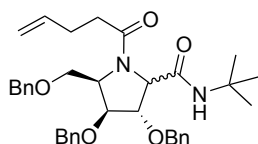


(25/75 EtOAc/toluene). 7:1 Mixture of rotamers; major rotamer: ¹H NMR (400 MHz, CDCl₃) δ 7.43 (d, J = 8.1 Hz, 1H, NH), 7.40 – 7.16 (m, 15H, CH_{Ar}), 5.88 – 5.72 (m, 1H, =CH pentenyl), 5.08 – 4.90 (m, 3H, =CH₂ pentenyl, CHH Bn-3), 4.69 (d, J = 11.6 Hz, 1H, CHH Bn-4), 4.61 – 4.42 (m, 4H, C-2, CHH Bn-3, CHH Bn-4, CHH Bn-6), 4.38 (d, J = 12.3 Hz, 1H, CHH Bn-6), 4.28 (dd, J = 9.7, 3.6 Hz, 1H, C-6a), 4.23 – 4.18 (m, 2H, C-3, C-4), 3.88 – 3.82 (m, 1H, C-5), 3.80 – 3.64 (m, 1H, CH Cy), 3.47 (dd, J = 9.8, 1.7 Hz, 1H, C-6b), 2.44 – 2.31 (m, 3H, CHHCH pentenyl, CH₂CO pentenyl), 2.29 – 2.18 (m, 1H, CHHCH pentenyl), 1.84 – 1.71 (m, 2H, CH₂ Cy), 1.66 – 1.49 (m, 3H, CH₂ Cy, CHH Cy), 1.33 – 1.19 (m, 2H, CH₂ Cy), 1.01 – 0.72 (m, 3H, CH₂ Cy, CHH Cy). ¹³C NMR (101 MHz, CDCl₃) δ 173.4 (NC=O pentenyl), 168.0 (NHC(O)-1), 137.9, 137.6, 137.3 (3x_q Bn), 137.1 (=CH pentenyl), 128.7, 128.5, 128.5, 128.4, 128.3, 128.2, 128.2, 127.9 (CH_{Ar}), 115.6 (=CH₂ pentenyl), 81.9 (C-3), 79.2 (C-4), 73.2, 73.1, 72.9 (3xCH₂ Bn), 66.0 (C-6), 63.4 (C-2), 60.2 (C-5), 48.5 (CH Cy), 33.4 (CH₂CH pentenyl), 33.0, 32.8 (2xCH₂ Cy), 28.7 (CH₂CO), 25.3, 25.2, 25.1 (3xCH₂ Cy). [α]²⁰_D: -23.8° (c = 1, CHCl₃). IR (neat): 696, 735, 912, 1001, 1026, 1074, 1098, 1206, 1256, 1306, 1329, 1364, 1404, 1452, 1537, 1657, 2853, 2928, 3318. HR-MS: [M+H]⁺ Calculated for C₃₈H₄₆N₂O₅: 611.34795; found: 611.34813. Spectroscopic data matched literature data.⁹

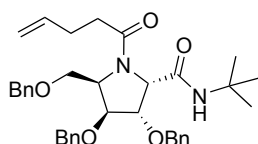
***N*-(cyclohexyl) [N-(pent-4-enoyl)-2,5-dideoxy-2,5-imino]-3,4,6-tri-*O*-benzyl-D-manno-hexonamide (19b).** R_f =



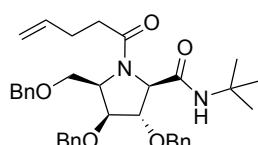
0.40 (25/75 EtOAc/toluene). 7:2 Mixture of rotamers; major rotamer: ¹H NMR (400 MHz, CDCl₃) δ 7.40 – 7.15 (m, 15H, CH_{Ar}), 6.01 (d, J = 8.1 Hz, 1H, NH), 5.91 – 5.70 (m, 1H, CH pentenyl), 5.10 – 4.91 (m, 2H, CH₂ pentenyl), 4.70 – 4.54 (m, 3H, C-5, CHH Bn-3, CHH Bn-6), 4.54 – 4.39 (m, 4H, CHH Bn-3, 2xCHH Bn-4, CHH Bn-6), 4.36 (s, 1H, C-2), 4.21 (s, 1H, C-4), 4.15 (s, 1H, C-3), 3.98 (dd, J = 8.8, 4.4 Hz, 1H, C-6a), 3.64 – 3.52 (m, 1H, CH Cy), 3.49 (dd, J = 10.5, 9.0 Hz, 1H, C-6b), 2.41 – 2.31 (m, 3H, CHHCH pentenyl, CH₂CO pentenyl), 2.30 – 2.21 (m, 1H, CHHCH pentenyl), 1.83 – 0.49 (m, 10H, CH₂ Cy). ¹³C NMR (101 MHz, CDCl₃) δ 173.0 (NC=O pentenyl), 168.8 (NHC(O)-1), 138.4, 137.1 (2x_q Bn), 137.0 (=CH pentenyl), 136.9 (C_q Bn), 128.6, 128.6, 128.5, 128.5, 128.3, 128.1, 127.8, 127.7, 127.7 (CH_{Ar}), 115.7 (=CH₂ pentenyl), 86.0 (C-3), 80.9 (C-4), 73.2 (CH₂ Bn-6), 71.8 (CH₂ Bn-3), 71.6 (CH₂ Bn-4), 69.1 (C-2), 66.7 (C-6), 64.0 (C-5), 48.6 (CH Cy), 34.0 (CH₂CH pentenyl), 32.8, 32.0 (2xCH₂ Cy), 28.9 (CH₂CO pentenyl), 25.3, 24.8, 24.8 (3xCH₂ Cy). [α]²⁰_D: -11.8° (c = 1, CHCl₃). IR (neat): 698, 737, 912, 1001, 1028, 1076, 1098, 1152, 1206, 1254, 1319, 1350, 1366, 1404, 1454, 1497, 1530, 1651, 2855, 2928, 3030, 3063. HR-MS: [M+H]⁺ Calculated for C₃₈H₄₆N₂O₅: 611.34795; found: 611.34821. Spectroscopic data matched literature data.⁹

***N*-(*tert*-butyl) [N-(pent-4-enoyl)-2,5-dideoxy-2,5-imino]-3,4,6-tri-*O*-benzyl-*D*-ido/*D*-gulo-hexonamide (20).**

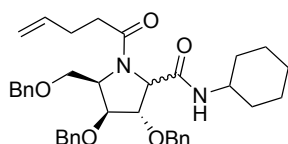
Crude 2,3,5-Tri-*O*-benzyl-4-deoxy-4-amino-*D*-xylose (**14**, 0.17 mmol) was dissolved in anhydrous MeOH (0.6 ml) and cooled to 0 °C. Next, pent-4-enoic acid (67 μ l, 0.66 mmol) and *tert*-butyl isocyanide (23 μ l, 0.21 mmol) were successively added and the reaction mixture was stirred overnight at 0–4 °C. NaHCO₃ (sat. aq.) was added to the mixture before allowing it to warm to room temperature while stirring. Ethyl acetate was added to the mixture and the organic phase was washed with NaHCO₃ (sat. aq.) and brine. The organic phase was dried over anhydrous MgSO₄, concentrated under reduced pressure and the product was isolated by silica gel chromatography (6–20% EtOAc/toluene; 2,3-*trans*-isomer **20b**: 6–7% EtOAc/toluene, 2,3-*cis*-isomer **20a** 7–20% EtOAc/toluene) yielding a separable 2,3-*cis*:2,3-*trans* mixture with a ratio of 43:57 in 39% combined yield (38 mg, 0.06 mmol) as a light yellow oil.

***N*-(*tert*-butyl) [N-(pent-4-enoyl)-2,5-dideoxy-2,5-imino]-3,4,6-tri-*O*-benzyl-*D*-ido-hexonamide (20a).** *R*_f = 0.40

(25/75 EtOAc/toluene). 5:4 Mixture of rotamers; major rotamer: ¹H NMR (400 MHz, CDCl₃) δ 7.44 – 7.16 (m, 15H, CH_{Ar}), 5.87 – 5.69 (m, 1H, =CH pentenyl), 5.28 (s, 1H, NH), 5.04 – 4.90 (m, 2H, =CH₂ pentenyl), 4.76 (d, *J* = 12.1 Hz, 1H, CHH Bn), 4.74 – 4.58 (m, 4H, C-3, 3xCHH Bn), 4.51 – 4.37 (m, 3H, 2xCHH Bn, C-4), 4.23 – 4.14 (m, 2H, C-1, C-5), 3.65 – 3.59 (m, 1H, C-6a), 3.53 (dd, *J* = 10.0, 3.2 Hz, 1H, C-6b), 2.42 – 2.23 (m, 3H, CH₂CO, CHHCH pentenyl), 2.21 – 2.14 (m, 1H, CHHCH pentenyl), 1.30 (s, 9H, 3xCH₃ *t*-butyl). ¹³C NMR (101 MHz, CDCl₃) δ 172.5 (NC=O pentenyl), 168.4 (NHC(O)-1), 138.3, 138.2, 137.9 (3x_q Bn), 137.5 (=CH pentenyl), 128.5, 128.5, 128.4, 128.4, 128.1, 127.9, 127.9, 127.8, 127.8, 127.7, 127.6, 127.5 (CH_{Ar}), 115.2 (=CH₂ pentenyl), 81.2 (C-3), 80.2 (C-4), 73.7, 73.6, 73.5 (CH₂ Bn), 68.5 (C-6), 62.8 (C-2), 56.7 (C-5), 51.6 (C_q *t*-butyl), 33.0 (CH₂CH pentenyl), 29.2 (CH₂CO), 28.7 (3xCH₃ *t*-butyl). [α]_D²⁰: 34.7° (*c* = 1, CHCl₃). IR (neat): 667, 698, 735, 802, 847, 912, 953, 1001, 1028, 1061, 1080, 1113, 1134, 1173, 1225, 1258, 1308, 1331, 1364, 1393, 1423, 1454, 1497, 1545, 1628, 1686, 1719, 1757, 2868, 2926, 2963, 3030, 3065, 3329. HR-MS: [M+H]⁺ Calculated for C₃₆H₄₄N₂O₅: 585.33230; found: 585.33234.

***N*-(*tert*-butyl) [N-(pent-4-enoyl)-2,5-dideoxy-2,5-imino]-3,4,6-tri-*O*-benzyl-*D*-gulo-hexonamide (20b).** *R*_f = 0.50

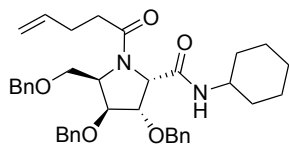
(25/75 EtOAc/toluene). 3:2 Mixture of rotamers; major rotamer: ¹H NMR (400 MHz, CDCl₃) δ 7.40 – 7.20 (m, 15H, CH_{Ar}), 7.03 (s, 1H, NH), 5.88 – 5.68 (m, 1H, =CH pentenyl), 5.08 – 4.89 (m, 3H, =CH₂, CHH Bn), 4.81 (d, *J* = 12.0 Hz, 1H, CHH Bn), 4.73 – 4.39 (m, 6H, C-5, C-3, 4xCHH Bn), 4.11 (d, *J* = 4.5 Hz, 1H, C-3), 4.03 (dd, *J* = 6.9, 5.8 Hz, 1H, C-2), 3.95 (dd, *J* = 9.8, 4.9 Hz, 1H, C-6a), 3.69 (dd, *J* = 9.9, 2.2 Hz, 1H, C-6b), 2.46 – 2.17 (m, 4H, CH₂CH pentenyl, CH₂CO pentenyl), 1.14 (s, 9H, *t*-butyl). ¹³C NMR (101 MHz, CDCl₃) δ 173.6 (NC=O pentenyl), 170.3 (NHC(O)-1), 137.8, 137.7, 137.6 (3x_q Bn), 137.1 (=CH pentenyl), 128.5, 128.5, 128.0, 127.9, 127.9, 127.9, 127.6 (CH_{Ar}), 115.6 (=CH₂ pentenyl), 84.6 (C-3), 81.0 (C-4), 73.7, 72.9, 72.1 (3xCH₂ Bn), 67.5 (C-2), 66.7 (C-6), 58.2 (C-5), 51.1 (C_q *t*-butyl), 33.2 (CH₂CO pentenyl), 29.1 (CH₂CH pentenyl), 28.3 (3xCH₃ *t*-butyl). [α]_D²⁰: 34.2° (*c* = 1, CHCl₃). IR (neat): 611, 631, 700, 735, 912, 1001, 1028, 1099, 1217, 1283, 1306, 1321, 1364, 1393, 1404, 1454, 1497, 1541, 1661, 1672, 2870, 2922, 2963, 3030, 3065, 3316. HR-MS: [M+H]⁺ Calculated for C₃₆H₄₄N₂O₅: 585.33230; found: 585.33240.

***N*-(cyclohexyl) [N-(pent-4-enoyl)-2,5-dideoxy-2,5-imino]-3,4,6-tri-*O*-benzyl-*D*-ido/*D*-gulo-hexonamide (21).**

Crude 2,3,5-Tri-*O*-benzyl-4-deoxy-4-amino-*D*-xylose (**14**, 0.17 mmol) was dissolved in anhydrous MeOH (0.55 ml) and cooled to 0 °C. Next, pent-4-enoic acid (67 μ l, 0.66 mmol) and cyclohexyl isocyanide (26 μ l, 0.21 mmol) were successively added and the reaction mixture was stirred overnight at 0–4 °C. NaHCO₃ (sat. aq.) was added to the mixture before allowing it to warm to room temperature while stirring. Ethyl acetate was added to the mixture and the organic phase was washed with NaHCO₃ (sat. aq.) and brine. The organic phase was dried over anhydrous MgSO₄, concentrated under reduced pressure and the product was isolated by silica gel chromatography (6–20% EtOAc/toluene; 2,3-*trans*-

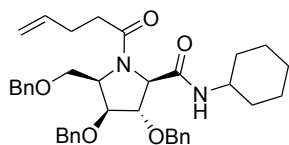
isomer **21b**: 6-7% EtOAc/toluene, 2,3-*cis*-isomer **21a** 7-20% EtOAc/toluene) yielding a separable 2,3-*cis*:2,3-*trans* mixture with a ratio of 45:55 in 37% combined yield (37 mg, 0.06 mmol) as a light yellow oil.

N-(cyclohexyl) [N-(pent-4-enoyl)-2,5-dideoxy-2,5-imino]-3,4,6-tri-O-benzyl-D-ido-hexonamide (21a). $R_f = 0.30$



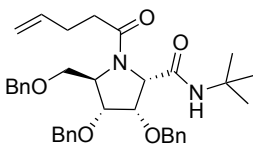
(25/75 EtOAc/toluene). 6:5 Mixture of rotamers; major rotamer: ^1H NMR (400 MHz, CDCl_3) δ 7.38 – 7.19 (m, 15H, CH_{Ar}), 5.84 – 5.70 (m, 1H, =CH pentenyl), 5.37 (d, $J = 8.1$ Hz, 1H, NH), 5.05 – 4.88 (m, 2H, = CH_2 pentenyl), 4.77 – 4.58 (m, 5H, C-3, 4xCHH Bn), 4.51 – 4.41 (m, 3H, C-4, 2xCHH Bn), 4.23 – 4.16 (m, 2H, C-2, C-5), 3.82 – 3.69 (m, 1H, CH Cy), 3.66 – 3.61 (m, 1H, C-6a), 3.54 (dd, $J = 10.0, 3.2$ Hz, 1H, C-6b), 2.38 – 2.27 (m, 3H, CHHCH pentenyl, CH_2CO pentenyl), 2.19 – 2.13 (m, 1H, CHHCH pentenyl), 2.01 – 0.70 (m, 10H, 5x CH_2 Cy). ^{13}C NMR (101 MHz, CDCl_3) δ 172.6 (NC=O pentenyl), 168.3 (NHC(O)-1), 138.7, 138.2, 138.0 (3x C_q Bn), 137.6 (=CH pentenyl), 128.6, 128.5, 128.5, 128.4, 128.1, 128.0, 127.9, 127.8, 127.8, 127.7, 127.6 (CH_{Ar}), 115.2 (=CH $_2$ pentenyl), 81.2 (C-3), 80.0 (C-4), 73.7, 73.5, 73.4 (CH_2 Bn), 68.5 (C-6), 61.1 (C-2), 56.8 (C-5), 48.8 (CH Cy), 33.1 (CH_2 Cy), 33.1 (CH_2CH pentenyl), 33.0 (CHCO pentenyl), 29.2, 25.6, 25.0, 24.9 (CH_2 Cy). $[\alpha]_D^{20}$: 37.5° ($c = 1$, CHCl_3). IR (neat): 681, 696, 735, 912, 1003, 1028, 1063, 1082, 1111, 1134, 1209, 1236, 1250, 1271, 1310, 1331, 1364, 1418, 1452, 1497, 1545, 1649, 2853, 2928, 3030, 3065, 3300. HR-MS: $[\text{M}+\text{H}^+]$ Calculated for $\text{C}_{38}\text{H}_{46}\text{N}_2\text{O}_5$: 611.34795; found: 611.34809.

N-(cyclohexyl) [N-(pent-4-enoyl)-2,5-dideoxy-2,5-imino]-3,4,6-tri-O-benzyl-D-gulo-hexonamide (21b). $R_f = 0.40$



(25/75 EtOAc/toluene). 4:3 Mixture of rotamers; major rotamer: ^1H NMR (400 MHz, CDCl_3) δ 7.42 – 7.17 (m, 16H, 15x CH_{Ar} , NH), 5.88 – 5.69 (m, 1H, =CH pentenyl), 5.07 – 4.90 (m, 2H, = CH_2), 4.80 (d, $J = 12.0$ Hz, 1H, CHH Bn), 4.69 – 4.43 (m, 6H, 5xCHH Bn, C-5), 4.43 – 4.38 (m, 1H, C-3), 4.20 (d, $J = 4.1$ Hz, 1H, C-2), 4.03 (dd, $J = 7.1, 5.4$ Hz, 1H, C-4), 3.99 (dd, $J = 9.7, 5.0$ Hz, 1H, C-6a), 3.70 (dd, $J = 9.7, 2.1$ Hz, 1H, C-6b), 3.60 – 3.47 (m, 1H, CH Cy), 2.41 – 2.25 (m, 3H, CHHCH pentenyl, CH_2CO pentenyl), 2.24 – 2.13 (m, 1H, CHHCH pentenyl), 1.88 – 0.44 (m, 10H, 5x CH_2 Cy). ^{13}C NMR (101 MHz, CDCl_3) δ 173.5 (NC=O pentenyl), 170.2 (NHC(O)-1), 137.6, 137.6 (3x C_q Bn), 137.2 (=CH pentenyl), 128.6, 128.5, 128.2, 128.0, 128.0, 127.9 (CH_{Ar}), 115.6 (=CH $_2$ pentenyl), 84.6 (C-3), 81.1 (C-4), 73.7, 72.9, 72.2 (3x CH_2 Bn), 67.0 (C-2), 66.6 (C-6), 58.3 (C-5), 48.4 (CHCy), 33.2 (CH_2 Cy), 32.7 (CH_2CH pentenyl), 32.2 (CH_2 Cy), 28.7 (CH_2CO pentenyl), 25.3, 25.1, 25.0 (3x CH_2 Cy). $[\alpha]_D^{20}$: 18.9° ($c = 1$, CHCl_3). IR (neat): 696, 737, 912, 1001, 1028, 1101, 1207, 1254, 1281, 1319, 1364, 1410, 1452, 1497, 1522, 1533, 1655, 1661, 2855, 2928, 3030, 3065, 3308. HR-MS: $[\text{M}+\text{H}^+]$ Calculated for $\text{C}_{38}\text{H}_{46}\text{N}_2\text{O}_5$: 611.34795; found: 611.34815.

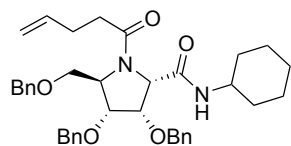
N-(tert-butyl) [N-(pent-4-enoyl)-2,5-dideoxy-2,5-imino]-3,4,6-tri-O-benzyl-D-altro-hexonamide (22a). Crude



2,3,5-Tri-*O*-benzyl-4-deoxy-4-amino-D-ribose (**15**, 0.21 mmol) was dissolved in anhydrous MeOH (0.7 ml) and cooled to 0 °C. Next, pent-4-enoic acid (86 μl , 0.84 mmol) and *tert*-butyl isocyanide (30 μl , 0.26 mmol) were successively added and the reaction mixture was stirred overnight at 0-4 °C. NaHCO_3 (sat. aq.) was added to the mixture before allowing it to warm to room temperature while stirring. Ethyl acetate was added to the mixture and the organic phase was washed with NaHCO_3 (sat. aq.) and brine. The organic phase was dried over anhydrous MgSO_4 , concentrated under reduced pressure and the product was isolated by silica gel chromatography (10-15% EtOAc/toluene) yielding the title compound as a single stereoisomer in 49% yield (60 mg, 0.10 mmol). $R_f = 0.55$ (25/75 EtOAc/toluene). ^1H NMR (400 MHz, CDCl_3) δ 7.38 – 7.26 (m, 13H, CH_{Ar} Bn), 7.19 – 7.14 (m, 2H, CH_{Ar} Bn), 6.76 (s, 1H, NH), 5.88 – 5.75 (m, 1H, =CH pentenyl), 5.05 – 4.92 (m, 2H, = CH_2 pentenyl), 4.76 (d, $J = 11.6$ Hz, 1H, CHH Bn-3), 4.70 (d, $J = 11.5$ Hz, 1H, CHH Bn-4), 4.65 (d, $J = 12.0$ Hz, 1H, CHH Bn-4), 4.61 (dd, $J = 9.1, 4.4$ Hz, 1H, C-3), 4.55 – 4.50 (m, 2H, C-5, CHH Bn-3), 4.44 (d, $J = 9.1$ Hz, 1H, C-2), 4.43 (d, $J = 12.0$ Hz, 1H, CHH Bn-6), 4.38 (d, $J = 11.9$ Hz, 1H, CHH Bn-6), 4.07 (d, $J = 4.4$ Hz, 1H, C-4), 3.66 (dd, $J = 9.9, 4.9$ Hz, 1H, C-6a), 3.53 (dd, $J = 9.9, 2.6$ Hz, 1H, C-6b), 2.40 – 2.31 (m, 4H, CH_2CH pentenyl, CH_2CO pentenyl), 1.06 (s, 9H, 3x CH_2 *tert*-butyl). ^{13}C NMR (101 MHz, CDCl_3) δ 173.3 (NC=O pentenyl), 168.9 (NHC(O)-1), 137.9, 137.8, 137.4 (3x C_q Bn), 137.3 (=CH pentenyl), 128.6, 128.5, 128.4, 128.3, 128.2, 127.9, 127.8,

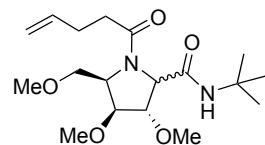
127.8, 127.5 (CH_{Ar} Bn), 115.3 ($=\text{CH}_2$ pentenyl), 79.7 (C-4), 79.0 (C-3), 73.5 (CH_2 Bn-6), 73.1 (CH_2 Bn-4), 72.9 (CH_2 Bn-3), 67.8 (C-6), 65.7 (C-2), 62.9 (C-5), 51.0 (C_q *tert*-butyl), 33.7 (CH_2CH pentenyl), 28.7 (CH_2CO pentenyl), 28.2 ($3\times\text{CH}_3$ *tert*-butyl). $[\alpha]_D^{20}$: 14.4° ($c = 1$, CHCl_3). IR (neat): 698, 737, 912, 1001, 1028, 1043, 4069, 1103, 1223, 1277, 1306, 1364, 1406, 1454, 1497, 1535, 1657, 1676, 2866, 2924, 2963, 3030, 3063, 3348. HR-MS: $[\text{M}+\text{H}^+]$ Calculated for $\text{C}_{36}\text{H}_{44}\text{N}_2\text{O}_5$: 585.33230; found: 585.33213.

***N*-(cyclohexyl) [N-(pent-4-enoyl)-2,5-dideoxy-2,5-imino]-3,4,6-tri-*O*-benzyl-D-altro-hexonamide (23a).** Crude



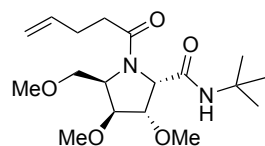
2,3,5-Tri-*O*-benzyl-4-deoxy-4-amino-D-ribose (**15**, 0.21 mmol) was dissolved in anhydrous MeOH (0.7 ml) and cooled to 0 °C. Next, pent-4-enoic acid (86 μl , 0.84 mmol) and cyclohexyl isocyanide (33 μl , 0.26 mmol) were successively added and the reaction mixture was stirred overnight at 0-4 °C. NaHCO_3 (sat. aq.) was added to the mixture before allowing it to warm to room temperature while stirring. Ethyl acetate was added to the mixture and the organic phase was washed with NaHCO_3 (sat. aq.) and brine. The organic phase was dried over anhydrous MgSO_4 , concentrated under reduced pressure and the product was isolated by silica gel chromatography (10-30% EtOAc/toluene) yielding the title compound as a single stereoisomer in 51% yield (65 mg, 0.11 mmol). $R_f = 0.50$ (25/75 EtOAc/toluene). ^1H NMR (400 MHz, CDCl_3) δ 7.48 – 7.21 (m, 13H, CH_{Ar} Bn), 7.19 – 7.12 (m, 2H, CH_{Ar} Bn), 6.85 (d, $J = 8.0$ Hz, 1H, NH), 5.87 – 5.71 (m, 1H, $=\text{CH}$ pentenyl), 5.05 – 4.91 (m, 2H, $=\text{CH}_2$), 4.73 (d, $J = 11.8$ Hz, 1H, CHH Bn-3), 4.64 (s, 2H, CH_2 Bn-4), 4.62 (dd, $J = 9.1, 4.4$ Hz, 1H, C-3), 4.56 – 4.50 (m, 3H, C-2, C-5, CHH Bn-3), 4.42 (d, $J = 11.9$ Hz, 1H, CHH Bn-6), 4.37 (d, $J = 11.9$ Hz, 1H, CHH Bn-6), 4.04 (d, $J = 4.4$ Hz, 1H, C-4), 3.67 (dd, $J = 9.9, 4.8$ Hz, 1H, C-6a), 3.65 – 3.55 (m, 1H, CH Cy), 3.52 (dd, $J = 9.9, 2.4$ Hz, 1H, C-6), 2.39 – 2.29 (m, 4H, CH_2CH pentenyl, CH_2CO pentenyl), 1.65 (d, $J = 12.2$ Hz, 1H, CHHCH Cy), 1.59 – 1.38 (m, 3H, CHHCH Cy, CHHCCH Cy, CHHCH $_2$ CH Cy), 1.24 – 1.07 (m, 2H, CHHCH $_2$ CH Cy, CHHCH $_2$ CH Cy), 0.95 – 0.80 (m, 2H, $\text{CH}_2\text{CH}_2\text{CH}_2$ Cy), 0.79 – 0.67 (m, 1H, CHHCH Cy), 0.67 – 0.52 (m, 1H, CHHCH Cy). ^{13}C NMR (101 MHz, CDCl_3) δ 173.2 (NC=O pentenyl), 168.7 (NHC(O)-1), 137.9, 137.7 ($3\times\text{C}_q$ Bn), 137.2 ($=\text{CH}$ pentenyl), 128.6, 128.5, 128.4, 128.2, 127.9, 127.8, 127.5 (CH_{Ar} Bn), 115.3 ($=\text{CH}_2$ pentenyl), 79.5 (C-4), 78.7 (C-3), 73.4 (CH_2 Bn-6), 72.9 (CH_2 Bn-4), 72.7 (CH_2 Bn-3), 67.8 (C-6), 64.9 (C-5), 62.8 (C-2), 48.4 (CH Cy), 33.7 (CHCH $_2$ pentenyl), 32.6 (CH_2CH Cy), 32.1 (CH_2CH Cy), 28.7 (CH_2CO pentenyl), 25.4 ($\text{CH}_2(\text{CH}_2)_2$ Cy), 24.8 ($\text{CH}_2\text{CH}_2\text{CH}$ Cy), 24.7 ($\text{CH}_2\text{CH}_2\text{CH}$ Cy). $[\alpha]_D^{20}$: 11.9° ($c = 1$, CHCl_3). IR (neat): 698, 737, 912, 1003, 1028, 1103, 1190, 1209, 1258, 1273, 1321, 1358, 1408, 1452, 1497, 1535, 1657, 2855, 2928, 3030, 3063, 3308, 3339. HR-MS: $[\text{M}+\text{H}^+]$ Calculated for $\text{C}_{38}\text{H}_{46}\text{N}_2\text{O}_5$: 611.34795; found: 611.34808.

***N*-(*tert*-butyl) [N-(pent-4-enoyl)-2,5-dideoxy-2,5-imino]-3,4,6-tri-*O*-methyl-D-ido/D-gulo-hexonamide (63).**



Crude 2,3,5-Tri-*O*-methyl-4-deoxy-4-amino-D-xylofuranose (**62**, 0.22 mmol) was dissolved in anhydrous MeOH (0.7 ml) and cooled to 0 °C. Next, pent-4-enoic acid (90 μl , 0.88 mmol) and *tert*-butyl isocyanide (31 μl , 0.28 mmol) were successively added and the reaction mixture was stirred overnight at 0-4 °C. NaHCO_3 (sat. aq.) was added to the mixture before allowing it to warm to room temperature while stirring. Ethyl acetate was added to the mixture and the organic phase was washed with NaHCO_3 (sat. aq.) and brine. The organic phase was dried over anhydrous MgSO_4 , concentrated under reduced pressure and the product was isolated by silica gel chromatography (20-70% EtOAc/toluene; 2,3-*trans*-isomer **63b**: 20-30% EtOAc/toluene, 2,3-*cis*-isomer **63a**: 30-70% EtOAc/toluene) yielding a separable 2,3-*cis*:2,3-*trans* mixture with a ratio of 44:56 in 46% combined yield (36 mg, 0.10 mmol).

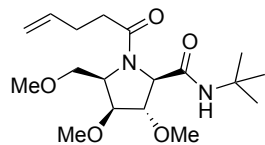
***N*-(*tert*-butyl) [N-(pent-4-enoyl)-2,5-dideoxy-2,5-imino]-3,4,6-tri-*O*-methyl-D-ido-hexonamide (63a).** $R_f = 0.35$



(75/25 EtOAc/toluene). 6:5 Mixture of rotamers; major rotamer: ^1H NMR (400 MHz, CDCl_3) δ 5.90 – 5.75 (m, 1H, $=\text{CH}$ pentenyl), 5.53 (s, 1H, NH), 5.11 – 4.93 (m, 2H, $=\text{CH}_2$), 4.37 (dd, $J = 9.0, 7.8$ Hz, 1H, C-4), 4.32 – 4.19 (m, 2H, C-2, C-5), 4.02 (t, $J = 8.6$ Hz, 1H, C-3), 3.56 – 3.51 (m, 1H, C-6a), 3.49 (s, 3H, CH_3 Me-3), 3.47 (s, 3H, CH_3 Me-4), 3.45 – 3.39 (m, 1H, C-6b), 3.32 (s, 3H, CH_3 Me-6), 2.50 –

2.42 (m, 1H, CHHCH pentenyl), 2.42 – 2.33 (m, 2H, CH₂CO), 2.28 – 2.19 (m, 1H, CHHCH pentenyl), 1.35 (s, 9H, 3xCH₃). ¹³C NMR (101 MHz, CDCl₃) δ 172.8 (NC=O pentenyl), 168.3 (NHC(O)-1), 137.6 (=CH pentenyl), 115.3 (=CH₂ pentenyl), 82.3 (C-4), 82.0 (C-3), 71.1 (C-6), 61.4 (C-2), 59.5 (CH₃ Me-3), 59.4 (CH₃ Me-4), 59.1 (CH₃ Me-6), 56.5 (C-5), 51.8 (C_q *tert*-butyl), 33.1 (CH₂CH pentenyl), 29.3 (CH₂CO), 28.8 (3xCH₃ *tert*-butyl). [α]²⁰_D: 32.3° (c = 1, CHCl₃). IR (neat): 910, 1011, 1067, 1115, 1202, 1258, 1364, 1393, 1422, 1450, 1549, 1630, 1668, 2828, 2851, 2926, 2967, 3076, 3318. HR-MS: [M+H]⁺ Calculated for C₁₈H₃₂N₂O₅: 357.23840; found: 357.23835.

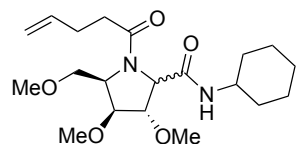
***N*-(*tert*-butyl) [*N*-(pent-4-enoyl)-2,5-dideoxy-2,5-imino]-3,4,6-tri-*O*-methyl-*D*-gulo-hexonamide (63b).** *R*_f = 0.60



(75/25 EtOAc/toluene). 2:1 Mixture of rotamers; major rotamer: ¹H NMR (400 MHz, CDCl₃) δ 5.92 – 5.75 (m, 1H, =CH pentenyl), 5.11 – 4.94 (m, 2H, =CH₂ pentenyl), 4.44 – 4.35 (m, 1H, C-5), 4.04 (t, *J* = 5.1 Hz, 1H, C-3), 3.99 (d, *J* = 4.6 Hz, 1H, C-2), 3.91 (dd, *J* = 9.7, 4.6 Hz, 1H, C-5), 3.72 (t, *J* = 7.3, 5.8 Hz, 1H, C-4), 3.55 (dd, *J* = 9.6, 1.8 Hz, 1H, C-6), 3.48 (s, 3H, CH₃ Me-3), 3.43 (s, 3H, CH₃ Me-4),

3.38 (s, 3H, CH₃ Me-6), 2.42 – 2.32 (m, 3H, CHHCH pentenyl, CH₂CO), 2.27 – 2.21 (m, 1H, CHHCH pentenyl), 1.33 (s, 9H, 3xCH₃ *tert*-butyl). ¹³C NMR (101 MHz, CDCl₃) δ 173.6 (NC=O pentenyl), 170.8 (NHC(O)-1), 137.2 (=CH pentenyl), 115.6 (=CH₂ pentenyl), 86.9 (C-3), 83.0 (C-4), 68.3 (C-6), 67.2 (C-2), 59.0 (CH₃ Me-6), 58.8 (CH₃ Me-4), 58.3 (CH₃ Me-3), 57.7 (C-5), 51.0 (C_q *tert*-butyl), 33.1 (CH₂CH pentenyl), 28.7 (CH₂CO pentenyl), 28.6 (3xCH₃ *tert*-butyl). [α]²⁰_D: 23.2° (c = 1, CHCl₃). IR (neat): 914, 995, 1057, 1111, 1198, 1225, 1285, 1321, 1364, 1393, 1454, 1545, 1663, 1676, 2835, 2926, 2963, 3310. HR-MS: [M+H]⁺ Calculated for C₁₈H₃₂N₂O₅: 357.23840; found: 357.23839.

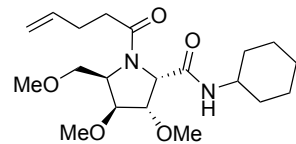
***N*-(cyclohexyl) [*N*-(pent-4-enoyl)-2,5-dideoxy-2,5-imino]-3,4,6-tri-*O*-methyl-*D*-ido/*D*-gulo-hexonamide (64).**



Crude 2,3,5-Tri-*O*-methyl-4-deoxy-4-amino-*D*-xylofuranose (**62**, 0.22 mmol) was dissolved in anhydrous MeOH (0.7 ml) and cooled to 0 °C. Next, pent-4-enoic acid (90 μl, 0.88 mmol) and cyclohexyl isocyanide (34 μl, 0.28 mmol) were successively added and the reaction mixture was stirred overnight at 0–4 °C. NaHCO₃ (sat. aq.) was added to the mixture before allowing it to

warm to room temperature while stirring. Ethyl acetate was added to the mixture and the organic phase was washed with NaHCO₃ (sat. aq.) and brine. The organic phase was dried over anhydrous MgSO₄, concentrated under reduced pressure and the product was isolated by silica gel chromatography (15–70% EtOAc/toluene; 2,3-*trans*-isomer **64b**: 15–30% EtOAc/toluene, 2,3-*cis*-isomer **64a** 40–70% EtOAc/toluene) yielding a separable 2,3-*cis*:2,3-*trans* mixture with a ratio of 46:54 in 53% combined yield (45 mg, 0.12 mmol).

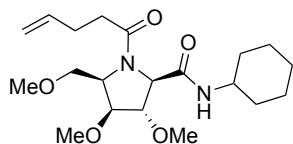
***N*-(cyclohexyl) [*N*-(pent-4-enoyl)-2,5-dideoxy-2,5-imino]-3,4,6-tri-*O*-methyl-*D*-ido-hexonamide (64a).** *R*_f = 0.35



(75/25 EtOAc/toluene). ¹H NMR (400 MHz, CDCl₃) δ 5.92 – 5.74 (m, 1H, =CH pentenyl), 5.70 (d, *J* = 8.1 Hz, 1H, NH), 5.09 – 4.94 (m, 2H, =CH₂ pentenyl), 4.40 – 4.22 (m, 3H, C-2, C-4, C-5), 4.05 (t, *J* = 8.6 Hz, 1H, C-3), 3.86 – 3.74 (m, 1H, CH Cy), 3.53 (dd, *J* = 10.2, 3.8 Hz, 1H, C-6a), 3.48 (s, 3H, CH₃ Me-3), 3.48 (s, 3H, CH₃ Me-4), 3.46 – 3.40 (m, 1H, C-6b), 3.32 (s, 3H, CH₃ Me-6), 2.52 –

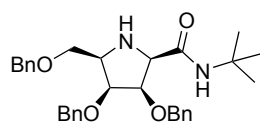
2.43 (m, 1H, CHHCH pentenyl), 2.43 – 2.32 (m, 2H, CH₂CO pentenyl), 2.28 – 2.17 (m, 1H, CHHCH pentenyl), 1.99 – 1.87 (m, 2H, CH₂ Cy), 1.75 – 1.55 (m, 4H, 2xCH₂ Cy), 1.44 – 1.28 (m, 2H, CH₂ Cy), 1.23 – 1.05 (m, 2H, CH₂ Cy). ¹³C NMR (101 MHz, CDCl₃) δ 173.2 (NC=O pentenyl), 168.3 (NHC(O)-1), 137.5 (=CH pentenyl), 115.4 (=CH₂ pentenyl), 82.5 (C-4), 82.0 (C-3), 70.9 (C-6), 61.0 (C-2), 59.6 (CH₃ Me-3), 59.4 (CH₃ Me-4), 59.2 (CH₃ Me-6), 56.6 (C-5), 48.8 (CH Cy), 33.2, 33.2, 33.0 (CH₂CH pentenyl, 2xCH₂ Cy), 29.2 (CH₂CO pentenyl), 25.7, 25.0, 24.9 (3xCH₂ Cy). [α]²⁰_D: 25.9° (c = 1, CHCl₃). IR (neat): 912, 959, 1011, 1065, 1113, 1202, 1250, 1350, 1418, 1449, 1549, 1653, 2830, 2855, 2928, 2980, 3292. HR-MS: [M+H]⁺ Calculated for C₂₀H₃₄N₂O₅: 383.25405; found: 383.25446.

***N*-(cyclohexyl) [N-(pent-4-enoyl)-2,5-dideoxy-2,5-imino]-3,4,6-tri-*O*-methyl-D-gulo-hexonamide (64b).** R_f = 0.55



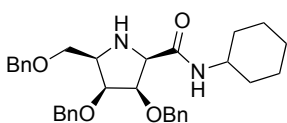
(75/25 EtOAc/toluene). 3:1 Mixture of rotamers; major rotamer: ^1H NMR (400 MHz, CDCl_3) δ 7.48 (d, J = 8.1 Hz, 1H, NH), 5.92 – 5.73 (m, 1H, =CH), 5.11 – 4.94 (m, 2H, =CH₂), 4.48 – 4.37 (m, 1H, C-5), 4.08 (d, J = 4.7 Hz, 1H, C-2), 4.02 (t, J = 5.2 Hz, 1H, C-3), 3.93 (dd, J = 9.7, 4.5 Hz, 1H, C-6), 3.78 – 3.69 (m, 2H, C-4, CH Cy), 3.55 (dd, J = 9.7, 1.8 Hz, 1H, C-6a), 3.48 (s, 3H, CH₃ Me-3), 3.43 (s, 3H, CH₃ Me-4), 3.40 (s, 3H, CH₃ Me-6), 2.51 – 2.28 (m, 3H, CHHCH pentenyl, CH₂CO), 2.28 – 2.16 (m, 1H, CHHCH pentenyl), 1.94 – 1.80 (m, 2H, CH₂ Cy), 1.78 – 1.50 (m, 3H, CHH Cy, CH₂ Cy), 1.43 – 1.28 (m, 3H, CHH Cy, CH₂ Cy), 1.22 – 1.00 (m, 2H, CH₂ Cy). ^{13}C NMR (101 MHz, CDCl_3) δ 173.5 (NC=O pentenyl), 170.6 (NHC(O)-1), 137.1 (=CH pentenyl), 115.6 (=CH₂ pentenyl), 87.0 (C-3), 83.1 (C-4), 68.3 (C-6), 66.6 (C-2), 58.9 (CH₃ Me-3), 58.9 (CH₃ Me-4), 58.4 (CH₃ Me-6), 57.6 (C-5), 48.3 (CH Cy), 33.2, 33.1, 33.0 (CH₂CH pentenyl, 2xCH₂ Cy), 28.7 (CH₂CO), 25.7, 25.1 (2xCH₂ Cy). $[\alpha]_D^{20}$: 21.4° (c = 1, CHCl_3). IR (neat): 912, 957, 980, 997, 1051, 1196, 1225, 1256, 1277, 1319, 1418, 1449, 1539, 1659, 1734, 2853, 2928, 2980, 3304. HR-MS: $[\text{M}+\text{H}]^+$ Calculated for $\text{C}_{20}\text{H}_{34}\text{N}_2\text{O}_5$: 383.25405; found: 383.25444.

***N*-(*tert*-butyl)-2,5-dideoxy-2,5-imino-3,4,6-tri-*O*-benzyl-D-galacto-hexonamide (24).** *N*-(*tert*-butyl) [N-(pent-4-enoyl)-2,5-dideoxy-2,5-imino]-3,4,6-tri-*O*-benzyl-D-galacto-hexonamide (16a, 62



mg, 0.11 mmol) was dissolved in a mixture of THF (1.5 ml) and water (0.5 ml). Iodine (81 mg, 0.3 mmol) was added and the reaction stirred for 30 minutes. A mixture of 1M $\text{Na}_2\text{S}_2\text{O}_3$ (aq.) and NaHCO_3 (sat. aq., 1/1 v/v, 5 ml) was added and the mixture vigorously stirred for 5 minutes. The suspension was extracted with EtOAc and the combined organic layers washed with brine, dried over anhydrous MgSO_4 and concentrated. The product was purified by flash chromatography (40-80% EtOAc/toluene) yielding the title compound in 78% yield (42 mg, 83 μmol). R_f = 0.15 (40/60 EtOAc/toluene). ^1H NMR (400 MHz, CDCl_3) δ 7.36 (s, 1H, NH *tert*-butyl), 7.35 – 7.22 (m, 15H, CH_{Ar}), 4.76 (d, J = 11.7 Hz, 1H, CHH Bn-3), 4.66 (d, J = 11.7 Hz, 1H, CHH Bn-3), 4.64 (d, J = 11.9 Hz, 1H, CHH Bn-4), 4.55 (s, 2H, CH₂ Bn-6), 4.51 (d, J = 11.9 Hz, 1H, CHH Bn-4), 4.29 (dd, J = 6.2, 4.0 Hz, 1H, C-3), 3.98 (dd, J = 6.3, 4.0 Hz, 1H, C-4), 3.84 (d, J = 6.3 Hz, 1H, C-2), 3.79 (dd, J = 9.5, 4.4 Hz, 1H, C-6a), 3.73 – 3.67 (m, 1H, C-6b), 3.61 – 3.55 (m, 1H, C-5), 1.22 (s, 9H, 3xCH₃ *tert*-butyl). ^{13}C NMR (101 MHz, CDCl_3) δ 170.2 (C-1), 138.6, 138.4, 138.3 (C_q Bn), 128.5, 128.4, 128.2, 127.9, 127.8, 127.6, 127.6, 127.4 (CH_{Ar} Bn), 79.8 (C-3), 79.7 (C-4), 73.8 (CH₂ Bn-3), 73.7 (CH₂ Bn-6), 72.9 (CH₂ Bn-4), 71.6 (C-6), 62.3 (C-2), 58.1 (C-5), 50.6 (C_q *tert*-butyl), 28.7 (3xCH₃ *tert*-butyl). $[\alpha]_D^{20}$: 7.3° (c = 1, CHCl_3). IR (neat): 696, 737, 910, 949, 1026, 1057, 1099, 1109, 1144, 1215, 1275, 1364, 1393, 1454, 1497, 1531, 1663, 2868, 2924, 2965, 3030, 3063, 3321. HR-MS: $[\text{M}+\text{H}]^+$ Calculated for $\text{C}_{31}\text{H}_{38}\text{N}_2\text{O}_4$: 503.29043; found: 503.29011.

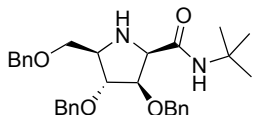
***N*-(cyclohexyl)-2,5-dideoxy-2,5-imino-3,4,6-tri-*O*-benzyl-D-galacto-hexonamide (25).** *N*-(cyclohexyl) [N-(pent-4-enoyl)-2,5-dideoxy-2,5-imino]-3,4,6-tri-*O*-benzyl-D-galacto-hexonamide (17a,



75 mg, 0.12 mmol) was dissolved in a mixture of THF (1.7 ml) and water (0.5 ml). Iodine (93 mg, 0.37 mmol) was added and the reaction stirred for 30 minutes. A mixture of 1M $\text{Na}_2\text{S}_2\text{O}_3$ (aq.) and NaHCO_3 (sat. aq., 1/1 v/v, 5 ml) was added and the mixture vigorously stirred for 5 minutes. The suspension was extracted with EtOAc and the combined organic layers washed with brine, dried over anhydrous MgSO_4 and concentrated. The product was purified by flash chromatography (40-80% EtOAc/toluene) yielding the title compound in 71% yield (46 mg, 86 μmol). R_f = 0.35 (40/60 EtOAc/toluene). ^1H NMR (400 MHz, CDCl_3) δ 7.46 (d, J = 8.3 Hz, 1H, NH Cy), 7.38 – 7.20 (m, 15H, CH_{Ar} Bn), 4.71 (d, J = 11.6 Hz, 1H, CHH Bn-3), 4.67 (d, J = 11.7 Hz, 1H, CHH Bn-3), 4.62 (d, J = 11.8 Hz, 1H, CHH Bn-4), 4.53 (s, 2H, 2xCHH Bn-6), 4.50 (d, J = 11.8 Hz, 1H, CHH Bn-4), 4.41 (dd, J = 6.2, 3.9 Hz, 1H, C-3), 4.06 (d, J = 6.4 Hz, 1H, C-2), 4.04 (dd, J = 6.1, 3.9 Hz, 1H, C-4), 3.79 – 3.63 (m, 4H, C-5, C-6, CH Cy), 1.79 – 1.71 (m, 1H, CHHCH Cy), 1.67 – 1.42 (m, 4H, CHHCH Cy, 2xCHHCH₂CH Cy, CHH(CH₂)₂ Cy), 1.36 – 1.01 (m, 4H, CHHCH Cy, 2xCHHCH₂CH Cy, CHH(CH₂)₂ Cy), 1.00 – 0.90 (m, 1H, CHHCH Cy). ^{13}C NMR (101 MHz, CDCl_3) δ 169.4 (C-1), 138.4, 138.2, 138.0 (3xC_q Bn), 128.5, 128.5, 128.3, 128.0, 127.8, 127.8, 127.7, 127.6, 127.5 (CH_{Ar} Bn), 79.7 (C-3), 79.4 (C-

4), 73.9 (CH₂ Bn-3), 73.6 (CH₂ Bn-6), 72.9 (CH₂ Bn-4), 71.0 (C-6), 61.5 (C-2), 58.2 (C-5), 47.9 (CH Cy), 32.7 (2xCH₂CH Cy), 25.6 (CH₂(CH₂)₂ Cy), 24.7, 24.7 (2xCH₂CH₂CH Cy). [α]_D²⁰: 3.6° (c = 0.9, CHCl₃). IR (neat): 696, 735, 891, 912, 957, 1028, 1057, 1094, 1126, 1150, 1209, 1254, 1312, 1350, 1360, 1404, 1452, 1497, 1526, 1653, 1717, 2853, 2928, 3030, 3063, 3321. HR-MS: [M+H]⁺ Calculated for C₃₃H₄₀N₂O₄: 529.30608; found: 529.30583. Spectroscopic data matched literature data.⁹

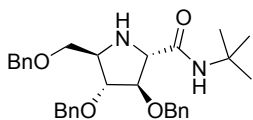
***N*-(*tert*-butyl)-2,5-dideoxy-2,5-imino-3,4,6-tri-*O*-benzyl-*D*-gluco-hexonamide (26a).** *N*-(*tert*-butyl) [*N*-(pent-4-



enoyl)-2,5-dideoxy-2,5-imino]-3,4,6-tri-*O*-benzyl-*D*-gluco-hexonamide (**18a**, 49 mg, 84 μ mol) was dissolved in a mixture of THF (1.2 ml) and water (0.4 ml). Iodine (64 mg, 0.25 mmol) was added and the reaction stirred for 30 minutes. A

mixture of 1M Na₂S₂O₃ (aq.) and NaHCO₃ (sat. aq., 1/1 v/v, 5 ml) was added and the mixture vigorously stirred for 5 minutes. The suspension was extracted with EtOAc and the combined organic layers washed with brine, dried over anhydrous MgSO₄ and concentrated. The product was purified by flash chromatography (14-25% EtOAc/toluene) yielding the title compound in 52% yield (22 mg, 44 μ mol). *R*_f = 0.40 (40/60 EtOAc/toluene). ¹H NMR (400 MHz, CDCl₃) δ 7.37 – 7.20 (m, 15H, CH_{Ar}), 7.18 (s, 1H, NH *tert*-butyl), 4.60 (d, *J* = 11.8 Hz, 1H, CHH Bn-3), 4.53 (d, *J* = 12.1 Hz, 1H, CHH Bn-6), 4.51 – 4.47 (m, 1H, CHH Bn-6), 4.46 (d, *J* = 11.9 Hz, 1H, CHH Bn-4), 4.45 (d, *J* = 11.8 Hz, 1H, CHH Bn-3), 4.39 (d, *J* = 11.9 Hz, 1H, CHH Bn-4), 4.23 (dd, *J* = 5.5, 1.4 Hz, 1H, C-3), 4.00 (d, *J* = 5.5 Hz, 1H, C-2), 3.85 – 3.80 (m, 1H, C-4), 3.57 – 3.43 (m, 3H, C-5, C-6), 1.30 (s, 9H, 3xCH₃ *tert*-butyl). ¹³C NMR (101 MHz, CDCl₃) δ 170.1 (C-1), 138.4, 138.2, 137.9 (3xC_q Bn), 128.5, 128.5, 128.3, 127.9, 127.9, 127.8, 127.8, 127.7, 127.7 (CH_{Ar} Bn), 83.8 (C-4), 83.3 (C-3), 73.3 (CH₂ Bn-6), 73.0 (CH₂ Bn-3), 72.5 (C-6), 71.5 (CH₂ Bn-4), 65.3 (C-2), 62.6 (C-5), 50.6 (C_q *tert*-butyl), 28.9 (3xCH₃ *tert*-butyl). [α]_D²⁰: 2.0° (c = 1, CHCl₃). IR (neat): 696, 735, 910, 943, 1003, 1028, 1070, 1094, 1207, 1229, 1256, 1271, 1364, 1391, 1454, 1497, 1522, 1670, 1722, 2857, 2922, 2963, 3030, 3325. HR-MS: [M+H]⁺ Calculated for C₃₁H₃₈N₂O₄: 502.29043; found: 502.28966. Spectroscopic data matched literature data.⁹

***N*-(*tert*-butyl)-2,5-dideoxy-2,5-imino-3,4,6-tri-*O*-benzyl-*D*-manno-hexonamide (26b).** *N*-(*tert*-butyl) [*N*-(pent-4-



enoyl)-2,5-dideoxy-2,5-imino]-3,4,6-tri-*O*-benzyl-*D*-manno-hexonamide (**18b**, 47 mg, 80 μ mol) was dissolved in a mixture of THF (1.1 ml) and water (0.3 ml). Iodine (61 mg, 0.24 mmol) was added and the reaction stirred for 15 minutes. A

mixture of 1M Na₂S₂O₃ (aq.) and NaHCO₃ (sat. aq., 1/1 v/v, 5 ml) was added and the mixture vigorously stirred for 5 minutes. The suspension was extracted with EtOAc and the combined organic layers washed with brine, dried over anhydrous MgSO₄ and concentrated. The product was purified by flash chromatography (10% EtOAc/toluene) yielding the title compound in 60% yield (24 mg, 48 μ mol). *R*_f = 0.65 (40/60 EtOAc/toluene). ¹H NMR (400 MHz, CDCl₃) δ 7.55 (s, 1H, NH *tert*-butyl), 7.38 – 7.21 (m, 15H, CH_{Ar} Bn), 4.76 (d, *J* = 11.8 Hz, 1H, CHH Bn-3), 4.61 (d, *J* = 11.8 Hz, 1H, CHH Bn-3), 4.55 (d, *J* = 11.7 Hz, 1H, CHH Bn-4), 4.51 (d, *J* = 12.1 Hz, 1H, CHH Bn-6), 4.47 (d, *J* = 12.1 Hz, 1H, CHH Bn-6), 4.43 (d, *J* = 11.7 Hz, 1H, CHH Bn-4), 4.34 (t, *J* = 2.9 Hz, 1H, C-3), 3.88 (dd, *J* = 5.4, 3.1 Hz, 1H, C-4), 3.65 (d, *J* = 2.5 Hz, 1H, C-2), 3.57 (dd, *J* = 9.6, 4.3 Hz, 1H, C-6a), 3.53 (dd, *J* = 9.6, 5.7 Hz, 1H, C-6b), 3.26 – 3.20 (m, 1H, C-5), 1.32 (s, 9H, 3xCH₃ Bn). ¹³C NMR (101 MHz, CDCl₃) δ 171.3 (C-1), 138.4, 138.1, 138.0 (3xC_q Bn), 128.6, 128.5, 128.4, 128.0, 128.0, 127.9, 127.9, 127.8, 127.7 (CH_{Ar} Bn), 87.5 (C-3), 85.1 (C-4), 73.4 (CH₂ Bn-6), 72.0 (CH₂ Bn-4), 71.8 (CH₂ Bn-3), 69.1 (C-6), 66.2 (C-2), 62.5 (C-5), 50.5 (C_q *tert*-butyl), 28.8 (3xCH₃ *tert*-butyl). [α]_D²⁰: -0.8° (c = 1, CHCl₃). IR (neat): 625, 637, 696, 735, 804, 824, 851, 908, 957, 1003, 1028, 1074, 1092, 1177, 1207, 1227, 1269, 1306, 1331, 1364, 1391, 1454, 1497, 1516, 1670, 2795, 2859, 2920, 2963, 3030, 3063, 3088, 3326. HR-MS: [M+H]⁺ Calculated for C₃₁H₃₈N₂O₄: 503.29043; found: 503.28954. Spectroscopic data matched literature data.⁹

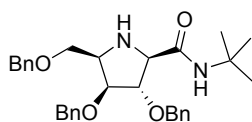
***N*-(cyclohexyl)-2,5-dideoxy-2,5-imino-3,4,6-tri-*O*-benzyl-*D*-gluco-hexonamide (27a).** *N*-(cyclohexyl) [*N*-(pent-4-enoyl)-2,5-dideoxy-2,5-imino]-3,4,6-tri-*O*-benzyl-*D*-gluco-hexonamide (**19a**, 62 mg, 0.10 mmol) was dissolved in a mixture of THF (1.4 ml) and water (0.4 ml). Iodine (77 mg, 0.3 mmol) was added and the reaction stirred for 30 minutes. A mixture of 1M Na₂S₂O₃ (aq.) and NaHCO₃ (sat. aq., 1/1 v/v, 5 ml) was added and the mixture vigorously stirred for 5 minutes. The suspension was extracted with EtOAc and the combined organic layers washed with brine, dried over anhydrous MgSO₄ and concentrated. The product was purified by flash chromatography (30-40% EtOAc/toluene) yielding the title compound in 85% yield (46 mg, 87 μmol). *R*_f = 0.30 (40/60 EtOAc/toluene). ¹H NMR (400 MHz, CDCl₃) δ 7.40 – 7.15 (m, 16H, NH Cy, CH_{Ar}), 4.59 (d, *J* = 11.7 Hz, 1H, CHH Bn-3), 4.54 – 4.46 (m, 3H, CHH Bn-4, 2xCHH Bn-6), 4.44 (d, *J* = 11.7 Hz, 1H, CHH Bn-3), 4.40 (d, *J* = 11.9 Hz, 1H, CHH Bn-4), 4.29 (dd, *J* = 5.5, 1.4 Hz, 1H, C-3), 4.13 (d, *J* = 5.6 Hz, 1H, C-2), 3.86 – 3.83 (m, 1H, C-4), 3.81 – 3.69 (m, 1H, CH Cy), 3.54 – 3.45 (m, 3H, C-5, C-6), 1.88 – 1.79 (m, 1H, CHHCH Cy), 1.79 – 1.70 (m, 1H, CHHCH Cy), 1.70 – 1.50 (m, 3H, 2xCHHCH₂CH Cy, CHH(CH₂)₂ Cy), 1.43 – 1.27 (m, 2H, 2xCHHCH₂CH), 1.21 – 0.98 (m, 3H, 2xCHHCH Cy, CHH(CH₂)₂ Cy). ¹³C NMR (101 MHz, CDCl₃) δ 169.8 (C-1), 138.3, 138.1, 137.9 (3x_C_q Bn), 128.5, 128.5, 128.3, 127.9, 127.9, 127.8, 127.8, 127.7 (CH_{Ar}), 83.5 (C-4), 83.1 (C-3), 73.3 (CH₂ Bn-6), 73.0 (CH₂ Bn-3), 72.2 (C-6), 71.5 (CH₂ Bn-4), 64.6 (C-2), 62.6 (C-5), 47.7 (CH Cy), 33.1, 33.0 (2xCH₂CH Cy), 25.7 (CH₂(CH₂)₂ Cy), 24.9, 24.8 (2xCH₂CH₂CH Cy). [α]²⁰_D: 11.5° (c = 1, CHCl₃). IR (neat): 696, 733, 891, 908, 957, 1003, 1028, 1070, 1090, 1206, 1252, 1315, 1362, 1393, 1452, 1497, 1520, 1659, 2853, 2926, 3319, 3329. HR-MS: [M+H]⁺ Calculated for C₃₃H₄₀N₂O₄: 529.30608; found: 529.30558.

***N*-(cyclohexyl)-2,5-dideoxy-2,5-imino-3,4,6-tri-*O*-benzyl-*D*-manno-hexonamide (27b).** *N*-(cyclohexyl) [*N*-(pent-4-enoyl)-2,5-dideoxy-2,5-imino]-3,4,6-tri-*O*-benzyl-*D*-manno-hexonamide (**19b**, 26 mg, 42 μmol) was dissolved in a mixture of THF (0.6 ml) and water (0.2 ml). Iodine (32 mg, 0.13 mmol) was added and the reaction stirred for 30 minutes. A mixture of 1M Na₂S₂O₃ (aq.) and NaHCO₃ (sat. aq., 1/1 v/v, 5 ml) was added and the mixture vigorously stirred for 5 minutes. The suspension was extracted with EtOAc and the combined organic layers washed with brine, dried over anhydrous MgSO₄ and concentrated. The product was purified by flash chromatography (10-16% EtOAc/toluene) yielding the title compound in 80% yield (18 mg, 34 μmol). *R*_f = 0.60 (40/60 EtOAc/toluene). ¹H NMR (400 MHz, CDCl₃) δ 7.56 (d, *J* = 8.7 Hz, 1H, NH Cy), 7.43 – 7.15 (m, 15H, CH_{Ar}), 4.77 (d, *J* = 11.8 Hz, 1H, CHH Bn-3), 4.62 (d, *J* = 11.8 Hz, 1H, CHH Bn-3), 4.54 – 4.44 (m, 3H, CHH Bn-4, 2xCHH Bn-6), 4.41 (d, *J* = 11.6 Hz, 1H, CHH Bn-4), 4.36 (t, *J* = 2.9 Hz, 1H, C-3), 3.88 (dd, *J* = 5.6, 3.2 Hz, 1H, C-4), 3.73 (d, *J* = 2.6 Hz, 1H, C-2), 3.77 – 3.65 (m, 1H, CH Cy), 3.58 (dd, *J* = 9.6, 4.2 Hz, 1H, C-6a), 3.53 (dd, *J* = 9.6, 5.6 Hz, 1H, C-6b), 3.24 – 3.18 (m, 1H, C-5), 1.91 – 1.84 (m, 1H, CHHCH Cy), 1.79 – 1.52 (m, 4H, CHHCH Cy, 2xCHHCH₂CH Cy, CHH(CH₂)₂ Cy), 1.43 – 1.27 (m, 2H, 2xCHHCH₂CH Cy), 1.21 – 1.02 (m, 3H, 2xCHHCH Cy, CHH(CH₂)₂ Cy). ¹³C NMR (101 MHz, CDCl₃) δ 171.1 (C-1), 138.3, 138.1, 138.0 (3x_C_q Bn), 128.6, 128.5, 128.4, 128.2, 128.1, 127.9, 127.9, 127.8, 127.8 (CH_{Ar}), 87.3 (C-3), 85.0 (C-4), 73.4 (CH₂ Bn-6), 72.0 (CH₂ Bn-4), 71.7 (CH₂ Bn-3), 69.0 (C-6), 65.8 (C-2), 62.5 (C-5), 47.8 (CH Cy), 33.1 (2xCH₂CH Cy), 25.7 (CH₂(CH₂)₂ Cy), 25.0, 24.9 (2xCH₂CH₂CH Cy). [α]²⁰_D: 2.2° (c = 1, CHCl₃). IR (neat): 613, 696, 735, 822, 847, 891, 908, 957, 1001, 1028, 1072, 1092, 1207, 1252, 1310, 1342, 1354, 1452, 1497, 1514, 1667, 1726, 2853, 2926, 3030, 3063, 3325. HR-MS: [M+H]⁺ Calculated for C₃₃H₄₀N₂O₄: 529.30608; found: 529.30544.

***N*-(*tert*-butyl)-2,5-dideoxy-2,5-imino-3,4,6-tri-*O*-benzyl-*D*-ido-hexonamide (28a).** *N*-(*tert*-butyl) [*N*-(pent-4-enoyl)-2,5-dideoxy-2,5-imino]-3,4,6-tri-*O*-benzyl-*D*-ido-hexonamide (**20a**, 28 mg, 47 μmol) was dissolved in a mixture of THF (0.7 ml) and water (0.2 ml). Iodine (36 mg, 0.14 mmol) was added and the reaction stirred for 15 minutes. A mixture of 1M Na₂S₂O₃ (aq.) and NaHCO₃ (sat. aq., 1/1 v/v, 5 ml) was added and the mixture vigorously stirred for 5 minutes. The suspension was extracted with EtOAc and the combined organic layers washed with brine, dried over anhydrous MgSO₄ and concentrated. The product was purified by flash

chromatography (10-25% EtOAc/toluene) yielding the title compound in 75% yield (18 mg, 35 μmol). $R_f = 0.40$ (40/60 EtOAc/toluene). $^1\text{H NMR}$ (400 MHz, CDCl_3) δ 7.37 – 7.26 (m, 14H, CH_{Ar} Bn, NH *tert*-butyl), 7.20 – 7.15 (m, 2H, CH_{Ar} Bn), 4.62 (d, $J = 11.9$ Hz, 1H, *CHH* Bn-3), 4.53 (s, 2H, $2\times\text{CHH}$ Bn-6), 4.49 (d, $J = 7.2$ Hz, 1H, *CHH* Bn-3), 4.46 (d, $J = 7.2$ Hz, 1H, *CHH* Bn-4), 4.30 (d, $J = 11.7$ Hz, 1H, *CHH* Bn-4), 4.29 (dd, $J = 5.4, 1.3$ Hz, 1H, C-3), 4.01 (d, $J = 5.1$ Hz, 1H, C-2), 3.83 (dd, $J = 3.5, 1.0$ Hz, 1H, C-4), 3.71 – 3.61 (m, 2H, C-5, C-6a), 3.56 (dd, $J = 9.2, 7.1$ Hz, 1H, C-6b), 1.33 (s, 9H, $3\times\text{CH}_3$ *tert*-butyl). $^{13}\text{C NMR}$ (101 MHz, CDCl_3) δ 170.4 (C-1), 138.3, 138.2, 138.0 ($3\times\text{C}_q$ Bn), 128.6, 128.5, 128.3, 128.0, 127.9, 127.9, 127.8, 127.7 (CH_{Ar} Bn), 82.8 (C-4), 82.5 (C-3), 73.5 (CH_2 Bn-6), 73.4 (CH_2 Bn-3), 71.9 (CH_2 Bn-4), 68.9 (C-6), 64.5 (C-2), 60.1 (C-5), 50.6 (C_q *tert*-butyl), 28.9 ($3\times\text{CH}_3$ *tert*-butyl). $[\alpha]_{\text{D}}^{20}$: 5.8° ($c = 1$, CHCl_3). IR (neat): 847, 912, 1003, 1028, 1078, 1098, 1177, 1225, 1267, 1364, 1393, 1454, 1497, 1526, 1609, 1653, 1668, 2855, 2922, 2963, 3030, 3063, 3088, 3291, 3310. HR-MS: $[\text{M}+\text{H}^+]$ Calculated for $\text{C}_{31}\text{H}_{38}\text{N}_2\text{O}_4$: 503.29043; found: 503.28988.

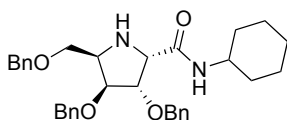
***N*-(*tert*-butyl)-2,5-dideoxy-2,5-imino-3,4,6-tri-*O*-benzyl-D-gulo-hexonamide (28b).** *N*-(*tert*-butyl) [*N*-(pent-4-



enoyl]-2,5-dideoxy-2,5-imino]-3,4,6-tri-*O*-benzyl-D-gulo-hexonamide (**20b**, 33 mg, 56 μmol) was dissolved in a mixture of THF (0.8 ml) and water (0.2 ml). Iodine (43 mg, 0.17 mmol) was added and the reaction stirred for 15 minutes. A mixture of 1M $\text{Na}_2\text{S}_2\text{O}_3$ (aq.) and NaHCO_3 (sat. aq., 1/1 v/v, 5 ml) was added and

the mixture vigorously stirred for 5 minutes. The suspension was extracted with EtOAc and the combined organic layers washed with brine, dried over anhydrous MgSO_4 and concentrated. The product was purified by flash chromatography (10-15% EtOAc/toluene) yielding the title compound in 89% yield (25 mg, 50 μmol). $R_f = 0.50$ (40/60 EtOAc/toluene). $^1\text{H NMR}$ (400 MHz, CDCl_3) δ 7.61 (s, 1H, NH *tert*-butyl), 7.38 – 7.17 (m, 15H, CH_{Ar}), 4.71 (d, $J = 11.8$ Hz, 1H, *CHH* Bn-3), 4.60 – 4.52 (m, 3H, *CHH* Bn-3, $2\times\text{CHH}$ Bn-6), 4.50 (d, $J = 12.0$ Hz, 1H, *CHH* Bn-4), 4.32 (s, 1H, C-3), 4.31 (d, $J = 12.0$ Hz, 1H, *CHH* Bn-4), 3.88 (d, $J = 4.1$ Hz, 1H, C-4), 3.82 – 3.72 (m, 2H, C-5, C-6a), 3.71 (s, 1H, C-2), 3.60 (dd, $J = 8.8, 7.2$ Hz, 1H, C-5), 1.21 (s, 9H, $3\times\text{CH}_3$ *tert*-butyl). $^{13}\text{C NMR}$ (101 MHz, CDCl_3) δ 171.7 (C-1), 138.5, 138.1, 138.1 (C_q Bn), 128.6, 128.5, 128.4, 127.8, 127.8, 127.7, 127.7, 127.7 (CH_{Ar}), 85.0 (C-3), 81.4 (C-4), 73.5 (CH_2 Bn-6), 71.6 (CH_2 Bn-4), 71.2 (CH_2 Bn-3), 70.9 (C-6), 66.0 (C-2), 60.7 (C-4), 50.3 (C_q *tert*-butyl), 28.6 ($3\times\text{CH}_3$ *tert*-butyl). $[\alpha]_{\text{D}}^{20}$: 4.7° ($c = 1$, CHCl_3). IR (neat): 822, 849, 908, 937, 1003, 1028, 1074, 1090, 1177, 1207, 1227, 1267, 1308, 1364, 1391, 1454, 1497, 1522, 1607, 1667, 1724, 2859, 2920, 2963, 3030, 3063, 3304. HR-MS: $[\text{M}+\text{H}^+]$ Calculated for $\text{C}_{31}\text{H}_{38}\text{N}_2\text{O}_4$: 503.29043; found: 503.28975.

***N*-(cyclohexyl)-2,5-dideoxy-2,5-imino-3,4,6-tri-*O*-benzyl-D-ido-hexonamide (29a).** *N*-(cyclohexyl) [*N*-(pent-4-

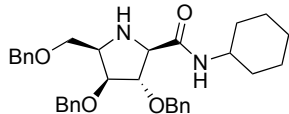


enoyl]-2,5-dideoxy-2,5-imino]-3,4,6-tri-*O*-benzyl-D-ido-hexonamide (**21a**, 20 mg, 33 μmol) was dissolved in a mixture of THF (0.5 ml) and water (0.1 ml). Iodine (25 mg, 0.10 mmol) was added and the reaction stirred for 15 minutes. A mixture of 1M $\text{Na}_2\text{S}_2\text{O}_3$ (aq.) and NaHCO_3 (sat. aq., 1/1 v/v, 5 ml) was added and the mixture vigorously stirred for 5 minutes. The suspension

was extracted with EtOAc and the combined organic layers washed with brine, dried over anhydrous MgSO_4 and concentrated. The product was purified by flash chromatography (15-25% EtOAc/toluene) yielding the title compound in 51% yield (9 mg, 16 μmol). $R_f = 0.35$ (40/60 EtOAc/toluene). $^1\text{H NMR}$ (400 MHz, CDCl_3) δ 7.43 (d, $J = 8.7$ Hz, 1H, NH Cy), 7.38 – 7.23 (m, 13H, CH_{Ar} Bn), 7.21 – 7.15 (m, 2H, CH_{Ar}), 4.61 (d, $J = 11.8$ Hz, 1H, *CHH* Bn-3), 4.54 (s, 2H, $2\times\text{CHH}$ Bn-6), 4.50 – 4.45 (m, 2H, *CHH* Bn-3, *CHH* Bn-4), 4.33 (dd, $J = 5.1, 1.0$ Hz, 1H, C-3), 4.30 (d, $J = 11.8$ Hz, 1H, *CHH* Bn-4), 4.10 (d, $J = 5.1$ Hz, 1H, C-2), 3.83 (dd, $J = 3.5, 1.5$ Hz, 1H, C-4), 3.81 – 3.71 (m, 1H, CH Cy), 3.71 – 3.61 (m, 2H, C-5, C-6a), 3.56 (dd, $J = 9.0, 7.2$ Hz, 1H, C-6b), 1.91 – 1.51 (m, 5H, $2\times\text{CHHCH}$ Cy, $2\times\text{CHHCH}_2\text{CH}$ Cy, $\text{CHH}(\text{CH}_2)_2$ Cy), 1.44 – 1.03 (m, 5H, $2\times\text{CHHCH}$ Cy, $2\times\text{CHHCH}_2\text{CH}$ Cy, $\text{CHH}(\text{CH}_2)_2$ Cy). $^{13}\text{C NMR}$ (101 MHz, CDCl_3) δ 170.3 (C-1), 138.3, 138.1, 138.0 ($3\times\text{C}_q$ Bn), 128.6, 128.5, 128.3, 128.0, 127.9, 127.8, 127.7 (CH_{Ar} Bn), 82.7 (C-4), 82.4 (C-3), 73.6 (CH_2 Bn-6), 73.3 (CH_2 Bn-3), 71.9 (CH_2 Bn-4), 69.1 (C-6), 64.2 (C-2), 60.3 (C-5), 47.8 (CH Cy), 33.4, 33.1 ($2\times\text{CH}_2\text{CH}$ Cy), 25.8 ($\text{CH}_2(\text{CH}_2)_2$ Cy), 25.1, 25.0 ($2\times\text{CH}_2\text{CH}_2\text{CH}$ Cy). $[\alpha]_{\text{D}}^{20}$: -4.1° ($c = 1$, CHCl_3). IR (neat): 841, 891,

912, 1028, 1078, 1099, 1209, 1254, 1314, 1350, 1364, 1452, 1497, 1528, 1653, 1722, 2795, 2853, 2926, 3007, 3030, 3061, 3088, 3200, 3296. HR-MS: $[M+H]^+$ Calculated for $C_{33}H_{40}N_2O_4$: 529.30608; found: 529.30566.

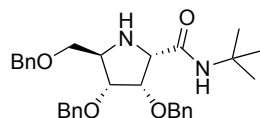
***N*-(cyclohexyl)-2,5-dideoxy-2,5-imino-3,4,6-tri-*O*-benzyl-*D*-gulo-hexonamide (29b).** *N*-(cyclohexyl) [*N*-(pent-4-enoyl)-2,5-dideoxy-2,5-imino]-3,4,6-tri-*O*-benzyl-*D*-gulo-hexonamide (21b,



27 mg, 44 μ mol) was dissolved in a mixture of THF (0.6 ml) and water (0.2 ml). Iodine (33 mg, 0.13 mmol) was added and the reaction stirred for 30 minutes. A mixture of 1M $Na_2S_2O_3$ (aq.) and $NaHCO_3$ (sat. aq., 1/1 v/v, 5 ml)

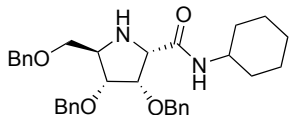
was added and the mixture vigorously stirred for 5 minutes. The suspension was extracted with EtOAc and the combined organic layers washed with brine, dried over anhydrous $MgSO_4$ and concentrated. The product was purified by flash chromatography (15-25% EtOAc/toluene) yielding the title compound in 60% yield (14 mg, 26 μ mol). $R_f = 0.50$ (40/60 EtOAc/toluene). 1H NMR (400 MHz, $CDCl_3$) δ 7.58 (d, $J = 8.5$ Hz, 1H, NH Cy), 7.37 – 7.23 (m, 13H, CH_{Ar} Bn), 7.21 – 7.16 (m, 2H, CH_{Ar} Bn), 4.71 (d, $J = 11.8$ Hz, 1H, CHH Bn-3), 4.60 – 4.51 (m, 3H, CHH Bn-3, 2xCHH Bn-6), 4.45 (d, $J = 11.6$ Hz, 1H, CHH Bn-4), 4.35 (s, 1H, C-3), 4.28 (d, $J = 11.6$ Hz, 1H, CHH Bn-4), 3.88 (d, $J = 4.2$ Hz, 1H, C-4), 3.82 – 3.77 (m, 1H, C-5), 3.79 (s, 1H, C-2), 3.72 (dd, $J = 9.1, 5.5$ Hz, 1H, C-6a), 3.65 – 3.58 (m, 1H, CH Cy), 3.59 (dd, $J = 8.9, 7.5$ Hz, 1H, C-6b), 1.86 – 1.76 (m, 1H, CHHCH Cy), 1.69 – 1.59 (m, 1H, CHHCH₂CH Cy), 1.57 – 1.40 (m, 3H, CHHCH Cy, CHHCH₂CH Cy, CHH(CH₂)₂ Cy), 1.38 – 1.27 (m, 1H, CHHCH₂CH), 1.24 – 1.02 (m, 3H, CHHCH Cy, CHHCH₂CH Cy, CHH(CH₂)₂ Cy), 0.92 – 0.77 (m, 1H, CHHCH Cy). ^{13}C NMR (101 MHz, $CDCl_3$) δ 171.4 (C-1), 138.5, 138.1, 138.0 (C_q Bn), 128.6, 128.5, 128.3, 128.0, 127.9, 127.9 (CH_{Ar} Bn), 84.9 (C-3), 81.3 (C-4), 73.5 (CH_2 Bn-6), 71.7 (CH_2 Bn-4), 71.3 (CH_2 Bn-3), 70.9 (C-6), 65.6 (C-2), 60.6 (C-5), 47.6 (CH Cy), 33.0, 32.6 (2x CH_2 CH Cy), 25.7 (CH_2 (CH_2)₂ Cy), 24.9, 24.8 (2x CH_2 CH₂CH Cy). $[\alpha]^{20}_D$: -3.5° (c = 1, $CHCl_3$). IR (neat): 822, 849, 891, 910, 845, 955, 1003, 1028, 1074, 1090, 1207, 1254, 1314, 1364, 1395, 1452, 1497, 1518, 1607, 1661, 1717, 1799, 1853, 2926, 3030, 3063, 3326. HR-MS: $[M+H]^+$ Calculated for $C_{33}H_{40}N_2O_4$: 529.30608; found: 529.30566.

***N*-(*tert*-butyl)-2,5-dideoxy-2,5-imino-3,4,6-tri-*O*-benzyl-*D*-altro-hexonamide (30).** *N*-(*tert*-butyl) [*N*-(pent-4-enoyl)-2,5-dideoxy-2,5-imino]-3,4,6-tri-*O*-benzyl-*D*-altro-hexonamide (22a,



62 mg, 0.11 mmol) was dissolved in a mixture of THF (1.5 ml) and water (0.4 ml). Iodine (80 mg, 0.32 mmol) was added and the reaction stirred for 30 minutes. A mixture of 1M $Na_2S_2O_3$ (aq.) and $NaHCO_3$ (sat. aq., 1/1 v/v, 5 ml) was added and the mixture vigorously stirred for 5 minutes. The suspension was extracted with EtOAc and the combined organic layers washed with brine, dried over anhydrous $MgSO_4$ and concentrated. The product was purified by flash chromatography (12-25% EtOAc/toluene) yielding the title compound in 44% yield (24 mg, 47 μ mol). $R_f = 0.45$ (70/30 EtOAc/toluene). 1H NMR (400 MHz, $CDCl_3$) δ 7.48 (s, 1H, NH *tert*-butyl), 7.40 – 7.20 (m, 15H, CH_{Ar} Bn), 4.73 (d, $J = 11.6$ Hz, 1H, CHH Bn-3), 4.67 (d, $J = 11.5$ Hz, 1H, CHH Bn-3), 4.48 (d, $J = 11.9$ Hz, 1H, CHH Bn-4), 4.46 (d, $J = 11.9$ Hz, 1H, CHH Bn-6), 4.43 – 4.39 (m, 1H, CHH Bn-6), 4.41 – 4.38 (m, 1H, C-3), 4.28 (d, $J = 12.0$ Hz, 1H, CHH Bn-4), 3.82 – 3.78 (m, 1H, C-4), 3.79 (d, $J = 4.1$ Hz, 1H, C-2), 3.63 (dd, $J = 10.0, 3.0$ Hz, 1H, C-6a), 3.54 (dd, $J = 10.0, 3.3$ Hz, 1H, C-6b), 3.46 (dt, $J = 9.3, 3.1$ Hz, 1H, C-5), 1.31 (s, 9H, 3x CH_3 *tert*-butyl). ^{13}C NMR (101 MHz, $CDCl_3$) δ 170.2 (C-1), 138.8, 138.1, 138.0 (3x C_q Bn), 128.5, 128.5, 128.5, 128.2, 128.2, 127.9, 127.9, 127.9, 127.8, 127.5 (CH_{Ar} Bn), 80.4 (C-4), 78.2 (C-3), 74.0 (CH_2 Bn-3), 73.3 (CH_2 Bn-6), 72.2 (CH_2 Bn-4), 68.0 (C-6), 63.6 (C-2), 60.0 (C-5), 50.6 (C_q *tert*-butyl), 28.9 (3x CH_3 *tert*-butyl). $[\alpha]^{20}_D$: 12° (c = 0.5, $CHCl_3$). IR (neat): 698, 737, 910, 1028, 1047, 1074, 1115, 1177, 1217, 1281, 1312, 1364, 1393, 1454, 1497, 1533, 1609, 1661, 1721, 2862, 2870, 2926, 2967, 3030, 3063, 3088, 3310. HR-MS: $[M+H]^+$ Calculated for $C_{31}H_{38}N_2O_4$: 503.29043; found: 503.29008.

***N*-(cyclohexyl)-2,5-dideoxy-2,5-imino-3,4,6-tri-*O*-benzyl-*D*-altro-hexonamide (31).** *N*-(cyclohexyl) [*N*-(pent-4-enoyl)-2,5-dideoxy-2,5-imino]-3,4,6-tri-*O*-benzyl-*D*-altro-hexonamide (23a,



95 mg, 0.16 mmol) was dissolved in a mixture of THF (2.5 ml) and water (0.3 ml). Iodine (118 mg, 0.47 mmol) was added and the reaction stirred for 15 minutes. A mixture of 1M $Na_2S_2O_3$ (aq.) and $NaHCO_3$ (sat. aq., 1/1 v/v, 10 ml)

was added and the mixture vigorously stirred for 5 minutes. The suspension was extracted with EtOAc and the combined organic layers washed with brine, dried over anhydrous MgSO_4 and concentrated. The product was purified by preparative HPLC chromatography. This yielded the title compound in 29% yield (24 mg, 45 μmol). $R_f = 0.4$ (70/30 EtOAc/toluene). $^1\text{H NMR}$ (400 MHz, CD_3CN) δ 7.43 (d, $J = 8.1$ Hz, 1H, NH Cy), 7.37 – 7.21 (m, 15H, CH_{Ar} Bn), 4.65 (d, $J = 11.3$ Hz, 1H, CHH Bn), 4.62 (d, $J = 11.8$ Hz, 1H, CHH Bn), 4.60 (d, $J = 11.3$ Hz, 1H, CHH Bn), 4.50 (d, $J = 11.9$ Hz, 1H, CHH Bn), 4.45 (d, $J = 11.8$ Hz, 1H, CHH Bn), 4.44 (d, $J = 11.9$ Hz, 1H, CHH Bn), 4.37 (t, $J = 4.1$ Hz, 1H, C-3), 3.82 (dd, $J = 9.2, 3.7$ Hz, 1H, C-4), 3.80 (d, $J = 4.7$ Hz, 1H, C-2), 3.68 – 3.57 (m, 1H, CH Cy), 3.62 (dd, $J = 10.1, 3.1$ Hz, 1H, C-6a), 3.50 (dd, $J = 10.1, 4.3$ Hz, 1H, C-6b), 3.32 – 3.26 (m, 1H, C-5), 1.80 – 1.50 (m, 5H, 2xCHHCH Cy, 2xCHHCH₂CH Cy, CHH(CH₂)₂ Cy), 1.40 – 1.21 (m, 2H, 2xCHHCH₂CH Cy), 1.21 – 1.04 (m, 3H, 2xCHHCH Cy, CHH(CH₂)₂ Cy). $^{13}\text{C NMR}$ (101 MHz, CD_3CN) δ 170.7 (C-1), 140.1, 139.5 (3x C_q Bn), 129.3, 129.0, 128.8, 128.8, 128.6, 128.6, 128.5, 128.3 (CH_{Ar} Bn), 82.1 (C-4), 79.8 (C-3), 74.7, 73.6, 72.8 (3xCH₂ Bn), 69.8 (C-6), 63.7 (C-2), 60.9 (C-5), 48.5 (CH Cy), 33.7, 33.6 (2xCH₂CH Cy), 26.3 (CH₂(CH₂)₂ Cy), 25.6, 25.6 (2xCH₂CH₂CH Cy). $[\alpha]_D^{20}$: 23.3° ($c = 0.2$, CH_3CN). IR (neat): 602, 635, 696, 733, 800, 822, 847, 891, 912, 959, 1003, 1026, 1063, 1086, 1107, 1128, 1206, 1252, 1310, 1348, 1362, 1402, 1452, 1497, 1518, 1651, 2853, 2928, 3030, 3341. HR-MS: $[\text{M}+\text{H}^+]$ Calculated for $\text{C}_{33}\text{H}_{40}\text{N}_2\text{O}_4$: 529.30608; found: 529.30593.

References and notes

- [1] Domling, A.; Ugi, I. *Angew. Chem. Int. Ed.* **2000**, *39*, 3168-3210, 10.1002/1521-3773(20000915)39:18<3168::AID-ANIE3168>3.0.CO;2-U.
- [2] Domling, A. *Chem. Rev.* **2006**, *106*, 17-89, 10.1021/cr0505728.
- [3] Ruijter, E.; Scheffelaar, R.; Orru, R. V. A. *Angew. Chem. Int. Ed.* **2011**, *50*, 6234-6246, 10.1002/anie.201006515.
- [4] El Kaim, L.; Grimaud, L. *Tetrahedron* **2009**, *65*, 2153-2171, 10.1016/j.tet.2008.12.002.
- [5] Ugi, I.; Meyr, R. *Chem. Ber.* **1961**, *94*, 2229-2233, 10.1002/cber.19610940844.
- [6] Timmer, M. S. M.; Risseeuw, M. D. P.; Verdoes, M.; Filippov, D. V.; Plaisier, J. R.; van der Marel, G. A.; Overkleeft, H. S.; van Boom, J. H. *Tetrahedron Asymm.* **2005**, *16*, 177-185, 10.1016/j.tetasy.2004.11.079.
- [7] Bongers, K. M.; Wennekes, T.; Filippov, D. V.; Lodder, G.; van der Marel, G. A.; Overkleeft, H. S. *Eur. J. Org. Chem.* **2008**, 3678-3688, 10.1002/ejoc.200800340.
- [8] Wennekes, T.; Bongers, K. M.; Vogel, K.; van den Berg, R. J. B. H. N.; Strijland, A.; Donker-Koopman, W. E.; Aerts, J. M. F. G.; van der Marel, G. A.; Overkleeft, H. S. *Eur. J. Org. Chem.* **2012**, 6420-6454, 10.1002/ejoc.201200923.
- [9] Bongers, K. M.; Wennekes, T.; de Lavoie, S. V. P.; Esposito, D.; den Berg, R. J. B. H. N.; Litjens, R. E. J. N.; van der Marel, G. A. *QSAR Comb. Sci.* **2006**, *25*, 491-503, 10.1002/qsar.200540198.
- [10] Chapman, T. M.; Davies, I. G.; Gu, B.; Block, T. M.; Scopes, D. I. C.; Hay, P. A.; Courtney, S. M.; McNeill, L. A.; Schofield, C. J.; Davis, B. G. *J. Am. Chem. Soc.* **2005**, *127*, 506-507, 10.1021/ja0439241.

- [11] Banfi, L.; Basso, A.; Guanti, G.; Riva, R. *Tetrahedron Lett.* **2004**, *45*, 6637-6640, 10.1016/j.tetlet.2004.07.015.
- [12] Banfi, L.; Basso, A.; Guanti, G.; Merlo, S.; Repetto, C.; Riva, R. *Tetrahedron* **2008**, *64*, 1114-1134, 10.1016/j.tet.2007.10.058.
- [13] Cerulli, V.; Banfi, L.; Basso, A.; Rocca, V.; Riva, R. *Org. Biomol. Chem.* **2012**, *10*, 1255-1274, 10.1039/c1ob06632c.
- [14] Flanagan, D. M.; Joullie, M. M. *Synth. Commun.* **1989**, *19*, 1-12, 10.1080/00397918908050946.
- [15] Bowers, M. M.; Carroll, P.; Joullie, M. M. *J. Chem. Soc., Perkin Trans. 1* **1989**, 857-865, 10.1039/p19890000857.
- [16] de Graaff, C.; Ruijter, E.; Orru, R. V. A. *Chem. Soc. Rev.* **2012**, *41*, 3969-4009, 10.1039/c2cs15361k.
- [17] In this chapter carbohydrate numbering is used.
- [18] Product ratios are determined by ^1H NMR at 393K to allow free rotation around the newly formed tertiary amide bond.
- [19] Larsen, C. H.; Ridgway, B. H.; Shaw, J. T.; Smith, D. M.; Woerpel, K. A. *J. Am. Chem. Soc.* **2005**, *127*, 10879-10884, 10.1021/ja0524043.
- [20] Smith, D. M.; Tran, M. B.; Woerpel, K. A. *J. Am. Chem. Soc.* **2003**, *125*, 14149-14152, 10.1021/ja0375176.
- [21] Maeda, S.; Komagawa, S.; Uchiyama, M.; Morokuma, K. *Angew. Chem. Int. Ed.* **2011**, *50*, 644-649, 10.1002/anie.201005336.
- [22] Cheron, N.; Ramozzi, R.; El Kaim, L.; Grimaud, L.; Fleurat-Lessard, P. *J. Org. Chem.* **2012**, *77*, 1361-1366, 10.1021/jo2021554.
- [23] The stereoselectivity of the Ugi reaction of the per-*O*-methylated xylo derived imine was similar to that for the Ugi reaction of its per-*O*-benzylated counterpart.
- [24] Several bicyclic intermediates can be formed in this reaction step, differing in the stereochemistry of the newly formed hemiaminal linkage and the stereochemistry of the double bond. The lowest energy intermediate is shown in the figure.
- [25] Although the addition of the isocyanide to the imine can also be envisioned to proceed via an $\text{S}_{\text{N}}2$ -like pathway in which the incoming isocyanide displaces an anomeric (covalent) acetate, this pathway is deemed to be less likely given the stabilities of the intermediate iminium ions and the polarity of the solvent.
- [26] Chao, C. S.; Lin, C. Y.; Mulani, S.; Hung, W. C.; Mong, K. K. T. *Chem. Eur. J.* **2011**, *17*, 12193-12202, 10.1002/chem.201100732.

- [27] The steric penalty can be estimated at $1.8 \text{ kcal mol}^{-1}$ from corresponding *syn*-butanol interactions, while in the transition state the energy differences actually increase by $0.7 \text{ kcal mol}^{-1}$ over the ground state conformers. A rough estimate for the stabilizing interaction could therefore be the sum of these two at $2.5 \text{ kcal mol}^{-1}$.
- [28] When all iminium ions are compared it becomes clear that the 3E Ara is the most stable conformer of the four isomers (ΔE ; 3E Lyxo = $1.00 \text{ kcal mol}^{-1}$, 3E Ara = $0.00 \text{ kcal mol}^{-1}$, E_3 Xylo = $0.96 \text{ kcal mol}^{-1}$, E_3 Ribo = $0.99 \text{ kcal mol}^{-1}$).
- [29] Spartan '04, Kong, J. *et al.*, Wavefunction Inc. **2004**.
- [30] Gaussian 03 (Revision D.01), Frisch, M. J. *et al.*, Gaussian, Inc. **2004**.
- [31] Naka, T.; Minakawa, N.; Abe, H.; Kaga, D.; Matsuda, A. *J. Am. Chem. Soc.* **2000**, *122*, 7233-7243, Doi 10.1021/Ja000541o.

Chapter 5

A library of lipophilic iminosugars based on all eight stereoisomeric pentofuranosyl iminosugars

5.1 Introduction

Iminosugars are carbohydrates in which the endocyclic oxygen is replaced by nitrogen. They can act as inhibitors for glycosidases and glycosyl transferases owing to their structural similarity with the putative transition states of the corresponding enzymatic transformations.¹⁻⁷ Furanosyl based iminosugars are attractive as potential inhibitors for

furanose processing enzymes, because furanose containing oligosaccharides are not produced in humans or other mammals but do play important roles in microbial organisms.⁸⁻¹⁰ In addition they can serve as interesting lead compounds to develop inhibitors for pyranose processing enzymes, because their three-dimensional structures can effectively mimic the pyranosyl oxocarbenium ions.^{7,11} For example, 1,4-dideoxy-1,4-imino-D-arabinitol is known to be a powerful inhibitor of a range of α -glucosidases.^{1,4,11-15}

Eight different stereoisomers are possible in the pentofuranose iminosugar family. Different strategies towards the synthesis of each of the eight iminosugars have been developed, the first one being reported in 1968 to access 1,4-dideoxy-1,4-imino-L-xylitol.¹⁶ Although new approaches are still regularly being published to synthesize these iminosugars, most of these studies comprise the synthesis of only a single or a limited number of the eight diastereomers.^{12-13,17-23} To effectively generate a library of furanosyl iminosugars, encompassing all stereoisomers, a general route of synthesis to access them all is desirable. In this Chapter a general strategy is described to access all eight stereoisomeric furanosyl iminosugars. These have been used to generate a library of functionalized iminosugars in which the iminosugar amines are alkylated with 7 different alkyl chains to produce a library of 64 furanosyl iminosugars. The choice of alkyl chains has been made based on the successful iminosugar therapeutic agents that are currently on the market, that is Zavesca (Miglustat, *N*-butyl 1-deoxynojirimycin)¹⁴ and Glyset (Miglitol, *N*-hydroxyethyl 1-deoxynojirimycin),¹⁴ as well as the library of alkylated pyranosyl iminosugars that has been compiled in-house.²⁴⁻²⁶ The different alkyl chains are depicted in Figure 5.1, alongside the panel of different iminosugar stereoisomers.

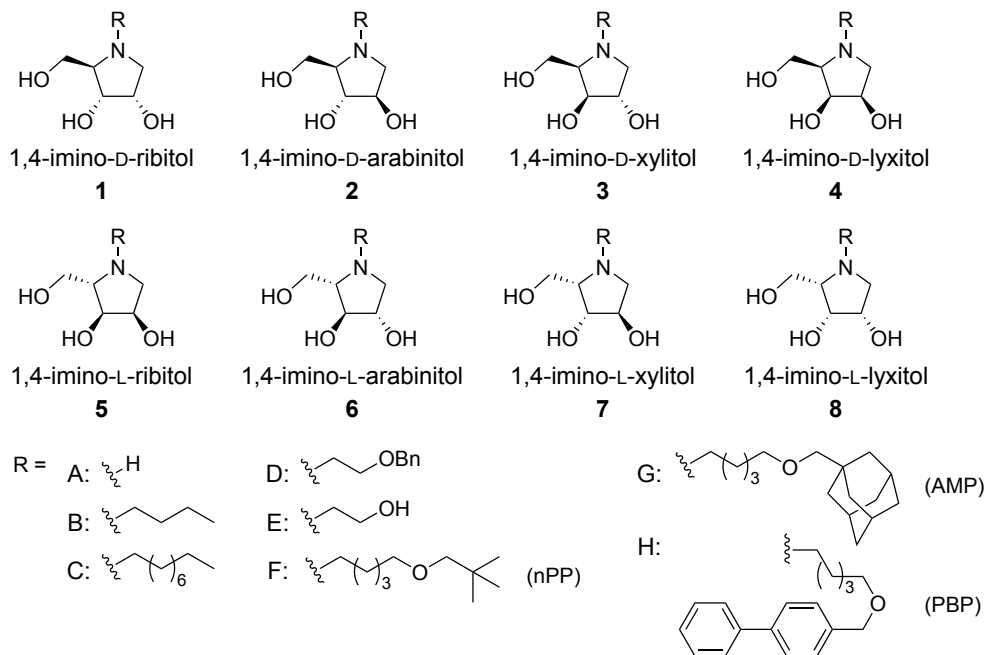


Figure 5.1 Target furanose iminosugars.

5.2 Results and discussion

Most of the published approaches for the synthesis of iminosugars are based on either a double reductive amination strategy or on a nucleophilic substitution of one or both of the hydroxyl groups with a nitrogen nucleophile such as azide or benzylamine.¹² To access all eight furanose iminosugars, the synthetic strategy that is retrosynthetically outlined in Figure 5.2 was selected. In this strategy a double nucleophilic S_N2 displacement of the C1- and C4-hydroxyls with benzylamine is used. To this end the C1- and C4 hydroxyls of otherwise perbenzylated pentitols were transformed into good leaving groups. Because the S_N2 substitutions lead to inversion of stereochemistry at C4, the use of D-furanosyl starting compounds lead to products having the L-configuration and vice versa. All D-pentoses as well as L-arabinose and L-xylose are commercially available at reasonable cost and can therefore be used as starting material. The remaining two, L-ribose and L-lyxose, are too expensive and therefore a double inversion strategy was devised in which the D-sugars are used as starting materials. In this approach the C1- and C4-hydroxyls are first displaced by iodine to give the 1,4-di-iodo-L-pentoses that are then subjected to the second double displacement with benzylamine to give the protected D-iminosugars.

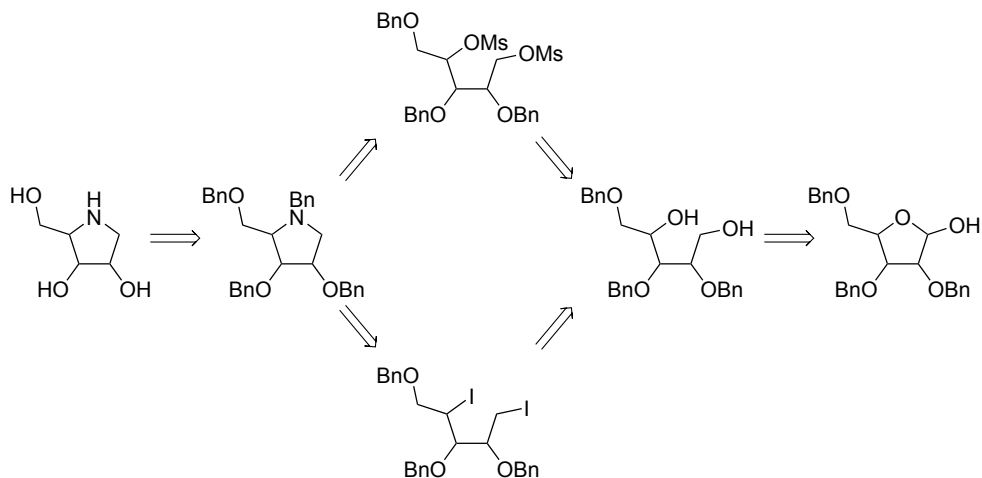
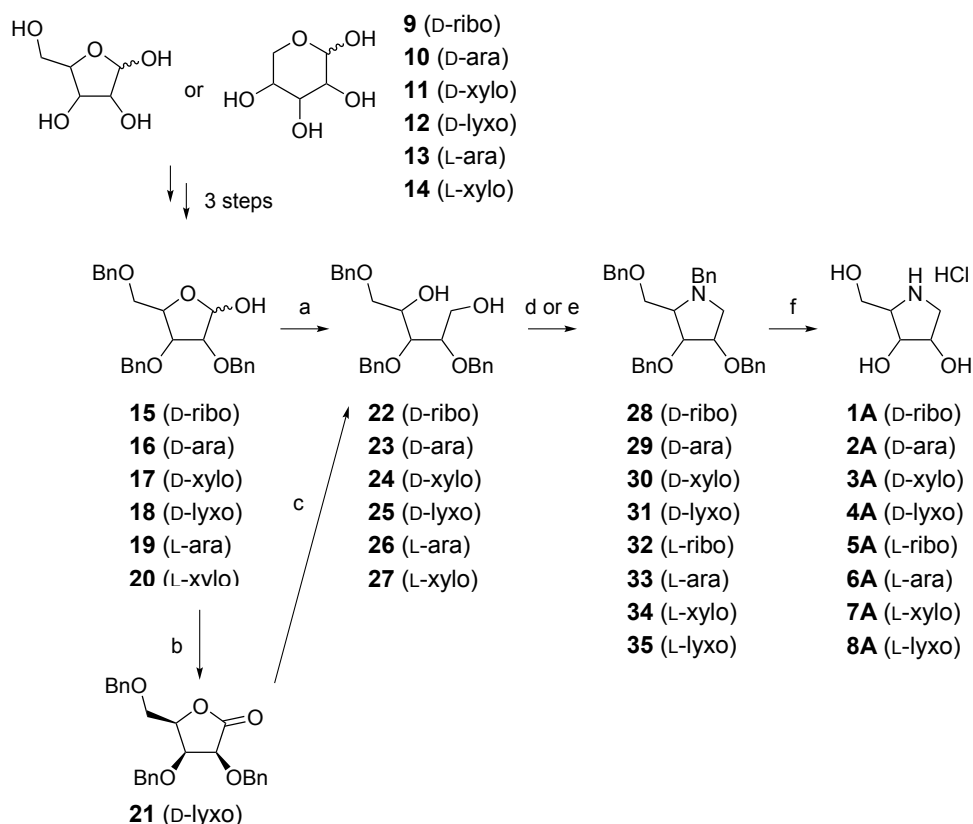


Figure 5.2 Retrosynthetic analysis of the target iminosugars based on a double displacement strategy.

The syntheses of the eight stereoisomeric iminosugars **1-8** is depicted in Scheme 5.1, starting from the six commercially available furanoses, D-ribose (**9**), D-arabinose (**10**), D-xylose (**11**), D-lyxose (**12**), L-arabinose (**13**) and L-xylose (**14**). These were transformed, *via* a three step reaction sequence entailing: 1) a kinetic Fischer methylation to give the methyl furanosides; 2) complete benzylation of the remaining alcohols and 3) the acid catalyzed hydrolysis of the methyl acetal, into the lactols **15-20**.²⁷⁻³⁰ Because it proved to be difficult to purify the D-lyxo-furanoside from its pyranosyl counterpart at this stage, the lactol (**18**) was oxidized to provide the crystalline furanolactone (**21**) that was obtained in an overall yield of 64% over 4 steps. The five tri-*O*-benzylated pentofuranoses (**15-17**, **19**, **20**) were reduced using sodium borohydride to give the corresponding diols (**22-24,26-27**) with yields ranging from 92 to 98%. For the reduction of D-lyxonolactone **21** a stronger reducing agent was required, and therefore lithium aluminum hydride was employed to deliver lyxitol **25**. All six diols were di-mesyated using mesyl chloride in pyridine, after which a double displacement with benzylamine led to the fully protected iminosugars **29**, **30**, **32-35** (in 46% - 92% yield). The remaining two protected iminosugars were synthesized using the double inversion protocol. Therefore 2,3,5-tri-*O*-benzyl D-ribitol (**22**) and D-lyxitol (**25**) were subjected to a Garegg-Samuelson reaction using iodine, triphenylphosphine and imidazole.³¹ Because tetrahydrofuran side products are readily formed in this reaction (generated from activation of the primary alcohol and subsequent ring closure by nucleophilic displacement of the secondary alcohol), it proved to be challenging to optimize these reactions. The best conditions were found in stirring the reaction mixture at low temperature (-30 °C to -20 °C) for a prolonged period of time (\pm 4 days) to allow for the formation of the bis(triphenylphosphonium oxides). Next the mixtures were

concentrated, taken up in toluene and brought to reflux temperature to effect the displacement with iodine resulting in the 1,4-di-iodo L-pentitols. The di-iodides were then subjected to benzylamine at 55 °C to generate the perbenzylated iminofuranoses having the D-ribose (**28**) and D-lyxose (**31**) configuration in 69% and 55% yield over the last two steps, respectively. Global deprotection of the perbenzylated iminosugars was accomplished by subjection of the eight protected iminosugars to a 4.5-5 bar hydrogen overpressure in the presence of palladium on carbon in a slightly acidic medium to deliver all the unprotected iminosugars as hydrochloride salt (**1A-8A**) in very high to quantitative yields.

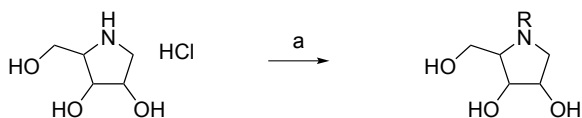
Scheme 5.1 Synthesis of the iminofuranoses (**1A-8A**, see Figure 5.1 for stereochemistry).



Reagents and conditions: (a) NaBH₄, EtOH, **22** (from **15**): 97%, **23** (from **16**): 98%, **24** (from **17**): 97%, **26** (from **19**): 85%, **27** (from **20**): 92%; (b) Ac₂O, DMSO; (c) LiAlH₄, THF, 0 °C, **25** (from **21**): 89%; (d) i) PPh₃, I₂, imidazole, DCM, -30 °C to -20 °C, ii) toluene, Δ; iii) BnNH₂, 55 °C, **28** (from **22**): 69% over 2 steps, **31** (from **25**): 55% over 2 steps; (e) i) MsCl, pyridine, 0 °C; ii) BnNH₂, 55 °C, **29** (from **27**): 84% over 2 steps, **30** (from **26**): 92% over 2 steps, **32** (from **25**): 88% over 2 steps, **33** (from **24**): 71% over 2 steps, **34** (from **23**): 46% over 2 steps, **35** (from **22**): 70% over 2 steps. (f) H₂, Pd/C, HCl, EtOH, H₂O, **1A** (from **28**): 99%, **2A** (from **29**): quant., **3A** (from **30**): quant., **4A** (from **31**): 98%, **5A** (from **32**): quant., **6A** (from **33**): quant., **7A** (from **34**): quant., **8A** (from **35**): quant.

Next, the introduction of the various alkyl chains was undertaken. Initially the alkylation was attempted using K_2CO_3 as base in combination with the relevant alkyl bromides in DMF, conditions previously reported for the alkylation of a large variety of pyranosyl iminosugars.²⁵⁻²⁶ Unfortunately the use of these reagents led to the concomitant formation of carbamate and cyclic carbonate side products. Formation of these byproducts can be explained by attack of the carbonate anion on the alkylating agent to give a dialkyl carbonate, which can be substituted by the iminosugar amine to give a stable carbamate, or be used to form a cyclic carbonate by the *cis*-diol systems in de ribo and lyxo configured iminosugars. To circumvent the formation of these side products, the base was changed to *N,N*-diisopropylethylamine (DiPEA), which indeed led to clean alkylation reactions. Table 5.1 summarizes the yields for all the alkylation reactions, ranging from 5% to 59%. The variation in yields for these reactions can in part be accounted for by losses during the column chromatography purification step that was required to remove ammonium salt byproducts. The last of the substituents, the hydroxyethyl group, was generated by debenzoylation of the benzyloxyethyl substituent. All these debenzylations proceeded quantitatively to yield the *N*-hydroxyethyl iminofuranoses as hydrochloride salts.

Table 5.1 *N*-alkylation of the iminofuranoses.



R =	D-ribo	D-ara	D-xylo	D-lyxo	L-ribo	L-ara	L-xylo	L-lyxo
Butyl ^a	1B 35%	2B 13%	3B 27%	4B 14%	5B 12%	6B 45%	7B 5%	8B 7%
Nonyl ^a	1C 44%	2C 47%	3C 43%	4C 29%	5C 59%	6C 46%	7C 36%	8C 29%
EtOBn ^a	1D 32%	2D 26%	3D 25%	4D 16%	5D 27%	6D 25%	7D 26%	8D 16%
EtOH ^b	1E 31%	2E 25%	3E 11%	4E 13%	5E 25%	6E 22%	7E 23%	8E 15%
nPP ^a	1F 44%	2F 26%	3F 31%	4F 22%	5F 27%	6F 45%	7F 36%	8F 21%
AMP ^a	1G 33%	2G 37%	3G 36%	4G 12%	5G 36%	6G 36%	7G 40%	8G 9%
PBP ^a	1H 41%	2H 34%	3H 36%	4H 16%	5H 25%	6H 25%	7H 38%	8H 15%

Reagents and conditions: (a) R-Br, DiPEA, DMF, 60 °C. (b) Alkylated derivatives **1D-8D** were treated with: H_2 , Pd/C, HCl, EtOH, H_2O (yield over 2 steps).

5.3 Conclusion

The synthesis of all eight stereoisomeric pentofuranosyl iminosugars has been described, using a double displacement strategy of suitably functionalized alditols. A library consisting of 64 compounds was constructed by alkylation of the eight diastereomers, to give a collection of lipophilic iminosugars that have the potential to inhibit glycolipid processing enzymes. Using the free energy surface scanning method outlined in Chapter 2 and 3, the conformational preferences of the iminosugars can be mapped and the outcome of these studies will be valuable in the interpretation of results emanating from enzyme inhibition studies using the here described iminosugar library.

Experimental section

General. All reagents were of commercial grade and used as received. All moisture sensitive reactions were performed under an argon atmosphere. Reactions were performed at room temperature unless stated otherwise and were monitored by TLC analysis with detection by UV (254 nm) and where applicable by spraying with a solution of $(\text{NH}_4)_6\text{Mo}_7\text{O}_{24}\cdot 4\text{H}_2\text{O}$ (25 g/L) and $(\text{NH}_4)_4\text{Ce}(\text{SO}_4)_4\cdot 2\text{H}_2\text{O}$ (10 g/L) in 10% sulfuric acid (aq.) or a solution of KMnO_4 (20 g/L) and K_2CO_3 (10 g/L) in H_2O followed by charring at $\sim 150^\circ\text{C}$. Flash column chromatography was performed on silica gel (40–63 μm). ^1H and ^{13}C spectra were recorded on a Bruker AV 600 or AV 400 in CDCl_3 or CD_3OD . Chemical shifts (δ) are given in ppm relative to tetramethylsilane as internal standard (^1H NMR in CDCl_3) or the residual signal of the deuterated solvent. Coupling constants (J) are given in Hz. All ^{13}C spectra are proton decoupled. NMR peak assignments were made using COSY and HSQC experiments.

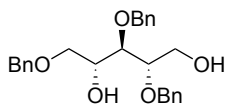
General procedure A: Pd/C catalyzed hydrogenolysis: The perbenzylated iminosugar (7.5 mmol – 8 mmol) was dissolved in a mixture of 2M HCl (aq.) / EtOH (0.05 M, 3/1, v/v) and transferred to a Parr high pressure hydrogenation flask. The atmosphere was exchanged to argon after which a catalytic amount of palladium on carbon (~ 0.1 eq, 10 wt. % on carbon) was added. The flask was put under reduced pressure and ventilated with hydrogen gas. This procedure was repeated twice after which the pressure was adjusted to 4.5–5 bar hydrogen overpressure. The reaction was allowed to react for 24 hours while mechanically shaken and the pressure being maintained at the value initially set. The mixture was filtered over a glass microfiber filter, followed by rinsing the filter with EtOH. The mixture was concentrated under reduced pressure followed by several coevaporation steps with EtOH and MeOH to yield the deprotected iminosugar as hydrochloride salt.

General procedure B: base catalyzed alkylation: The unprotected iminosugar (0.50 mmol) as hydrochloride salt was dissolved in DMF (0.2 M, 2.5 ml) after which alkyl bromide (1.5 eq, 0.75 mmol) and *N,N*-diisopropylethylamine (3 eq, 260 μl , 1.5 mmol) were added. The reaction mixture was stirred overnight at 70°C after which the reaction mixture was concentrated. The crude product was purified by silica gel column chromatography and subsequently by preparative reversed phase HPLC purification (solvent A: H_2O + 0.1% TFA, solvent B: ACN) yielding the compound as TFA salt. When DiPEA TFA salt was present as impurity, the compound was neutralized with NH_4OH (aq., 1 eq) and purified by reversed phase column chromatography ($\text{H}_2\text{O}/\text{MeOH}$) yielding the product as free base.

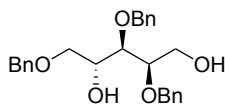
General procedure C: small scale Pd/C catalyzed hydrogenolysis: The ethyloxybenzyl iminosugar (0.07 mmol – 0.18 mmol) was dissolved in a mixture of 0.25M HCl (aq.) / EtOH (0.01 M, 12/1, v/v) and transferred to a Parr high pressure hydrogenation flask. The atmosphere was exchanged to argon after which a catalytic amount of palladium on carbon (~ 0.1 eq, 10 wt. % on carbon) was added. The flask was put under reduced pressure and

ventilated with hydrogen gas. This procedure was repeated twice after which the pressure was adjusted to 4.5-5 bar hydrogen overpressure. The reaction was allowed to react for 4 hours-overnight while mechanically shaken and the pressure being maintained at the value initially set. The mixture was filtered over a glass microfiber filter, followed by rinsing the filter with EtOH. The mixture was concentrated under reduced pressure followed by several coevaporation steps with EtOH and MeOH to yield the deprotected iminosugar as hydrochloride salt.

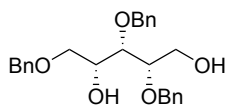
2,3,5-Tri-O-benzyl-D-ribose (22). 2,3,5-Tri-O-benzyl-D-ribofuranose (**15**, 25 g, 60 mmol) was dissolved in EtOH (600 ml) and cooled to 0 °C. Sodium borohydride (5.3 g, 139 mmol) was added and the reaction stirred at room temperature for 3 hours. The pH of the reaction mixture was adjusted to pH 4-5 with acetic acid and the mixture concentrated. The residue was taken up in EtOAc and washed with 1 M HCl (aq.), NaHCO₃ (sat. aq.), and brine. The organic layer was dried over anhydrous MgSO₄, filtered and concentrated under reduced pressure. The residue was purified by flash chromatography (30-60% EtOAc/pentane) yielding the title compound (25 g, 58 mmol, 97 % yield). *R*_f = 0.45 (50/50 EtOAc/pentane). ¹H NMR (400 MHz, CDCl₃) δ 7.47 – 7.13 (m, 15H, CH_{Ar} Bn), 4.72 (d, *J* = 11.2 Hz, 1H, CHH Bn), 4.63 (d, *J* = 11.6 Hz, 1H, CHH Bn), 4.58 (d, *J* = 11.7 Hz, 1H, CHH Bn), 4.58 (d, *J* = 11.2 Hz, 1H, CHH Bn), 4.51 (d, *J* = 11.9 Hz, 1H, CHH Bn), 4.47 (d, *J* = 11.9 Hz, 1H, CHH Bn), 4.05 – 3.95 (m, 1H, C-4), 3.89 – 3.72 (m, 4H, C-1, C-2, C-3), 3.60 (dd, *J* = 9.8, 3.7 Hz, 1H, C-5a), 3.56 (dd, *J* = 9.7, 5.9 Hz, 1H, C-5b), 2.91 (s, 1H, OH-4), 2.54 (s, 1H, OH-1). ¹³C NMR (101 MHz, CDCl₃) δ 138.1, 138.1, 137.9 (C_q Bn), 128.6, 128.5, 128.5, 128.1, 128.0, 128.0, 127.9 (CH_{Ar} Bn), 79.5, 79.4 (C-2, C-3), 74.1, 73.5, 72.1 (3xCH₂ Bn), 71.1 (C-5), 70.7 (C-4), 61.1 (C-1). [α]_D²⁰ = 18.1° (c = 1, CHCl₃). IR (neat): 602, 694, 733, 806, 520, 849, 908, 1026, 1067, 1088, 1207, 1273, 1314, 1329, 1360, 1395, 1452, 1497, 1719, 2866, 3030, 3063, 3348. HR-MS: [M+H]⁺ Calculated for C₂₆H₃₀O₅: 423.21660; found: 423.21622.



2,3,5-Tri-O-benzyl-D-arabinose (23). 2,3,5-Tri-O-benzyl-D-arabinofuranose (**16**, 17 g, 41 mmol) was dissolved in ethanol (410 ml) and cooled to 0 °C. Sodium borohydride (3.6 g, 95 mmol) was added and the reaction stirred for 5 hours at room temperature. The pH of the reaction mixture was adjusted to pH 4-5 with acetic acid and the mixture concentrated. The residue was taken up in EtOAc and washed with 1M HCl (aq.), NaHCO₃ (sat. aq.) and brine. The solution was dried over anhydrous MgSO₄, filtered and concentrated under reduced pressure. The crude product was purified by flash chromatography (20-70% EtOAc/pentane) yielding the title compound (17 g, 41 mmol, 98 % yield). *R*_f = 0.7 (50/50 EtOAc/pentane). ¹H NMR (400 MHz, CDCl₃) δ 7.37 – 7.22 (m, 15H, CH_{Ar} Bn), 4.64 (d, *J* = 11.8 Hz, 1H, CHH Bn), 4.61 (d, *J* = 11.8 Hz, 1H, CHH Bn), 4.59 (d, *J* = 11.5 Hz, 1H, CHH Bn), 4.56 (d, *J* = 11.4 Hz, 1H, CHH Bn), 4.54 (d, *J* = 12.2 Hz, 1H, CHH Bn), 4.51 (d, *J* = 12.0 Hz, 1H, CHH Bn), 4.04 – 3.98 (m, 1H, C-4), 3.83 – 3.67 (m, 4H, C-1, C-2, C-3), 3.68 – 3.59 (m, 2H, C-5), 2.67 (s, 2H, 2xOH). ¹³C NMR (101 MHz, CDCl₃) δ 138.0, 137.9, 137.9 (C_q Bn), 128.6, 128.6, 128.4, 128.3, 128.1, 128.0, 127.9 (CH_{Ar} Bn), 79.5 (C-2), 78.4 (C-3), 73.8, 73.6, 72.9 (3xCH₂ Bn), 71.1 (C-5), 70.6 (C-4), 61.5 (C-1). [α]_D²⁰ = 4.6° (c = 1, CHCl₃). IR (neat): 602, 696, 733, 806, 820, 851, 880, 910, 1001, 1026, 1069, 1086, 1207, 1271, 1315, 1350, 1396, 1452, 1497, 1705, 1717, 2866, 2920, 3030, 3063, 3445. HR-MS: [M+H]⁺ Calculated for C₂₆H₃₀O₅: 423.21660; found: 423.21637.



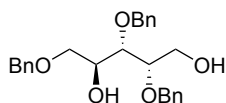
2,3,5-Tri-O-benzyl-D-xylitol (24). 2,3,5-Tri-O-benzyl-D-xylofuranose (**17**, 23 g, 54 mmol) was dissolved in ethanol (550 ml), put under an argon atmosphere and cooled to 0 °C. Sodium borohydride (4.7 g, 123 mmol) was added and the reaction stirred at room temperature for 4 hours. The pH of the reaction was adjusted to pH 4-5 by addition of acetic acid and the resulting mixture was concentrated. The residue was taken up in EtOAc and washed with 1M HCl (aq.), NaHCO₃ (sat. aq.) and brine. The solution was dried over anhydrous MgSO₄, filtered and concentrated under reduced pressure. The product was purified by flash chromatography (25-60% EtOAc/pentane) yielding the title compound (22 g, 52 mmol, 97% yield). *R*_f = 0.65 (50/50 EtOAc/pentane). ¹H NMR (400 MHz, CDCl₃) δ 7.36 – 7.24 (m, 13H, CH_{Ar} Bn), 7.24 – 7.21 (m, 2H, CH_{Ar} Bn), 4.65 (d, *J* = 11.4 Hz, 1H, CHH



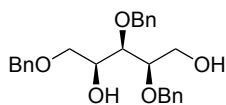
Bn-3), 4.61 (d, $J = 11.9$ Hz, 1H, CHH Bn-2), 4.57 (d, $J = 11.8$ Hz, 1H, CHH Bn-2), 4.51 – 4.46 (m, 2H, CHH Bn-3, CHH Bn-5), 4.42 (d, $J = 11.9$ Hz, 1H, CHH Bn-5), 4.07 – 4.01 (m, 1H, C-4), 3.81 – 3.73 (m, 2H, C-1), 3.73 – 3.63 (m, 2H, C-2, C-3), 3.50 (dd, $J = 9.4, 6.4$ Hz, 1H, C-5a), 3.41 (dd, $J = 9.4, 6.2$ Hz, 1H, C-5b), 3.02 (s, 1H, OH-4), 2.86 (s, 1H, OH-1). ^{13}C NMR (101 MHz, CDCl_3) δ 138.1, 138.0, 137.9 (C_q Bn), 128.5, 128.5, 128.5, 128.4, 128.0, 128.0, 127.9, 127.8 (CH_{Ar} Bn), 78.7 (C-2), 77.3 (C-3), 74.2 (CH_2 Bn-3), 73.3 (CH_2 Bn-5), 72.4 (CH_2 Bn-2), 71.3 (C-5), 68.6 (C-4), 60.6 (C-1). $[\alpha]_D^{20} = -9.7^\circ$ ($c = 1, \text{CHCl}_3$). IR (neat): 694, 716, 733, 822, 881, 903, 918, 980, 1018, 1024, 1057, 1084, 1096, 1206, 1248, 1279, 1294, 1366, 1385, 1400, 1452, 1497, 1578, 1726, 2471, 2542, 2716, 2866, 3028, 3343. HR-MS: $[\text{M}+\text{H}^+]$ Calculated for $\text{C}_{26}\text{H}_{30}\text{O}_5$: 423.21660; found: 423.21633.

2,3,5-Tri-O-benzyl-D-lyxitol (25). 2,3,5-Tri-O-benzyl-D-lyxono-1,4-lactone (**21**, 12 g, 28 mmol) in THF (120 ml) was slowly added to a solution of lithium aluminum hydride (2.6 g, 68 mmol) in THF (120 ml) at 0 °C. The reaction mixture was stirred for 1.5 hour at 0 °C, after which the reaction was quenched with EtOAc. Sodium potassium tartrate (sat. aq.) was slowly added and the mixture was stirred for 30 minutes before ethyl acetate was added and the layers separated. The organic layer was washed with NaHCO_3 (sat. aq.) and brine before being dried over anhydrous MgSO_4 , filtered and concentrated under reduced pressure. The residue was purified by flash chromatography (50% EtOAc/pentane) yielding the title compound (11 g, 25 mmol, 89 % yield). $R_f = 0.6$ (50/50 EtOAc/pentane). ^1H NMR (400 MHz, CDCl_3) δ 7.39 – 7.24 (m, 15H, CH_{Ar} Bn), 4.73 (d, $J = 11.1$ Hz, 1H, CHH Bn), 4.61 (s, 2H, CH_2 Bn), 4.52 (d, $J = 11.1$ Hz, 1H, CHH Bn), 4.51 (d, $J = 12.0$ Hz, 1H, CHH Bn), 4.46 (d, $J = 11.9$ Hz, 1H, CHH Bn), 4.00 (td, $J = 6.1, 2.1$ Hz, 1H, C-4), 3.90 – 3.82 (m, 1H, C-1a), 3.79 (dd, $J = 6.4, 2.1$ Hz, 1H, C-3), 3.76 – 3.71 (m, 1H, C-1b), 3.71 – 3.68 (m, 1H, C-2), 3.53 (dd, $J = 9.4, 6.1$ Hz, 1H, C-5a), 3.46 (dd, $J = 9.5, 6.1$ Hz, 1H, C-5b), 2.49 (s, 2H, OH-1, OH-4). ^{13}C NMR (101 MHz, CDCl_3) δ 138.0, 137.9, 137.9 (C_q Bn), 128.6, 128.5, 128.3, 128.0, 128.0, 128.0, 127.9 (CH_{Ar} Bn), 79.6 (C-2), 77.1 (C-3), 74.4, 73.5, 72.5 ($3\times\text{CH}_2$ Bn), 71.3 (C-5), 69.8 (C-4), 60.6 (C-1). $[\alpha]_D^{20} = -18.9^\circ$ ($c = 1, \text{CHCl}_3$). IR (neat): 602, 646, 694, 733, 820, 851, 868, 910, 959, 1026, 1049, 1090, 1207, 1246, 1265, 1308, 1327, 1362, 1395, 1454, 1497, 2864, 2920, 3030, 3061. HR-MS: $[\text{M}+\text{H}^+]$ Calculated for $\text{C}_{26}\text{H}_{30}\text{O}_5$: 423.21660; found: 423.21629.

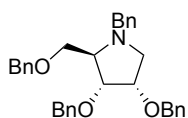
2,3,5-Tri-O-benzyl-L-arabinitol (26). Synthesized as in Chapter 4.



2,3,5-Tri-O-benzyl-L-xylylitol (27). 2,3,5-Tri-O-benzyl-L-xylofuranose (**20**, 12g, 28 mmol) was dissolved in ethanol (285 ml), cooled to 0 °C and sodium borohydride (2.5 g, 65 mmol) added. The reaction was stirred for 5 hours at room temperature after which the pH of the reaction mixture was adjusted to pH 4-5 with acetic acid and the mixture concentrated. The residue was taken up in EtOAc and washed with 1M HCl (aq.), NaHCO_3 (sat. aq.) and brine. The solution was dried over anhydrous MgSO_4 , filtered and concentrated under reduced pressure. The residue was purified by flash chromatography (70% EtOAc/pentane) yielding the title compound (11 g, 26 mmol, 92 % yield). $[\alpha]_D^{20} = 10.6^\circ$ ($c = 1, \text{CHCl}_3$). Analytical data was the same as for its enantiomer (**24**).

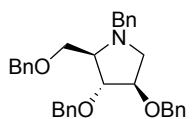


1,4-Dideoxy-1,4-benzylimino-2,3,5-tri-O-benzyl-D-ribitol (28). 2,3,5-Tri-O-benzyl-D-ribitol (**22**, 7.6 g, 18 mmol), triphenylphosphine (11 g, 41 mmol) and imidazole (3.7 g, 54 mmol) were coevaporated thrice with dry toluene before being dissolved in DCM (180 ml) and cooled to -30 °C. Iodine (11 g, 43 mmol) was slowly added and the reaction mixture stirred for 2 days at -30 °C, then 1 day at -20 °C. The solution was concentrated under reduced pressure, dry



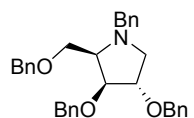
toluene (180 ml) added and the mixture refluxed for 2 hours. The reaction mixture was diluted with Et₂O, washed with Na₂S₂O₃ (sat. aq.) and brine, dried over anhydrous MgSO₄, filtered and concentrated under reduced pressure. The residue was coevaporated with Et₂O to remove residual toluene and then dissolved in Et₂O after which it was filtered to remove most of the Ph₃PO. The crude 1,4-Dideoxy-1,4-diiodo-2,3,5-tri-*O*-benzyl-L-lyxitol (18 mmol) was dissolved in benzylamine (59 ml, 540 mmol) and stirred for 2 days at 55 °C. The mixture was diluted with EtOAc, washed with 1M HCl (aq.), NaHCO₃ (sat. aq.) and brine, dried over anhydrous MgSO₄, filtered and concentrated under reduced pressure. The residue was purified by flash chromatography (15-22.5% Et₂O/pentane) yielding the title compound (6.1 g, 12 mmol, 69% yield over 2 steps). *R*_f = 0.55 (40/60 Et₂O/pentane). ¹H NMR (400 MHz, CDCl₃) δ 7.35 – 7.20 (m, 20H, *CH*_{Ar}, Bn), 4.64 (d, *J* = 12.2 Hz, 1H, *CHH*-Bn-3), 4.59 (d, *J* = 12.2 Hz, 1H, *CHH* Bn-3), 4.52 – 4.42 (m, 4H, 2*xCHH* Bn-2, 2*xCHH* Bn-5), 3.99 (d, *J* = 12.9 Hz, 1H, *CHH* *N*-Bn), 3.90 (dt, *J* = 7.9, 5.5 Hz, 1H, C-2), 3.85 (dd, *J* = 5.1, 3.6 Hz, 1H, C-3), 3.58 (d, *J* = 13.0 Hz, 1H, *CHH* *N*-Bn), 3.39 (dd, *J* = 9.9, 4.6 Hz, 1H, C-5a), 3.32 (dd, *J* = 9.9, 6.2 Hz, 1H, C-5b), 3.11 (dd, *J* = 9.0, 5.7 Hz, 1H, C-1a), 3.05 (dt, *J* = 6.1, 4.3 Hz, 1H, C-4), 2.68 (dd, *J* = 8.8, 8.3 Hz, 1H, C-1b). ¹³C NMR (101 MHz, CDCl₃) δ 139.2 (C_q *N*-Bn), 138.6, 138.4, 138.4 (C_q *O*-Bn), 129.0, 128.4, 128.4, 128.3, 128.2, 127.7, 127.7, 127.6, 127.6, 127.1 (CH_{Ar}, Bn), 79.0 (C-3), 76.5 (C-2), 73.4, 71.6 (CH₂ Bn-2, CH₂ Bn-5), 71.4 (CH₂ Bn-3), 71.1 (C-5), 68.2 (C-4), 60.2 (CH₂ *N*-Bn), 55.9 (C-1). [α]_D²⁰ = -32.9° (c = 1, CHCl₃). IR (neat): 602, 694, 731, 820, 845, 908, 1026, 1051, 1072, 1092, 1207, 1258, 1310, 1321, 1364, 1452, 1495, 2799, 2857, 3028, 3061. HR-MS: [M+H]⁺ Calculated for C₃₃H₃₅NO₃: 494.26897; found: 494.26796.

1,4-Dideoxy-1,4-benzylimino-2,3,5-tri-*O*-benzyl-*D*-arabinitol (29). 2,3,5-Tri-*O*-benzyl-L-xylytol (**27**, 11 g, 25 mmol)



was dissolved in pyridine (52 ml), cooled to 0 °C and methanesulfonyl chloride (9.7 ml, 124 mmol) added. The reaction mixture was stirred at this temperature after which the reaction was quenched with H₂O and diluted with EtOAc. The suspension was washed with 1M HCl (aq.), NaHCO₃ (sat. aq.) and brine. The solution was dried over anhydrous MgSO₄ and concentrated. The crude 1,4-Di-*O*-methanesulfonyl-2,3,5-tri-*O*-benzyl-L-xylytol (14 g, 25 mmol) was dissolved in benzylamine (81 ml, 750 mmol) and stirred at 55 °C overnight after which the reaction mixture was allowed to cool to room temperature and subsequently diluted with EtOAc. The mixture was washed with 1M HCl (aq.), NaHCO₃ (sat. aq.) and brine before being dried over anhydrous MgSO₄, filtered and concentrated under reduced pressure. The residue was purified by flash chromatography (10-15% Et₂O/pentane) yielding the title pyrrolidine (11 g, 21 mmol, 84 % yield over 2 steps). *R*_f = 0.9 (10/90 acetone/toluene). ¹H NMR (400 MHz, CDCl₃) δ 7.37 – 7.19 (m, 20H, *CH*_{Ar}, Bn), 4.52 (s, 2H, CH₂ Bn-5), 4.50 (s, 2H, CH₂ Bn-3), 4.45 (d, *J* = 12.2 Hz, 1H, *CHH* Bn-2), 4.37 (d, *J* = 12.2 Hz, 1H, *CHH* Bn-2), 4.14 (d, *J* = 13.3 Hz, 1H, *CHH* *N*-Bn), 3.93 – 3.86 (m, 2H, C-2, C-3), 3.60 (d, *J* = 5.7 Hz, 2H, C-5), 3.49 (d, *J* = 13.8 Hz, 1H, *CHH* *N*-Bn), 3.04 (d, *J* = 10.7 Hz, 1H, C-1a), 2.86 (q, *J* = 5.3 Hz, 1H, C-4), 2.56 (dd, *J* = 10.7, 5.1 Hz, 1H, C-1b). ¹³C NMR (101 MHz, CDCl₃) δ 138.9, 138.5, 138.3, 138.3 (C_q Bn), 129.1, 128.5, 128.3, 127.9, 127.8, 127.7, 127.7, 127.6, 127.0 (CH_{Ar}, Bn), 86.0 (C-3), 81.6 (C-2), 73.3 (CH₂ Bn-5), 71.5 (CH₂ Bn-3), 71.4 (C-5), 71.0 (CH₂ Bn-2), 68.5 (C-4), 59.2 (CH₂ *N*-Bn), 57.1 (C-1). [α]_D²⁰ = -40.0° (c = 1, CHCl₃). IR (neat): 602, 694, 731, 820, 845, 908, 951, 1026, 1074, 1092, 1153, 1206, 1258, 1333, 1366, 1452, 1495, 2797, 2857, 2891, 3028, 3061. HR-MS: [M+H]⁺ Calculated for C₃₃H₃₅NO₃: 494.26897; found: 494.26795.

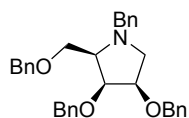
1,4-Dideoxy-1,4-benzylimino-2,3,5-tri-*O*-benzyl-*D*-xylytol (30). 2,3,5-Tri-*O*-benzyl-*L*-arabinitol (**26**, 10 g, 24 mmol)



was dissolved in pyridine (50 ml), cooled to 0 °C and methanesulfonyl chloride (9.2 ml, 118 mmol) added. The mixture was stirred at this temperature for 5 hours. The reaction was quenched with H₂O and the mixture taken up in a mixture of EtOAc and 1M HCl (aq.), washed with 1M HCl (aq.), NaHCO₃ (sat. aq.) and brine. The solution was dried over anhydrous MgSO₄, filtered and concentrated. The crude 1,4-Di-*O*-methanesulfonyl-2,3,5-tri-*O*-benzyl-*L*-arabinitol (13.7 g, 23.7 mmol) was dissolved in benzylamine (78 ml, 710 mmol) and stirred at 55 °C overnight. The reaction mixture was diluted with EtOAc and washed with 1M HCl (aq.), Na₂CO₃ (sat. aq.) and brine. The solution was dried over anhydrous MgSO₄, filtered and concentrated under reduced pressure. The residue was purified by

flash chromatography (10-17.5% Et₂O/pentane) yielding the title pyrrolidine (11 g, 22 mmol, 92 % yield over 2 steps). $R_f = 0.7$ (40/60 Et₂O/pentane). ¹H NMR (400 MHz, CDCl₃) δ 7.41 – 7.24 (m, 20H, CH_{Ar} Bn), 4.66 (d, $J = 12.1$ Hz, 1H, CHH Bn-3), 4.61 (d, $J = 12.1$ Hz, 1H, CHH Bn-3), 4.59 (d, $J = 12.0$ Hz, 1H, CHH Bn-5), 4.55 (d, $J = 12.0$ Hz, 1H, CHH Bn-5), 4.46 (s, 2H, CH₂ Bn-2), 4.16 (d, $J = 13.3$ Hz, 1H, CHH N-Bn), 4.11 (dd, $J = 6.2, 2.9$ Hz, 1H, C-3), 4.04 (td, $J = 5.9, 3.0$ Hz, 1H, C-2), 3.90 (dd, $J = 9.6, 6.0$ Hz, 1H, C-5a), 3.70 (dd, $J = 9.6, 5.2$ Hz, 1H, C-5b), 3.52 (d, $J = 13.3$ Hz, 1H, CHH N-Bn), 3.31 (dd, $J = 10.2, 6.3$ Hz, 1H, C-1a), 3.18 (q, $J = 5.8$ Hz, 1H, C-4), 2.36 (dd, $J = 10.2, 5.5$ Hz, 1H, C-1b). ¹³C NMR (101 MHz, CDCl₃) δ 139.1, 138.6, 138.5, 138.3 (C_q Bn), 129.1, 128.5, 128.5, 128.4, 128.3, 127.9, 127.8, 127.7, 127.6, 127.0 (CH_{Ar} Bn), 83.6 (C-3), 82.2 (C-2), 73.6 (CH₂ Bn-5), 72.2 (CH₂ Bn-3), 71.5 (CH₂ Bn-2), 69.6 (C-5), 65.4 (C-4), 59.5 (CH₂ N-Bn), 57.3 (C-1). $[\alpha]_D^{20} = -35.5^\circ$ ($c = 1$, CHCl₃). IR (neat): 602, 694, 731, 820, 845, 908, 966, 1003, 1026, 1072, 1088, 1206, 1246, 1308, 1344, 1364, 1452, 1495, 2799, 2859, 2911, 3028, 3061. HR-MS: $[M+H]^+$ Calculated for C₃₃H₃₅NO₃: 494.26897; found: 494.26807.

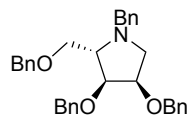
1,4-Dideoxy-1,4-benzylimino-2,3,5-tri-O-benzyl-D-lyxitol (31), 2,3,5-Tri-O-benzyl-D-lyxitol (**25**, 5.3 g, 13 mmol),



triphenylphosphine (7.5 g, 28.8 mmol) and imidazole (2.6 g, 38 mmol) were coevaporated thrice with dry toluene before being dissolved in DCM (125 ml) and cooled to -30 °C. Iodine (7.6 g, 30 mmol) was slowly added and the reaction mixture stirred for 3 days at -35 °C, then 1 day at -25 °C. The solution was concentrated under

reduced pressure, dry toluene (125 ml) added and the mixture refluxed for 2 hours. The reaction mixture was diluted with Et₂O, washed with Na₂S₂O₃ (sat. aq.) and brine, dried over anhydrous MgSO₄, filtered and concentrated under reduced pressure. The residue was coevaporated with Et₂O to remove residual toluene and then dissolved in Et₂O after which it was filtered to remove most of the Ph₃PO. The crude 1,4-Dideoxy-1,4-diiodo-2,3,5-tri-O-benzyl-L-ribitol (12.5 mmol) was dissolved in benzylamine (41 ml, 375 mmol) and stirred for 2 days at 55 °C. The mixture was diluted with EtOAc, washed with 1M HCl (aq.), NaHCO₃ (sat. aq.) and brine, dried over anhydrous MgSO₄, filtered and concentrated under reduced pressure. The residue was purified by flash chromatography (12.5-15% Et₂O/pentane) yielding the title compound (3.4 g, 6.8 mmol, 55% over 2 steps). $R_f = 0.55$ (40/60 Et₂O/pentane). ¹H NMR (400 MHz, CDCl₃) δ 7.44 – 7.14 (m, 20H, CH_{Ar} Bn), 4.74 (d, $J = 12.1$ Hz, 1H, CHH Bn-3), 4.61 (d, $J = 12.1$ Hz, 1H, CHH Bn-3), 4.54 (d, $J = 12.4$ Hz, 1H, CHH Bn-2), 4.52 (d, $J = 12.3$ Hz, 1H, CHH Bn-2), 4.50 (s, 2H, CHH Bn-5), 4.07 (t, $J = 5.3$ Hz, 1H, C-3), 4.05 (d, $J = 13.7$ Hz, 1H, CHH N-Bn), 3.95 (dt, $J = 6.1, 5.0$ Hz, 1H, C-2), 3.91 (dd, $J = 9.4, 6.1$ Hz, 1H, C-5a), 3.68 (dd, $J = 9.4, 6.0$ Hz, 1H, C-5b), 3.59 (d, $J = 13.6$ Hz, 1H, CHH N-Bn), 3.17 (q, $J = 6.0$ Hz, 1H, C-4), 3.07 (dd, $J = 10.7, 4.9$ Hz, 1H, C-1a), 2.56 (dd, $J = 10.7, 6.1$ Hz, 1H, C-1b). ¹³C NMR (101 MHz, CDCl₃) δ 139.4 (C_q N-Bn), 138.8, 138.7, 138.6 (C_q O-Bn), 128.9, 128.4, 128.4, 128.3, 128.3, 127.8, 127.8, 127.6, 127.5, 126.9 (CH_{Ar} Bn), 78.8 (C-3), 77.4 (C-2), 73.5 (CH₂ Bn-5), 73.0 (CH₂ Bn-3), 71.7 (CH₂ Bn-2), 70.7 (C-5), 64.4 (C-4), 59.8 (CH₂ N-Bn), 54.9 (C-1). $[\alpha]_D^{20} = -36.0^\circ$ ($c = 1$, CHCl₃). IR (neat): 602, 617, 636, 694, 731, 808, 820, 847, 907, 953, 1026, 1061, 1090, 1142, 1207, 1256, 1281, 1308, 1344, 1364, 1398, 1452, 1495, 2793, 2862, 2913, 3028, 3061. HR-MS: $[M+H]^+$ Calculated for C₃₃H₃₅NO₃: 494.26897; found: 494.26804.

1,4-Dideoxy-1,4-benzylimino-2,3,5-tri-O-benzyl-L-ribitol (32), 2,3,5-Tri-O-benzyl-D-lyxitol (**25**, 4.7 g, 11 mmol)



was dissolved in pyridine (24 ml), cooled to 0 °C and methanesulfonyl chloride (4.4 ml, 56 mmol) added. The mixture was stirred at this temperature for 5 hours. The reaction was quenched with H₂O and the mixture taken up in a mixture of EtOAc and 1M HCl (aq.), washed with 1M HCl (aq.), NaHCO₃ (sat. aq.) and brine. The solution was dried over anhydrous MgSO₄, filtered and concentrated.

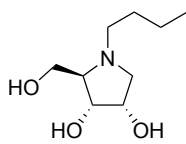
The crude 1,4-Di-O-methanesulfonyl-2,3,5-tri-O-benzyl-D-ribitol (6.2 g, 11 mmol) was dissolved in benzylamine (35 ml, 323 mmol) and stirred overnight at 55 °C. The reaction mixture was diluted with EtOAc and washed with 1M HCl (aq.), Na₂CO₃ (sat. aq.) and brine. The solution was dried over anhydrous MgSO₄, filtered and concentrated under reduced pressure. The residue was purified by flash chromatography (10-20% Et₂O/pentane) yielding the title pyrrolidine (4.7 g, 9.5 mmol, 88 % yield over 2 steps). $[\alpha]_D^{20} = 30.7^\circ$ ($c = 1$, CHCl₃). Analytical data was the same as for its enantiomer (**28**).

1,4-Dideoxy-1,4-benzylimino-2,3,5-tri-*O*-benzyl-L-arabinitol (33). 2,3,5-Tri-*O*-benzyl-D-xylitol (**24**, 10 g, 24 mmol) was dissolved in pyridine (50 ml), cooled to 0 °C and methanesulfonyl chloride (9.2 ml, 118 mmol) added. The mixture was stirred at this temperature for 4 hours. The reaction was quenched with H₂O and the mixture taken up in a mixture of EtOAc and 1M HCl (aq.), washed with 1M HCl (aq.), NaHCO₃ (sat. aq.) and brine. The solution was dried over anhydrous MgSO₄, filtered and concentrated under reduced pressure. The crude 1,4-Di-*O*-methanesulfonyl-2,3,5-tri-*O*-benzyl-D-xylitol (13 g, 22 mmol) was dissolved in benzylamine (71 ml, 650 mmol) and stirred overnight at 55 °C. The reaction mixture was diluted with EtOAc and washed with 1M HCl (aq.), NaHCO₃ (sat. aq.) and brine. The solution was dried over anhydrous MgSO₄, filtered and concentrated under reduced pressure. The residue was purified by flash chromatography (10-15% Et₂O/pentane) yielding the title pyrrolidine (7.6 g, 15 mmol, 71% yield over 2 steps). $[\alpha]_D^{20} = 38.0^\circ$ (*c* = 1, CHCl₃). Analytical data was the same as for its enantiomer (**29**).

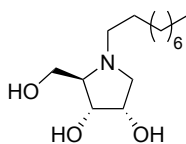
1,4-Dideoxy-1,4-benzylimino-2,3,5-tri-*O*-benzyl-L-xylitol (34). 2,3,5-Tri-*O*-benzyl-D-arabinitol (**23**, 10 g, 24 mmol) was dissolved in pyridine (50 ml), cooled to 0 °C and methanesulfonyl chloride (9.2 ml, 118 mmol) added. The reaction mixture was stirred at this temperature for 5 hours after which the reaction was quenched with H₂O and diluted with EtOAc. The suspension was washed with 1M HCl (aq.), NaHCO₃ (sat. aq.) and brine. The solution was dried over anhydrous MgSO₄ and concentrated. The crude 1,4-Di-*O*-methanesulfonyl-2,3,5-tri-*O*-benzyl-D-arabinitol (12.9 g, 22.3 mmol) was dissolved in benzylamine (73 ml, 670 mmol) and stirred at 55 °C overnight after which the reaction mixture was allowed to cool to room temperature and subsequently diluted with EtOAc. The mixture was washed with 1M HCl (aq.), Na₂CO₃ (sat. aq.) and brine before being dried over anhydrous MgSO₄, filtered and concentrated under reduced pressure. The residue was purified by flash chromatography (2-3% EtOAc/toluene) yielding the title pyrrolidine (5.0 g, 10 mmol, 46 % yield over 2 steps). $[\alpha]_D^{20} = 34.1^\circ$ (*c* = 1, CHCl₃). Analytical data was the same as for its enantiomer (**30**).

1,4-Dideoxy-1,4-benzylimino-2,3,5-tri-*O*-benzyl-L-lyxitol (35). 2,3,5-Tri-*O*-benzyl-D-ribitol (**22**, 6.3 g, 15 mmol) was dissolved in pyridine (32 ml), cooled to 0 °C and methanesulfonyl chloride (5.8 ml, 75 mmol) added. The reaction mixture was stirred at this temperature for 2.5 hours after which the reaction was quenched with H₂O and diluted with EtOAc. The suspension was washed with 1M HCl (aq.), NaHCO₃ (sat. aq.) and brine. The solution was dried over anhydrous MgSO₄ and concentrated. The crude 1,4-Di-*O*-methanesulfonyl-2,3,5-tri-*O*-benzyl-D-ribitol (8.5 g, 15 mmol) was dissolved in benzylamine (49 ml, 450 mmol) and stirred at 55 °C for 2 days after which the reaction mixture was allowed to cool to room temperature and subsequently diluted with EtOAc. The mixture was washed with 1M HCl (aq.), Na₂CO₃ (sat. aq.) and brine before being dried over anhydrous MgSO₄, filtered and concentrated under reduced pressure. The residue was purified by flash chromatography (12.5-20% Et₂O/pentane) yielding the title pyrrolidine (5.2 g, 11 mmol, 70 % yield over 2 steps). $[\alpha]_D^{20} = 34.9^\circ$ (*c* = 1, CHCl₃). Analytical data was the same as for its enantiomer (**31**).

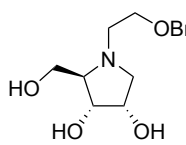
1,4-Dideoxy-1,4-imino-D-ribitol hydrochloride (1A). 1,4-Dideoxy-1,4-benzylimino-2,3,5-tri-*O*-benzyl-D-ribitol (**28**, 4.0 g, 8.0 mmol) was subjected to *General procedure A* yielding the title compound (1.4 g, 7.9 mmol, 99%). ¹H NMR (600 MHz, MeOD) δ 4.26 (td, *J* = 4.0, 1.9 Hz, 1H, C-2), 4.13 (dd, *J* = 8.3, 4.0 Hz, 1H, C-3), 3.91 (dd, *J* = 12.0, 3.3 Hz, 1H, C-5a), 3.78 (dd, *J* = 12.0, 5.9 Hz, 1H, C-5b), 3.54 (ddd, *J* = 8.8, 5.9, 3.3 Hz, 1H, C-4), 3.39 (dd, *J* = 12.4, 4.0 Hz, 1H, C-1a), 3.26 (dd, *J* = 12.5, 2.0 Hz, 1H, C-1b). ¹³C NMR (151 MHz, MeOD) δ 72.9 (C-3), 71.1 (C-2), 63.9 (C-4), 59.4 (C-5), 51.1 (C-1). $[\alpha]_D^{20} = 51.6^\circ$ (*c* = 1, MeOH). IR (neat): 754, 922, 967, 980, 1003, 1034, 1051, 1098, 1132, 1192, 1233, 1323, 1385, 1418, 1449, 2475, 2538, 2596, 2695, 2716, 2747, 2849, 2895, 2938, 3256, 3289, 3345, 3383. HR-MS: $[M+H]^+$ Calculated for C₅H₁₁NO₃: 134.08117; found: 134.08173.

1,4-Dideoxy-1,4-butylimino-D-ribitol (1B). 1,4-Dideoxy-1,4-imino-D-ribitol hydrochloride (**1A**, 85 mg, 0.50 mmol)

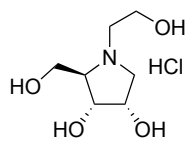
was alkylated with 1-bromobutane (103 mg, 0.75 mmol) in *General procedure B*. Silica gel column chromatography (12.5-17.5% MeOH/EtOAc), HPLC purification and reversed phase column chromatography yielded the title compound (33 mg, 0.17 mmol, 35%). ^1H NMR (600 MHz, MeOD) δ 4.06 (q, $J = 5.8$ Hz, 1H, C-2), 3.88 (t, $J = 5.1$ Hz, 1H, C-3), 3.62 (dd, $J = 11.5, 5.0$ Hz, 1H, C-5a), 3.60 (dd, $J = 11.6, 4.5$ Hz, 1H, C-5b), 3.29 (dd, $J = 10.1, 6.0$ Hz, 1H, C-1a), 2.92 – 2.87 (m, 1H, N-CHH butyl), 2.68 (q, $J = 4.7$ Hz, 1H, C-4), 2.56 – 2.45 (m, 2H, C-1a, N-CHH butyl), 1.56 – 1.45 (m, 2H, N-CH₂CH₂ butyl), 1.41 – 1.28 (m, 2H, CH₂CH₃ butyl), 0.95 (t, $J = 7.4$ Hz, 3H, CH₃ butyl). ^{13}C NMR (151 MHz, MeOD) δ 73.9 (C-3), 72.9 (C-4), 70.9 (C-2), 62.3 (C-5), 58.9 (C-1), 57.2 (N-CH₂ butyl), 30.9 (N-CH₂CH₂ butyl), 21.6 (CH₂CH₃ butyl), 14.3 (CH₃ butyl). $[\alpha]_{\text{D}}^{20} = -33.9^\circ$ ($c = 0.7$, MeOH). HR-MS: $[\text{M}+\text{H}^+]$ Calculated for C₉H₁₉NO₃: 190.14377; found: 190.14488.

1,4-Dideoxy-1,4-nonylimino-D-ribitol (1C). 1,4-Dideoxy-1,4-imino-D-ribitol hydrochloride (**1A**, 85 mg, 0.50 mmol)

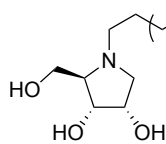
was alkylated with 1-bromononane (155 mg, 0.75 mmol) in *General procedure B*. Silica gel column chromatography (10-12.5% MeOH/EtOAc), HPLC purification (26.5-29% A/B in 10 minutes) and reversed phase column chromatography yielded the title compound (57 mg, 0.22 mmol, 44%). ^1H NMR (600 MHz, MeOD) δ 4.09 – 4.02 (m, 1H, C-2), 3.88 (t, $J = 5.1$ Hz, 1H, C-3), 3.60 (d, $J = 5.0$ Hz, 2H, C-5), 3.27 (dd, $J = 9.8, 5.8$ Hz, 1H, C-1a), 2.86 (ddd, $J = 11.8, 9.9, 6.9$ Hz, 1H, N-CHH nonyl), 2.65 (q, $J = 4.7$ Hz, 1H, C-4), 2.52 – 2.42 (m, 2H, C-1a, N-CHH), 1.58 – 1.44 (m, 2H, N-CH₂CH₂ nonyl), 1.39 – 1.22 (m, 12H, 6xCH₂ nonyl), 0.90 (t, $J = 7.1$ Hz, 3H, CH₃ nonyl). ^{13}C NMR (151 MHz, MeOD) δ 74.0 (C-3), 72.8 (C-4), 70.9 (C-2), 62.5 (C-5), 59.0 (C-1), 57.4 (N-CH₂ nonyl), 33.0, 30.7, 30.6, 30.4 (4xCH₂ nonyl), 28.9 (N-CH₂CH₂ nonyl), 28.5, 23.7 (2xCH₂ nonyl), 14.5 (CH₃ nonyl). $[\alpha]_{\text{D}}^{20} = -34.5^\circ$ ($c = 1$, MeOH). HR-MS: $[\text{M}+\text{H}^+]$ Calculated for C₁₄H₂₉NO₃: 260.22202; found: 260.22259.

1,4-Dideoxy-1,4-(N-(2-benzyloxyethyl))imino-D-ribitol (1D). 1,4-Dideoxy-1,4-imino-D-ribitol hydrochloride (**1A**,

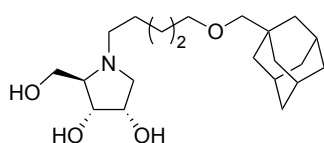
85 mg, 0.50 mmol) was alkylated with 2-bromo(benzyloxy)ethane (161 mg, 0.75 mmol) in *General procedure B*. Silica gel column chromatography (10-15% MeOH/EtOAc), HPLC purification (12.5-16% A/B in 10 minutes) and reversed phase column chromatography yielded the title compound (42 mg, 0.16 mmol, 32%). ^1H NMR (600 MHz, MeOD) δ 7.38 – 7.32 (m, 4H, 2x *o*-CH_{Ar} Bn, 2x *m*-CH_{Ar} Bn), 7.30 – 7.25 (m, 1H, *p*-CH_{Ar} Bn), 4.53 (s, 2H, CH₂ Bn), 4.05 (q, $J = 5.7$ Hz, 1H, C-2), 3.89 (t, $J = 5.2$ Hz, 1H, C-3), 3.68 – 3.54 (m, 4H, C-5, N-CH₂CH₂ ethyl), 3.34 – 3.32 (m, 1H, C-1a), 3.15 (ddd, $J = 12.3, 6.9, 4.9$ Hz, 1H, N-CHH ethyl), 2.80 – 2.73 (m, 2H, C-4, N-CHH ethyl), 2.62 (dd, $J = 9.9, 6.4$ Hz, 1H, C-1b). ^{13}C NMR (151 MHz, MeOD) δ 139.3 (C_q Bn), 129.4, 129.0 (*o*-CH_{Ar} Bn, *m*-CH_{Ar} Bn), 128.8 (*p*-CH_{Ar} Bn), 74.1 (CH₂ Bn), 73.8 (C-3), 72.7 (C-4), 71.1 (C-2), 69.3 (N-CH₂CH₂), 62.0 (C-5), 59.6 (C-1), 56.4 (N-CH₂). $[\alpha]_{\text{D}}^{20} = -18.8^\circ$ ($c = 0.8$, MeOH). HR-MS: $[\text{M}+\text{H}^+]$ Calculated for C₁₄H₂₁NO₄: 268.15433; found: 268.15586.

1,4-Dideoxy-1,4-(N-(2-hydroxyethyl))imino-D-ribitol hydrochloride (1E). 1,4-Dideoxy-1,4-(N-(2-

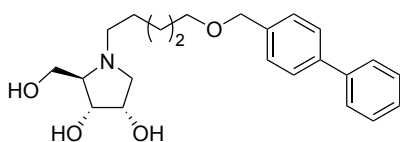
benzyloxyethyl))imino-D-ribitol (**1D**, 15 mg, 0.06 mmol) was subjected to *General procedure C* yielding the title compound (12 mg, 0.06 mmol, quant.). ^1H NMR (600 MHz, MeOD) δ 4.31 – 4.23 (m, 1H, C-2), 4.15 – 4.09 (m, 1H, C-3), 4.02 (dd, $J = 12.3, 3.2$ Hz, 1H, C-5a), 3.94 – 3.83 (m, 3H, C-5b, N-CH₂CH₂ ethyl), 3.79 (dd, $J = 12.5, 3.8$ Hz, 1H, C-1b), 3.68 – 3.59 (m, 2H, C-4, N-CHH ethyl), 3.40 (d, $J = 10.3$ Hz, 2H, C-1a, N-CHH ethyl). ^{13}C NMR (151 MHz, MeOD) δ 72.8 (C-4), 72.6 (C-3), 70.5 (C-2), 61.3 (N-CH₂ ethyl), 59.7 (C-1), 58.6 (C-5), 57.5 (N-CH₂CH₂ ethyl). $[\alpha]_{\text{D}}^{20} = 16.6^\circ$ ($c = 0.7$, MeOH). HR-MS: $[\text{M}+\text{H}^+]$ Calculated for C₇H₁₅NO₄: 178.10738; found: 178.10762.

1,4-Dideoxy-1,4-(N-(5-neopentoxypentyl))imino-D-ribitol (1F).

(**1A**, 85 mg, 0.50 mmol) was alkylated with 5-bromo-1-neopentylloxypentane (178 mg, 0.75 mmol) in *General procedure B*. Silica gel column chromatography (10-12.5% MeOH/EtOAc), HPLC purification (21-25% A/B in 10 minutes) and reversed phase column chromatography yielded the title compound (64 mg, 0.22 mmol, 44%). ^1H NMR (600 MHz, MeOD) δ 4.05 (q, $J = 5.8$ Hz, 1H, C-2), 3.88 (t, $J = 5.1$ Hz, 1H, C-3), 3.61 (dd, $J = 11.5, 5.0$ Hz, 1H, C-5a), 3.59 (dd, $J = 11.6, 4.4$ Hz, 1H, C-5b), 3.42 (t, $J = 6.4$ Hz, 2H, O-CH₂ pentyl), 3.28 (dd, $J = 9.8, 5.8$ Hz, 1H, C-1a), 3.06 (s, 2H, OCH₂ neopentyl), 2.91 – 2.84 (m, 1H, N-CHH pentyl), 2.65 (q, $J = 4.6$ Hz, 1H, C-4), 2.52 – 2.44 (m, 2H, C-1b, N-CHH pentyl), 1.65 – 1.48 (m, 4H, N-CH₂CH₂ pentyl, O-CH₂CH₂ pentyl), 1.46 – 1.32 (m, 2H, N-(CH₂)₂CH₂ pentyl), 0.90 (s, 9H, 3xCH₃ neopentyl). ^{13}C NMR (151 MHz, MeOD) δ 82.4 (O-CH₂ neopentyl), 74.0 (C-3), 72.8 (C-4), 72.3 (O-CH₂ pentyl), 70.9 (C-2), 62.4 (C-5), 58.9 (C-1), 57.3 (N-CH₂ pentyl), 32.9 (C_q neopentyl), 30.5 (O-CH₂CH₂ pentyl), 28.7 (N-CH₂CH₂ pentyl), 27.2 (3xCH₃ neopentyl), 25.1 (N-(CH₂)₂CH₂ pentyl). $[\alpha]_{\text{D}}^{20} = -31.7^\circ$ ($c = 1$, MeOH). HR-MS: $[\text{M}+\text{H}^+]$ Calculated for C₁₅H₃₁NO₄: 290.23258; found: 290.23279.

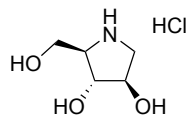
1,4-Dideoxy-1,4-(N-(5-(adamantane-1-yl-methoxy)pentyl))imino-D-ribitol (1G).

hydrochloride (**1A**, 85 mg, 0.50 mmol) was alkylated with 5-bromo-1-(adamantane-1-yl-methoxy)pentane (236 mg, 0.75 mmol) in *General procedure B*. Silica gel column chromatography (10-12.5% MeOH/EtOAc), HPLC purification (33-37% A/B in 10 minutes) and reversed phase column chromatography yielded the title compound (60 mg, 0.16 mmol, 33%). ^1H NMR (600 MHz, MeOD) δ 4.04 (q, $J = 5.8$ Hz, 1H, C-2), 3.86 (t, $J = 5.0$ Hz, 1H, C-3), 3.59 (d, $J = 4.8$ Hz, 2H, C-5), 3.39 (t, $J = 6.4$ Hz, 2H, O-CH₂ pentyl), 3.26 (dd, $J = 9.6, 5.9$ Hz, 1H, C-1a), 2.97 (s, 2H, O-CH₂ adamantanemethyl), 2.90 – 2.79 (m, 1H, N-CHH pentyl), 2.61 (q, $J = 4.7$ Hz, 1H, C-4), 2.51 – 2.39 (m, 2H, C-1b, N-CHH pentyl), 1.95 (s, 3H, 3xCH adamantanemethyl), 1.80 – 1.65 (m, 6H, 3xC_qCH₂ adamantanemethyl), 1.64 – 1.46 (m, 10H, N-CH₂CH₂ pentyl, O-CH₂CH₂ pentyl, 3xCHCH₂ adamantanemethyl), 1.46 – 1.27 (m, 2H, N-(CH₂)₂CH₂ pentyl). ^{13}C NMR (151 MHz, MeOD) δ 83.0 (O-CH₂ adamantanemethyl), 74.0 (C-3), 72.9 (C-4), 72.4 (O-CH₂ pentyl), 70.9 (C-2), 62.6 (C-5), 59.0 (C-1), 57.2 (N-CH₂ pentyl), 40.8 (3xC_qCH₂ adamantanemethyl), 38.3 (3xCHCH₂ adamantanemethyl), 35.1 (C_q adamantanemethyl), 30.5 (O-CH₂CH₂ pentyl), 29.7 (3xCH adamantanemethyl), 28.8 (N-CH₂CH₂ pentyl), 25.2 (N-(CH₂)₂CH₂ pentyl). $[\alpha]_{\text{D}}^{20} = -23.4^\circ$ ($c = 1$, MeOH). HR-MS: $[\text{M}+\text{H}^+]$ Calculated for C₂₁H₃₇NO₄: 368.27954; found: 368.27952.

1,4-Dideoxy-1,4-(N-(5-(*p*-phenylbenzyloxy)pentyl))imino-D-ribitol (1H).

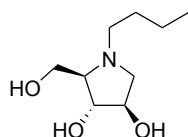
hydrochloride (**1A**, 85 mg, 0.50 mmol) was alkylated with 5-bromo-1-(*p*-phenylbenzyloxy)pentane (250 mg, 0.75 mmol) in *General procedure B*. Silica gel column chromatography (10-12.5% MeOH/EtOAc), HPLC purification (32.5-37% A/B in 10 minutes) and reversed phase column chromatography yielded the title compound (79 mg, 0.21 mmol, 41%). ^1H NMR (600 MHz, MeOD) δ 7.62 – 7.54 (m, 4H, 4xCH_{Ar} Ph), 7.44 – 7.37 (m, 4H, 4xCH_{Ar} Ph), 7.31 (t, $J = 7.4$ Hz, 1H, *p*-CH_{Ar} Ph), 4.51 (s, 2H, O-CH₂ phenylbenzyl), 4.04 (q, $J = 5.8$ Hz, 1H, C-2), 3.87 (t, $J = 5.1$ Hz, 1H, C-3), 3.58 (d, $J = 4.8$ Hz, 2H, C-5), 3.49 (t, $J = 6.5$ Hz, 2H, O-CH₂ pentyl), 3.25 (dd, $J = 9.7, 5.9$ Hz, 1H, C-1a), 2.88 – 2.79 (m, 1H, N-CHH pentyl), 2.61 (q, $J = 4.6$ Hz, 1H, C-4), 2.49 – 2.39 (m, 2H, C-1b, N-CHH pentyl), 1.68 – 1.57 (m, 2H, O-CH₂CH₂ pentyl), 1.56 – 1.47 (m, 2H, N-CH₂CH₂ pentyl), 1.46 – 1.32 (m, 2H, N-(CH₂)₂CH₂ pentyl). ^{13}C NMR (151 MHz, MeOD) δ 142.0, 141.7, 138.9 (3xC_q Ph), 129.8, 129.3 (4xCH_{Ar} Ph), 128.3 (*p*-CH_{Ar} Ph), 127.9, 127.9 (4xCH_{Ar} Ph), 74.0 (C-3), 73.5 (O-CH₂ phenylbenzyl), 72.8 (C-4), 71.2 (O-CH₂ pentyl), 70.9 (C-2), 62.6 (C-5), 58.9 (C-1), 57.1 (N-CH₂ pentyl), 30.6 (O-CH₂CH₂ pentyl), 28.7 (N-CH₂CH₂ pentyl), 25.1 (N-(CH₂)₂CH₂ pentyl). $[\alpha]_{\text{D}}^{20} = -31.2^\circ$ ($c = 1$, MeOH). HR-MS: $[\text{M}+\text{H}^+]$ Calculated for C₂₁H₃₇NO₄: 386.23258; found: 386.23266.

1,4-Dideoxy-1,4-imino-D-arabinitol hydrochloride (2A). 1,4-Dideoxy-1,4-benzylimino-2,3,5-tri-*O*-benzyl-D-



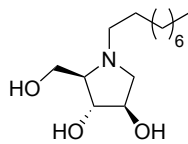
arabinitol (**29**, 4.0 g, 8.0 mmol) was subjected to *General procedure A* yielding the title compound (1.4 g, 8.0 mmol, quant.). $^1\text{H NMR}$ (600 MHz, MeOD) δ 4.22 – 4.18 (m, 1H, C-2), 3.98 (s, 1H, C-3), 3.90 (dd, $J = 11.6, 4.7$ Hz, 1H, C-5a), 3.80 (dd, $J = 11.6, 9.3$ Hz, 1H, C-5b), 3.52 (ddd, $J = 9.0, 4.5, 2.7$ Hz, 1H, C-4), 3.47 (dd, $J = 12.0, 4.0$ Hz, 1H, C-1a), 3.29 (d, $J = 12.0$ Hz, 1H, C-1b). $^{13}\text{C NMR}$ (151 MHz, MeOD) δ 77.4 (C-2), 76.1 (C-3), 69.8 (C-4), 60.9 (C-5), 51.9 (C-1). $[\alpha]_{\text{D}}^{20} = 36.4^\circ$ ($c = 1$, MeOH). IR (neat): 606, 714, 764, 823, 918, 966, 1003, 1038, 1074, 1109, 1167, 1215, 1260, 1298, 1360, 1375, 1396, 1449, 1576, 2488, 2745, 2762, 2833, 2887, 2941, 2959, 2968, 3022, 3277, 3372, 3416. HR-MS: $[\text{M}+\text{H}^+]$ Calculated for $\text{C}_5\text{H}_{11}\text{NO}_3$: 134.08117; found: 134.08169.

1,4-Dideoxy-1,4-butylimino-D-arabinitol (2B). 1,4-Dideoxy-1,4-imino-D-arabinitol hydrochloride (**2A**, 85 mg, 0.50



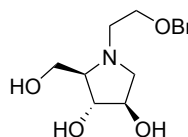
mmol) was alkylated with 1-bromobutane (103 mg, 0.75 mmol) in *General procedure B*. Silica gel column chromatography (10-15% MeOH/EtOAc), HPLC purification and reversed phase column chromatography yielded the title compound (12 mg, 0.06 mmol, 13%). $^1\text{H NMR}$ (600 MHz, MeOD) δ 4.07 – 4.02 (m, 1H, C-2), 3.94 – 3.89 (m, 1H, C-3), 3.79 (dd, $J = 11.5, 5.2$ Hz, 1H, C-5a), 3.77 (dd, $J = 11.5, 6.1$ Hz, 1H, C-5b), 3.27 (d, $J = 11.0$ Hz, 1H, C-1a), 3.14 – 3.07 (m, 1H, N-*CHH* butyl), 3.00 (dd, $J = 11.1, 4.6$ Hz, 1H, C-1b), 2.89 – 2.83 (m, 1H, C-4), 2.71 – 2.64 (m, 1H, N-*CHH* butyl), 1.64 – 1.56 (m, 2H, N- CH_2CH_2 butyl), 1.43 – 1.32 (m, 2H, CH_2CH_3 butyl), 0.96 (t, $J = 7.4$ Hz, 3H, CH_3 butyl). $^{13}\text{C NMR}$ (151 MHz, MeOD) δ 79.4 (C-3), 76.7 (C-2), 76.3 (C-4), 61.8 (C-5), 60.5 (C-1), 57.5 (N- CH_2 butyl), 30.0 (N- CH_2CH_2 butyl), 21.4 (CH_2CH_3 butyl), 14.2 (CH_3 butyl). $[\alpha]_{\text{D}}^{20} = -23.3^\circ$ ($c = 0.2$, MeOH). HR-MS: $[\text{M}+\text{H}^+]$ Calculated for $\text{C}_9\text{H}_{19}\text{NO}_3$: 190.14377; found: 190.14470.

1,4-Dideoxy-1,4-nonylimino-D-arabinitol (2C). 1,4-Dideoxy-1,4-imino-D-arabinitol hydrochloride (**2A**, 85 mg, 0.50

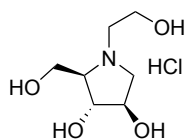


mmol) was alkylated with 1-bromononane (155 mg, 0.75 mmol) in *General procedure B*. Silica gel column chromatography (10-12.5% MeOH/EtOAc), HPLC purification (25-42% A/B in 8.5 minutes) and reversed phase column chromatography yielded the title compound (61 mg, 0.23 mmol, 47%). $^1\text{H NMR}$ (600 MHz, MeOD) δ 4.09 – 4.01 (m, 1H, C-2), 3.94 – 3.91 (m, 1H, C-3), 3.78 (d, $J = 5.7$ Hz, 2H, C-5), 3.28 (d, $J = 11.0$ Hz, 1H, C-1a), 3.14 – 3.06 (m, 1H, N-*CHH* nonyl), 3.00 (dd, $J = 11.0, 4.7$ Hz, 1H, C-1b), 2.89 – 2.85 (m, 1H, C-4), 2.71 – 2.65 (m, 1H, N-*CHH* nonyl), 1.66 – 1.57 (m, 2H, N- CH_2CH_2 nonyl), 1.39 – 1.24 (m, 12H, $6 \times \text{CH}_2$ nonyl), 0.90 (t, $J = 7.0$ Hz, 3H, CH_3 nonyl). $^{13}\text{C NMR}$ (151 MHz, MeOD) δ 79.4 (C-3), 76.6 (C-2), 76.3 (C-4), 61.8 (C-5), 60.5 (C-1), 57.7 (N- CH_2 nonyl), 33.0, 30.6, 30.5, 30.4, 28.2 ($5 \times \text{CH}_2$ nonyl), 27.8 (N- CH_2CH_2 nonyl), 23.7 (CH_2 nonyl), 14.5 (CH_3 nonyl). $[\alpha]_{\text{D}}^{20} = -18.9^\circ$ ($c = 1$, MeOH). HR-MS: $[\text{M}+\text{H}^+]$ Calculated for $\text{C}_{14}\text{H}_{29}\text{NO}_3$: 260.22202; found: 260.22228.

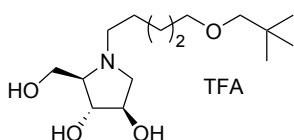
1,4-Dideoxy-1,4-(N-(2-benzyloxyethyl))imino-D-arabinitol (2D). 1,4-Dideoxy-1,4-imino-D-arabinitol



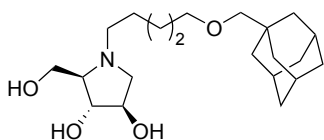
hydrochloride (**2A**, 85 mg, 0.50 mmol) was alkylated with 2-bromo(benzyloxy)ethane (161 mg, 0.75 mmol) in *General procedure B*. Silica gel column chromatography (10-12.5% MeOH/EtOAc), HPLC purification (11-20% A/B in 10 minutes) and reversed phase column chromatography yielded the title compound (35 mg, 0.13 mmol, 26%). $^1\text{H NMR}$ (600 MHz, MeOD) δ 7.38 – 7.31 (m, 4H, 2x *o*- CH_{Ar} Bn, 2x *m*- CH_{Ar} Bn), 7.30 – 7.25 (m, 1H, *p*- CH_{Ar} Bn), 4.53 (s, 2H, CH_2 Bn), 3.95 – 3.92 (m, 1H, C-2), 3.91 – 3.87 (m, 1H, C-3), 3.70 (dd, $J = 11.4, 4.5$ Hz, 1H, C-5a), 3.66 – 3.61 (m, 2H, C-5b, N- CH_2CHH ethyl), 3.60 (dd, $J = 10.2, 5.3$ Hz, 1H, N- CH_2CHH ethyl), 3.14 – 3.10 (m, 1H, N-*CHH* ethyl), 3.09 (d, $J = 9.4$ Hz, 1H, C-1a), 2.78 (dd, $J = 10.5, 5.4$ Hz, 1H, C-1b), 2.62 (dt, $J = 13.1, 5.1$ Hz, 1H, N-*CHH* ethyl), 2.53 (q, $J = 4.4$ Hz, 1H, C-4). $^{13}\text{C NMR}$ (151 MHz, MeOD) δ 139.5 (C_q Bn), 129.4, 129.0 (*o*- CH_{Ar} Bn, *m*- CH_{Ar} Bn), 128.7 (*p*- CH_{Ar} , *p*-Bn), 80.4 (C-3), 77.4 (C-2), 74.4 (C-4), 74.2 (CH_2 Bn), 69.8 (N- CH_2CH_2 ethyl), 62.2 (C-5), 61.1 (C-1), 55.5 (N- CH_2 ethyl). $[\alpha]_{\text{D}}^{20} = -22.6^\circ$ ($c = 0.7$, MeOH). HR-MS: $[\text{M}+\text{H}^+]$ Calculated for $\text{C}_{14}\text{H}_{21}\text{NO}_4$: 268.15433; found: 268.15420.

1,4-Dideoxy-1,4-(*N*-(2-hydroxyethyl))imino-D-arabinitol hydrochloride (2E).

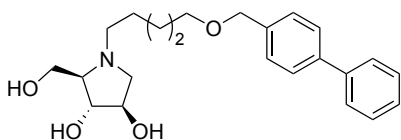
1,4-Dideoxy-1,4-(*N*-(2-benzyloxyethyl))imino-D-arabinitol (**2D**, 47 mg, 0.18 mmol) was subjected to *General procedure C* yielding the title compound (39 mg, 0.18 mmol, quant.). ^1H NMR (600 MHz, MeOD) δ 4.22 (s, 1H, C-2), 3.99 (s, 1H, C-3), 3.96 (d, $J = 6.6$ Hz, 2H, C-5), 3.95 – 3.86 (m, 2H, N-CH₂CH₂ ethyl), 3.72 (d, $J = 12.1$ Hz, 1H, C-1a), 3.66 – 3.54 (m, 3H, C-1b, C-4, N-CHH ethyl), 3.35 (s, 1H, N-CHH ethyl). ^{13}C NMR (151 MHz, MeOD) δ 78.3 (C-4), 77.6 (C-3), 75.7 (C-2), 61.5 (C-1), 60.6 (C-5), 60.4 (N-CH₂ ethyl), 57.9 (N-CH₂CH₂ ethyl). $[\alpha]^{20}_{\text{D}} = 5.9^\circ$ ($c = 0.8$, MeOH). HR-MS: $[\text{M}+\text{H}^+]$ Calculated for C₇H₁₅NO₄: 178.10738; found: 178.10816.

1,4-Dideoxy-1,4-(*N*-(5-neopentoxypentyl))imino-D-arabinitol trifluoroacetic acid (2F).

D-arabinitol hydrochloride (**2A**, 85 mg, 0.50 mmol) was alkylated with 5-bromo-1-neopentoxypentane (178 mg, 0.75 mmol) in *General procedure B*. Silica gel column chromatography (10-12.5% MeOH/EtOAc) and HPLC purification (21-26% A/B in 10 minutes) yielded the title compound (53 mg, 0.13 mmol, 26%). ^1H NMR (600 MHz, MeOD) δ 4.21 – 4.16 (m, 1H, C-2), 3.95 (s, 1H, C-3), 3.94 – 3.89 (m, 2H, C-5), 3.60 (d, $J = 11.8$ Hz, 1H, C-1a), 3.49 – 3.40 (m, 5H, C-1b, C-4, N-CHH pentyl, O-CH₂ pentyl), 3.19 – 3.11 (m, 1H, N-CHH pentyl), 3.07 (s, 2H, O-CH₂ neopentyl), 1.85 – 1.73 (m, 2H, N-CH₂CH₂ pentyl), 1.68 – 1.58 (m, 2H, N-(CH₂)₂CH₂), 1.51 – 1.40 (m, 2H, O-CH₂CH₂ pentyl), 0.90 (s, 9H, 3xCH₃ neopentyl). ^{13}C NMR (151 MHz, MeOD) δ 82.5 (O-CH₂ neopentyl), 78.6 (O-CH₂ pentyl), 77.7 (C-4), 75.7 (C-3), 72.0 (C-2), 60.9 (C-5), 60.6 (C-1), 58.9 (N-CH₂ pentyl), 32.9 (C_q neopentyl), 30.2 (O-CH₂CH₂ pentyl), 27.1 (3xCH₃ neopentyl), 26.1 (N-CH₂CH₂ pentyl), 24.5 (N-(CH₂)₂CH₂ pentyl). $[\alpha]^{20}_{\text{D}} = -1.2^\circ$ ($c = 1$, MeOH). HR-MS: $[\text{M}+\text{H}^+]$ Calculated for C₁₅H₃₁NO₄: 290.23258; found: 290.23312.

1,4-Dideoxy-1,4-(*N*-(5-(adamantane-1-yl-methoxy)pentyl))imino-D-arabinitol (2G).

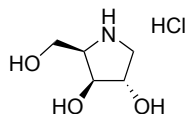
D-arabinitol hydrochloride (**2A**, 85 mg, 0.50 mmol) was alkylated with 5-bromo-1-(adamantane-1-yl-methoxy)pentane (236 mg, 0.75 mmol) in *General procedure B*. Silica gel column chromatography (10-12.5% MeOH/EtOAc), HPLC purification (25-58% A/B in 9.5 minutes) and reversed phase column chromatography yielded the title compound (68 mg, 0.19 mmol, 37%). ^1H NMR (600 MHz, MeOD) δ 4.03 – 3.96 (m, 1H, C-2), 3.94 – 3.89 (m, 1H, C-3), 3.74 (dd, $J = 11.5, 5.1$ Hz, 1H, C-5a), 3.71 (dd, $J = 11.4, 5.3$ Hz, 1H, C-5b), 3.39 (t, $J = 6.4$ Hz, 2H, O-CH₂ pentyl), 3.16 (d, $J = 10.7$ Hz, 1H, C-1a), 3.02 – 2.93 (m, 3H, N-CHH pentyl, O-CH₂ adamantanemethyl), 2.84 (dd, $J = 10.8, 4.9$ Hz, 1H, C-1b), 2.66 (q, $J = 4.7$ Hz, 1H, C-4), 2.56 – 2.48 (m, 1H, N-CHH pentyl), 1.95 (s, 3H, 3xCH adamantanemethyl), 1.80 – 1.65 (m, 6H, 3xC_qCH₂ adamantanemethyl), 1.63 – 1.53 (m, 10H, N-CH₂CH₂ pentyl, O-CH₂CH₂ pentyl, 3xCHCH₂ adamantanemethyl), 1.46 – 1.33 (m, 2H, N-(CH₂)₂CH₂). ^{13}C NMR (151 MHz, MeOD) δ 83.0 (O-CH₂ adamantanemethyl), 80.0 (C-3), 76.9 (C-2), 75.4 (C-4), 72.4 (O-CH₂ pentyl), 62.1 (C-5), 60.5 (C-1), 57.2 (N-CH₂ pentyl), 40.8 (3xC_qCH₂ adamantanemethyl), 38.3 (3xCHCH₂ adamantanemethyl), 35.1 (C_q adamantanemethyl), 30.5 (O-CH₂CH₂ pentyl), 29.7 (3xCH adamantanemethyl), 28.2 (N-CH₂CH₂ pentyl), 25.1 (N-(CH₂)₂CH₂). $[\alpha]^{20}_{\text{D}} = -22.8^\circ$ ($c = 1$, MeOH). HR-MS: $[\text{M}+\text{H}^+]$ Calculated for C₂₁H₃₇NO₄: 368.27954; found: 368.27953.

1,4-Dideoxy-1,4-(*N*-(5-(*p*-phenylbenzyloxy)pentyl))imino-D-arabinitol (2H).

D-arabinitol hydrochloride (**2A**, 85 mg, 0.50 mmol) was alkylated with 5-bromo-1-(*p*-phenylbenzyloxy)pentane (250 mg, 0.75 mmol) in *General procedure B*. Silica gel column chromatography (10-12.5% MeOH/EtOAc), HPLC purification (32-37% A/B in 10 minutes) and reversed phase column chromatography yielded the title compound (65 mg, 0.17 mmol, 34%). ^1H NMR (600 MHz, MeOD) δ 7.62 – 7.55 (m, 4H, 4xCH_{Ar} Ph), 7.44 – 7.37 (m, 4H, 4xCH_{Ar} Ph), 7.34 – 7.28 (m, 1H, *p*-CH_{Ar} Ph), 4.51 (s, 2H, O-CH₂ phenylbenzyl), 3.96 – 3.92 (m, 1H, C-2),

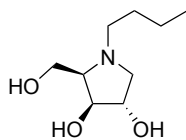
3.92 – 3.89 (m, 1H, C-3), 3.68 (dd, $J = 11.2, 4.9$ Hz, 1H, C-5a), 3.64 (dd, $J = 11.2, 4.2$ Hz, 1H, C-5b), 3.50 (t, $J = 6.5$ Hz, 2H, O-CH₂ pentyl), 3.01 (d, $J = 10.4$ Hz, 1H, C-1a), 2.86 – 2.78 (m, 1H, N-CHH pentyl), 2.63 (dd, $J = 10.4, 5.3$ Hz, 1H, C-1b), 2.42 (q, $J = 4.4$ Hz, 1H, C-4), 2.35 – 2.28 (m, 1H, N-CHH pentyl), 1.67 – 1.58 (m, 2H, O-CH₂CH₂ pentyl), 1.56 – 1.47 (m, 2H, N-CH₂CH₂ pentyl), 1.47 – 1.32 (m, 2H, N-(CH₂)₂CH₂ pentyl). ¹³C NMR (151 MHz, MeOD) δ 142.1, 141.7, 138.9 (3x_{C_q} Ph), 129.8, 129.3 (4x_{C_{Ar}} Ph), 128.3 (*p*-CH_{Ar} Ph), 127.9, 127.9 (4x_{C_{Ar}} Ph), 80.8 (C-3), 77.3 (C-2), 74.4 (C-4), 73.5 (O-CH₂ phenylbenzyl), 71.3 (O-CH₂ pentyl), 62.5 (C-5), 60.5 (C-1), 56.6 (N-CH₂ pentyl), 30.6 (O-CH₂CH₂ pentyl), 28.9 (N-CH₂CH₂ pentyl), 25.2 (N-(CH₂)₂CH₂ pentyl). $[\alpha]_{\text{D}}^{20} = -29.6^\circ$ ($c = 1$, MeOH). HR-MS: $[M+H]^+$ Calculated for C₂₁H₃₇NO₄: 386.23258; found: 368.23263.

1,4-Dideoxy-1,4-imino-D-xylitol hydrochloride (3A) 1,4-Dideoxy-1,4-benzylimino-2,3,5-tri-O-benzyl-D-xylitol (**30**,



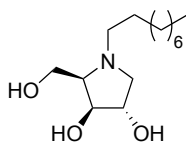
4.0 g, 8.0 mmol) was subjected to *General procedure A* yielding the title compound (1.4 g, 8.0 mmol, quant.). ¹H NMR (600 MHz, MeOD) δ 4.25 (dd, $J = 4.0, 1.5$ Hz, 1H, C-2), 4.16 (dd, $J = 3.3, 1.5$ Hz, 1H, C-3), 3.96 (dd, $J = 11.7, 4.5$ Hz, 1H, C-5a), 3.87 (dd, $J = 11.7, 9.1$ Hz, 1H, C-5b), 3.80 (ddd, $J = 9.1, 4.5, 3.2$ Hz, 1H, C-4), 3.56 (dd, $J = 12.3, 4.1$ Hz, 1H, C-1a), 3.16 (d, $J = 12.3$ Hz, 1H, C-1b). ¹³C NMR (151 MHz, MeOD) δ 76.1 (C-2), 75.8 (C-3), 65.1 (C-4), 59.0 (C-5), 52.0 (C-1). $[\alpha]_{\text{D}}^{20} = 13.3^\circ$ ($c = 1$, MeOH). IR (neat): 608, 718, 773, 822, 901, 918, 972, 1016, 1034, 1055, 1082, 1098, 1204, 1246, 1281, 1294, 1366, 1385, 1402, 1454, 1578, 2295, 2351, 2399, 2469, 2540, 2650, 2714, 2805, 2955, 3026, 3341. HR-MS: $[M+H]^+$ Calculated for C₅H₁₁NO₃: 134.08117; found: 134.08186.

1,4-Dideoxy-1,4-butylimino-D-xylitol (3B) 1,4-Dideoxy-1,4-imino-D-xylitol hydrochloride (**3A**, 85 mg, 0.50 mmol)



was alkylated with 1-bromobutane (103 mg, 0.75 mmol) in *General procedure B*. Silica gel column chromatography (15-17.5% MeOH/EtOAc), HPLC purification and reversed phase column chromatography yielded the title compound (25 mg, 0.13 mmol, 27%). ¹H NMR (600 MHz, MeOD) δ 4.08 – 3.97 (m, 2H, C-2, C-3), 3.80 (dd, $J = 11.1, 6.7$ Hz, 1H, C-5a), 3.66 (dd, $J = 11.1, 4.4$ Hz, 1H, C-5b), 3.38 (dd, $J = 10.5, 5.4$ Hz, 1H, C-1a), 2.86 – 2.79 (m, 1H, N-CHH ethyl), 2.78 – 2.74 (m, 1H, C-4), 2.38 – 2.32 (m, 1H, N-CHH butyl), 2.24 (dd, $J = 10.4, 5.2$ Hz, 1H, C-1b), 1.52 – 1.44 (m, 2H, N-CH₂CH₂ butyl), 1.41 – 1.27 (m, 2H, CH₂CH₃ butyl), 0.94 (t, $J = 7.4$ Hz, 3H, CH₃ butyl). ¹³C NMR (151 MHz, MeOD) δ 79.0 (C-3), 77.4 (C-2), 69.0 (C-4), 61.0 (C-5), 59.9 (C-1), 57.1 (N-CH₂ butyl), 31.2 (N-CH₂CH₂ butyl), 21.7 (CH₂CH₃ butyl), 14.4 (CH₃ butyl). $[\alpha]_{\text{D}}^{20} = -62.8^\circ$ ($c = 0.5$, MeOH). HR-MS: $[M+H]^+$ Calculated for C₉H₁₉NO₃: 190.14377; found: 190.14421.

1,4-Dideoxy-1,4-nonylimino-D-xylitol (3C) 1,4-Dideoxy-1,4-imino-D-xylitol hydrochloride (**3A**, 85 mg, 0.50 mmol)



was alkylated with 1-bromononane (155 mg, 0.75 mmol) in *General procedure B*. Silica gel column chromatography, HPLC purification (27-31% A/B in 8.5 minutes) and reversed phase column chromatography yielded the title compound (56 mg, 0.22 mmol, 43%). ¹H NMR (600 MHz, MeOD) δ 4.07 – 3.98 (m, 2H, C-2, C-3), 3.80 (dd, $J = 11.1, 6.7$ Hz, 1H, C-5a), 3.66 (dd, $J = 11.1, 4.4$ Hz, 1H, C-5b), 3.38 (dd, $J = 10.5, 5.4$ Hz, 1H, C-1a), 2.84 – 2.79 (m, 1H, N-CHH nonyl), 2.79 – 2.75 (m, 1H, C-4), 2.39 – 2.29 (m, 1H, N-CHH nonyl), 2.24 (dd, $J = 10.4, 5.2$ Hz, 1H, C-1b), 1.54 – 1.46 (m, 2H, N-CH₂CH₂ nonyl), 1.37 – 1.23 (m, 12H, 6xCH₂ nonyl), 0.90 (t, $J = 7.1$ Hz, 3H, CH₃ nonyl). ¹³C NMR (151 MHz, MeOD) δ 79.0 (C-3), 77.4 (C-2), 69.0 (C-4), 61.0 (C-5), 59.8 (C-1), 57.4 (N-CH₂ nonyl), 33.1, 30.7, 30.7, 30.4 (4xCH₂ nonyl), 29.0 (N-CH₂CH₂ nonyl), 28.6, 23.7 (2xCH₂ nonyl), 14.5 (CH₃ nonyl). $[\alpha]_{\text{D}}^{20} = -51.7^\circ$ ($c = 1$, MeOH). HR-MS: $[M+H]^+$ Calculated for C₁₄H₂₉NO₃: 260.22202; found: 260.22193.

1,4-Dideoxy-1,4-(*N*-(2-benzyloxyethyl))imino-D-xylitol (3D). 1,4-Dideoxy-1,4-imino-D-xylitol hydrochloride (**3A**, 85 mg, 0.50 mmol) was alkylated with 2-bromo(benzyloxy)ethane (161 mg, 0.75 mmol) in *General procedure B*. Silica gel column chromatography, HPLC purification (13.5-17% A/B in 9.5 minutes) and reversed phase column chromatography yielded the title compound (34 mg, 0.13 mmol, 25%). $^1\text{H NMR}$ (600 MHz, MeOD) δ 7.38 – 7.31 (m, 4H, *o*-CH_{Ar} Bn, *m*-CH_{Ar} Bn), 7.30 – 7.25 (m, 1H, *p*-CH_{Ar} Bn), 4.52 (s, 2H, CH₂ Bn), 4.04 – 3.98 (m, 2H, C-2, C-3), 3.79 (dd, $J = 11.3, 6.1$ Hz, 1H, C-5a), 3.66 (dd, $J = 11.3, 4.6$ Hz, 1H, C-5b), 3.64 – 3.56 (m, 2H, N-CH₂CH₂ ethyl), 3.41 (dd, $J = 10.5, 5.6$ Hz, 1H, C-1a), 3.11 – 3.04 (m, 1H, N-CHH ethyl), 2.85 (q, $J = 5.7$ Hz, 1H, C-4), 2.69 – 2.61 (m, 1H, N-CHH ethyl), 2.35 (dd, $J = 10.4, 5.2$ Hz, 1H, C-1b). $^{13}\text{C NMR}$ (151 MHz, MeOD) δ 139.5 (C_q Bn), 129.4, 128.9 (*o*-CH_{Ar} Bn, *m*-CH_{Ar} Bn), 128.7 (*p*-CH_{Ar} Bn), 79.0 (C-3), 77.5 (C-2), 74.1 (O-CH₂ Bn), 69.9 (N-CH₂CH₂ ethyl), 68.8 (C-4), 61.2 (C-5), 60.4 (C-1), 56.1 (N-CH₂CH₂). $[\alpha]_{\text{D}}^{20} = -30^\circ$ ($c = 0.7$, MeOH). HR-MS: $[\text{M}+\text{H}^+]$ Calculated for C₁₄H₂₁NO₄: 268.15433; found: 268.15469.

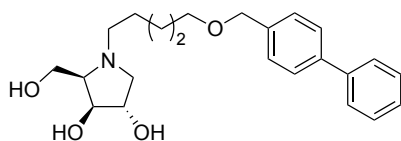
1,4-Dideoxy-1,4-(*N*-(2-hydroxyethyl))imino-D-xylitol hydrochloride (3E). 1,4-Dideoxy-1,4-(*N*-(2-benzyloxyethyl))imino-D-xylitol (**3D**, 15 mg, 0.06 mmol) was subjected to *General procedure C* yielding the title compound (12 mg, 0.06 mmol, quant.). $^1\text{H NMR}$ (600 MHz, MeOD) δ 4.26 – 4.21 (m, 2H, C-2, C-3), 4.08 – 4.01 (m, 2H, C-5), 3.94 – 3.82 (m, 4H, C-1a, C-4, N-CH₂CH₂ ethyl), 3.77 – 3.68 (m, 1H, N-CHH ethyl), 3.47 (d, $J = 12.6$ Hz, 1H, C-1b), 3.39 – 3.34 (m, 1H, N-CHH ethyl). $^{13}\text{C NMR}$ (151 MHz, MeOD) δ 76.6, 75.9 (C-2, C-3), 73.7 (C-4), 61.9 (N-CH₂ ethyl), 60.9 (C-1), 58.9 (C-5), 58.1 (N-CH₂CH₂). $[\alpha]_{\text{D}}^{20} = -16.7^\circ$ ($c = 0.2$, MeOH). HR-MS: $[\text{M}+\text{H}^+]$ Calculated for C₇H₁₅NO₄: 178.10738; found: 178.10800.

1,4-Dideoxy-1,4-(*N*-(5-neopentoxypentyl))imino-D-xylitol (3F). 1,4-Dideoxy-1,4-imino-D-xylitol hydrochloride (**3A**, 85 mg, 0.50 mmol) was alkylated with 5-bromo-1-neopentylloxypentane (178 mg, 0.75 mmol) in *General procedure B*. Silica gel column chromatography, HPLC purification (22-26% A/B in 9 minutes) and reversed phase column chromatography yielded the title compound (46 mg, 0.16 mmol, 31%). $^1\text{H NMR}$ (600 MHz, MeOD) δ 4.06 – 3.99 (m, 2H, C-2, C-3), 3.80 (dd, $J = 11.1, 6.7$ Hz, 1H, C-5a), 3.66 (dd, $J = 11.2, 4.4$ Hz, 1H, C-5b), 3.42 (t, $J = 6.4$ Hz, 2H, O-CH₂ pentyl), 3.38 (dd, $J = 10.4, 5.4$ Hz, 1H, C-1a), 3.06 (s, 2H, O-CH₂ neopentyl), 2.85 – 2.79 (m, 1H, N-CHH pentyl), 2.79 – 2.76 (m, 1H, C-4), 2.40 – 2.33 (m, 1H, N-CHH pentyl), 2.25 (dd, $J = 10.4, 5.1$ Hz, 1H, C-1b), 1.62 – 1.56 (m, 2H, O-CH₂CH₂ pentyl), 1.56 – 1.47 (m, 2H, N-CH₂CH₂ pentyl), 1.44 – 1.32 (m, 2H, N-(CH₂)₂CH₂ pentyl), 0.90 (s, 9H, 3xCH₃ neopentyl). $^{13}\text{C NMR}$ (151 MHz, MeOD) δ 82.4 (O-CH₂ neopentyl), 79.0 (C-3), 77.4 (C-2), 72.4 (O-CH₂ pentyl), 69.0 (C-4), 61.0 (C-5), 59.8 (C-1), 57.3 (N-CH₂ pentyl), 32.9 (C_q neopentyl), 30.6 (O-CH₂CH₂ pentyl), 28.8 (N-CH₂CH₂ pentyl), 27.2 (3xCH₃ neopentyl), 25.3 (N-(CH₂)₂CH₂ pentyl). $[\alpha]_{\text{D}}^{20} = -48.9^\circ$ ($c = 0.9$, MeOH). HR-MS: $[\text{M}+\text{H}^+]$ Calculated for C₁₅H₃₁NO₄: 290.23258; found: 290.23295.

1,4-Dideoxy-1,4-(*N*-(5-(adamantane-1-yl-methoxy)pentyl))imino-D-xylitol (3G). 1,4-Dideoxy-1,4-imino-D-xylitol hydrochloride (**3A**, 85 mg, 0.50 mmol) was alkylated with 5-bromo-1-(adamantane-1-yl-methoxy)pentane (236 mg, 0.75 mmol) in *General procedure B*. Silica gel column chromatography, HPLC purification (33-38% A/B in 9.5 minutes) and reversed phase column chromatography yielded the title compound (66 mg, 0.18 mmol, 36%). $^1\text{H NMR}$ (600 MHz, MeOD) δ 4.09 – 3.99 (m, 2H, C-2, C-3), 3.81 (dd, $J = 11.1, 6.7$ Hz, 1H, C-5a), 3.66 (dd, $J = 11.2, 4.4$ Hz, 1H, C-5b), 3.41 – 3.36 (m, 3H, C-1a, O-CH₂ pentyl), 2.97 (s, 2H, O-CH₂ adamantanemethyl), 2.87 – 2.81 (m, 1H, N-CHH pentyl), 2.81 – 2.76 (m, 1H, C-4), 2.40 – 2.34 (m, 1H, N-CHH pentyl), 2.26 (dd, $J = 10.4, 5.0$ Hz, 1H, C-1b), 1.95 (s, 3H, CH adamantanemethyl), 1.80 – 1.64 (m, 6H, 3xC_qCH₂ adamantanemethyl), 1.62 – 1.48 (m, 10H, N-CH₂CH₂ pentyl, O-CH₂CH₂ pentyl, 3xCHCH₂ adamantanemethyl), 1.42 – 1.31 (m, 2H, N-(CH₂)₂CH₂ pentyl). $^{13}\text{C NMR}$ (151

MHz, MeOD) δ 83.0 (O-CH₂ adamantanemethyl), 79.0 (C-3), 77.4 (C-2), 72.5 (O-CH₂ pentyl), 69.0 (C-4), 61.0 (C-5), 59.8 (C-1), 57.3 (N-CH₂ pentyl), 40.8 (3xC_qCH₂ adamantanemethyl), 38.3 (3xCHCH₂ adamantanemethyl), 35.1 (C_q adamantanemethyl), 30.6 (O-CH₂CH₂ pentyl), 29.7 (3xCH adamantanemethyl), 28.8 (N-CH₂CH₂ pentyl), 25.3 (N-(CH₂)₂CH₂ pentyl). [α]_D²⁰ = -37.2° (c = 1, MeOH). HR-MS: [M+H]⁺ Calculated for C₂₁H₃₇NO₄: 368.27954; found: 368.27963.

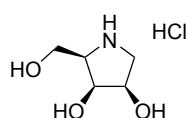
1,4-Dideoxy-1,4-(N-(5-(*p*-phenylbenzyloxy)pentyl))imino-D-xylitol (3H). 1,4-Dideoxy-1,4-imino-D-xylitol



hydrochloride (**3A**, 85 mg, 0.50 mmol) was alkylated with 5-bromo-1-(*p*-phenylbenzyloxy)pentane (250 mg, 0.75 mmol) in *General procedure B*. Silica gel column chromatography, HPLC purification (32-40% A/B in 9 minutes) and reversed phase column chromatography yielded the title compound (69 mg,

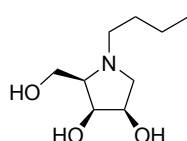
0.18 mmol, 36%). ¹H NMR (600 MHz, MeOD) δ 7.62 – 7.56 (m, 4H, 4xCH_{Ar} Ph), 7.44 – 7.37 (m, 4H, 4xCH_{Ar} Ph), 7.31 (t, *J* = 7.4 Hz, 1H, *p*-CH_{Ar} Ph), 4.51 (s, 2H, O-CH₂ phenylbenzyl), 4.08 – 4.01 (m, 2H, C-2, C-3), 3.81 (dd, *J* = 11.2, 6.6 Hz, 1H, C-5a), 3.68 (dd, *J* = 11.2, 4.5 Hz, 1H, C-5b), 3.49 (t, *J* = 6.5 Hz, 2H, O-CH₂ pentyl), 3.39 (dd, *J* = 10.5, 5.4 Hz, 1H, C-1a), 2.89 – 2.77 (m, 2H, C-4, N-CHH pentyl), 2.42 – 2.34 (m, 1H, N-CHH pentyl), 2.28 (dd, *J* = 10.5, 5.0 Hz, 1H, C-1b), 1.62 (p, *J* = 7.5, 7.0 Hz, 2H, O-CH₂CH₂ pentyl), 1.52 (p, *J* = 7.7 Hz, 2H, N-CH₂CH₂ pentyl), 1.44 – 1.32 (m, 2H, N-(CH₂)₂CH₂ pentyl). ¹³C NMR (151 MHz, MeOD) δ 142.0, 141.7, 138.9 (3xC_q Ph), 129.8, 129.3 (4xCH_{Ar} Ph), 128.3 (*p*-CH_{Ar} Ph), 127.9, 127.9 (4xCH_{Ar} Ph), 78.9 (C-3), 77.3 (C-2), 73.5 (O-CH₂ phenylbenzyl), 71.2 (O-CH₂ pentyl), 69.1 (C-4), 60.9 (C-5), 59.8 (C-1), 57.3 (N-CH₂ pentyl), 30.6 (O-CH₂CH₂ pentyl), 28.7 (N-CH₂CH₂ pentyl), 25.2 (N-(CH₂)₂CH₂ pentyl). [α]_D²⁰ = -48.1° (c = 1, MeOH). HR-MS: [M+H]⁺ Calculated for C₂₁H₃₇NO₄: 386.23258; found: 368.23253.

1,4-Dideoxy-1,4-imino-D-lyxitol hydrochloride (4A). 1,4-Dideoxy-1,4-benzylimino-2,3,5-tri-O-benzyl-D-lyxitol (**3I**,

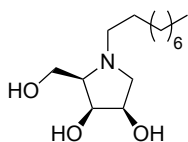


4.0 g, 8.0 mmol) was subjected to *General procedure A* yielding the title compound (1.3 g, 7.8 mmol, 98%). ¹H NMR (600 MHz, MeOD) δ 4.40 (td, *J* = 7.3, 4.0 Hz, 1H, C-2), 4.21 (t, *J* = 4.0 Hz, 1H, C-3), 3.94 (dd, *J* = 11.8, 4.6 Hz, 1H, C-5a), 3.89 (dd, *J* = 11.8, 8.9 Hz, 1H, C-5b), 3.64 (dt, *J* = 8.8, 4.4 Hz, 1H, C-4), 3.42 (dd, *J* = 11.7, 7.3 Hz, 1H, C-1a), 3.14 (dd, *J* = 11.7, 7.3 Hz, 1H, C-1b). ¹³C NMR (151 MHz, MeOD) δ 71.8 (C-2), 71.3 (C-3), 64.5 (C-4), 59.3 (C-5), 48.5 (C-1). [α]_D²⁰ = 23.4° (c = 1, MeOH). IR (neat): 61, 667, 899, 920, 982, 1040, 1115, 1202, 1269, 1287, 1350, 1412, 1460, 1601, 2480, 2583, 2666, 2716, 2733, 2783, 2891, 2930, 2976, 3221, 3404. HR-MS: [M+H]⁺ Calculated for C₅H₁₁NO₃: 134.08117; found: 134.08122.

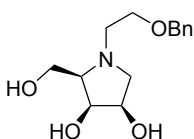
1,4-Dideoxy-1,4-butylimino-D-lyxitol (4B). 1,4-Dideoxy-1,4-imino-D-lyxitol hydrochloride (**4A**, 85 mg, 0.50 mmol)



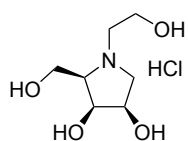
was alkylated with 1-bromobutane (103 mg, 0.75 mmol) in *General procedure B*. Silica gel column chromatography (15-17.5% MeOH/EtOAc), HPLC purification and reversed phase column chromatography yielded the title compound (14 mg, 0.07 mmol, 14%). ¹H NMR (600 MHz, MeOD) δ 4.21 (dd, *J* = 6.6, 5.2 Hz, 1H, C-3), 4.12 (td, *J* = 5.4, 3.5 Hz, 1H, C-2), 3.77 (dd, *J* = 11.1, 5.9 Hz, 1H, C-5a), 3.64 (dd, *J* = 11.1, 3.8 Hz, 1H, C-5b), 3.01 (dd, *J* = 10.7, 3.4 Hz, 1H, C-1a), 2.78 – 2.71 (m, 1H, N-CHH butyl), 2.69 – 2.64 (m, 1H, C-4), 2.53 (dd, *J* = 10.7, 5.7 Hz, 1H, C-1b), 2.37 – 2.30 (m, 1H, N-CHH butyl), 1.48 (p, *J* = 7.8 Hz, 2H, N-CH₂CH₂ butyl), 1.40 – 1.27 (m, 2H, CH₂CH₃ butyl), 0.94 (t, *J* = 7.4 Hz, 3H, CH₃ butyl). ¹³C NMR (151 MHz, MeOD) δ 73.3 (C-3), 71.4 (C-2), 68.8 (C-4), 60.9 (C-5), 59.4 (C-1), 56.8 (N-CH₂ butyl), 31.2 (N-CH₂CH₂ butyl), 21.7 (CH₂CH₃ butyl), 14.4 (CH₃ butyl). [α]_D²⁰ = -74.3° (c = 0.3, MeOH). HR-MS: [M+H]⁺ Calculated for C₉H₁₉NO₃: 190.14377; found: 190.14341.

1,4-Dideoxy-1,4-nonylimino-D-lyxitol (4C). 1,4-Dideoxy-1,4-imino-D-lyxitol hydrochloride (**4A**, 85 mg, 0.50 mmol)

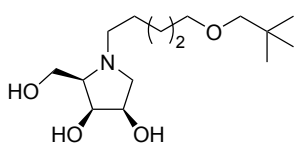
was alkylated with 1-bromononane (155 mg, 0.75 mmol) in *General procedure B*. Silica gel column chromatography (10-12.5% MeOH/EtOAc), HPLC purification (25-30% A/B in 10 minutes) and reversed phase column chromatography yielded the title compound (37 mg, 0.14 mmol, 29%). $^1\text{H NMR}$ (600 MHz, MeOD) δ 4.22 (dd, $J = 6.5, 5.2$ Hz, 1H, C-3), 4.13 (td, $J = 5.4, 3.7$ Hz, 1H, C-2), 3.78 (dd, $J = 11.1, 5.8$ Hz, 1H, C-5a), 3.65 (dd, $J = 11.1, 4.0$ Hz, 1H, C-5b), 3.03 (dd, $J = 10.7, 3.5$ Hz, 1H, C-1a), 2.76 (dt, $J = 11.9, 8.1$ Hz, 1H, N-CHH nonyl), 2.71 – 2.66 (m, 1H, C-4), 2.55 (dd, $J = 10.7, 5.7$ Hz, 1H, C-1b), 2.35 (dt, $J = 11.9, 7.5$ Hz, 1H, N-CHH nonyl), 1.56 – 1.40 (m, 2H, N-CH₂CH₂ nonyl), 1.38 – 1.21 (m, 12H, 6xCH₂ nonyl), 0.90 (t, $J = 7.0$ Hz, 3H, CH₃ nonyl). $^{13}\text{C NMR}$ (151 MHz, MeOD) δ 73.3 (C-3), 71.4 (C-2), 68.9 (C-4), 60.9 (C-5), 59.3 (C-1), 57.1 (N-CH₂ nonyl), 33.1, 30.7, 30.7, 30.4 (4xCH₂ nonyl), 29.0 (N-CH₂CH₂ nonyl), 28.6, 23.7 (2xCH₂ nonyl), 14.5 (CH₃ nonyl). $[\alpha]_{\text{D}}^{20} = -54.6^\circ$ ($c = 0.7$, MeOH). HR-MS: $[\text{M}+\text{H}^+]$ Calculated for C₁₄H₂₉NO₃: 260.22202; found: 260.22193.

1,4-Dideoxy-1,4-(N-(2-benzyloxyethyl))imino-D-lyxitol (4D). 1,4-Dideoxy-1,4-imino-D-lyxitol hydrochloride (**4A**,

85 mg, 0.50 mmol) was alkylated with 2-bromo(benzyloxy)ethane (161 mg, 0.75 mmol) in *General procedure B*. Silica gel column chromatography (10-15% MeOH/EtOAc), HPLC purification (12-16% A/B in 10 minutes) and reversed phase column chromatography yielded the title compound (22 mg, 0.08 mmol, 16%). $^1\text{H NMR}$ (600 MHz, MeOD) δ 7.38 – 7.31 (m, 4H, *o*-CH_{Ar} Ph, *m*-CH_{Ar} Ph), 7.31 – 7.25 (m, 1H, *p*-CH_{Ar} Ph), 4.53 (s, 2H, O-CH₂ Bn), 4.21 (dd, $J = 6.7, 5.0$ Hz, 1H, C-3), 4.14 – 4.09 (m, 1H, C-2), 3.76 (dd, $J = 11.3, 5.2$ Hz, 1H, C-5a), 3.67 (dd, $J = 11.3, 4.2$ Hz, 1H, C-5b), 3.66 – 3.58 (m, 2H, N-CH₂CH₂ ethyl), 3.11 – 3.03 (m, 2H, C-1a, N-CHH ethyl), 2.87 – 2.81 (m, 1H, C-4), 2.74 – 2.67 (m, 2H, C-1b, N-CHH ethyl). $^{13}\text{C NMR}$ (151 MHz, MeOD) δ 139.5 (C_q Bn), 129.4, 129.0 (2x *o*-CH_{Ar} Bn, 2x *m*-CH_{Ar} Bn), 128.7 (*p*-CH_{Ar} Bn), 74.2 (O-CH₂ Bn), 73.3 (C-3), 71.6 (C-2), 69.6 (N-CH₂CH₂ ethyl), 68.8 (C-4), 60.8 (C-5), 59.7 (C-1), 55.9 (N-CH₂ ethyl). $[\alpha]_{\text{D}}^{20} = -25.9^\circ$ ($c = 0.4$, MeOH). HR-MS: $[\text{M}+\text{H}^+]$ Calculated for C₁₄H₂₁NO₄: 268.15433; found: 268.15462.

1,4-Dideoxy-1,4-(N-(2-hydroxyethyl))imino-D-lyxitol hydrochloride (4E). 1,4-Dideoxy-1,4-(N-(2-

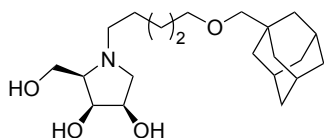
benzyloxyethyl))imino-D-lyxitol (**4D**, 18 mg, 0.07 mmol) was subjected to *General procedure C* yielding the title compound (16 mg, 0.07 mmol, quant.). $^1\text{H NMR}$ (600 MHz, MeOD) δ 4.45 – 4.41 (m, 1H, C-2), 4.41 – 4.36 (m, 1H, C-3), 4.05 (dd, $J = 12.4, 7.6$ Hz, 1H, C-5a), 4.00 (dd, $J = 12.4, 4.3$ Hz, 1H, C-5b), 3.93 – 3.84 (m, 2H, N-CH₂CH₂ ethyl), 3.76 – 3.71 (m, 1H, C-4), 3.68 – 3.62 (m, 1H, N-CHH ethyl), 3.59 (dd, $J = 12.0, 5.2$ Hz, 1H, C-1a), 3.50 (dd, $J = 12.0, 5.7$ Hz, 1H, C-1b), 3.33 – 3.28 (m, 1H, N-CHH ethyl). $^{13}\text{C NMR}$ (151 MHz, MeOD) δ 72.0 (C-4), 71.9 (C-3), 70.7 (C-2), 59.4 (N-CH₂ ethyl), 59.3 (C-5), 58.3 (C-1), 57.7 (N-CH₂CH₂ ethyl). $[\alpha]_{\text{D}}^{20} = -9.4^\circ$ ($c = 0.3$, MeOH). HR-MS: $[\text{M}+\text{H}^+]$ Calculated for C₇H₁₅NO₄: 178.10738; found: 178.10777.

1,4-Dideoxy-1,4-(N-(5-neopentoxypentyl))imino-D-lyxitol (4F). 1,4-Dideoxy-1,4-imino-D-lyxitol hydrochloride

(**4A**, 85 mg, 0.50 mmol) was alkylated with 5-bromo-1-neopentoxypentane (178 mg, 0.75 mmol) in *General procedure B*. Silica gel column chromatography (12.5-15% MeOH/EtOAc), HPLC purification (21-24% A/B in 10 minutes) and reversed phase column chromatography yielded the title compound (33 mg, 0.11 mmol, 22%). $^1\text{H NMR}$ (600 MHz, MeOD) δ 4.22 (dd, $J = 6.5, 5.2$ Hz, 1H, C-3), 4.13 (td, $J = 5.4, 3.6$ Hz, 1H, C-2), 3.78 (dd, $J = 11.1, 5.8$ Hz, 1H, C-5a), 3.66 (dd, $J = 11.1, 4.0$ Hz, 1H, C-5b), 3.42 (t, $J = 6.4$ Hz, 2H, O-CH₂ pentyl), 3.06 (s, 2H, O-CH₂ neopentyl), 3.03 (dd, $J = 10.7, 3.4$ Hz, 1H, C-1a), 2.81 – 2.75 (m, 1H, N-CHH pentyl), 2.73 – 2.67 (m, 1H, C-4), 2.56 (dd, $J = 10.7, 5.7$ Hz, 1H, C-1b), 2.40 – 2.34 (m, 1H, N-CHH pentyl), 1.59 (p, $J = 6.9$ Hz, 2H, O-CH₂CH₂ pentyl), 1.53 (p, $J = 8.0$ Hz, 2H, N-CH₂CH₂ pentyl), 1.45 – 1.30 (m, 2H, N-(CH₂)₂CH₂ pentyl), 0.90 (s, 9H, 3xCH₃ neopentyl). $^{13}\text{C NMR}$ (151 MHz, MeOD) δ 82.4 (O-CH₂ neopentyl), 73.3 (C-3), 72.4 (O-CH₂ pentyl), 71.4 (C-2), 68.9 (C-4), 60.8 (C-5), 59.3 (C-1), 57.1 (N-CH₂ pentyl), 32.9

(C_q neopentyl), 30.6 (O-CH₂CH₂ pentyl), 28.8 (N-CH₂CH₂ pentyl), 27.2 (3xCH₃ neopentyl), 25.2 (N-(CH₂)₂CH₂ pentyl). [α]²⁰_D = -47.6° (c = 0.7, MeOH). HR-MS: [M+H⁺] Calculated for C₁₅H₃₁NO₄: 290.23258; found: 290.23286.

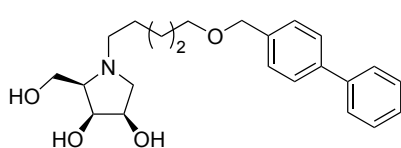
1,4-Dideoxy-1,4-(N-(5-(adamantane-1-yl-methoxy)pentyl))imino-D-lyxitol (4G).



hydrochloride (**4A**, 85 mg, 0.50 mmol) was alkylated with 5-bromo-1-(adamantane-1-yl-methoxy)pentane (236 mg, 0.75 mmol) in *General procedure B*. Silica gel column chromatography (12.5-15% MeOH/EtOAc), HPLC purification (32-37% A/B in 10 minutes) and reversed phase column chromatography yielded the title compound (22

mg, 0.06 mmol, 12%). ¹H NMR (600 MHz, MeOD) δ 4.23 (dd, *J* = 6.4, 5.1 Hz, 1H, C-3), 4.16 – 4.12 (m, 1H, C-2), 3.79 (dd, *J* = 11.2, 5.7 Hz, 1H, C-5a), 3.69 (dd, *J* = 11.2, 4.2 Hz, 1H, C-5b), 3.39 (t, *J* = 6.4 Hz, 2H, O-CH₂ pentyl), 3.06 (dd, *J* = 10.7, 3.5 Hz, 1H, C-1a), 2.97 (s, 2H, O-CH₂ neopentyl), 2.87 – 2.78 (m, 1H, N-CHH pentyl), 2.79 – 2.73 (m, 1H, C-4), 2.62 (dd, *J* = 10.7, 5.7 Hz, 1H, C-1b), 2.46 – 2.38 (m, 1H, N-CHH pentyl), 1.97 – 1.92 (m, 3H, 3xC_H adamantanemethyl), 1.79 – 1.65 (m, 6H, 3xCHCH₂ adamantanemethyl), 1.63 – 1.49 (m, 10H, 3xC_qCH₂ adamantanemethyl, O-CH₂CH₂ pentyl, N-CH₂CH₂ pentyl), 1.44 – 1.28 (m, 2H, N-(CH₂)₂CH₂ pentyl). ¹³C NMR (151 MHz, MeOD) δ 83.1 (O-CH₂ adamantanemethyl), 73.2 (C-3), 72.5 (O-CH₂ pentyl), 71.4 (C-2), 69.1 (C-4), 60.8 (C-5), 59.2 (C-1), 57.1 (N-CH₂ pentyl), 40.8 (3xC_qCH₂ adamantanemethyl), 38.3 (3xCHCH₂ adamantanemethyl), 35.2 (C_q adamantanemethyl), 30.5 (O-CH₂CH₂ pentyl), 29.8 (3xCH adamantanemethyl), 28.6 (N-CH₂CH₂ pentyl), 25.2 (N-(CH₂)₂CH₂ pentyl). [α]²⁰_D = -32.3° (c = 0.4, MeOH). HR-MS: [M+H⁺] Calculated for C₂₁H₃₇NO₄: 368.27954; found: 368.27956.

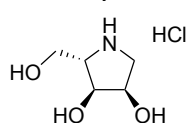
1,4-Dideoxy-1,4-(N-(5-(*p*-phenylbenzyloxy)pentyl))imino-D-lyxitol (4H).



hydrochloride (**4A**, 85 mg, 0.50 mmol) was alkylated with 5-bromo-1-(*p*-phenylbenzyloxy)pentane (250 mg, 0.75 mmol) in *General procedure B*. Silica gel column chromatography (12.5-15% MeOH/EtOAc), HPLC purification (31-38% A/B in 10 minutes) and reversed phase column chromatography yielded

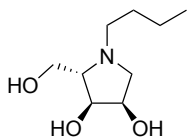
the title compound (32 mg, 0.08 mmol, 16%). ¹H NMR (600 MHz, MeOD) δ 7.65 – 7.56 (m, 4H, 4xCH_{Ar} Ph), 7.44 – 7.38 (m, 4H, 4xCH_{Ar} Ph), 7.35 – 7.29 (m, 1H, *p*-CH_{Ar} Ph), 4.53 (s, 2H, O-CH₂ phenylbenzyl), 4.24 (dd, *J* = 6.2, 4.9 Hz, 1H, C-3), 4.21 – 4.15 (m, 1H, C-2), 3.83 (dd, *J* = 11.5, 5.3 Hz, 1H, C-5a), 3.76 (dd, *J* = 11.5, 5.2 Hz, 1H, C-5b), 3.52 (t, *J* = 6.4 Hz, 2H, O-CH₂ pentyl), 3.14 (dd, *J* = 11.0, 3.8 Hz, 1H, C-1a), 3.01 – 2.88 (m, 2H, C-4, N-CHH pentyl), 2.74 (dd, *J* = 10.5, 5.5 Hz, 1H, C-1b), 2.60 – 2.50 (m, 1H, N-CHH pentyl), 1.64 (p, *J* = 6.9 Hz, 2H, O-CH₂CH₂ pentyl), 1.61 – 1.53 (m, 3H, N-CH₂CH₂ pentyl), 1.47 – 1.36 (m, 2H, N-(CH₂)₂CH₂ pentyl). ¹³C NMR (151 MHz, MeOD) δ 142.1, 141.8, 138.9 (3xC_q Ph), 129.9, 129.4 (4xCH_{Ar} Ph), 128.3 (*p*-CH_{Ar} Ph), 127.9, 127.9 (CH_{Ar} Ph), 73.5 (O-CH₂ phenylbenzyl), 72.9 (C-3), 71.2 (C-2), 71.2 (O-CH₂ pentyl), 69.7 (C-4), 60.5 (C-5), 58.7 (C-1), 57.2 (N-CH₂ pentyl), 30.4 (O-CH₂CH₂ pentyl), 27.9 (N-CH₂CH₂ pentyl), 25.0 (N-(CH₂)₂CH₂ pentyl). [α]²⁰_D = -25° (c = 0.6, MeOH). HR-MS: [M+H⁺] Calculated for C₂₁H₃₇NO₄: 386.23258; found: 368.23260.

1,4-Dideoxy-1,4-imino-L-ribitol hydrochloride (5A).

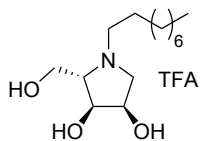


4.0 g, 8.0 mmol) was subjected to *General procedure A* yielding the title compound (1.4 g, 7.8 mmol, quant.). [α]²⁰_D = -61.2° (c = 1, MeOH). Analytical data was the same as for its enantiomer (**1A**).

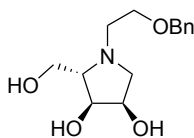
1,4-Dideoxy-1,4-butylimino-L-ribitol (5B). 1,4-Dideoxy-1,4-imino-L-ribitol hydrochloride (**5A**, 85 mg, 0.50 mmol) was alkylated with 1-bromobutane (103 mg, 0.75 mmol) in *General procedure B*. Silica gel column chromatography (12.5-15% MeOH/EtOAc), HPLC purification and reversed phase column chromatography yielded the title compound (12 mg, 0.06 mmol, 12%). $[\alpha]_D^{20} = 14.2^\circ$ ($c = 0.2$, MeOH). Analytical data was the same as for its enantiomer (**1B**).



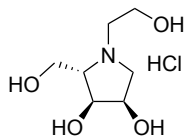
1,4-Dideoxy-1,4-nonylimino-L-ribitol trifluoroacetic acid (5C). 1,4-Dideoxy-1,4-imino-L-ribitol hydrochloride (**5A**, 85 mg, 0.50 mmol) was alkylated with 1-bromononane (155 mg, 0.75 mmol) in *General procedure B*. Silica gel column chromatography (10-15% MeOH/EtOAc) and HPLC purification (25-42% A/B in 8.5 minutes) yielded the title compound (111 mg, 0.30 mmol, 59%). $^1\text{H NMR}$ (600 MHz, MeOD) δ 4.27 – 4.23 (m, 1H, C-2), 4.08 (dd, $J = 7.8, 4.2$ Hz, 1H, C-3), 3.96 (dd, $J = 12.3, 3.3$ Hz, 1H, C-5a), 3.82 (dd, $J = 12.3, 5.3$ Hz, 1H, C-5b), 3.68 (dd, $J = 12.6, 4.6$ Hz, 1H, C-1a), 3.51 – 3.48 (m, 1H, C-4), 3.48 – 3.42 (m, 1H, N-CHH nonyl), 3.25 (dd, $J = 12.6, 3.2$ Hz, 1H, C-1b), 3.23 – 3.16 (m, 1H, N-CH nonyl), 1.78 – 1.69 (m, 2H, N-CH₂CH₂ nonyl), 1.41 – 1.26 (m, 12H, 6xCH₂ nonyl), 0.90 (t, $J = 7.1$ Hz, 3H, CH₃ nonyl). $^{13}\text{C NMR}$ (151 MHz, MeOD) δ 72.7 (C-4), 72.7 (C-3), 70.5 (C-2), 59.5 (N-CH₂ nonyl), 59.0 (C-1), 58.7 (C-5), 33.0, 30.5, 30.3, 30.2, 27.5 (5xCH₂ nonyl), 26.3 (N-CH₂CH₂ nonyl), 23.7 (CH₂ nonyl), 14.4 (CH₃ nonyl). $[\alpha]_D^{20} = -1.6^\circ$ ($c = 1$, MeOH). HR-MS: $[\text{M}+\text{H}^+]$ Calculated for C₁₄H₂₉NO₃: 260.22202; found: 260.22229.



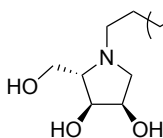
1,4-Dideoxy-1,4-(N-(2-benzyloxyethyl))imino-L-ribitol (5D). 1,4-Dideoxy-1,4-imino-L-ribitol hydrochloride (**5A**, 85 mg, 0.50 mmol) was alkylated with 2-bromo(benzyloxy)ethane (161 mg, 0.75 mmol) in *General procedure B*. Silica gel column chromatography (10-15% MeOH/EtOAc), HPLC purification (12-15% A/B in 10 minutes) and reversed phase column chromatography yielded the title compound (36 mg, 0.14 mmol, 27%). $[\alpha]_D^{20} = 16.7^\circ$ ($c = 0.7$, MeOH). Analytical data was the same as for its enantiomer (**1D**).



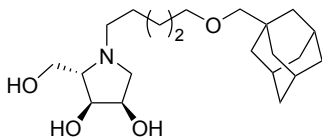
1,4-Dideoxy-1,4-(N-(2-hydroxyethyl))imino-L-ribitol hydrochloride (5E). 1,4-Dideoxy-1,4-(N-(2-benzyloxyethyl))imino-L-ribitol (**5D**, 33 mg, 0.12 mmol) was subjected to *General procedure C* yielding the title compound (30 mg, 0.12 mmol, quant.). $[\alpha]_D^{20} = -16.3^\circ$ ($c = 0.6$, MeOH). Analytical data was the same as for its enantiomer (**1E**).



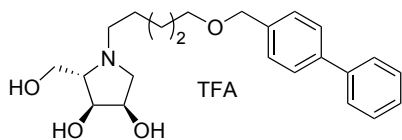
1,4-Dideoxy-1,4-(N-(5-neopentoxypentyl))imino-L-ribitol (5F). 1,4-Dideoxy-1,4-imino-L-ribitol hydrochloride (**5A**, 85 mg, 0.50 mmol) was alkylated with 5-bromo-1-neopentoxypentane (178 mg, 0.75 mmol) in *General procedure B*. Silica gel column chromatography (10-15% MeOH/EtOAc), HPLC purification (21-25% A/B in 9.5 minutes) and reversed phase column chromatography yielded the title compound (39 mg, 0.14 mmol, 27%). $[\alpha]_D^{20} = 21.3^\circ$ ($c = 0.8$, MeOH). Analytical data was the same as for its enantiomer (**1F**).



1,4-Dideoxy-1,4-(N-(5-(adamantane-1-yl-methoxy)pentyl))imino-L-ribitol (5G). 1,4-Dideoxy-1,4-imino-L-ribitol hydrochloride (**5A**, 85 mg, 0.50 mmol) was alkylated with 5-bromo-1-(adamantane-1-yl-methoxy)pentane (236 mg, 0.75 mmol) in *General procedure B*. Silica gel column chromatography (10-15% MeOH/EtOAc), HPLC purification (25-57% A/B in 9 minutes) and reversed phase column chromatography yielded the title compound (67 mg, 0.18 mmol, 36%). $[\alpha]_D^{20} = 18^\circ$ ($c = 1$, MeOH). Analytical data was the same as for its enantiomer (**1G**).



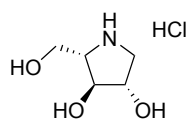
1,4-Dideoxy-1,4-(N-(5-(*p*-phenylbenzyloxy)pentyl))imino-L-ribitol trifluoroacetic acid (5H).



1,4-Dideoxy-1,4-imino-L-ribitol hydrochloride (**5A**, 85 mg, 0.50 mmol) was alkylated with 5-bromo-1-(*p*-phenylbenzyloxy)pentane (250 mg, 0.75 mmol) in *General procedure B*. Silica gel column chromatography (10-15% MeOH/EtOAc) and HPLC purification (31-37% A/B in 10 minutes) yielded the title compound (62 mg,

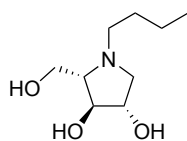
0.12 mmol, 25%). $^1\text{H NMR}$ (600 MHz, MeOD) δ 7.63 – 7.58 (m, 4H, $4\times\text{CH}_{\text{Ar}}$ Ph), 7.45 – 7.39 (m, 4H, $4\times\text{CH}_{\text{Ar}}$ Ph), 7.33 (t, $J = 7.4$ Hz, 1H, $p\text{-CH}_{\text{Ar}}$ Ph), 4.53 (s, 2H, O- CH_2 phenylbenzyl), 4.25 – 4.21 (m, 1H, C-2), 4.10 – 4.05 (m, 1H, C-3), 3.94 (dd, $J = 12.3$, 3.1 Hz, 1H, C-5a), 3.81 (dd, $J = 12.3$, 5.2 Hz, 1H, C-5b), 3.66 (dd, $J = 12.2$, 3.6 Hz, 1H, C-1a), 3.54 (t, $J = 6.2$ Hz, 2H, O- CH_2 pentyl), 3.46 (dd, $J = 20.4$, 9.3 Hz, 2H, C-4, N- CHH pentyl), 3.27 – 3.13 (m, 2H, C-1b, N- CHH pentyl), 1.76 (p, $J = 8.0$ Hz, 2H, O- CH_2CH_2 pentyl), 1.70 – 1.64 (m, 2H, N- CH_2CH_2 pentyl), 1.48 (p, $J = 7.3$, 6.6 Hz, 2H, N-(CH_2) $_2\text{CH}_2$ pentyl). $^{13}\text{C NMR}$ (151 MHz, MeOD) δ 142.0, 141.8, 138.8 ($3\times\text{C}_\alpha$ Ph), 129.9, 129.4 ($4\times\text{CH}_{\text{Ar}}$ Ph), 128.4 ($p\text{-CH}_{\text{Ar}}$ Ph), 127.9, 127.9 ($4\times\text{CH}_{\text{Ar}}$ Ph), 73.6 (O- CH_2 phenylbenzyl), 72.7 (C-4), 72.7 (C-3), 70.9 (O- CH_2 pentyl), 70.4 (C-2), 59.3 (N- CH_2 pentyl), 59.0 (C-1), 58.6 (C-5), 30.1 (O- CH_2CH_2 pentyl), 26.0 (N- CH_2CH_2 pentyl), 24.4 (N-(CH_2) $_2\text{CH}_2$ pentyl). $[\alpha]^{20}_D = -1^\circ$ ($c = 1$, MeOH). HR-MS: $[\text{M}+\text{H}^+]$ Calculated for $\text{C}_{21}\text{H}_{37}\text{NO}_4$: 386.23258; found: 368.23269.

1,4-Dideoxy-1,4-imino-L-arabinitol hydrochloride (6A).



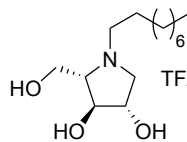
1,4-Dideoxy-1,4-benzylimino-2,3,5-tri-O-benzyl-L-arabinitol (**33**, 3.7 g, 7.5 mmol) was subjected to *General procedure A* yielding the title compound (1.3 g, 7.5 mmol, quant.). $[\alpha]^{20}_D = -38.9^\circ$ ($c = 1$, MeOH). Analytical data was the same as for its enantiomer (**2A**).

1,4-Dideoxy-1,4-butylimino-L-arabinitol (6B).



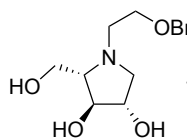
1,4-Dideoxy-1,4-imino-L-arabinitol hydrochloride (**6A**, 85 mg, 0.50 mmol) was alkylated with 1-bromobutane (103 mg, 0.75 mmol) in *General procedure B*. Silica gel column chromatography (12.5-15% MeOH/EtOAc), HPLC purification and reversed phase column chromatography yielded the title compound (43 mg, 0.23 mmol, 45%). $[\alpha]^{20}_D = 10.1^\circ$ ($c = 0.9$, MeOH). Analytical data was the same as for its enantiomer (**2B**).

1,4-Dideoxy-1,4-nonylimino-L-arabinitol trifluoroacetic acid (6C).



1,4-Dideoxy-1,4-imino-L-arabinitol hydrochloride (**6A**, 85 mg, 0.50 mmol) was alkylated with 1-bromononane (155 mg, 0.75 mmol) in *General procedure B*. Silica gel column chromatography (0-15% MeOH/EtOAc) and HPLC purification (25-43% A/B in 9 minutes) yielded the title compound (85 mg, 0.23 mmol, 46%). $^1\text{H NMR}$ (600 MHz, MeOD) δ 4.21 – 4.17 (m, 1H, C-2), 3.96 – 3.94 (m, 1H, C-3), 3.94 – 3.89 (m, 2H, C-5), 3.59 (d, $J = 11.8$ Hz, 1H, C-1a), 3.48 – 3.38 (m, 3H, C-1b, C-4, N- CHH nonyl), 3.17 – 3.09 (m, 1H, N- CHH nonyl), 1.81 – 1.70 (m, 2H, N- CH_2CH_2 nonyl), 1.41 – 1.24 (m, 12H, $6\times\text{CH}_2$ nonyl), 0.90 (t, $J = 7.1$ Hz, 3H, CH_3 nonyl). $^{13}\text{C NMR}$ (151 MHz, MeOD) δ 78.6 (C-4), 77.7 (C-3), 75.8 (C-2), 60.9 (C-5), 60.6 (C-1), 58.9 (N- CH_2 nonyl), 33.0, 30.5, 30.3, 30.2, 27.7 ($5\times\text{CH}_2$ nonyl), 26.3 (N- CH_2CH_2 nonyl), 23.7 (CH_2 nonyl), 14.4 (CH_3 nonyl). $[\alpha]^{20}_D = 0^\circ$ ($c = 1$, MeOH). HR-MS: $[\text{M}+\text{H}^+]$ Calculated for $\text{C}_{14}\text{H}_{29}\text{NO}_3$: 260.22202; found: 260.22206.

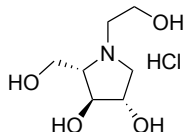
1,4-Dideoxy-1,4-(N-(2-benzyloxyethyl))imino-L-arabinitol trifluoroacetic acid (6D).



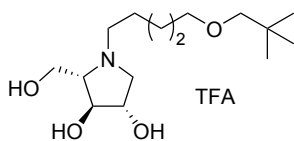
1,4-Dideoxy-1,4-imino-L-arabinitol hydrochloride (**6A**, 85 mg, 0.50 mmol) was alkylated with 2-bromo(benzyloxy)ethane (161 mg, 0.75 mmol) in *General procedure B*. Silica gel column chromatography (0-15% MeOH/EtOAc) and HPLC purification (15-23% A/B in 8 minutes) yielded the title compound (49 mg, 0.13 mmol, 25%). $^1\text{H NMR}$ (600 MHz, MeOD) δ 7.40 – 7.34 (m, 4H, $2\times o\text{-CH}_{\text{Ar}}$ Bn, $2\times m\text{-CH}_{\text{Ar}}$ Bn), 7.33 – 7.29 (m, 1H,

p-CH_{Ar} Bn), 4.58 (s, 2H, O-CH₂ Bn), 4.20 – 4.16 (m, 1H, C-2), 3.97 – 3.95 (m, 1H, C-3), 3.95 – 3.91 (m, 2H, C-5), 3.85 (ddd, *J* = 10.3, 7.3, 2.9 Hz, 1H, N-CH₂CHH ethyl), 3.79 (ddd, *J* = 11.6, 6.2, 2.9 Hz, 1H, N-CH₂CHH ethyl), 3.73 (ddd, *J* = 13.4, 6.1, 2.8 Hz, 1H, N-CHH ethyl), 3.64 (d, *J* = 12.0 Hz, 1H, C-1a), 3.59 – 3.52 (m, 2H, C-1b, C-4), 3.45 (ddd, *J* = 13.4, 7.3, 2.7 Hz, 1H, N-CHH ethyl). ¹³C NMR (151 MHz, MeOD) δ 138.7 (C_q Bn), 129.5, 129.2 (2x *o*-CH_{Ar} Bn, 2x *m*-CH_{Ar} Bn), 129.0 (*p*-CH_{Ar} Bn), 78.5 (C-4), 77.6 (C-3), 75.8 (C-2), 74.3 (O-CH₂ Bn), 65.8 (N-CH₂CH₂ ethyl), 61.6 (C-1), 60.7 (C-5), 58.0 (N-CH₂ ethyl). [α]²⁰_D = -10.5° (*c* = 1, MeOH). HR-MS: [M+H]⁺ Calculated for C₁₄H₂₁NO₄: 268.15433; found: 268.15417.

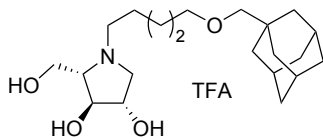
1,4-Dideoxy-1,4-(*N*-(2-hydroxyethyl))imino-L-arabinitol hydrochloride (6E). 1,4-Dideoxy-1,4-(*N*-(2-benzyloxyethyl))imino-L-arabinitol trifluoroacetic acid (**6D**, 29 mg, 0.11 mmol) was subjected to *General procedure C* yielding the title compound (25 mg, 0.11 mmol, quant.). [α]²⁰_D = -10.9° (*c* = 0.5, MeOH). Analytical data was the same as for its enantiomer (**2E**).



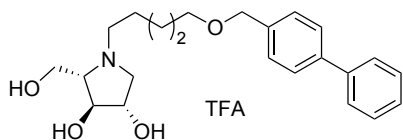
1,4-Dideoxy-1,4-(*N*-(5-neopentoxypentyl))imino-L-arabinitol trifluoroacetic acid (6F). 1,4-Dideoxy-1,4-imino-L-arabinitol hydrochloride (**6A**, 85 mg, 0.50 mmol) was alkylated with 5-bromo-1-neopentoxypentane (178 mg, 0.75 mmol) in *General procedure B*. Silica gel column chromatography and HPLC purification (21-26% A/B in 9.5 minutes) yielded the title compound (92 mg, 0.23 mmol, 45%). ¹H NMR (600 MHz, MeOD) δ 4.21 – 4.17 (m, 1H, C-2), 3.96 – 3.94 (m, 1H, C-3), 3.94 – 3.89 (m, 2H, C-5), 3.59 (d, *J* = 11.8 Hz, 1H, C-1a), 3.50 – 3.39 (m, 5H, C-1b, C-4, O-CH₂ pentyl, N-CHH pentyl), 3.19 – 3.11 (m, 1H, N-CHH pentyl), 3.07 (s, 2H, O-CH₂ neopentyl), 1.82 – 1.75 (m, 2H, N-CH₂CH₂ pentyl), 1.67 – 1.60 (m, 2H, O-CH₂CH₂ pentyl), 1.46 (p, *J* = 7.7 Hz, 2H, N-(CH₂)₂CH₂ pentyl), 0.90 (s, 9H, 3xCH₃ neopentyl). ¹³C NMR (151 MHz, MeOD) δ 82.5 (O-CH₂ neopentyl), 78.6 (C-4), 77.7 (C-3), 75.8 (C-2), 72.0 (O-CH₂ pentyl), 60.9 (C-5), 60.6 (C-1), 58.9 (N-CH₂ pentyl), 32.9 (C_q neopentyl), 30.2 (O-CH₂CH₂ pentyl), 27.1 (3xCH₃ neopentyl), 26.2 (N-CH₂CH₂ pentyl), 24.6 (N-(CH₂)₂CH₂ pentyl). [α]²⁰_D = 0.2° (*c* = 1, MeOH). HR-MS: [M+H]⁺ Calculated for C₁₅H₃₁NO₄: 290.23258; found: 290.23270.



1,4-Dideoxy-1,4-(*N*-(5-(adamantane-1-yl-methoxy)pentyl))imino-L-arabinitol trifluoroacetic acid (6G). 1,4-Dideoxy-1,4-imino-L-arabinitol hydrochloride (**6A**, 85 mg, 0.50 mmol) was alkylated with 5-bromo-1-(adamantane-1-yl-methoxy)pentane (236 mg, 0.75 mmol) in *General procedure B*. Silica gel column chromatography (10-15% MeOH/EtOAc) and HPLC purification (25-60% A/B in 10 minutes) yielded the title compound (87 mg, 0.18 mmol, 36%). ¹H NMR (600 MHz, MeOD) δ 4.22 – 4.17 (m, 1H, C-2), 3.95 (s, 1H, C-3), 3.94 – 3.89 (m, 2H, C-5), 3.59 (d, *J* = 11.7 Hz, 1H, C-1a), 3.49 – 3.42 (m, 3H, C-1b, C-4, N-CHH pentyl), 3.40 (t, *J* = 6.2 Hz, 2H, O-CH₂ pentyl), 3.18 – 3.12 (m, 1H, N-CHH pentyl), 2.98 (s, 2H, O-CH₂ adamantanemethyl), 1.98 – 1.91 (m, 3H, 3xCH adamantanemethyl), 1.82 – 1.65 (m, 8H, N-CH₂CH₂ pentyl, 3xCHCH₂ adamantanemethyl), 1.65 – 1.59 (m, 2H, O-CH₂CH₂ pentyl), 1.58 – 1.54 (m, 6H, 3xC_qCH₂ adamantanemethyl), 1.45 (p, *J* = 7.6 Hz, 2H, N-(CH₂)₂CH₂ pentyl). ¹³C NMR (151 MHz, MeOD) δ 83.1 (O-CH₂ adamantanemethyl), 78.6 (C-4), 77.7 (C-3), 75.8 (C-2), 72.0 (O-CH₂ pentyl), 60.9 (C-5), 60.6 (C-1), 58.9 (N-CH₂ pentyl), 40.8 (3xC_qCH₂ adamantanemethyl), 38.3 (3xCHCH₂ adamantanemethyl), 35.1 (C_q adamantanemethyl), 30.1 (O-CH₂CH₂ pentyl), 29.7 (3xCH adamantanemethyl), 26.1 (N-CH₂CH₂ pentyl), 24.6 (N-(CH₂)₂CH₂ pentyl). [α]²⁰_D = 0.6° (*c* = 1, MeOH). HR-MS: [M+H]⁺ Calculated for C₂₁H₃₇NO₄: 368.27954; found: 368.27965.

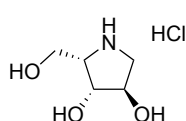


1,4-Dideoxy-1,4-(N-(5-(*p*-phenylbenzyloxy)pentyl))imino-L-arabinitol trifluoroacetic acid (6H). 1,4-Dideoxy-1,4-



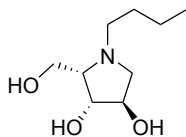
imino-L-arabinitol hydrochloride (**6A**, 85 mg, 0.50 mmol) was alkylated with 5-bromo-1-(*p*-phenylbenzyloxy)pentane (250 mg, 0.75 mmol) in *General procedure B*. Silica gel column chromatography (10-15% MeOH/EtOAc) and HPLC purification (28-48% A/B in 9 minutes) yielded the title compound (63 mg, 0.13 mmol, 25%). ¹H NMR (600 MHz, MeOD) δ 7.63 – 7.58 (m, 4H, 4xCH_{Ar} Ph), 7.45 – 7.40 (m, 4H, CH_{Ar} Ph), 7.33 (t, *J* = 7.4 Hz, 1H, *p*-CH_{Ar} Ph), 4.54 (s, 2H, O-CH₂ phenylbenzyl), 4.16 (s, 1H, C-2), 3.94 (s, 1H, C-3), 3.93 – 3.88 (m, 2H, C-5), 3.58 – 3.52 (m, 3H, C-1a, O-CH₂ pentyl), 3.49 – 3.43 (m, 1H, N-CHH pentyl), 3.43 – 3.38 (m, 2H, C-1b, C-4), 3.17 – 3.10 (m, 1H, N-CHH pentyl), 1.82 – 1.74 (m, 2H, N-CH₂CH₂ pentyl), 1.72 – 1.63 (m, 2H, O-CH₂CH₂ pentyl), 1.47 (p, *J* = 7.7 Hz, 2H, N-(CH₂)₂CH₂ pentyl). ¹³C NMR (151 MHz, MeOD) δ 142.0, 141.8, 138.9 (3x_C Ph), 129.9, 129.4 (4xCH_{Ar} Ph), 128.4 (*p*-CH_{Ar} Ph), 127.9, 127.9 (4xCH_{Ar} Ph), 78.6 (C-4), 77.7 (C-3), 75.7 (C-2), 73.6 (O-CH₂ phenylbenzyl), 70.9 (O-CH₂ pentyl), 60.9 (C-5), 60.6 (C-1), 58.8 (N-CH₂ pentyl), 30.1 (O-CH₂CH₂ pentyl), 26.1 (N-CH₂CH₂ pentyl), 24.5 (N-(CH₂)₂CH₂ pentyl). [α]_D²⁰ = 0.2° (c = 1, MeOH). HR-MS: [M+H]⁺ Calculated for C₂₁H₃₇NO₄: 386.23258; found: 368.23271.

1,4-Dideoxy-1,4-imino-L-xylytol hydrochloride (7A). 1,4-Dideoxy-1,4-benzylimino-2,3,5-tri-*O*-benzyl-L-xylytol (**3A**,



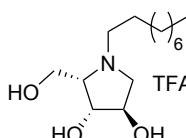
3A, 3.95 g, 8 mmol) was subjected to *General procedure A* yielding the title compound (1.44 g, 8.0 mmol, quant.). [α]_D²⁰ = -17.8° (c = 1, MeOH). Analytical data was the same as for its enantiomer (**3A**).

1,4-dideoxy-1,4-butylimino-L-xylytol (7B). 1,4-Dideoxy-1,4-imino-L-xylytol hydrochloride (**7A**, 85 mg, 0.50 mmol)



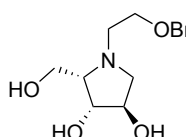
was alkylated with 1-bromobutane (103 mg, 0.75 mmol) in *General procedure B*. Silica gel column chromatography (12.5-17.5% MeOH/EtOAc), HPLC purification and reversed phase column chromatography yielded the title compound (5 mg, 0.03 mmol, 5%). [α]_D²⁰ = 80° (c = 0.1, MeOH). Analytical data was the same as for its enantiomer (**3B**).

1,4-Dideoxy-1,4-nonylimino-L-xylytol trifluoroacetic acid (7C). 1,4-Dideoxy-1,4-imino-L-xylytol hydrochloride (**7A**,



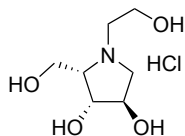
85 mg, 0.50 mmol) was alkylated with 1-bromononane (155 mg, 0.75 mmol) in *General procedure B*. Silica gel column chromatography (10-12.5% MeOH/EtOAc) and HPLC purification (25-43% A/B in 9 minutes) yielded the title compound (68 mg, 0.18 mmol, 36%). ¹H NMR (600 MHz, MeOD) δ 4.23 – 4.18 (m, 2H, C-2, C-3), 4.06 – 3.99 (m, 2H, C-5), 3.84 (dd, *J* = 12.6, 3.8 Hz, 1H, C-1a), 3.76 (td, *J* = 6.9, 3.3 Hz, 1H, C-4), 3.60 – 3.53 (m, 1H, N-CHH pentyl), 3.22 (d, *J* = 12.6 Hz, 1H, C-1b), 3.19 – 3.10 (m, 1H, N-CHH pentyl), 1.81 – 1.70 (m, 2H, N-CH₂CH₂ pentyl), 1.42 – 1.26 (m, 12H, 6xCH₂ pentyl), 0.90 (t, *J* = 7.1 Hz, 3H, CH₃ pentyl). ¹³C NMR (151 MHz, MeOD) δ 76.8 (C-3), 75.6 (C-2), 73.2 (C-4), 60.3 (C-1), 59.7 (N-CH₂ pentyl), 59.1 (C-5), 33.0, 30.4, 30.3, 30.2, 27.6 (5xCH₂ pentyl), 26.5 (N-CH₂CH₂ pentyl), 23.7 (CH₂ pentyl), 14.4 (CH₃ pentyl). [α]_D²⁰ = 22.4° (c = 1, MeOH). HR-MS: [M+H]⁺ Calculated for C₁₄H₂₉NO₃: 260.22202; found: 260.22217.

1,4-Dideoxy-1,4-(N-(2-benzyloxyethyl))imino-L-xylytol (7D). 1,4-Dideoxy-1,4-imino-L-xylytol hydrochloride (**7A**, 85

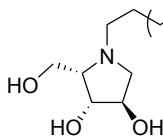


mg, 0.50 mmol) was alkylated with 2-bromo(benzyloxy)ethane (161 mg, 0.75 mmol) in *General procedure B*. Silica gel column chromatography (10-12.5% MeOH/EtOAc), HPLC purification (11.5-20% A/B in 10 minutes) and reversed phase column chromatography yielded the title compound (34 mg, 0.13 mmol, 26%). [α]_D²⁰ = 12.1° (c = 0.7, MeOH). Analytical data was the same as for its enantiomer (**3D**).

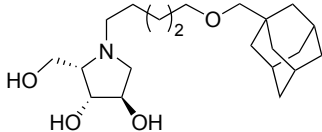
1,4-Dideoxy-1,4-(*N*-(2-hydroxyethyl))imino-L-xylitol hydrochloride (7E). 1,4-Dideoxy-1,4-(*N*-(2-benzyloxyethyl))imino-L-xylitol (**7D**, 31 mg, 0.12 mmol) was subjected to *General procedure C* yielding the title compound (27 mg, 0.12 mmol, quant.). $[\alpha]_D^{20} = 13.2^\circ$ ($c = 0.5$, MeOH). Analytical data was the same as for its enantiomer (**3E**).



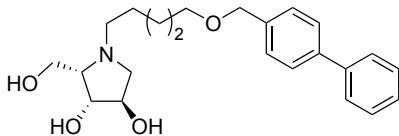
1,4-Dideoxy-1,4-(*N*-(5-neopentoxypentyl))imino-L-xylitol (7F). 1,4-Dideoxy-1,4-imino-L-xylitol hydrochloride (**7A**, 85 mg, 0.50 mmol) was alkylated with 5-bromo-1-neopentylpentane (178 mg, 0.75 mmol) in *General procedure B*. Silica gel column chromatography (12.5-15% MeOH/EtOAc), HPLC purification (22-26% A/B in 10 minutes) and reversed phase column chromatography yielded the title compound (52 mg, 0.18 mmol, 36%). $[\alpha]_D^{20} = 26.7^\circ$ ($c = 1$, MeOH). Analytical data was the same as for its enantiomer (**3F**).



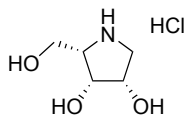
1,4-Dideoxy-1,4-(*N*-(5-(adamantane-1-yl-methoxy)pentyl))imino-L-xylitol (7G). 1,4-Dideoxy-1,4-imino-L-xylitol hydrochloride (**7A**, 85 mg, 0.50 mmol) was alkylated with 5-bromo-1-(adamantane-1-yl-methoxy)pentane (236 mg, 0.75 mmol) in *General procedure B*. Silica gel column chromatography (10-12.5% MeOH/EtOAc), HPLC purification (25-60% A/B in 10 minutes) and reversed phase column chromatography yielded the title compound (73 mg, 0.20 mmol, 40%). $[\alpha]_D^{20} = 25.7^\circ$ ($c = 1$, MeOH). Analytical data was the same as for its enantiomer (**3G**).



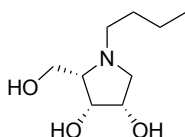
1,4-Dideoxy-1,4-(*N*-(5-(*p*-phenylbenzyloxy)pentyl))imino-L-xylitol (7H). 1,4-Dideoxy-1,4-imino-L-xylitol hydrochloride (**7A**, 85 mg, 0.50 mmol) was alkylated with 5-bromo-1-(*p*-phenylbenzyloxy)pentane (250 mg, 0.75 mmol) in *General procedure B*. Silica gel column chromatography (10-12.5% MeOH/EtOAc), HPLC purification (32-39% A/B in 10 minutes) and reversed phase column chromatography yielded the title compound (72 mg, 0.19 mmol, 38%). $[\alpha]_D^{20} = 16.5^\circ$ ($c = 1$, MeOH). Analytical data was the same as for its enantiomer (**3H**).



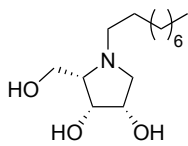
1,4-Dideoxy-1,4-imino-L-lyxitol hydrochloride (8A). 1,4-Dideoxy-1,4-benzylimino-2,3,5-tri-*O*-benzyl-L-lyxitol (**35**, 4.0 g, 8.0 mmol) was subjected to *General procedure A* yielding the title compound (1.37 g, 8.0 mmol, quant.). $[\alpha]_D^{20} = -28.5^\circ$ ($c = 0.9$, MeOH). Analytical data was the same as for its enantiomer (**4A**).



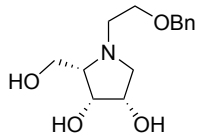
1,4-Dideoxy-1,4-butylimino-L-lyxitol (8B). 1,4-Dideoxy-1,4-imino-L-lyxitol hydrochloride (**8A**, 85 mg, 0.50 mmol) was alkylated with 1-bromobutane (103 mg, 0.75 mmol) in *General procedure B*. Silica gel column chromatography (12.5-17.5% MeOH/EtOAc), HPLC purification and reversed phase column chromatography yielded the title compound (7 mg, 0.04 mmol, 7%). $[\alpha]_D^{20} = 54.3^\circ$ ($c = 0.1$, MeOH). Analytical data was the same as for its enantiomer (**4B**).



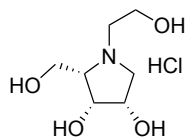
1,4-Dideoxy-1,4-nonylimino-L-lyxitol (8C). 1,4-Dideoxy-1,4-imino-L-lyxitol hydrochloride (**8A**, 85 mg, 0.50 mmol) was alkylated with 1-bromononane (155 mg, 0.75 mmol) in *General procedure B*. Silica gel column chromatography (12.5-17.5% MeOH/EtOAc), HPLC purification (25-30% A/B in 10 minutes) and reversed phase column chromatography yielded the title compound (38 mg, 0.15 mmol, 29%). $[\alpha]_D^{20} = 50.3^\circ$ ($c = 0.8$, MeOH). Analytical data was the same as for its enantiomer (**4C**).



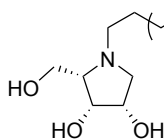
1,4-Dideoxy-1,4-(N-(2-benzyloxyethyl))imino-L-lyxitol (8D). 1,4-Dideoxy-1,4-imino-L-lyxitol hydrochloride (**8A**, 85 mg, 0.50 mmol) was alkylated with 2-bromo(benzyloxy)ethane (161 mg, 0.75 mmol) in *General procedure B*. Silica gel column chromatography (12.5-17.5% MeOH/EtOAc), HPLC purification (12-16% A/B in 10 minutes) and reversed phase column chromatography yielded the title compound (21 mg, 0.08 mmol, 16%). $[\alpha]_D^{20} = 24.8^\circ$ ($c = 0.4$, MeOH). Analytical data was the same as for its enantiomer (**4D**).



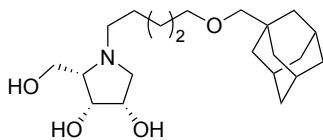
1,4-Dideoxy-1,4-(N-(2-hydroxyethyl))imino-L-lyxitol hydrochloride (8E). 1,4-Dideoxy-1,4-(N-(2-benzyloxyethyl))imino-L-lyxitol (**8D**, 21 mg, 0.08 mmol) was subjected to *General procedure C* yielding the title compound (17 mg, 0.08 mmol, quant.). $[\alpha]_D^{20} = 6.5^\circ$ ($c = 0.3$, MeOH). Analytical data was the same as for its enantiomer (**4E**).



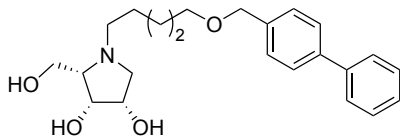
1,4-Dideoxy-1,4-(N-(5-neopentoxypentyl))imino-L-lyxitol (8F). 1,4-Dideoxy-1,4-imino-L-lyxitol hydrochloride (**8A**, 85 mg, 0.50 mmol) was alkylated with 5-bromo-1-neopentoxypentane (178 mg, 0.75 mmol) in *General procedure B*. Silica gel column chromatography (15-17.5% MeOH/EtOAc), HPLC purification (21-24% A/B in 10 minutes) and reversed phase column chromatography yielded the title compound (30 mg, 0.10 mmol, 21%). $[\alpha]_D^{20} = 45^\circ$ ($c = 0.6$, MeOH). Analytical data was the same as for its enantiomer (**4F**).



1,4-Dideoxy-1,4-(N-(5-(adamantane-1-yl-methoxy)pentyl))imino-L-lyxitol (8G). 1,4-Dideoxy-1,4-imino-L-lyxitol hydrochloride (**8A**, 85 mg, 0.50 mmol) was alkylated with 5-bromo-1-(adamantane-1-yl-methoxy)pentane (236 mg, 0.75 mmol) in *General procedure B*. Silica gel column chromatography (15-17.5% MeOH/EtOAc), HPLC purification (34-40% A/B in 10 minutes) and reversed phase column chromatography yielded the title compound (17 mg, 0.05 mmol, 10%). $[\alpha]_D^{20} = 28.2^\circ$ ($c = 0.3$, MeOH). Analytical data was the same as for its enantiomer (**4G**).



1,4-Dideoxy-1,4-(N-(5-(p-phenylbenzyloxy)pentyl))imino-L-lyxitol (8H). 1,4-Dideoxy-1,4-imino-L-lyxitol hydrochloride (**8A**, 85 mg, 0.50 mmol) was alkylated with 5-bromo-1-(p-phenylbenzyloxy)pentane (250 mg, 0.75 mmol) in *General procedure B*. Silica gel column chromatography (15-17.5% MeOH/EtOAc), HPLC purification (31-38% A/B in 10 minutes) and reversed phase column chromatography yielded the title compound (29 mg, 0.08 mmol, 15%). $[\alpha]_D^{20} = 55.2^\circ$ ($c = 0.6$, MeOH). Analytical data was the same as for its enantiomer (**4H**).



References and notes

- [1] Fleet, G. W. J.; Nicholas, S. J.; Smith, P. W.; Evans, S. V.; Fellows, L. E.; Nash, R. J. *Tetrahedron Lett.* **1985**, *26*, 3127-3130, 10.1016/s0040-4039(00)98636-2.
- [2] Liu, K. K. C.; Kajimoto, T.; Chen, L. R.; Zhong, Z. Y.; Ichikawa, Y.; Wong, C. H. *J. Org. Chem.* **1991**, *56*, 6280-6289, 10.1021/jo00022a013.
- [3] Winchester, B.; Aldaher, S.; Carpenter, N. C.; Dibello, I. C.; Choi, S. S.; Fairbanks, A. J.; Fleet, G. W. J. *Biochem. J.* **1993**, *290*, 743-749.
- [4] Kato, A.; Adachi, I.; Miyauchi, M.; Ikeda, K.; Komae, T.; Kizu, H.; Kameda, Y.; Watson, A. A.; Nash, R. J.; Wormald, M. R.; Fleet, G. W. J.; Asano, N. *Carbohydr. Res.* **1999**, *316*, 95-103, 10.1016/s0008-6215(99)00043-9.
- [5] Takebayashi, M.; Hiranuma, S.; Kanie, Y.; Kajimoto, T.; Kanie, O.; Wong, C. H. *J. Org. Chem.* **1999**, *64*, 5280-5291, 10.1021/jo9902446.
- [6] Saotome, C.; Kanie, Y.; Kanie, O.; Wong, C. H. *Bioorg. Med. Chem.* **2000**, *8*, 2249-2261, 10.1016/s0968-0896(00)00170-x.
- [7] Saotome, C.; Wong, C. H.; Kanie, O. *Chem. Biol.* **2001**, *8*, 1061-1070, 10.1016/s1074-5521(01)00074-6.
- [8] Pedersen, L. L.; Turco, S. J. *Cell. Mol. Life Sci.* **2003**, *60*, 259-266, 10.1007/s000180300021.
- [9] Chlubnova, I.; Legentil, L.; Dureau, R.; Pennec, A.; Almendros, M.; Daniellou, R.; Nugier-Chauvin, C.; Ferrieres, V. *Carbohydr. Res.* **2012**, *356*, 44-61, 10.1016/j.carres.2012.04.002.
- [10] Taha, H. A.; Richards, M. R.; Lowary, T. L. *Chem. Rev.* **2013**, *113*, 1851-1876, 10.1021/cr300249c.
- [11] da Cruz, F. P.; Newberry, S.; Jenkinson, S. F.; Wormald, M. R.; Butters, T. D.; Alonzi, D. S.; Nakagawa, S.; Becq, F.; Norez, C.; Nash, R. J.; Kato, A.; Fleet, G. W. J. *Tetrahedron Lett.* **2011**, *52*, 219-223, 10.1015/j.tetlet.2010.10.173.
- [12] Bouillon, M. E.; Pyne, S. G. *Tetrahedron Lett.* **2014**, *55*, 475-478, 10.1016/j.tetlet.2013.11.068.
- [13] Suzuki, K.; Nakahara, T.; Kanie, O. *Curr. Top. Med. Chem.* **2009**, *9*, 34-57, 10.2174/156802609787354315.
- [14] Jenkinson, S. F.; Best, D.; Saville, A. W.; Mui, J.; Martinez, R. F.; Nakagawa, S.; Kunimatsu, T.; Alonzi, D. S.; Butters, T. D.; Norez, C.; Becq, F.; Blieriot, Y.; Wilson, F. X.; Weymouth-Wilson, A. C.; Kato, A.; Fleet, G. W. J. *J. Org. Chem.* **2013**, *78*, 7380-7397, 10.1021/jo4005487.

- [15] Minami, Y.; Kurlyarna, C.; Ikeda, K.; Kato, A.; Takebayashi, K.; Adachi, I.; Fleet, G. W. J.; Kettawan, A.; Karnoto, T.; Asano, N. *Bioorg. Med. Chem.* **2008**, *16*, 2734-2740, 10.1016/j.bmc.2008.01.032.
- [16] Paulsen, H.; Bruning, J.; Propp, K.; Heyns, K. *Tetrahedron Lett.* **1968**, 999-8, 10.1016/s0040-4039(01)98844-6.
- [17] Dangerfield, E. M.; Gulab, S. A.; Plunkett, C. H.; Timmer, M. S. M.; Stocker, B. L. *Carbohydr. Res.* **2010**, *345*, 1360-1365, 10.1016/j.carres.2010.03.016.
- [18] Kim, J. Y.; Mu, Y.; Jin, X.; Park, S. H.; Pham, V. T.; Song, D. K.; Lee, K. Y.; Ham, W. H. *Tetrahedron* **2011**, *67*, 9426-9432, 10.1016/j.tet.2011.09.084.
- [19] Wang, G. N.; Yang, L.; Zhang, L. H.; Ye, X. S. *J. Org. Chem.* **2011**, *76*, 2001-2009, 10.1021/jo1020322.
- [20] Choi, H. G.; Park, D. S.; Lee, W. K.; Sim, T. *Tetrahedron Lett.* **2013**, *54*, 5775-5777, 10.1016/j.tetlet.2013.08.040.
- [21] Stocker, B. L.; Jongkees, S. A. K.; Win-Mason, A. L.; Dangerfield, E. M.; Withers, S. G.; Timmer, M. S. M. *Carbohydr. Res.* **2013**, *367*, 29-32, 10.1016/j.carres.2012.11.011.
- [22] Ansari, A. A.; Vankar, Y. D. *RSC Adv.* **2014**, *4*, 12555-12567, 10.1039/c3ra47555g.
- [23] Chirke, S. S.; Rajender, A.; Rao, B. V. *Tetrahedron* **2014**, *70*, 103-109, 10.1016/j.tet.2013.11.004.
- [24] Wennekes, T.; van den Berg, R. J. B. H. N.; Donker, W.; van der Marel, G. A.; Donker, W.; van der Marel, G. A.; Strijland, A.; Aerts, J. M. F. G.; Overkleeft, H. S. *J. Org. Chem.* **2007**, *72*, 1088-1097, 10.1021/jo061280p.
- [25] Ghisaidoobe, A.; Bikker, P.; de Bruijn, A. C. J.; Godschalk, F. D.; Rogaar, E.; Guijt, M. C.; Hagens, P.; Halma, J. M.; van't Hart, S. M.; Luitjens, S. B.; van Rixel, V. H. S.; Wijzenbroek, M.; Zweegers, T.; Donker-Koopman, W. E.; Strijland, A.; Boot, R.; van der Marel, G.; Overkleeft, H. S.; Aerts, J. M. F. G.; van den Berg, R. J. B. H. N. *ACS Med. Chem. Lett.* **2011**, *2*, 119-123, 10.1021/ml100192b.
- [26] Ghisaidoobe, A. T.; van den Berg, R. J. B. H. N.; Butt, S. S.; Strijland, A.; Donker-Koopman, W. E.; Scheij, S.; van den Nieuwendijk, A. M. C. H.; Koomen, G.-J.; van Loevezijn, A.; Leemhuis, M.; Wennekes, T.; van der Stelt, M.; van der Marel, G. A.; van Boeckel, C. A. A.; Aerts, J. M. F. G.; Overkleeft, H. S. *J. Med. Chem.* **2014**, 10.1021/jm501181z.
- [27] Ayers, B.; Long, H.; Sim, E.; Smellie, I. A.; Wilkinson, B. L.; Fairbanks, A. J. *Carbohydr. Res.* **2009**, *344*, 739-746, 10.1016/j.carres.2009.02.006.
- [28] Behr, J. B.; Guillerme, G. *Tetrahedron Asymm.* **2002**, *13*, 111-113, 10.1016/s0957-4166(02)00081-2.

- [29] Postema, M. H. D.; Calimente, D.; Liu, L.; Behrmann, T. L. *J. Org. Chem.* **2000**, *65*, 6061-6068, 10.1021/jo0005159.
- [30] Wennekes, T.; Bongers, K. M.; Vogel, K.; van den Berg, R. J. B. H. N.; Strijland, A.; Donker-Koopman, W. E.; Aerts, J. M. F. G.; van der Marel, G. A.; Overkleeft, H. S. *Eur. J. Org. Chem.* **2012**, 6420-6454, 10.1002/ejoc.201200923.
- [31] Guo, L. N.; Liu, Y. H.; Wan, Y.; Wang, P. G.; Zhao, W. *Tetrahedron Lett.* **2013**, *54*, 2579-2582, 10.1016/j.tetlet.2013.02.115.

Chapter 6

Stereoelectronic substituent effects determine the conformational preferences of mannuronic acid based iminosugar cations

6.1 Introduction

Stereoelectronic effects of substituents on a cyclic compound have a profound effect on its three-dimensional structure. Where substituents on a cyclic compound generally have a preference for an (pseudo)-equatorial position for steric reasons, the electronic spatial preferences depend on different forces such as charge-charge and dipole-dipole interactions.¹ The conformation and reactivity of carbohydrates is determined to a large

extent by the nature and orientation of the substituents. This influence becomes apparent in glycosylation reactions, where the amount, nature and orientation of the hydroxyl groups, protected with electron withdrawing esters or more electron neutral ether groups, determine the overall reactivity.²⁻⁴ It has long been known that in glycosylations axial substituents are less deactivating or “disarming” than their equatorially positioned equivalents.⁵⁻⁹ Similarly, the basicity of iminosugars (or “azasugars”), carbohydrates of which the endocyclic oxygen is replaced by an amine, is influenced by the orientation of the ring substituents and azasugars bearing more axially positioned hydroxyl groups are more basic than their stereoisomers bearing equatorially positioned substituents.¹⁰⁻¹³ These effects can be explained by the interaction of the electronegative oxygen substituents with the positive charge present on the azasugar ring in a protonated state and the (partial) positive charge of oxocarbenium ion (-like) intermediates in glycosylation reactions. Two explanations can be forwarded to account for the more favorable interaction of axially positioned oxygen substituents with the positive charge in the carbohydrate and azasugar rings. Firstly, the interaction of the dipole moment associated with the ring substituent and the positive charge is less unfavorable if the substituent is positioned axially.^{10,12-13} Secondly, properly positioned oxygen substituents can donate electron density into the electron-depleted carbocations.¹⁴⁻¹⁶

Insightful studies of the Woerpel laboratory, involving a series of addition reactions onto mono-substituted five and six-membered oxocarbenium ions, have shown that electronegative substituents at the C3 position in furanosides and at the C3 and C4 position in pyranosides, prefer to adopt a pseudoaxial orientation in an oxocarbenium ion, thereby determining which envelope (the ³E or E₃) or half chair (the ³H₄ or ⁴H₃) is energetically more favorable.^{1,14-20} In Chapter 2 a free energy surface (FES) scanning method was introduced to determine the energies of all possible conformers of fully substituted furanosyl oxocarbenium ions. The calculations described in this work corroborated the axial preference for the furanosyl ring C3 substituent, determined experimentally by the Woerpel laboratory, and also provided detailed insight into the overall effect of the full decoration of the furanosyl rings.

In glycuronic acids, pyranosides having a C5 carboxylic acid appendage, the electron withdrawing carboxylic acid functionality also has a profound effect on the reactivity of the pyranoside, making glycuronic acids generally less reactive than their “non-oxidized” counterparts.²¹⁻²² In studies towards the glycosylation properties of mannuronic acids it has been noted that mannuronic acid derived glycosyl donors display an unusual high reactivity.²³⁻²⁵ In addition, glycosylation reactions of mannuronic acid donors proceed with a striking stereoselectivity to provide the 1,2-*cis*-linked products.^{22-24,26-28} To account for these results it has been postulated that the ³H₄ oxocarbenium ion plays a decisive role. In

this oxocarbenium ion conformer the C3 and C4 oxygen substituents take up their preferred axial orientation, where the C2 oxygen atom is placed equatorially to allow for a hyperconjugative stabilization of the neighboring oxocarbenium ion. Importantly, the C5 carboxylic acid is placed in an axial position in this half chair, an orientation that is energetically significantly favored over the alternative equatorial position.^{25,27} Thus, all ring substituents can adopt an energetically most favorable orientation in the 3H_4 half chair oxocarbenium ion, making this species relatively favorable. It has also been observed that various manuronic acid donors are inclined to undergo a conformational flip towards the “axially rich” 1C_4 chair and this unusual conformational behavior has been rationalized by linking their structural preference to that of the manuronic acid oxocarbenium ion.²⁸

Because of the parallel between glycosyl donor reactivity, conformational behavior and azasugar basicity the properties of manuronic acid based azasugars are studied in this chapter. Bols and co-workers have previously described a great variety of azasugars and related their basicity to the amount of axially oriented substituents.^{12-13,29} They also noted that in specific cases azasugar rings flip their conformation to position the substituents such that their electron withdrawing effect is minimized.¹² Here the conformational behavior of a set of manuronic acid based azasugars is described as studied by NMR spectroscopy and through DFT calculations (Figure 6.1). It is shown that the conformational flexibility displayed by (fully protected) manuronic acid glycosyl donors (in apolar solvents) extends to manuronic acid azasugars in very polar solvents (H_2O).

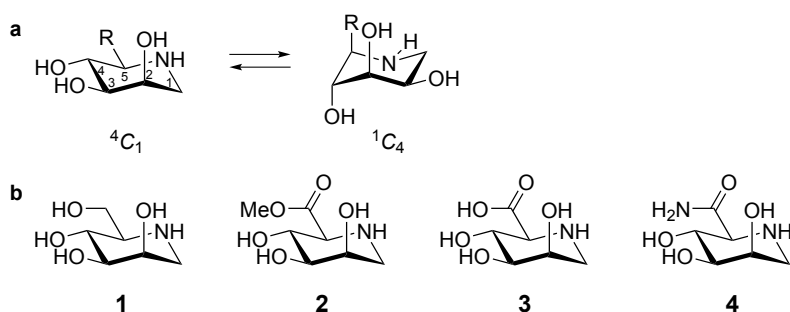
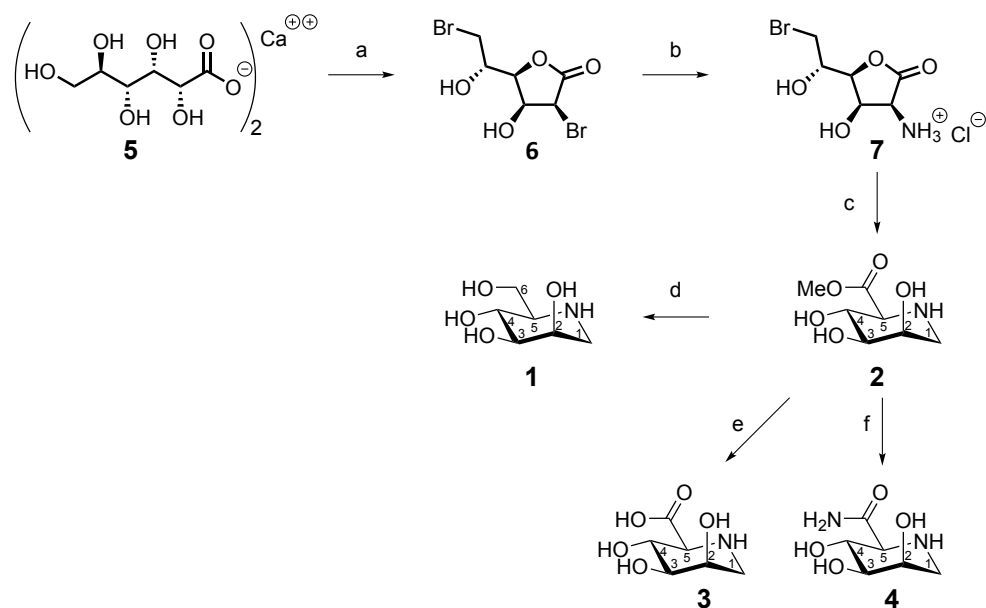


Figure 6.1 a) The 4C_1 and 1C_4 chair conformations. b) The investigated iminosugars, DMJ (**1**), DMJ methyl ester (**2**), DMJ acid (**3**), DMJ amide (**4**).

6.2 Results and discussion

The four azasugars investigated here are depicted in Figure 6.1 and they include the mannuronic acid ester azasugar **2**, the free acid **3** and amide **4** and the “reduced” counterpart, 1-deoxymannojirimicin **1** (DMJ) for comparison. The synthesis of DMJ **1** and its C5 analogs was achieved according to the route devised by Wrodnigg and co-workers.³⁰ As depicted in Scheme 6.1, methyl 2,6-dideoxy-2,6-imino-D-mannonate (**2**) was obtained in four steps from the commercially available calcium D-gluconate monohydrate (**5**).³¹ Acid **5** was treated with HBr in acetic acid to form 3,5-di-O-acetyl-2,6-dideoxy-2,6-dibromo-D-manno-1,4-lactone after a series of acid catalyzed transformations (*i.e.* substitution of the C2 and C6 hydroxyl groups, intramolecular ring closure and acetylation of the remaining hydroxyl groups). Next the acetyl groups at O3 and O5 were removed in an acid catalyzed transesterification with methanol to provide the pure dibromolactone **6** after crystallization from chloroform/water in 26% yield over the two steps. Regioselective displacement of the C2-bromide with an azide occurred with retention of configuration, which Bock et al.³² proposed to originate from epimerization of the C2-bromide to the higher reactive glucose configuration before introduction of the azide. This reaction gave, after palladium catalyzed reduction of the intermediate azide and subsequent crystallization from ethanol, the 2-amino-6-bromo-lactone (**7**) as its hydrochloric acid salt in 55%. Treatment of the salt with triethylamine in methanol led to ring opening and intramolecular bromide displacement by the C2 amine to give methyl ester **2**. Purification of this compound from the triethylammonium and sodium salts formed in the reaction proved difficult, because of the high polarity of the compound as well as the lability of the methyl ester towards hydrolysis. Attempts to crystallize the compound were to no avail. Therefore, all hydroxyl groups in **2** were capped with trimethylsilyl groups³³ to allow for the purification of the compound by chromatography. After desilylation, the pure methyl ester (**2**) was obtained as its hydrochloric acid salt. DMJ (**1**) was synthesized from **2** by a sodium borohydride mediated reduction and was obtained in 29% yield after column chromatography. D-Mannonic acid **3** and amide **4** were obtained from **2** through saponification with sodium hydroxide or aminolysis with methanolic ammonia respectively.

Scheme 6.1 Synthesis of DMJ and its C5 analogs for this study.

Reagents and conditions: (a) i) HBr, AcOH; ii) MeOH, 26% over 2 steps; (b) i) NaN_3 , acetone; ii) H_2 , Pd/C, HCl (aq.), MeOH, 55% over 2 steps; (c) Et_3N , MeOH, quant.; (d) NaBH_4 , EtOH, 29%; (e) NaOH, H_2O , quant.; (f) NH_3 , MeOH, quant.

The conformational behavior at different pH^* (the pH measured in D_2O) values of the set of azasugars was investigated by NMR spectroscopy.³⁴ In Figure 6.2, the ^1H NMR spectra of DMJ (**1**) in D_2O at pH^* 1-12 are shown. From pH^* 1 to pH^* 6.5 no changes are observed in either chemical shifts or coupling constants. The coupling constants are indicative of a “normal” $^4\text{C}_1$ chair conformation for the azasugar ring. Going from pH^* 6.5 to pH^* 12 a significant shift in chemical shift is observed for all ring protons, with the direct neighbors of the amino group experiencing the largest shift. No changes occur in the coupling constants of the ring protons, indicating that no major conformation change takes place.

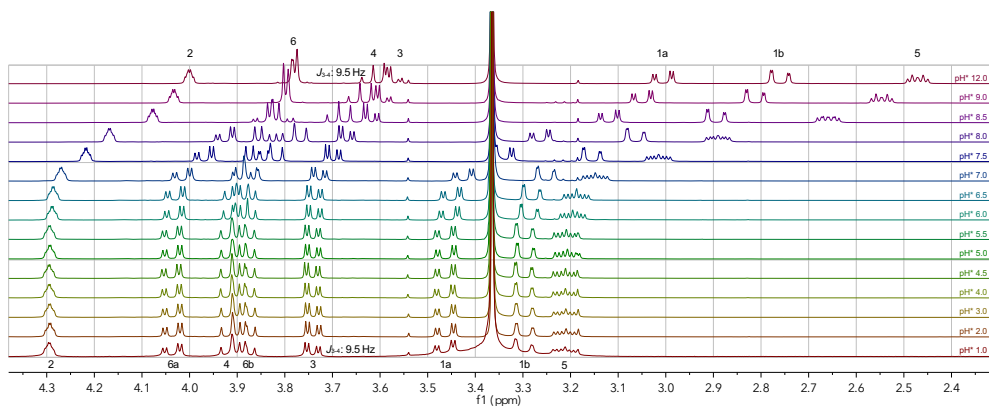


Figure 6.2 ^1H NMR spectra for DMJ (**1**) under different pH^* ; spectra are referenced to residual methanol, intensities are aligned to H2.

In Figure 6.3, the ^1H NMR spectra of methyl ester **2** at different pH^* values are displayed. Because hydrolysis of the methyl ester was observed above pH^* 8, no spectra were recorded above this pH^* . Large chemical shift changes are seen with increasing pH^* . Especially H5 undergoes a large chemical shift change and shifts from $\delta = 4.04$ at pH^* 2 to 3.22 at pH^* 8. Also a change in coupling constants is observed for the ring protons. For example, the $J_{3,4}$ changes from 9.4 Hz at basic pH^* to 7.5 Hz at acidic pH^* , indicative of a change in conformation of the azasugar ring. At high pH^* the azasugar adopts a single conformation, where both the $^1\text{C}_4$ and $^4\text{C}_1$ conformers are present at low pH^* (*vide infra*).

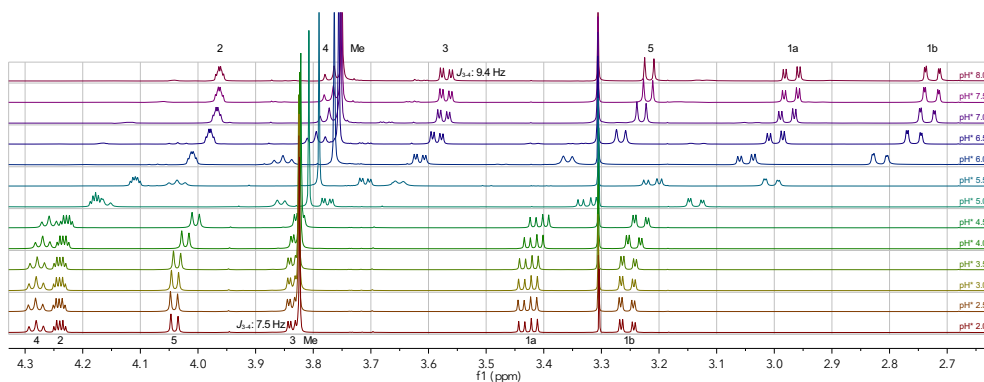


Figure 6.3 ^1H NMR spectra for 2,6-dideoxy-2,6-imino-mannonic acid methyl ester (**2**) under different pH^* ; spectra are referenced to residual methanol, intensities are aligned to the methyl ester.

Mannonic acid **3** can occur in three different charged states: the fully protonated state, the neutral zwitterionic state and the negatively charged state. In Figure 6.4, the ^1H NMR spectra of **3** are shown from pH^* 1 to pH^* 12. Again large chemical shift changes are observed (especially for H5 shifting from 3.9 to 2.9 ppm). Also a small change in coupling constants is apparent. The $J_{3,4}$ changes from 9.8 at high pH^* to 8.8 Hz at neutral pH^* to 8.3

Hz at acidic pH*. In line with the conformational behavior of methyl ester **2**, mannuronic acid **3** can change its conformation in a pH-dependent manner.

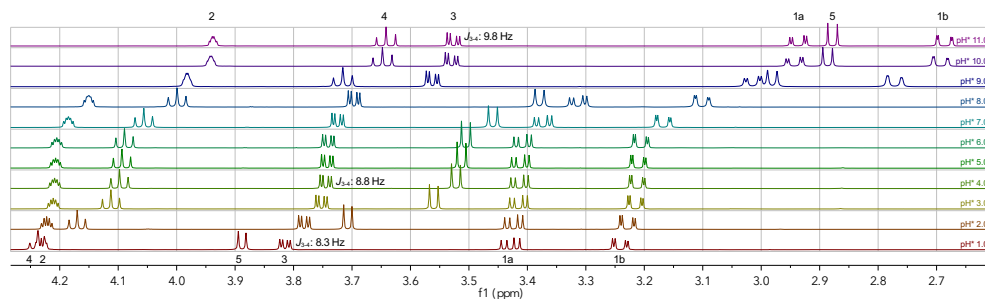


Figure 6.4 ^1H NMR spectra for 2,6-dideoxy-2,6-imino-mannonic acid (**3**) under different pH*; spectra are referenced to water, intensities are aligned to H4.

Figure 6.5 displays the collection of ^1H NMR spectra for amide **4** at different pH* values. Smaller changes are observed for the chemical shift change of H5 and there is no significant change of the coupling constants, indicating minimal conformation changes going from high to low pH*.

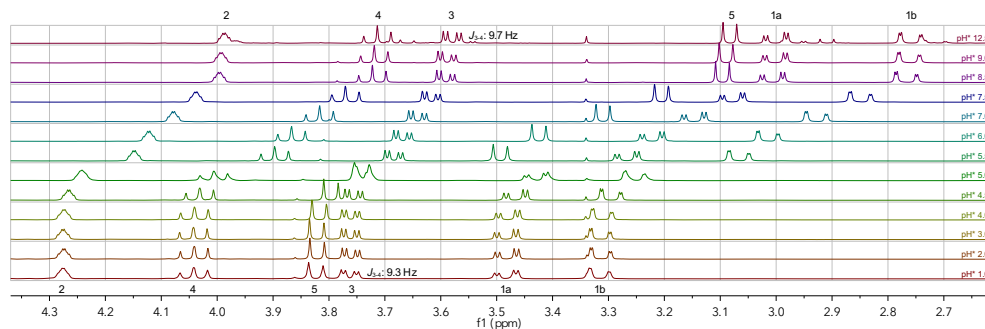


Figure 6.5 ^1H NMR spectra for 2,6-dideoxy-2,6-imino-mannonic amide (**4**) under different pH*; spectra are referenced to water, intensities are aligned to H2.

Although it is clear from the ^1H NMR spectra depicted above that both the methyl ester **2** and the acid **3** can undergo a pH-dependent conformational change, it is not possible to accurately determine the ratio of $^1\text{C}_4$ and $^4\text{C}_1$ conformers present because the interconversion between the two chair forms is too fast at ambient temperature, leading to coalescence of the resonances of both conformers. Therefore DFT calculations were used to determine the coupling constants of the two conformers of both the protonated and deprotonated azasugars. To this end a set of starting conformers was generated and the structures were optimized with Gaussian 03³⁵, by employing the B3LYP density functional and the 6-31G* basis set. The solvation in these optimizations was accounted for using the polarizable continuum model (PCM) function for the solvent used (H_2O or

methanol). The structures of relevant optimized chair conformers are depicted in Figure 6.6. The energies associated with the structures were determined by single point calculation employing the 6-311++G** basis set. The ^1H NMR coupling constants were generated from the optimized structures using the Gauge-Independent Atomic Orbital (GIAO) NMR method with the 6-311+G(2d,p) basis set, by employing the SpinSpin and Mixed options. The energies of the different conformers were used to determine the distribution of the two present in solution at room temperature. Table 6.1 shows the measured coupling constants ($J_{3,4}$) for the four azasugars at low and high pH*, the calculated $J_{3,4}$ values for the $^1\text{C}_4$ and $^4\text{C}_1$ conformers, the ratio of the two conformers, established from the measured average coupling constants, the difference in free energy established by the DFT calculations as well as the theoretical ratio of the two conformers, based on the difference in calculated free energy.

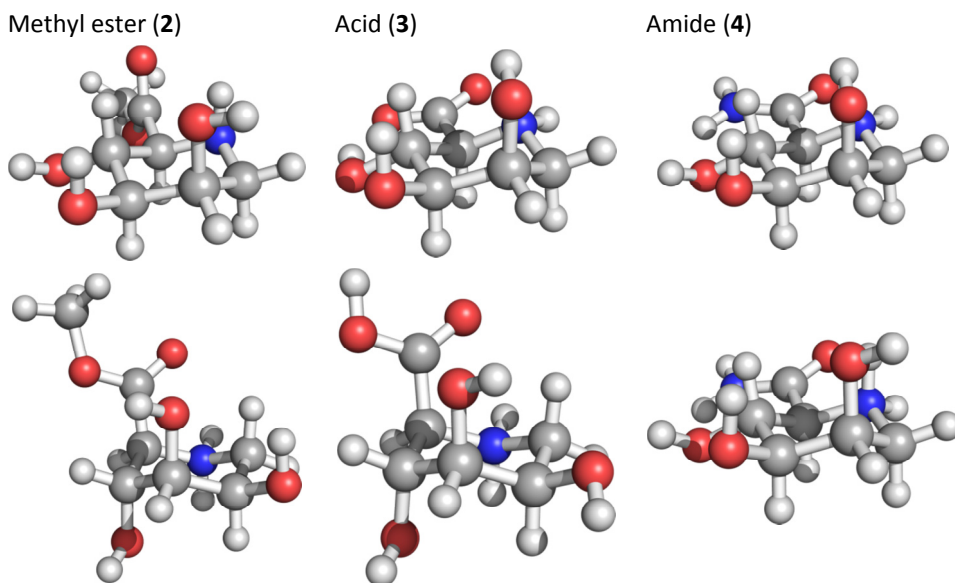
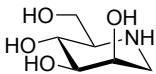
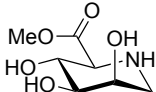
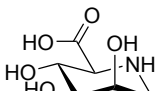
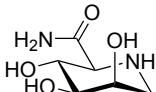
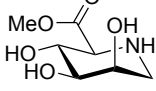


Figure 6.6 Calculated non-protonated (top) and protonated (bottom) optimized structures.

Table 6.1 Measured and calculated ratios in D₂O and MeOD.

Compound	pH* / TFA	$J_{3,4}$ Obs.	$J_{3,4}$ calc. 4C_1 1C_4		Ratio by NMR ${}^4C_1: {}^1C_4$	ΔE [${}^1C_4-{}^4C_1$] (kcal·mol ⁻¹)	Ratio theory ${}^4C_1: {}^1C_4$	pK _a
In D ₂ O:								
1 	9	9.5	9.0	3.3	100:0	4.0	100:0	7.4
	2	9.5	9.4	4.3	100:0	2.3	98:2	
2 	8	9.4	9.4	3.9	99:1	2.4	98:2	5.3
	2	7.5	9.5	4.9	56:44	0.3	64:36	
3 	11	9.8	9.3	3.1	100:0	3.2	100:0	7.5
	5	8.8	9.1	3.8	94:6	3.7	100:0	
	1	8.3	9.5	4.7	75:25	0.1	54:46	
4 	9	9.7	9.0	2.8	100:0	3.4	100:0	5.8
	2	9.3	9.1	4.7	100:0	1.7	95:5	
----- In MeOD:								
2 	0 μl	9.2	9.3	4.2	99:1	2.4	98:2	
	25 μl	4.8	9.3	4.7	1:99	-0.1	45:55	

As can be seen from Table 6.1, there is good agreement between the calculated and measured coupling constants at high pH*. With the two extreme values for $J_{3,4}$ the ratio of the 1C_4 and 4C_1 conformers was established and it is clear that DMJ takes up a single 4C_1 conformation at both low and high pH values. The calculated difference in energy between the possible 1C_4 and 4C_1 conformers was calculated to be 4.0 kcal mol⁻¹ for the unprotonated amine, and 2.3 kcal mol⁻¹ for the protonated amine. Although the difference in energy between the two conformers is significantly smaller for the protonated amine, it is so large that the 4C_1 conformer is almost exclusively present at both high and low pH values. For the methyl ester **2** the situation is different. For the unprotonated amine, present at high pH values, the difference in energy between the two chair conformers is 2.4 kcal mol⁻¹ in favor of the 4C_1 chair. In the protonated form however, the energy difference is minimal (0.3 kcal mol⁻¹), explaining the conformational mixture. With the calculated values of the coupling constants for both conformers (9.5 Hz and 4.9 Hz) and the measured average coupling constant (7.5 Hz) the ratio of the two conformers was established to be 56:44. This ratio is well in line with the ratio determined from the energy difference determined by the DFT calculations (0.3 kcal mol⁻¹), being 64:36.³⁶

In a similar vein the ratio of the two chair conformers of the acid (**3**) was determined at three different pH values. As can be seen in Table 6.1, there is reasonable agreement between the theoretical calculations and the measured ratios. At high pH, the anionic azasugar **3** is present as a single conformer. At pH 5 the measured average coupling constant indicates a 94:6 mixture of conformers, where theory predicts a single conformer. At low pH two conformers are observed in a 75:25 4C_1 : 1C_4 ratio, where the theoretical ratio is 54:46.³⁶ Finally, for the amide **4**, at both high and low pH the 4C_1 chair is almost exclusively present.

The pK_a values for the four compounds were determined by titration, and these data are also tabularized in Table 6.1. For DMJ a pK_a value of 7.4 was measured, which is in line with the pK_a previously established for this compound (7.5).¹² The pK_a 's of methyl ester **2**, amino acid **3** and amide **4** were determined to be 5.3, 7.5 and 5.8, respectively. The drop in pK_a value for the ester and the amide is a clear manifestation of the electron withdrawing effect of the carboxylic acid ester and amide functionalities. In acid **3** the electron withdrawing effect of the carboxylate is minimized because of its negative charge.

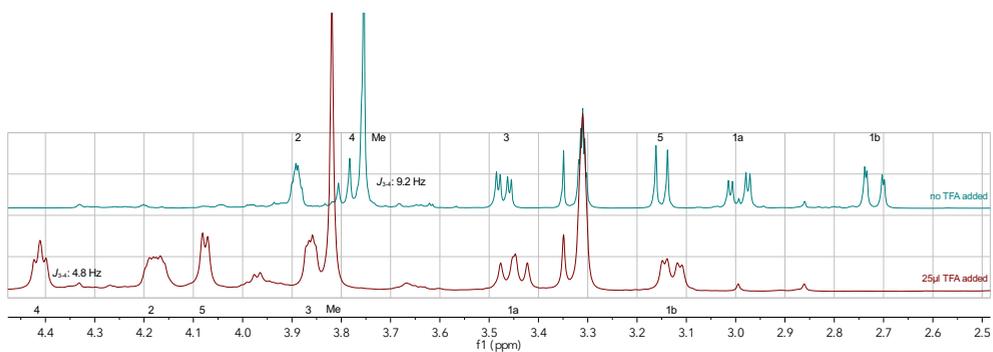


Figure 6.7 DMJ Methyl ester (**2**) in MeOD with non-protonated (no TFA added, top) and protonated (25 μ l TFA added, bottom)

Finally the azasugar showing the largest conformational change, that is methyl ester **2**, in a less polar solvent (MeOD) was investigated. In Figure 6.7 the spectra of the non-protonated and protonated azasugar are depicted. In this medium the $J_{3,4}$ coupling constant changes from 9.2 Hz to 4.8 Hz upon protonation, indicating a much stronger conformational flip than the one observed in D_2O . Also for this solvent the structures of the two chair conformers were optimized, and the associated energies and coupling constants calculated as described above. Using the obtained values (depicted in Table 6.1) for the coupling constants of the protonated and deprotonated species, it is concluded that the non-protonated azasugar almost exclusively resides in the 4C_1 conformation where the protonated species is found in the opposite 1C_4 conformation. Although the

theoretical free energy difference between the two chairs predicts the 1C_4 chair to be most favorable, the difference between the two chair forms is smaller than what is concluded from the NMR measurements (${}^4C_1 : {}^1C_4$ calculated = 45:55; ${}^4C_1 : {}^1C_4$ measured = 1:99).³⁶

The NMR results together with the DFT calculations show that DMJ analogues having a methyl ester or carboxylic acid at C5 (as in **2** and **3**, respectively) change their conformation from the 4C_1 chair to the opposite 1C_4 chair upon protonation. This conformational change is seen even in a highly polar medium such as water and is significantly enhanced in a more apolar solvent (MeOD). The nature of the substituent at the C5 of the DMJ analogues is of major importance, because DMJ (**1**) and the C5 amide DMJ (**4**) do not display a change in conformational preference. The difference between the ester and amide is notable, because both functional groups, the C5 ester and C5 amide respectively, have a similar effect on the basicity of the azasugars. The electron withdrawing effect of both groups leads to a significant drop in the pK_a values for **2** and **3**, with the strongest electron withdrawing functionality -the ester- having the strongest inductive effect. The conformational flip of ester **2** and acid **3** can be accounted for by taking into account that electron withdrawing groups prefer to occupy an axial position on a positively charged carbohydrate ring to minimize their destabilizing effect. The fact that amide **4** does not change its conformation to accommodate this intrinsic preference may be due to internal hydrogen bonds that can be formed between the amide $-NH_2$ and the C4-OH which provides an extra stabilizing factor in the 4C_1 amide (See DMJ amide pictures in Figure 6.6).³⁷

6.3 Conclusion

Mannuronic acid based azasugars can change their conformation upon protonation of the endocyclic amine from a “normal” 4C_1 chair to the inverted 1C_4 chair conformation. The molecules thereby position their substituents such that they are optimally positioned to accommodate the positive charge. Although the conformational behavior of any other glycuronic acid based azasugars, having different substituent configurations has not yet been studied in detail, it is likely that the spatial preferences of the substituents in the mannuronic acid azasugar work in concert to affect the ring flip. This behavior is in line with the conformational effects observed for fully protected mannuronic acid glycosyl donors and therefore the results described here provide an extra indication that the (partial) positive charge at the anomeric center of these donors is responsible for the observed unusual ring flip. The flexibility of the mannuronic acid azasugars may be exploited in the inhibition of specific mannosidases, enzymes that cleave mannosyl residues from oligosaccharides. For example, the cleavage of mannosyl residues by

mannosidases belonging to glycosyl hydrolase family 47 (GH47) occurs through a pathway in which the mannosyl substrate follows a ${}^3S_1 \rightarrow {}^3H_4 \ddagger \rightarrow {}^1C_4$ itinerary.³⁸⁻⁴⁰ To mimic the 3H_4 transition state of this reaction, the flexible mannuronic acid based azasugars may be well suited.

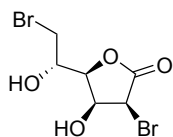
Experimental section

Calculations. All calculations were performed with DFT *ab initio* calculations with the B3LYP model. A set of conformers was optimized by starting from a conformer distribution search option included in the Spartan 04⁴¹ program in gas phase at 6-31G(d) as basis set. All generated geometries were optimized with Gaussian 03³⁵ at 6-31G*, their zero-point energy corrections calculated, and further optimized with incorporated polarizable continuum model (PCM) to correct for solvation in water or methanol. The energies for each of the structures were calculated by a single point calculation employing the PCM with corresponding solvent and a larger diffuse function containing 6-311++G** basis set.⁴² The 1H NMR coupling constants for the structures were generated for the two lowest energy 4C_1 and 1C_4 conformers using the Gauge-Independent Atomic Orbital (GIAO) NMR method with 6-311+G(2d,p) basis set, by employing the SpinSpin and Mixed options.

Synthesis

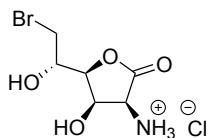
General. All reagents were of commercial grade and used as received unless stated otherwise. Reactions were performed at room temperature unless stated otherwise. Molecular sieves (4Å) were flame dried before use. Flash column chromatography was performed on silica gel (40-63 μ m). 1H and ${}^{13}C$ NMR spectra were recorded on a Bruker AV 600, Bruker AV 400 or a Bruker DPX 400 spectrometer in D_2O or CD_3OD . Chemical shifts (δ) are given in ppm relative to the solvent residual signals. Coupling constants (J) are given in Hz. All given ${}^{13}C$ spectra are proton decoupled. Compound names are given using the standard iminosugar nomenclature numbering, resulting in a different numbering system than in the article.

2,6-dibromo-2,6-dideoxy-D-mannono-1,4-lactone (6). Calcium D-gluconate monohydrate **5** (126 g, 280 mmol)



was put under an argon atmosphere before being dissolved in 33% HBr in acetic acid (500 ml, 3.0 mol). The reaction mixture was stirred for 18 hours to form acetylated **6**. MeOH (1 l) was added and the mixture was refluxed for 2 hours. After refluxing the mixture was concentrated to half the volume under reduced pressure before adding another 500 ml of MeOH. The reaction was left to stir overnight after which the mixture was concentrated resulting in a slightly oily residue. This was co-evaporated with 100 ml of MeOH and three times with H_2O . The residue was extracted with diethyl ether (4 x 100 ml), the organic layers were combined, dried with $MgSO_4$, filtered and concentrated under vacuum yielding a yellow oily residue. This was crystallized from $CHCl_3 / H_2O$ to yield a white crystalline solid (44 g, 146 mmol, 26% yield). 1H NMR (400 MHz, D_2O): δ 5.20 (1H, d, $J = 4.5$ Hz, C-2), 4.64 (2H, m, C-4, C-3), 4.19 (1H, m, C-5), 3.77 (1H, dd, $J = 11.4, 2.4$ Hz, C-6a), 3.65 (1H, dd, $J = 11.4, 4.9$ Hz, C-6b). ${}^{13}C$ NMR (101 MHz, D_2O): δ 174.0 (C-1), 81.6 (C-4), 69.1 (C-3), 66.2 (C-5), 47.6 (C-2), 36.6 (C-6). Melting point: 130 °C. $[\alpha]_D^{20}$: +58,6° (c = 1, MeOH)

2-amino-6-bromo-2,6-dideoxy-D-mannono-1,4-lactone hydrochloride (7). 2,6-Dibromo-2,6-dideoxy-D-mannono-



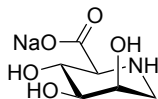
1,4-lactone (**6**, 5.0 g, 16.5 mmol) was put under argon and dissolved in dry acetone ($MgSO_4$, 100 ml). Sodium azide (15.0 g, 231 mmol) was added and the suspension was refluxed for 20 hours. The mixture was filtrated and the filtrate concentrated under reduced pressure. The residue was dissolved in H_2O (50 ml) and extracted with diethyl ether (5 x 100 ml), the organic layers were combined, dried over $MgSO_4$, filtered and

concentrated under reduced pressure to give a brown oil which was identified as the 2-azido compound but included some of its diastereoisomer. ^1H NMR (400 MHz, D_2O): δ 4.68 (1H, dd, $J = 4.5, 3.3$ Hz, C-3), 4.56 (1H, d, $J = 4.6$ Hz, C-2), 4.46 (1H, dd, $J = 9.2, 2.7$ Hz, C-4), 4.09 (1H, m, C-5), 3.69 (1H, dd, $J = 11.4, 2.7$ Hz, C-6a), 3.56 (1H, dd, $J = 11.5, 4.9$ Hz, C-6b). ^{13}C NMR (101 MHz, D_2O): δ 174.1 (C-1), 81.0 (C-4), 69.6, 65.7 (C-3, C-5), 62.3 (C-2), 36.6 (C-6). The crude compound (16.5 mmol) was put under argon and dissolved in MeOH (100 ml). Palladium on activated carbon (10%, 300 mg, 0.3 mmol) and HCl (37% in H_2O , 10 ml, 121 mmol) were added and the suspension charged with hydrogen atmosphere. The reaction mixture was stirred for 22 hours after which the catalyst was filtered off over a Whatman microfilter. The filtrate was concentrated under reduced pressure and co-evaporated once with HCl (37% in H_2O , 60 ml), thrice with toluene (60 ml) and once with CHCl_3 (50 ml). Crystallization from EtOH yielded 2-amino-6-bromo-2,6-dideoxy-D-mannono-1,4-lactone hydrochloride (**7**) as white crystals (2.6 g, 9.2 mmol, 55% over two steps). ^1H NMR (400 MHz, D_2O): δ 4.83 (1H, dd, $J = 4.8, 2.8$ Hz, C-3), 4.63 (1H, dd, $J = 9.2, 2.7$ Hz, C-4), 4.59 (1H, d, $J = 4.9$ Hz, C-2), 4.20 (1H, m, C-5), 3.77 (1H, dd, $J = 11.5, 2.6$ Hz, C-6a), 3.65 (1H, dd, $J = 11.4, 5.0$ Hz, C-6b). ^{13}C NMR (101 MHz, D_2O): δ 172.1 (C-1), 78.9 (C-4), 64.1 (C-3), 62.9 (C-5), 50.2 (C-2), 33.7 (C-6). Melting point: 207 °C (decomposed). $[\alpha]_{\text{D}}^{20}$: +41.6° (c = 1, MeOH).

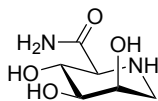
1-Deoxymannojirimycin (1). 2-amino-6-bromo-2,6-dideoxy-D-mannono-1,4-lactone hydrochloride (**7**, 501 mg, 1.8 mmol), was three times co-evaporated with dry toluene, put under argon and suspended in dry MeOH (10 ml). The suspension was cooled to 0 °C before addition of distilled triethylamine (1.0 ml, 7.2 mmol) and the resulting clear solution was stirred overnight. The reaction mixture was concentrated under reduced pressure yielding the methyl ester as a white semi-crystalline solid. The residue was put under argon, dissolved in dry EtOH (molsieves, 10 ml) and cooled to 0°C. Sodium borohydride (709 mg, 19 mmol) was added and the suspension was stirred overnight. Dry MeOH (20 ml) was added before the mixture was filtered, concentrated under reduced pressure and co-evaporated with 1M HCl in MeOH (3x, 10 ml). The residue was purified by column chromatography (1:1 EtOAc/EtOH \rightarrow 100% EtOH) yielding a pure sample of DMJ (**1**) in 29% yield (105 mg, 0.50 mmol). ^1H NMR (399 MHz, D_2O): δ 3.99 (1H, dt, $J = 2.9, 1.6$ Hz, C-3), 3.76 (1H, dd, $J = 12.5, 3.9$ Hz, C-7), 3.71 (1H, dd, $J = 12.5, 5.5$ Hz, C-7a), 3.60 (1H, t, $J = 9.7$ Hz, C-5), 3.53 (1H, dd, $J = 9.6, 3.1$ Hz, C-4), 3.03 (1H, dd, $J = 14.2, 2.8$ Hz, C-2a), 2.80 (1H, dd, $J = 14.2, 1.5$ Hz, C-2b), 2.57 (1H, ddd, $J = 9.7, 4.9, 3.4$ Hz, C-6). ^{13}C NMR (101 MHz, MeOD): δ 74.4 (C-4), 67.6 (C-5), 67.5 (C-3), 62.4 (C-6), 59.6 (C-7), 48.9 (C-2). $[\alpha]_{\text{D}}^{20}$: -14.0° (c = 0.5, MeOH).

Methyl 2,6-dideoxy-2,6-imino-D-mannonate hydrochloride (2). 2-amino-6-bromo-2,6-dideoxy-D-mannono-1,4-lactone hydrochloride (**7**, 0.60 g, 2.2 mmol), was co-evaporated thrice with dry toluene, put under argon and suspended in dry MeOH (12 ml). The suspension was cooled to 0 °C before addition of distilled triethylamine (1.2 ml, 8.7 mmol) and the resulting clear solution was stirred overnight. The reaction mixture was concentrated under reduced pressure before being taken up in acetonitrile (15 ml) charged with 1,1,1,3,3,3-hexamethylidisilazane (2.5 ml, 12 mmol) and copper sulphate pentahydrate (cat.). After 1 hour, the reaction mixture was concentrated and a fraction of 234 mg (0.57 mmol) was purified by column chromatography (1-2.5% 1,4-dioxane/DCM) to give 162 mg (0.40 mmol) of the per-TMSylated compound. The protected product was put under argon, dissolved in MeOH (8 ml) and acetyl chloride added to generate HCl *in situ*. The mixture was stirred for 0.5 hour, after which the compound was concentrated and coevaporated with MeOH yielding the title compound (98 mg, 0.40 mmol, 70% over 2 steps). ^1H NMR (400 MHz, MeOD) δ 4.40 (dd, $J = 5.3, 4.8$ Hz, 1H, C-5), 4.17 (ddd, $J = 9.5, 4.1, 2.8$ Hz, 1H, C-3), 4.09 (d, $J = 4.4$ Hz, 1H, C-6), 3.86 (dd, $J = 5.6, 2.7$ Hz, 1H, C-4), 3.82 (s, 3H, OCH_3), 3.44 (dd, $J = 12.2, 9.6$ Hz, 1H, C-2a), 3.13 (dd, $J = 12.2, 4.2$ Hz, 1H, C-2b). ^{13}C NMR (101 MHz, MeOD) δ 168.1 (C-7), 71.1 (C-4), 69.9 (C-5), 64.2 (C-3), 58.8 (C-6), 53.4 (OCH_3), 43.5 (C-2). $[\alpha]_{\text{D}}^{20}$: +31.8 (c = 1, MeOH).

Sodium 2,6-dideoxy-2,6-imino-D-mannonate (3). Methyl 2,6-dideoxy-2,6-imino-D-mannonate hydrochloride (**2**, 24 mg, 0.10 mmol), was dissolved in H₂O (0.5 ml). A sodium hydroxide solution (1M aq., 170 μ l, 0.17 mmol) was added and the mixture stirred for 2 hours. The mixture was concentrated under reduced pressure yielding the title compound, pure but with added sodium hydroxide. ¹H NMR (400 MHz, D₂O): δ 4.01 (1H, m, C-3), 3.71 (1H, t, J = 9.7 Hz, C-5), 3.60 (1H, dd, J = 9.6, 3.2 Hz, C-4), 3.01 (1H, dd, J = 14.6, 2.7 Hz, C-2a), 2.95 (1H, d, J = 9.8 Hz, C-6), 2.75 (1H, dd, J = 14.6, 1.6 Hz, C-2b). ¹³C NMR (101 MHz, D₂O): δ 178.4 (C-7), 74.1 (C-4), 70.6 (C-5), 69.1 (C-3), 65.2 (C-6), 47.9 (C-2). $[\alpha]_D^{20}$: -7.2 (c = 1, MeOH).



2,6-dideoxy-2,6-imino-D-mannonic amide (4). 2-amino-6-bromo-2,6-dideoxy-D-mannono-1,4-lactone hydrochloride (**7**, 500 mg, 1.8 mmol), was co-evaporated thrice with dry toluene, put under argon and suspended in dry MeOH (10 ml). The suspension was cooled to 0 °C before addition of distilled triethylamine (1.0 ml, 7.2 mmol) and the resulting clear solution was stirred overnight. The reaction mixture was concentrated under reduced pressure yielding the methyl ester as a white semi-crystalline solid. The residue was dissolved in 6M ammonia in MeOH (10 ml, 60 mmol) and was stirred overnight. The reaction mixture was concentrated under reduced pressure yielding 2,6-dideoxy-2,6-imino-D-mannonic amide (**4**) in quantitative yield. An analytical sample was made by crystallisation from pure MeOH (133 mg, 0.76 mmol, 42%). ¹H NMR (399 MHz, D₂O): δ 3.97 (1H, m, C-3), 3.70 (1H, t, J = 9.7 Hz, C-5), 3.57 (1H, dd, J = 9.6, 3.1 Hz, C-4), 3.07 (1H, d, J = 9.8 Hz, C-6), 2.99 (1H, dd, J = 14.6, 2.7 Hz, C-2a), 2.75 (1H, dd, J = 14.6, 1.6 Hz, C-2b). ¹³C NMR (101 MHz, DMSO): δ 173.5 (C-7), 74.9 (C-4), 70.0 (C-5), 68.7 (C-3), 63.3 (C-6), 49.1 (C-2). $[\alpha]_D^{20}$: -31.6° (c = 0.5, H₂O). HR-MS: $[M+H]^+$ calculated for C₆H₁₂O₄N₂: 177.08698; found: 177.08683.



References and notes

- [1] Smith, D. M.; Woerpel, K. A. *Org. Biomol. Chem.* **2006**, *4*, 1195-1201, 10.1039/b600056h.
- [2] Fraser-Reid, B.; Wu, Z. F.; Udodong, U. E.; Ottosson, H. *J. Org. Chem.* **1990**, *55*, 6068-6070, 10.1021/jo00312a004.
- [3] Mootoo, D. R.; Konradsson, P.; Udodong, U.; Fraser-Reid, B. *J. Am. Chem. Soc.* **1988**, *110*, 5583-5584, 10.1021/ja00224a060.
- [4] Pedersen, C. M.; Marinescu, L. G.; Bols, M. *ChemComm* **2008**, 2465-2467, 10.1039/b801305e.
- [5] Overend, W. G.; Sequeira, J. S.; Rees, C. W. *J. Chem. Soc.* **1962**, 3429-3439, 10.1039/jr9620003429.
- [6] Paulsen, H. *Angew. Chem. Int. Ed.* **1982**, *21*, 155-173, 10.1002/anie.198201553.
- [7] Zhang, Z. Y.; Ollmann, I. R.; Ye, X. S.; Wischnat, R.; Baasov, T.; Wong, C. H. *J. Am. Chem. Soc.* **1999**, *121*, 734-753, 10.1021/ja982232s.
- [8] Ritter, T. K.; Mong, K. K. T.; Liu, H. T.; Nakatani, T.; Wong, C. H. *Angew. Chem. Int. Ed.* **2003**, *42*, 4657-4660, 10.1002/anie.200351534.
- [9] McDonnell, C.; Lopez, O.; Murphy, P.; Bolanos, J. G. F.; Hazell, R.; Bols, M. *J. Am. Chem. Soc.* **2004**, *126*, 12374-12385, 10.1021/ja04746t.

- [10] Jensen, H. H.; Lyngbye, L.; Bols, M. *Angew. Chem. Int. Ed.* **2001**, *40*, 3447-3449, 10.1002/1521-3773(20010917)40:18<3447::aid-anie3447>3.0.co;2-8.
- [11] Bols, M.; Liang, X. F.; Jensen, H. H. *J. Org. Chem.* **2002**, *67*, 8970-8974, 10.1021/jo0205356.
- [12] Jensen, H. H.; Lyngbye, L.; Jensen, A.; Bols, M. *Chem. Eur. J.* **2002**, *8*, 1218-1226, 10.1002/1521-3765(20020301)8:5<1218::aid-chem1218>3.0.co;2-x.
- [13] Jensen, H. H.; Bols, M. *Acc. Chem. Res.* **2006**, *39*, 259-265, 10.1021/ar050189p.
- [14] Romero, J. A. C.; Tabacco, S. A.; Woerpel, K. A. *J. Am. Chem. Soc.* **2000**, *122*, 168-169, 10.1021/ja993366o.
- [15] Ayala, L.; Lucero, C. G.; Romero, J. A. C.; Tabacco, S. A.; Woerpel, K. A. *J. Am. Chem. Soc.* **2003**, *125*, 15521-15528, 10.1021/ja037935a.
- [16] Chamberland, S.; Ziller, J. W.; Woerpel, K. A. *J. Am. Chem. Soc.* **2005**, *127*, 5322-5323, 10.1021/ja050830i.
- [17] Larsen, C. H.; Ridgway, B. H.; Shaw, J. T.; Woerpel, K. A. *J. Am. Chem. Soc.* **1999**, *121*, 12208-12209, 10.1021/ja993349z.
- [18] Larsen, C. H.; Ridgway, B. H.; Shaw, J. T.; Smith, D. M.; Woerpel, K. A. *J. Am. Chem. Soc.* **2005**, *127*, 10879-10884, 10.1021/ja0524043.
- [19] Lucero, C. G.; Woerpel, K. A. *J. Org. Chem.* **2006**, *71*, 2641-2647, 10.1021/jo0522963.
- [20] Yang, M. T.; Woerpel, K. A. *J. Org. Chem.* **2009**, *74*, 545-553, 10.1021/jo8017846.
- [21] Codée, J. D. C.; Christina, A. E.; Walvoort, M. T. C.; Overkleeft, H. S.; Van der Marel, G. A., *Top. Curr. Chem.* **2011**, *301*, 253-289, 10.1007/128_2010_111.
- [22] van den Bos, L. J.; Codée, J. D. C.; Litjens, R. E. J. N.; Dinkelaar, J.; Overkleeft, H. S.; van der Marel, G. A. *Eur. J. Org. Chem.* **2007**, 3963-3976, 10.1002/ejoc.200700101.
- [23] Codée, J. D. C.; Walvoort, M. T. C.; de Jong, A. R.; Lodder, G.; Overkleeft, H. S.; van der Marel, G. A. *J. Carbohydr. Chem.* **2011**, *30*, 438-457, 10.1080/07328303.2011.624284.
- [24] Walvoort, M. T. C.; de Witte, W.; van Dijk, J.; Dinkelaar, J.; Lodder, G.; Overkleeft, H. S.; Codée, J. D. C.; van der Marel, G. A. *Org. Lett.* **2011**, *13*, 4360-4363, 10.1021/ol2016862.
- [25] Codée, J. D. C.; van den Bos, L. J.; de Jong, A. R.; Dinkelaar, J.; Lodder, G.; Overkleeft, H. S.; van der Marel, G. A. *J. Org. Chem.* **2009**, *74*, 38-47, 10.1021/jo8020192.
- [26] Walvoort, M. T. C.; Lodder, G.; Mazurek, J.; Overkleeft, H. S.; Codée, J. D. C.; van der Marel, G. A. *J. Am. Chem. Soc.* **2009**, *131*, 12080-12081, 10.1021/ja905008p.
- [27] Walvoort, M. T. C.; Dinkelaar, J.; van den Bos, L. J.; Lodder, G.; Overkleeft, H. S.; Codée, J. D. C.; van der Marel, G. A. *Carbohydr. Res.* **2010**, *345*, 1252-1263, 10.1016/j.carres.2010.02.027.

- [28] Walvoort, M. T. C.; Lodder, G.; Overkleeft, H. S.; Codée, J. D. C.; van der Marel, G. A. *J. Org. Chem.* **2010**, *75*, 7990-8002, 10.1021/jo101779v.
- [29] Pedersen, C. M.; Bols, M. *Tetrahedron* **2005**, *61*, 115-122, 10.1016/j.tet.2004.10.039.
- [30] Malle, B. M.; Lundt, I.; Wrodnigg, T. M. *Org. Biomol. Chem.* **2008**, *6*, 1779-1786, 10.1039/b719631h.
- [31] Bock, K.; Lundt, I.; Pedersen, C. *Carbohydr. Res.* **1979**, *68*, 313-319, 10.1016/s0008-6215(00)83780-5.
- [32] Bock, K.; Lundt, I.; Pedersen, C. *Acta. Chem. Scand., Ser. B* **1987**, *41*, 435-441, 10.3891/acta.chem.scand.41b-0435.
- [33] Akhlaghinia, B.; Tavakoli, S. *Synthesis* **2005**, 1775-1778, 10.1055/s-2005-865318.
- [34] The pH* defines the pH measured in D₂O.
- [35] Gaussian 03 (Revision E.01), Frisch, M. J. *et al.*, Gaussian, Inc. **2004**.
- [36] The PCM used for the solvents places the molecule in a cavity to account for solvent effects but does not account for intermolecular hydrogen bonding. The use of explicit solvent molecules within the calculations should enhance the precision of the calculated conformers and energies.
- [37] It has previously been observed that mannuronic acid ester thiodonors take up a ¹C₄ conformation when fully protected, while they reside in a ⁴C₁ conformation when the C4-OH is free. This contrasting conformational behavior can also be accounted for by a stabilizing hydrogen bond between the C5-carboxylic acid ester and the C4-OH in the ⁴C₁ chair conformation.
- [38] Davies, G. J.; Planas, A.; Rovira, C. *Acc. Chem. Res.* **2012**, *45*, 308-316, 10.1021/ar2001765.
- [39] Thompson, A. J.; Dabin, J.; Iglesias-Fernandez, J.; Ardevol, A.; Dinev, Z.; Williams, S. J.; Bande, O.; Siriwardena, A.; Moreland, C.; Hu, T. C.; Smith, D. K.; Gilbert, H. J.; Rovira, C.; Davies, G. J. *Angew. Chem. Int. Ed.* **2012**, *51*, 10997-11001, 10.1002/anie.201205338.
- [40] Williams, R. J.; Iglesias-Fernandez, J.; Stepper, J.; Jackson, A.; Thompson, A. J.; Lowe, E. C.; White, J. M.; Gilbert, H. J.; Rovira, C.; Davies, G. J.; Williams, S. J. *Angew. Chem. Int. Ed.* **2014**, *53*, 1087-1091, 10.1002/anie.201308334.
- [41] Spartan '04, Kong, J. *et al.*, Wavefunction Inc. **2004**.
- [42] Csonka, G. I.; French, A. D.; Johnson, G. P.; Stortz, C. A. *J. Chem. Theory Comput.* **2009**, *5*, 679-692, 10.1021/ct8004479.

Chapter 7

Summary and future prospects

The research in this thesis is focused on delineating the stereoelectronic effects exerted by ring substituents on carbohydrate derived oxocarbenium, iminium and ammonium ions. The electronegative oxygen substituents on the carbohydrate rings have an intrinsic (inductive) destabilizing effect on the positive charge of these cations. The magnitude of the destabilization depends on the nature of the substituent, its position and orientation on the carbohydrate ring. For example, it has long been known that axially positioned alkoxy groups at the C4 of pyranosides are less destabilizing than their equatorially

oriented counterparts. This becomes apparent in the higher reactivity of galactosyl donors in comparison to identically functionalized glucosyl donors and the faster hydrolysis of nitrophenol galactosides with respect to their glucosyl congeners. This reactivity difference can be explained by the stabilization of the electron depleted anomeric center by through space electron density donation of the axially positioned oxygen substituent. In addition, the interaction of the C4-O dipole with the positive charge at the anomeric center is more favorable in the galactose case than in the glucose case. To allow for the most optimal stabilization or to diminish the destabilizing effect of the substituents, carbohydrates can change their conformation to optimally position the ring substituents. The conformation of the carbohydrate ring can be a decisive factor in determining the stereochemical course of an addition reaction to the anomeric center. Similarly, protonation of iminosugars can change their conformation, thereby influencing the affinity of the molecule for the active site of its enzyme target.

In **Chapter 1** a general introduction is given on stereoelectronic effects and how they guide conformational preferences. The stereoelectronic effects of individual substituents in furanoses and pyranoses is summarized, as well as the stereoelectronic effects that are at play in polyhydroxylated iminosugars.

Chapter 2 describes a study toward substitution reactions of the four possible D-pentofuranosyl (*i.e.* ribosyl, arabinosyl, xylosyl and lyxosyl) acetates with [D]triethylsilane. It was observed that all furanosides gave the 1,2-*cis* products with good to excellent stereoselectivity. This striking result was explained using the conformational preferences of the intermediate oxocarbenium ions, which were assessed by calculating free energy surface (FES) maps of the complete conformational space for these molecules. Using the “inside attack model” the results from the [D]triethylsilane substitution reactions could be correlated to the most stable oxocarbenium ion conformers found with the FES. The results corroborated previous findings that a C2 alkoxy group prefers a pseudoequatorial position for optimal stabilization of the oxocarbenium ion, while the C3 alkoxy group prefers to be positioned pseudoaxial. In contrast to previous results, the C4 methyleneoxyalkyl substituent proved to be of great importance. The C5-oxygen can take up a *gg*, *tg*, *gt* orientation with respect to the C4 atom and the different rotamers have distinctly different FES maps. Most stabilization can be provided by the *gg*-C5-oxygen if the C4 substituent is positioned in an axial fashion to allow for optimal through-space interactions. Also the interplay between the different substituents became apparent from the different FES maps. The methodology of Chapter 2 was extended to anomeric tertiary oxocarbenium ions in **Chapter 3**. Reduction of furanosyl ketoses with triethylsilane provides access to (naturally occurring) C-glycosides and it was shown that addition of the hydride to the ketoses occurred preferentially in a 1,2-*cis* manner. While an alkyl

substituent on the anomeric carbon did not change the stereoselectivity in the [D]TES addition reactions when compared to the analogous reaction with the aldoses as described in Chapter 2, a phenyl substituent did give some erosion of stereoselectivity in two out of four cases. Also in this case, the calculated FES could be used to account for the (diminished) stereoselectivity of the reactions. There was a slight difference in stereochemical outcome found in the experiments and those determined from the calculated oxocarbenium ion conformer preferences. The secondary cations described in Chapter 2 are less stable than the ketose oxocarbenium ions of Chapter 3 and therefore the structures in the transition states of the addition reactions will more closely resemble the oxocarbenium ion structure in the aldose case than in the ketose case. In other words: the transition state in the aldose case will be earlier. In the ketose case the transition state will also be more crowded because of the tertiary nature of the cations. Thus, the differences in ground state energy of the oxocarbenium ion conformers are a better predictor for the product ratio found in the reactions of the aldoses than for those seen with the ketoses.

The methodology used in Chapter 2 and 3 can be expanded to all kinds of five-membered rings to examine their stability and conformational preferences. It can provide an attractive means to investigate the influence of ring substituents on oxocarbenium ion intermediates. Relevant examples of groups that are commonly employed in oligosaccharide and natural product synthesis include azides, amides and carbamates employed to mask amino groups,¹ esters and carbonates used to protect alcohol groups,¹ fluorides that are often used as a mimic for hydroxyl groups and as stabilizing groups for anomeric linkages,²⁻³ and carboxylates esters as present in masked glycuronic acids.⁴⁻⁶ To dissect the electronic and steric effects of the C4 methyleneoxy group, it would be of interest to investigate the C4 propyl analogues. Figure 7.1 depicts the FES maps calculated for a set of arabinosyl oxocarbenium ions featuring a C2-azide, a C2-fluoride, a C4-carboxylate or a C4-propyl group. The FES map for the protected 2-azido arabinofuranose oxocarbenium ion (**1**) in Figure 7.1 shows that **1** has a broader conformational preference than its C2-OMe analogue (See Chapter 2). The preference for the all-equatorial oxocarbenium ion has decreased and the favorable conformers now also include the flat- and E_3 envelope with a small ring pucker. The C4-C5 *gg* rotamer provides the most stable oxocarbenium ion conformers in line with the C2-OMe arabinosyl ion. It is likely that the broader conformation preference will result in addition reactions that proceed with less selectivity, but this has to be established experimentally.

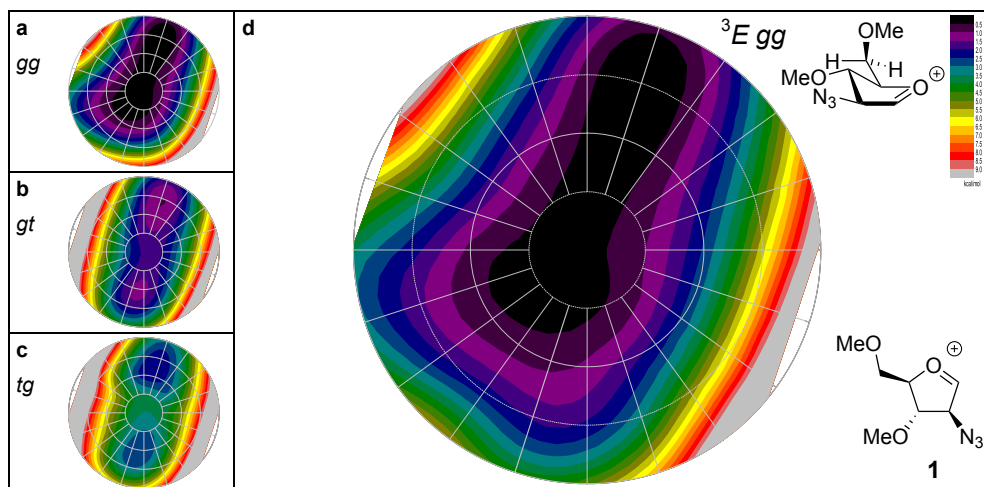


Figure 7.1 FES map of the 2-azidoarabinofuranosyl oxocarbenium ion (**1**). a) FES of the *gg* conformer. b) FES of the *gt* conformer. c) FES of the *tg* conformer. d) Global minimal FES of **1** showing the lowest-energy 3E (*gg*) conformer.

The 2-fluoro arabinofuranosyl oxocarbenium ion FES map (**2**, Figure 7.2) more closely resembles that of the C2-OMe arabinosyl ion. However, the E_3 conformer now is not as unfavorable. This is likely the result of the smaller size of the C2 fluorine leading to a decrease in steric interaction between the C2 and C4 substituents in the E_3 envelope.

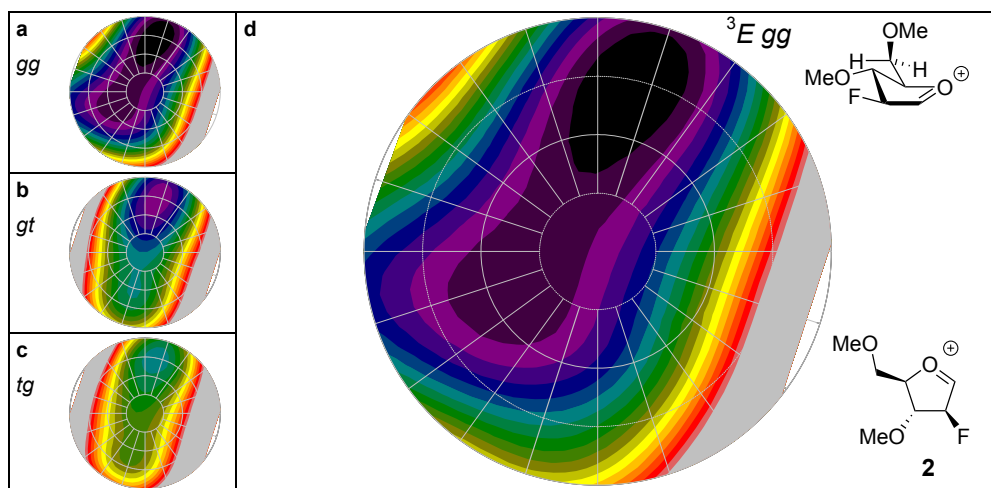


Figure 7.2 FES map of the 2-fluoroarabinofuranosyl oxocarbenium ion (**2**). a) FES of the *gg* conformer. b) FES of the *gt* conformer. c) FES of the *tg* conformer. d) Global minimal FES of **2** showing the lowest-energy 3E (*gg*) conformer.

The effect of a C4 carboxylic ester on the relative stability of the oxocarbenium ion conformers is visualized in Figure 7.3a-c using arabinosyl oxocarbenium ion **3**. In contrast to the three staggered rotamers that the methyleneoxymethyl group can adopt, the

methyl ester can be found in two relatively favorable positions: *syn*, with the carbonyl pointing towards O4 and *anti*, with the carbonyl opposite O4 (Figure 7.3d). The calculations of the individual *syn*- and *anti*-conformers show that there is only a very small difference between the *anti* and *syn* conformers. Notably, the FES map now shows two local minima one on the side of the 3E envelope and one on the opposite side of the E_3 envelope. In line with the findings described for the mannuronic acid oxocarbenium ions, (see Chapter 1 and 6) the stability of the E_3 envelope (which was unfavorable for the “non-oxidized” arabinosyl oxocarbenium ion, see Chapter 2) can result from extra stabilization by the axial C4 carboxylic ester⁴ and the smaller steric requirements for this group.

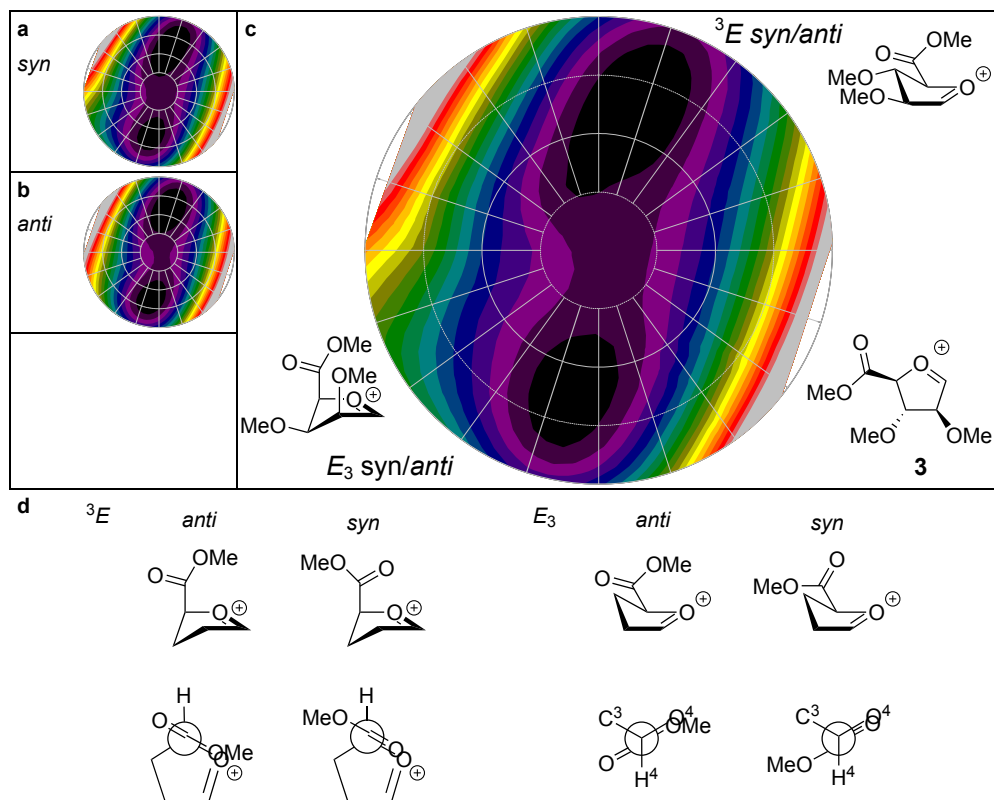


Figure 7.3 FES map of the C4 carboxylic ester arabinofuranosyl oxocarbenium ion (**3**). a) FES of the *syn* conformer. b) FES of the *anti* conformer. c) Global minimal FES of **3**. d) Possible rotamers around C4-C5 for the C5 carboxylate.

When O5 is replaced by a methylene group as in arabinose analogue **4**, the *gg* rotamer is no longer the most favorable rotamer (Figure 7.4). Instead the ‘electronically neutral’ alkyl prefers a *gt*-orientation for steric reasons. The FES map of arabinose **4** shows two local energy minima, an absolute minimum on the side of the 3E conformation and a minimum (+0.9 kcal mol⁻¹) for the E_3 conformer.

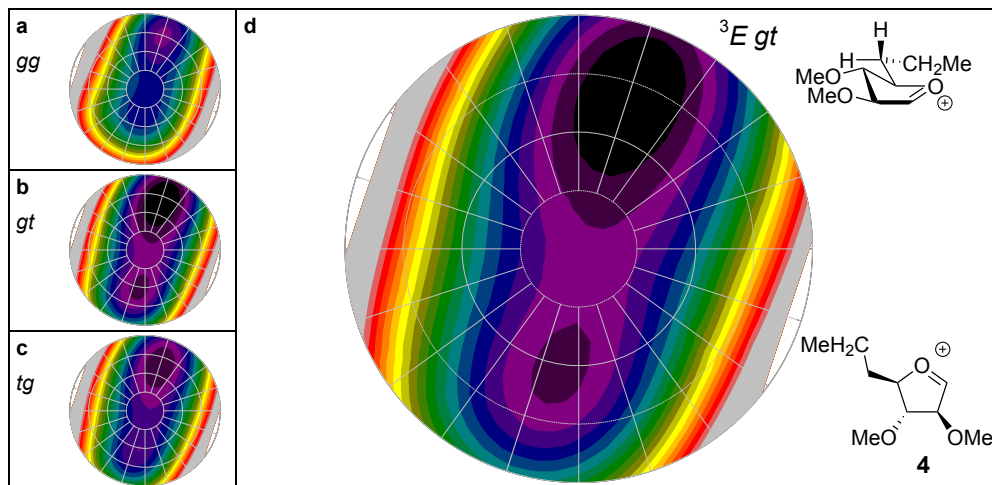


Figure 7.4 FES map of the 5-deoxy-5-ethyl arabinofuranosyl oxocarbenium ion (**4**). a) FES of the *gg* conformer. b) FES of the *gt* conformer. c) FES of the *tg* conformer. d) Global minimal FES of **4** showing the lowest-energy 3E (*gt*) conformer.

It will be of interest to also map the FES of the *ribo*-, *xylo*-, and *lyxo*-configured oxocarbenium ions to deliver a detailed picture on the influence of the different functional groups. Similarly all the “stripped” analogues, featuring a single substituent, will provide information on the effect of the isolated substituent. The theoretical studies should be complemented by experiments to validate the outcome of the studies. This will provide an in-depth understanding of the stereoelectronic effects of the ring substituents, both in a stand-alone situation and in concert with other ring substituents.

In **Chapter 4**, a combination of experiments and calculations is described to investigate the conformation of carbohydrate derived iminium ions as well as the stereochemical course of the Ugi multicomponent reaction. To this end, the four possible D-pentofuranosyl imines were generated and reacted with a carboxylic acid and an isocyanide. The results indicated that the stereoselectivity of the Ugi reaction is determined in the addition step of the isocyanide to the iminium ion. It was therefore concluded that the studied reactions proceeded under kinetic control, in contrast to common conception that the Ugi reaction proceeds under thermodynamic control. The calculations show that after formation of the nitrilium adduct an exothermic and irreversible step provides the imidate, which then rearranges into the product in another exothermic reaction. It was also found that an axial C3-alkoxy substituent plays a role in the transition state of the cyanide addition step as it stabilizes the developing positive charge on the forming iminium ion. It would therefore be interesting to investigate the Ugi reaction using differentially substituted imines, for example those devoid of a substituent at C3 or imines featuring azides or fluorides in analogy to the studies described above.

Chapter 5 describes the generation of an extensive library of lipophilic furanosyl iminosugars. To this extent, a highly efficient synthesis route was used to generate all eight D- and L-iminofuranoses employing a double displacement cyclization delivering the amines in 6-7 steps from the unprotected pentoses. The eight stereoisomers were alkylated with seven different alkyl groups to furnish a library consisting of 64 compounds. The compounds can be subjected to enzyme inhibition assays to determine their activity in the search for novel glycolipid-processing enzyme inhibitors.⁷

The conformation of the furanosyl iminosugars of Chapter 5 can be analyzed using the FES mapping method developed in this Thesis. Protonation of the endocyclic nitrogen can lead to important structural changes as outlined before. As an initial example both the non-protonated and protonated *N*-methylated arabinose iminosugar were investigated (Figure 7.5). The non-protonated iminosugar preferably takes up a conformation around the 0E envelope where all its substituents are in a sterically favored pseudoequatorial position. In the protonated ammonium ion, the preference shifts towards the E_1 , a conformer with more pseudoaxial substituents. This shift can be explained to result from the stereoelectronic effects that develop upon protonation of the endocyclic amine. In contrast to the C4-C5 *gg*-rotamer that the unprotonated amine adopts, the protonated iminosugar preferentially adopts a C4-C5 *gt*-conformation because of an increased C2-C4 steric repulsion. The arabinosyl iminosugar **7** was analyzed by ${}^1\text{H}$ NMR and its conformation was identified by a mathematical approach.⁸⁻⁹ It was determined that the arabinosyl iminosugar takes up an E_1 envelope structure, in line with the results of the FES map.

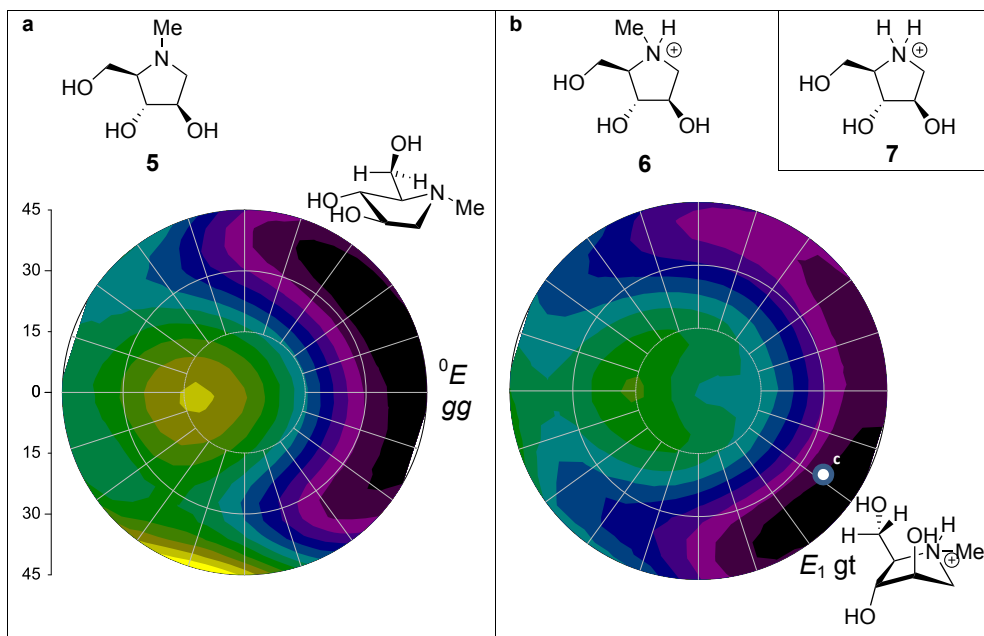


Figure 7.5 a) Global FES map of N-methyl arabinose iminosugar **5**. b) Global FES map of protonated N-methyl arabinose iminosugar **6**. c) Conformation identified from ^1H NMR for protonated arabinosyl iminosugar **7** (P: 122° , τ_m : 36).

Furanosyl iminosugars are known to not only target furanose processing enzymes but also inhibit pyranosidases.¹⁰ The smaller size of the five membered ring iminosugars allows them to fit into the active site of pyranose processing enzymes. The substituent configuration plays an important role in the selectivity of inhibitors. Arabinosyl iminosugar **8** for example is a good inhibitor of both glucosidases and mannosidases. This inhibitory activity can be explained by comparing the optimal 0E arabinosyl iminosugar conformation with D-glucose (**10**) and D-mannose (**11**), residing both in a 4C_1 chair conformation (Figure 7.6). The C2-C4 furanosyl substituents can be aligned with C3-C5 pyranosyl substituents, indicating that the substitution pattern of the 1,4-imino arabinitol allows for proper interactions with the active site (**9**).¹¹ However it should be noted that protonation of the amino groups can lead to a major conformational change and it remains to be seen how this influences the potency and selectivity of the furanosyl inhibitors. Studying the conformational preferences of both the protonated and non-protonated furanosyl (and pyranosyl) iminosugars will provide detailed insight to account for observed structure-activity-relationships.

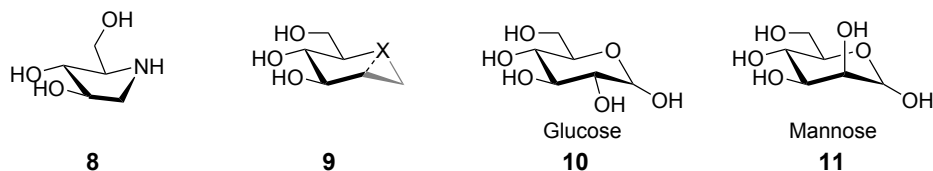


Figure 7.6 Structure of glucosyl and mannosyl inhibitor **8** aligned as in **9** with 4C_1 D-glucose (**10**) or D-mannose (**11**).

The conformational flexibility displayed by mannuronic acid iminosugars upon protonation is described in **Chapter 6**. Mannuronic acid donors show remarkable 1,2-*cis*-stereoselectivity and reactivity in glycosylation reactions. It has been proposed that the mannuronic acid 3H_4 oxocarbenium is at the basis of the striking reactivity. In this oxocarbenium ion all ring substituents are optimally positioned to stabilize the electron depleted anomeric center.¹² In Chapter 6 the conformational behavior of a set of mannuronic acid derived iminosugars was studied by NMR spectroscopy and through DFT calculations. It was found that the conformational flexibility displayed by mannuronic acid glycosyl donors extends to mannuronic acid iminosugars. Deoxymannojirimycin (DMJ) and three C6-oxidized analogues (the acid, the methyl ester and the amide) were studied. DMJ and the amide did not show any conformational change upon protonation, while both the acid and methyl ester gave a mixture of the 4C_1 and 1C_4 chair conformers. In D₂O the methyl ester gave a 56:44 mixture of the two chairs while in MeOD, a more apolar solvent in which the stereoelectronic stabilizing effects are more pronounced, the preference of the methyl ester for the “ring-flipped” 1C_4 chair was even stronger, and the molecule was found to adopt solely this conformation. The amide did not change conformation and the calculations revealed that the more stable 4C_1 conformation is caused by a hydrogen bond between the amide NH and O4. This molecule may be more prone to undergo a conformational change if this hydrogen bond can not form. Dimethylamide **12** is therefore an interesting iminosugar to investigate. Other C-5 substituents that are worthwhile to probe for their effect on the conformational equilibrium are the ketone **13** and CF₃-ketone **14**.

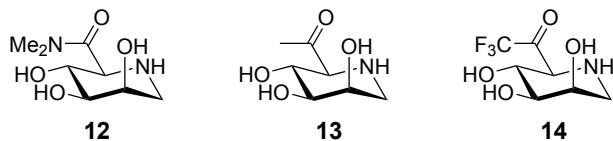


Figure 7.7 C5 analogues for mannuronic acid iminosugars interesting to investigate their conformational preferences.

The conformational flexibility of the mannuronic acid iminosugars may be used to generate selective enzyme inhibitors. For example, the cleavage of mannosyl residues by

mannosidases belonging to glycosyl hydrolase family 47 (GH47) occurs through a pathway in which the mannosyl substrate follows a ${}^3S_1 \rightarrow {}^3H_4^\ddagger \rightarrow {}^1C_4$ itinerary. The known mannosidase inhibitor mannoimidazole (**15**) effectively mimics the transition state by adopting a 3H_4 half-chair conformation (**16**). Under acidic conditions the mannuronic acid based iminosugars preferentially adopt a 1C_4 chair (**18**) that is conformationally close to the 3H_4 transition state and they may therefore be well suited as transition state mimics.

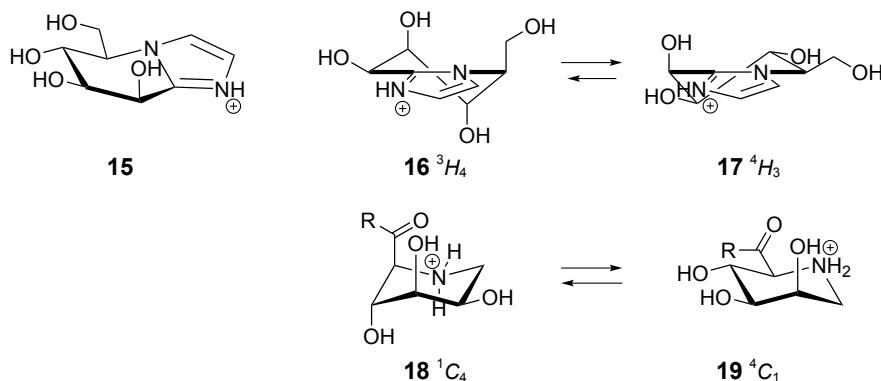


Figure 7.8 Mannosyl inhibitor mannoimidazole **15** adopts a 3H_4 half-chair, mannuronic acid based iminosugars (**18/19**) adopt a conformationally close 1C_4 chair.

References

- [1] Demchenko, A. V., *Handbook of Chemical Glycosylation*, **2008**.
- [2] Williams, S. J.; Withers, S. G. *Carbohydr. Res.* **2000**, 327, 27-46, 10.1016/s0008-6215(00)00041-0.
- [3] Walvoort, M. T. C.; Kallemeijn, W. W.; Willems, L. I.; Witte, M. D.; Aerts, J. M. F. G.; van der Marel, G. A.; Codée, J. D. C.; Overkleeft, H. S. *ChemComm* **2012**, 48, 10386-10388, 10.1039/c2cc35653h.
- [4] Dinkelaar, J.; de Jong, A. R.; van Meer, R.; Somers, M.; Lodder, G.; Overkleeft, H. S.; Codée, J. D. C.; van der Marel, G. A. *J. Org. Chem.* **2009**, 74, 4982-4991, 10.1021/jo900662v.
- [5] Walvoort, M. T. C.; Lodder, G.; Overkleeft, H. S.; Codée, J. D. C.; van der Marel, G. A. *J. Org. Chem.* **2010**, 75, 7990-8002, 10.1021/jo101779v.
- [6] de Jong, A. R.; Hagen, B.; van der Ark, V.; Overkleeft, H. S.; Codée, J. D. C.; van der Marel, G. A. *J. Org. Chem.* **2012**, 77, 108-125, 10.1021/jo201586r.
- [7] Ghisaidoobe, A.; Bikker, P.; de Bruijn, A. C. J.; Godschalk, F. D.; Rogaar, E.; Guijt, M. C.; Hagens, P.; Halma, J. M.; van't Hart, S. M.; Luitjens, S. B.; van Rixel, V. H. S.; Wijzenbroek, M.; Zweegers, T.; Donker-Koopman, W. E.; Strijland, A.; Boot, R.; van der Marel, G.;

- Overkleeft, H. S.; Aerts, J. M. F. G.; van den Berg, R. J. B. H. N. *ACS Med. Chem. Lett.* **2011**, *2*, 119-123, 10.1021/ml100192b.
- [8] Deleeuw, F.; Altona, C. J. *Comput. Chem.* **1983**, *4*, 428-437, 10.1002/jcc.540040319.
- [9] Hendrickx, P. M. S.; Martins, J. C. *Chem Cent J* **2008**, *2*, 10.1186/1752-153x-2-20.
- [10] Fleet, G. W. J.; Nicholas, S. J.; Smith, P. W.; Evans, S. V.; Fellows, L. E.; Nash, R. J. *Tetrahedron Lett.* **1985**, *26*, 3127-3130, 10.1016/s0040-4039(00)98636-2.
- [11] Saotome, C.; Wong, C. H.; Kanie, O. *Chem. Biol.* **2001**, *8*, 1061-1070, 10.1016/s1074-5521(01)00074-6.
- [12] Walvoort, M. T. C.; Dinkelaar, J.; van den Bos, L. J.; Lodder, G.; Overkleeft, H. S.; Codée, J. D. C.; van der Marel, G. A. *Carbohydr. Res.* **2010**, *345*, 1252-1263, 10.1016/j.carres.2010.02.027.

Samenvatting

Stereoelektronische en conformationele effecten in van koolhydraat afgeleide oxocarbenium, iminium en ammonium ionen

Het onderzoek dat beschreven is in dit proefschrift heeft zich gericht op het in kaart brengen van de invloed van substituenten op koolhydraat (suiker) ringen op de reactiviteit van deze moleculen. Verschillende typen koolhydraat afgeleide kationen zijn bestudeerd: furanosyl oxocarbenium ionen, gekarakteriseerd door de aanwezigheid van een $C=O^+$ groep; furanosyl iminium ionen, gekarakteriseerd door de aanwezigheid van een $C=N^+$ groep en ammonium ionen, die een geprotoneerd amine R_3NH^+ bevatten. De elektronegatieve alkoxy substituenten op deze koolhydraat ringen hebben een destabiliserend effect op de positieve lading van de kationen. De grootte van deze destabilisatie is afhankelijk van de aard van de substituent, de positie en de oriëntatie op de koolhydraat ring. Het is bijvoorbeeld reeds lang bekend dat axiaal gepositioneerde alkoxy groepen op de C4 positie van pyranosyl oxocarbenium ionen minder destabiliserend zijn dan hun equatoriaal georiënteerde tegenhangers. Dit wordt duidelijk door de hogere reactiviteit van galactose donoren in vergelijking met hun gelijk gefunctionaliseerde glucose donoren en door de grotere hydrolysesnelheid van nitrofenol galactosides in vergelijking met nitrofenol glucosides onder licht zure omstandigheden. Het verschil in reactiviteit kan verklaard worden met behulp van de stabilisatie van het elektronenarme anomere centrum door donatie van elektronendichtheid vanuit de axiaal gepositioneerde C4-zuurstof substituent. Ook de interactie tussen de C4-zuurstof dipool en de positieve lading op het anomere centrum is gunstiger in galactose dan in glucose. Om optimaal stabiliserende of minimaal destabiliserende effecten van de substituenten te bewerkstelligen, kunnen koolhydraatmoleculen hun conformatie veranderen zodat de ring substituenten de meest gunstige ruimtelijke positie aannemen. De conformatie van de koolhydraatring kan een beslissende factor zijn in het bepalen van de stereochemische uitkomst van additie reacties op het anomere centrum. In een analoog proces, kan het protoneren van iminosuikers leiden tot het veranderen van de conformationele voorkeur van de suikerring.

Hoofdstuk 1 dient als een algemene inleiding over stereoelektronische effecten en hoe deze effecten conformationele voorkeuren in cyclische moleculen kunnen sturen. De stereoelektronische effecten van individuele substituenten op furanose en pyranose moleculen is in dit hoofdstuk samengevat, evenals de stereoelektronische effecten die van toepassing zijn op poly-gehydroxyleerde pyranose iminosuikers.

Hoofdstuk 2 beschrijft een onderzoek naar de invloed van het substitutiepatroon van furanoses op de uitkomst van substitutie reacties op het anomere centrum van de vier mogelijke D-pentofuranoses. Hiervoor werd een modelreactie gebruikt waarin de pentofuranosyl acetaat donoren onder invloed van een Lewis zuur werden gesubstitueerd met [D]triethylsilaan. Alle furanosides in deze substitutie reactie gaven het 1,2-*cis* product met hoge tot uitstekende selectiviteit. Dit opvallende resultaat kon verklaard worden aan de hand van de conformationele voorkeur van de oxocarbenium ionen, die optraden als reactief intermediair in deze reacties. De voorkeur hiervan werd bepaald door het berekenen van het vrije energie landschap van alle mogelijke conformaties die deze moleculen kunnen aannemen. Met behulp van een bestaand model waarbij is aangetoond dat het inkomende nucleofiel in deze reacties reageert aan de “binnenkant” van de meest gunstige envelop structuur, kon de vorming van de gevonden producten in de substitutie reactie verklaard worden. Uit de berekeningen en experimenten werd duidelijk dat de drie aanwezige ringsubstituenten een specifieke voorkeur hebben voor optimale stabilisatie van het elektronenarme anomere centrum en dat de samenwerking van de drie substituenten de conformationele voorkeur van het oxocarbenium ion bepaalt. De methode gebruikt in hoofdstuk 2 werd in **Hoofdstuk 3** uitgebreid naar tertiaire anomere oxocarbenium ionen. De reductie van de bestudeerde furanosyl methyl- en phenylketoses met behulp van triethylsilaan gaf toegang tot C-glycosiden en er werd aangetoond dat ook hier de reactie bij voorkeur via een 1,2-*cis* additie plaatsvond. De stereochemie in de bestudeerde reacties kon ook in dit geval verklaard worden met behulp van de berekende vrije energie landschappen. Over het algemeen verliepen de reacties met tertiaire phenyl oxocarbenium ionen minder stereoselectief dan de reacties met tertiaire methyl oxocarbenium ionen.

Hoofdstuk 4 beschrijft een onderzoek waarbij een combinatie van experimenten en berekeningen werd gebruikt om de conformationele voorkeur van koolhydraat afgeleide iminium ionen te bepalen en de reactiviteit van deze moleculen in Ugi multicomponent reacties te onderzoeken. Hiervoor werden de vier mogelijke pentofuranose imines gesynthetiseerd en deze werden onderworpen aan een reactie met een carbonzuur en een isocyanide. Het bleek dat de stereoselectiviteit van de bestudeerde Ugi reacties wordt bepaald in de stap waar het isocyanide aan het iminium ion bindt. Dit wijst erop dat de stereochemie kinetisch wordt bepaald en niet, zoals vaak aangenomen, het resultaat is

van thermodynamische controle. De berekeningen laten zien dat de kinetische controle bepaald wordt door een exotherme, irreversibele stap, die plaatsvindt direct na de additie van het isocyanide aan het iminium ion. Ook werd duidelijk dat het substitutiepatroon op de iminium ionen van doorslaggevend belang was voor de stereoselectiviteit in de reacties. Geheel in lijn met de bevindingen van hoofdstuk 2 en 3 bleek dat de drie ringsubstituenten een specifieke ruimtelijke voorkeur hebben in de positief geladen intermediairen en dat de stereoselectiviteit in de reacties werd bepaald door het gecombineerde effect van deze drie substituenten.

Hoofdstuk 5 beschrijft de synthese van een uitgebreide bibliotheek van lipofiele furanosyl iminosuikers met als doel om nieuwe remmers te vinden voor glycolipide modificerende enzymen. Er werd een efficiënte synthese route ontwikkeld om alle acht D- en L-iminofuranoses te verkrijgen via een dubbele substitutie reactie welke toegang verschaft tot de cyclische amines. In totaal waren er 6 of 7 stappen nodig vanaf de onbeschermd pentose koolhydraten om tot de iminosuikers te komen. De acht stereoisomeren werden gealkyleerd met zeven verschillende lipofiele groepen om een bibliotheek te geven van 64 moleculen.

De conformationele flexibiliteit van geprotoneerde mannuronzuur afgeleide iminosuikers is beschreven in **hoofdstuk 6**. De conformationele voorkeur van de mannuronzuur afgeleide iminosuikers werd bestudeerd met behulp van NMR spectroscopie en chemische berekeningen. Er werd gevonden dat de conformationele flexibiliteit die al beschreven is voor mannuronzuur donoren in glycosyleringsreacties, zich ook manifesteert in mannuronzuur iminosuikers. Om tot deze conclusie te komen werden deoxymannojirimycine (DMJ) en drie C6-geoxideerde analoga, het zuur, de methyl ester en het amide, bestudeerd. Hierbij werd gevonden dat bij protonatie DMJ en het amide geen conformationele verandering ondergaan en zich bevinden in een stabiele 4C_1 stoel conformatie. Wanneer het amine in het mannuronzuur en de methyl ester iminosuiker geprotoneerd wordt kunnen deze moleculen twee verschillende stoel conformaties, de 4C_1 en 1C_4 stoel, aannemen. In zwaar water (D_2O , gebruikt voor de NMR analyse), een extreem polair medium, werd voor de methyl ester een 1 : 1 mengsel gevonden van de twee stoel conformeren, terwijl in het meer apolaire methanol ($MeOH-d_4$) alleen de ongewone 1C_4 conformatie gevonden werd. De voorkeur voor de 1C_4 stoel conformatie is het resultaat van stereoelektronisch stabiliserende effecten van de substituenten op het iminosuiker cation die in dit geval een grotere rol spelen dan sterische effecten, die in deze structuur vrij ongunstig zijn.

List of Publications

Chiral pyrroline-based Ugi-three-component reactions are under kinetic Control

Erwin R. van Rijssel, Theodorus P. M. Goumans, Gerrit Lodder, Herman S. Overkleef, Gijsbert A. van der Marel, Jeroen D. C. Codée

Organic letters, **2013**, *15*, 3026-3029, doi 10.1021/ol4012053.

Potent and selective activity-based probes for GH27 human retaining α -galactosidases

Lianne I. Willems, Thomas J. M. Beenakker, Benjamin Murray, Saskia Scheij, Wouter W. Kallemeijn, Rolf G. Boot, Marri Verhoek, Wilma E. Donker-Koopman, Maria J. Ferraz, Erwin R. van Rijssel, Bogdan I. Florea, Jeroen D. C. Codée, Gijsbert A. van der Marel, Johannes M. F. G. Aerts, Herman S. Overkleef

Journal of the American Chemical Society, **2014**, *136*, 11622-11625, doi 10.1021/ja507040n.

Synthesis of α - and β -galactopyranose-configured isomers of cyclophellitol and cyclophellitol aziridine

Lianne I. Willems, Thomas J. M. Beenakker, Benjamin Murray, Berend Gagestein, Hans van den Elst, Erwin R. van Rijssel, Jeroen D. C. Codée, Wouter W. Kallemeijn, Johannes M. F. G. Aerts, Gijsbert A. van der Marel, Herman S. Overkleef

European Journal of Organic Chemistry, **2014**, 6044-6056, doi 10.1002/ejoc.201402589.

Furanosyl oxocarbenium ion stability and stereoselectivity

Erwin R. van Rijssel, Pieter van Delft, Gerrit Lodder, Herman S. Overkleef, Gijsbert A. van der Marel, Dmitri V. Filippov, Jeroen D. C. Codée

Angewandte Chemie International Edition, **2014**, *53*, 10381-10385, doi 10.1002/anie.201405477.

Angewandte Chemie, **2014**, *126*, 10549-10553, doi 10.1002/ange.201405477.

Stereoselectivity in the Lewis acid mediated reduction of ketofuranosides

Erwin R. van Rijssel, Pieter van Delft, Stefan M. Bijvoets, Herman S. Overkleef, Gijsbert A. van der Marel, Dmitri V. Filippov, Jeroen D. C. Codée

Manuscript for publication in preparation

A library of lipophilic iminosugars based on all eight stereoisomeric pentofuranosyl iminosugars

Erwin R. van Rijssel, Herman S. Overkleef, Gijsbert A. van der Marel, Jeroen D. C. Codée

Manuscript for publication in preparation

Stereoelectronic substituent effects determine the conformational preferences of mannuronic acid based iminosugar cations

Erwin R. van Rijssel, Antonius P. A. Janssen, Herman S. Overkleef, Gijsbert A. van der Marel, Jeroen D. C. Codée

Manuscript for publication in preparation

Curriculum Vitae

Erwin van Rijssel werd op 16 april 1987 geboren in Hoofddorp. Van 1999 tot 2004 heeft hij zijn middelbaar onderwijs gevolgd bij het Herbert Vissers College in Nieuw-Vennep en behaalde hij daar zijn HAVO diploma (profielen Natuur&Techniek en Natuur&Gezondheid). In 2004 is hij vervolgens begonnen aan de HBO opleiding Hoger Laboratorium Onderwijs bij de Hogeschool Leiden en daar heeft hij in 2008 zijn bachelordiploma behaald met als specialisatie Organische Synthese. Als deel van deze studie heeft hij een onderzoeksstage uitgevoerd bij TNO Defensie & Veiligheid in Rijswijk, in het kader waarvan gefosforyleerde peptiden zijn gesynthetiseerd voor de verbetering van de diagnose voor blootstelling aan organofosfaten. Aansluitend is hij begonnen met de Master opleiding Chemistry aan de Universiteit Leiden met als specialisatie Design & Synthesis. Als onderdeel van deze Master opleiding heeft hij twee onderzoeksstages gedaan. Gedurende het eerste jaar heeft hij in de werkgroep Bio-Organische Synthese remmers voor matrix metalloproteases gesynthetiseerd. Deze remmers waren gebaseerd op korte peptide sequenties uitgerust met een epoxide keton als covalent bindende warhead. Als tweede onderzoeksproject heeft hij gewerkt bij de Medicinale Chemie afdeling van MSD in Oss. Dit onderzoek omvatte de synthese van peptide-conjugaten voor de optimalisatie van PTH receptor agonisten. In september 2010 behaalde hij het Master diploma.

Opvolgend aan zijn Master opleiding begon hij als assistent in opleiding bij de werkgroep Bio-Organische Synthese onder leiding van prof. dr. G. A. van der Marel en dr. J. D. C. Codée. Het resultaat van dit onderzoek is beschreven in dit proefschrift.

Momenteel is hij aangesteld als postdoctoraal onderzoeker in de werkgroep Bio-Organische Synthese.

Appendix

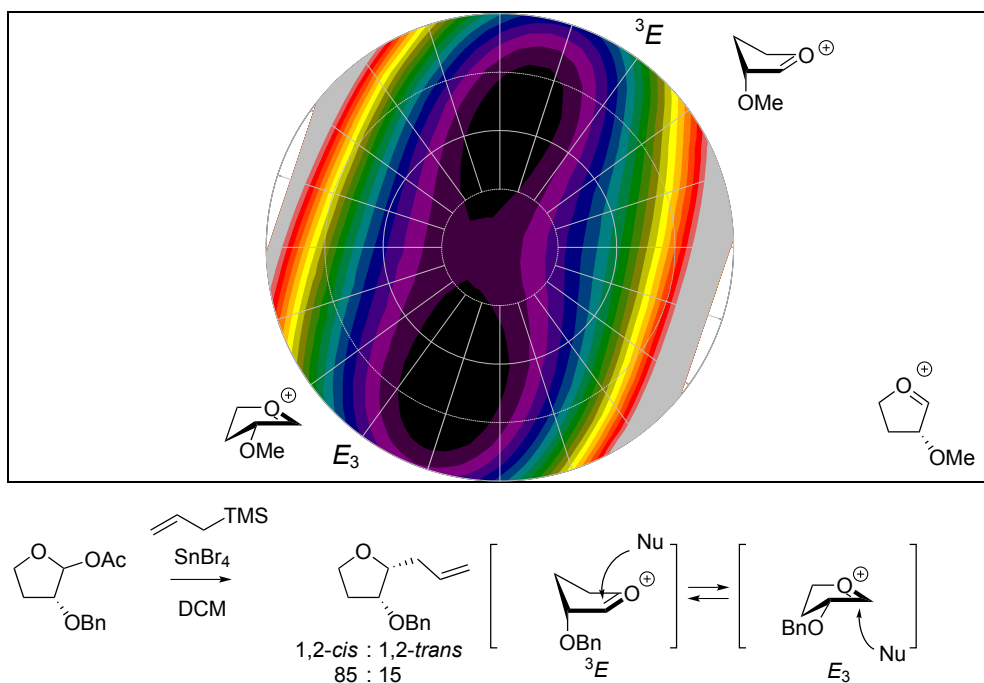
This Appendix provides additional free energy surface (FES) maps that have been calculated for mono- and disubstituted tetrahydrofuranyl oxocarbenium ions (“stripped pentofuranosyl oxocarbenium ions”, Schemes A.1-A.9). The maps are reported alongside the C-allylation reactions, described by Woerpel and co-workers, in which they occur as possible intermediates. Overall, there is good to excellent agreement between the calculated lowest energy oxocarbenium ions and the experimentally observed product

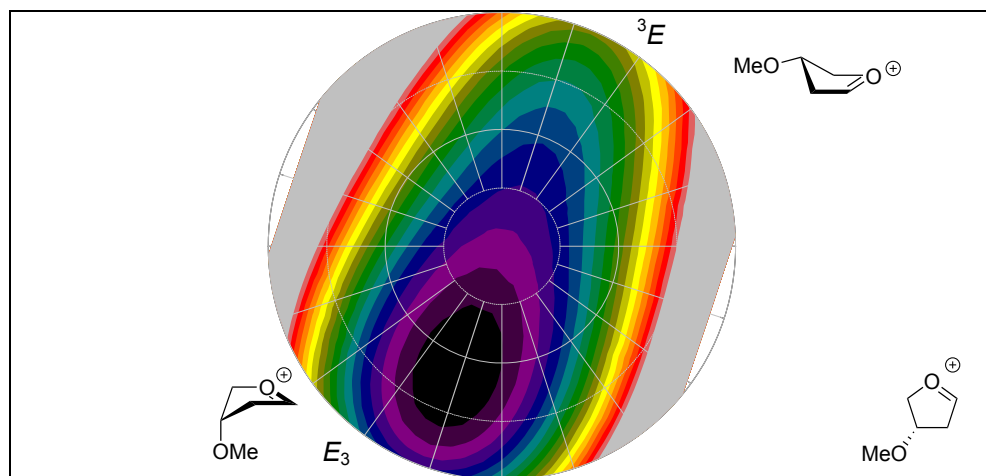
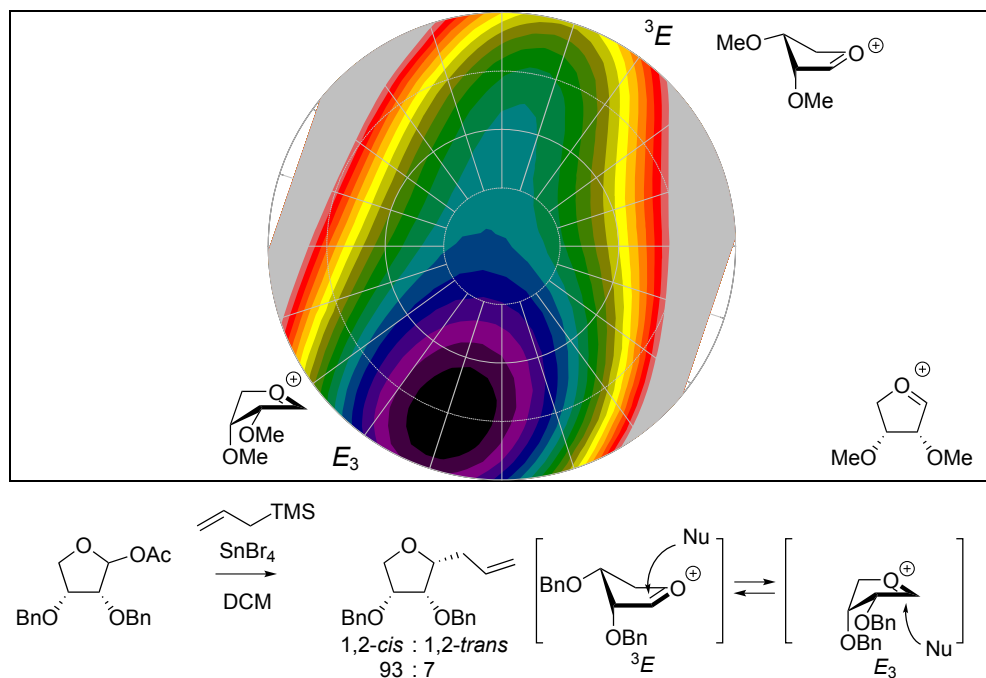
ratio's, taking into account the inside attack model as described in Chapters 1-3. The FES maps provide a clear picture on the influence of the different single ring substituents.

Figures A.1-A.4 depict the FES maps that have been calculated for the two possible anomers of the four D-furanosyl triflates. The most favorable structures are depicted in these Figures and the differences in energy between the α - and β -anomers have been determined based on the energies of their lowest energy conformers.

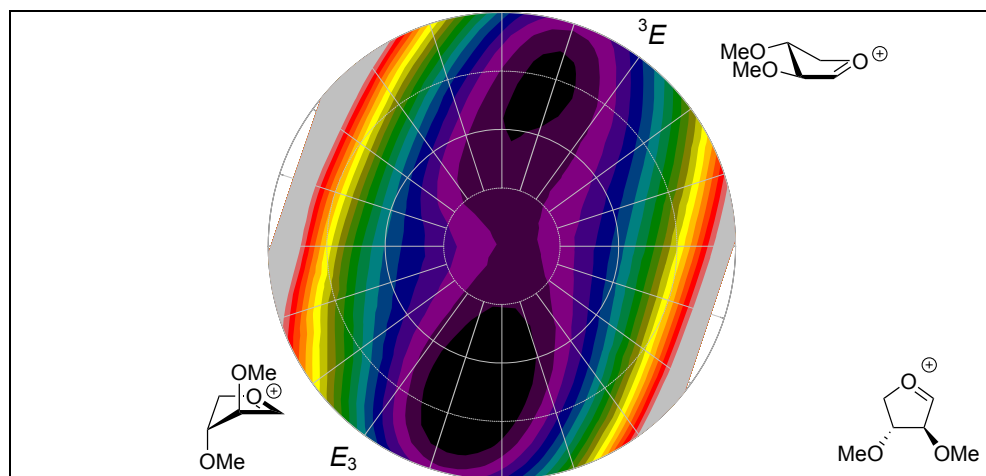
For the results of the C-allylation reactions see: Larsen, C. H.; Ridgway, B. H.; Shaw, J. T.; Smith, D. M.; Woerpel, K. A., *J. Am. Chem. Soc.* **2005**, *127*, 10879-10884, 10.1021/ja0524043.

Scheme A.1 (*R*)-4-methoxy-3,4-dihydro-2H-furan-1-ium.

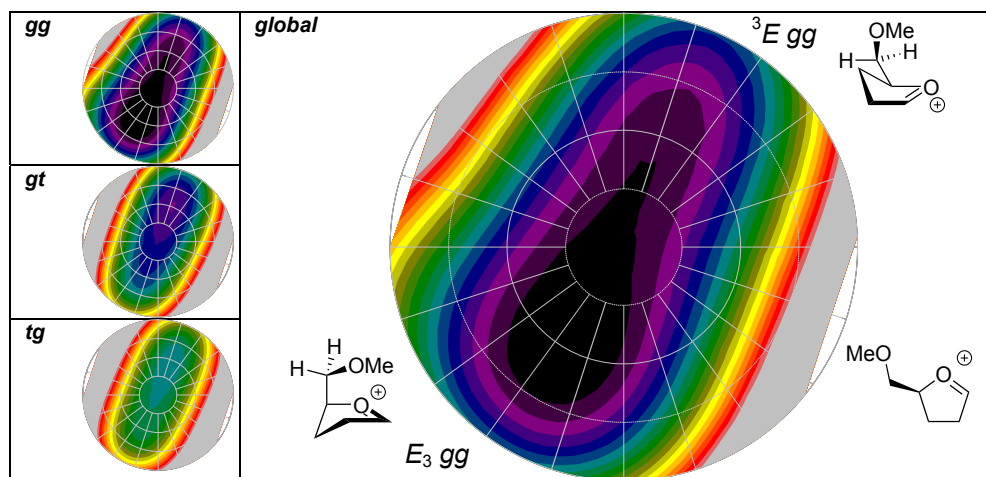


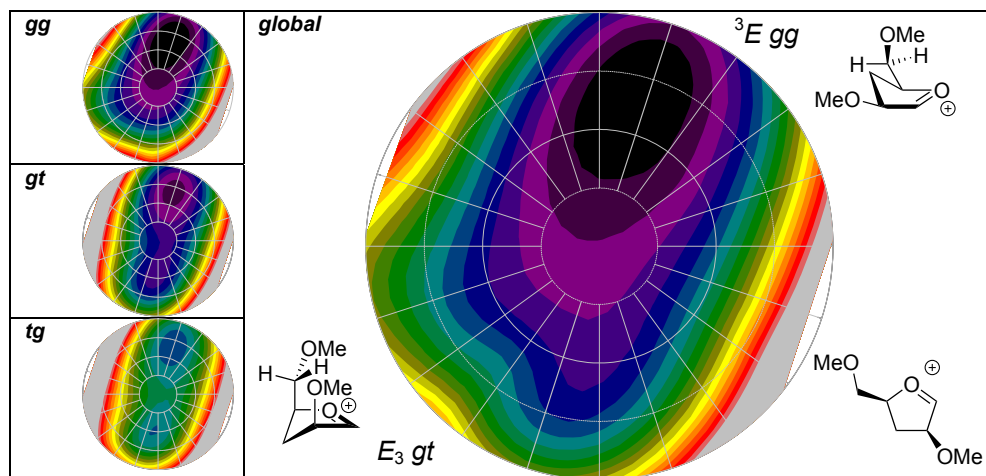
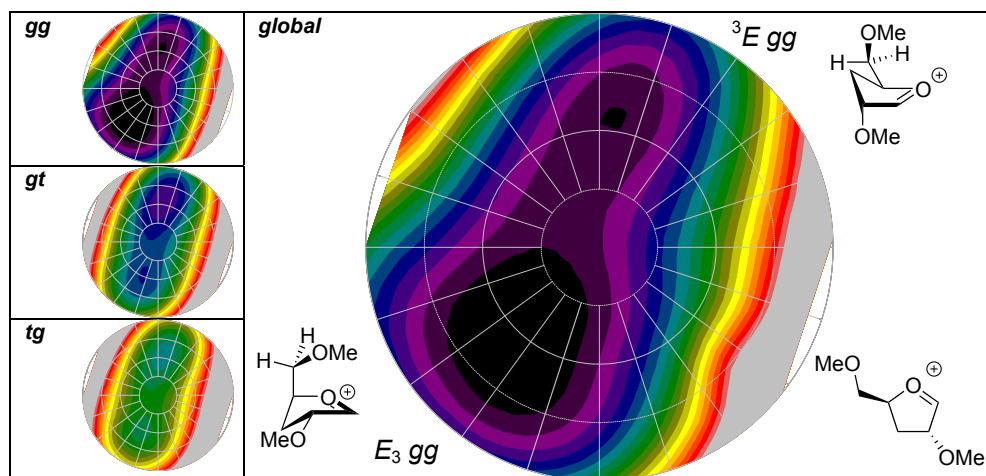
Scheme A.2 (*S*)-3-methoxy-3,4-dihydro-2H-furan-1-ium.Scheme A.3 (3*R*,4*R*)-3,4-dimethoxy-3,4-dihydro-2H-furan-1-ium.

Scheme A.4 (3*R*,4*S*)-3,4-dimethoxy-3,4-dihydro-2H-furan-1-ium.

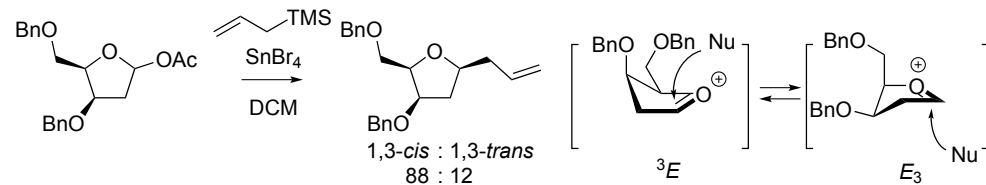
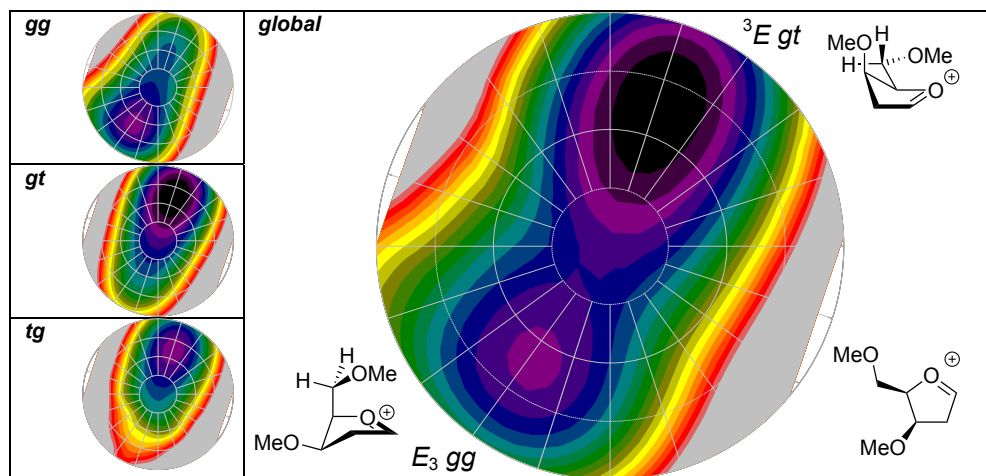


Scheme A.5 (S)-2-(methoxymethyl)-3,4-dihydro-2H-furan-1-ium.

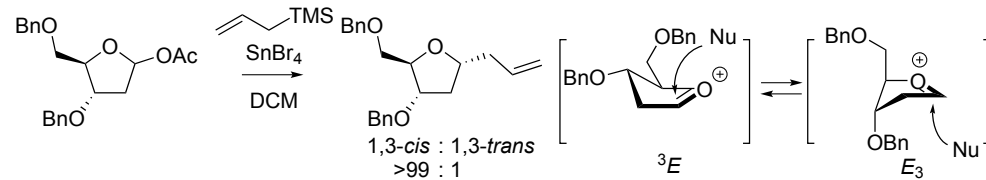
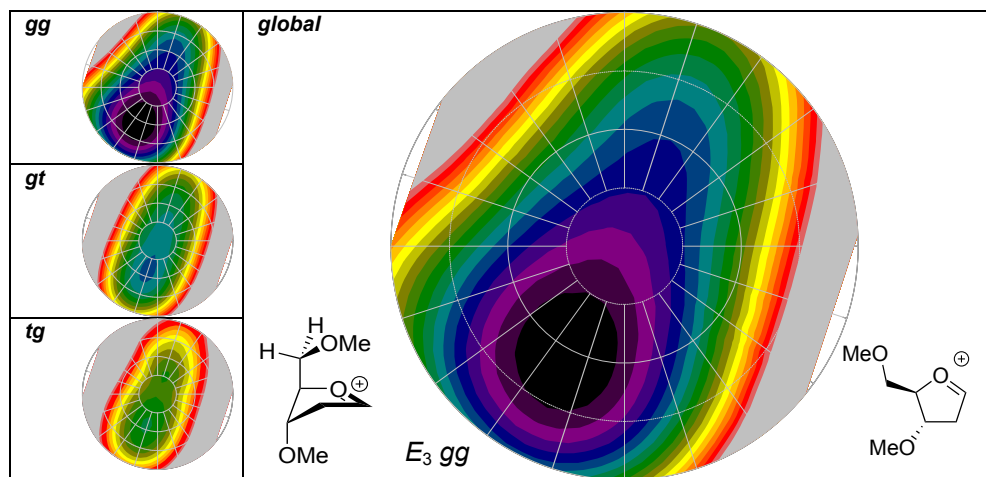


Scheme A.6 (2*S*,4*S*)-4-methoxy-2-(methoxymethyl)-3,4-dihydro-2H-furan-1-ium.Scheme A.7 (2*S*,4*R*)-4-methoxy-2-(methoxymethyl)-3,4-dihydro-2H-furan-1-ium.

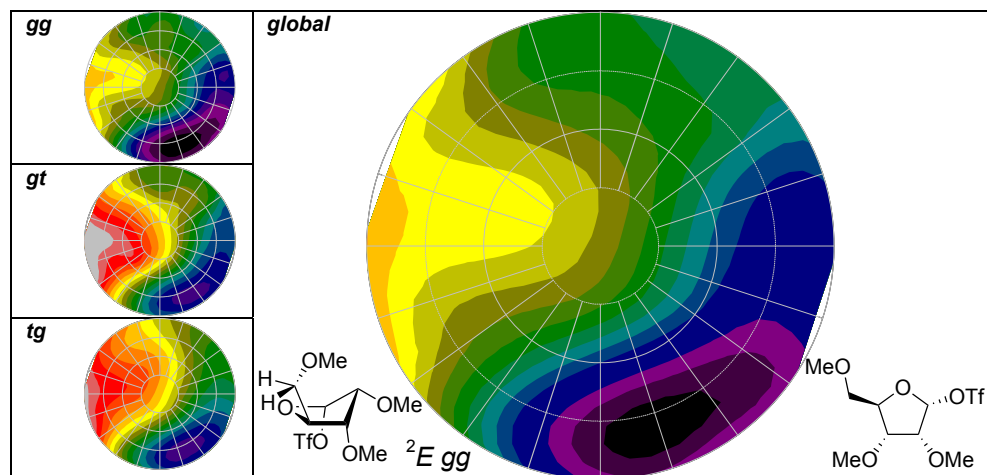
Scheme A.8 (2*R*,3*R*)-3-methoxy-2-(methoxymethyl)-3,4-dihydro-2*H*-furan-1-ium.



Scheme A.9 (2*R*,3*R*)-3-methoxy-2-(methoxymethyl)-3,4-dihydro-2*H*-furan-1-ium.



(α)



(β)

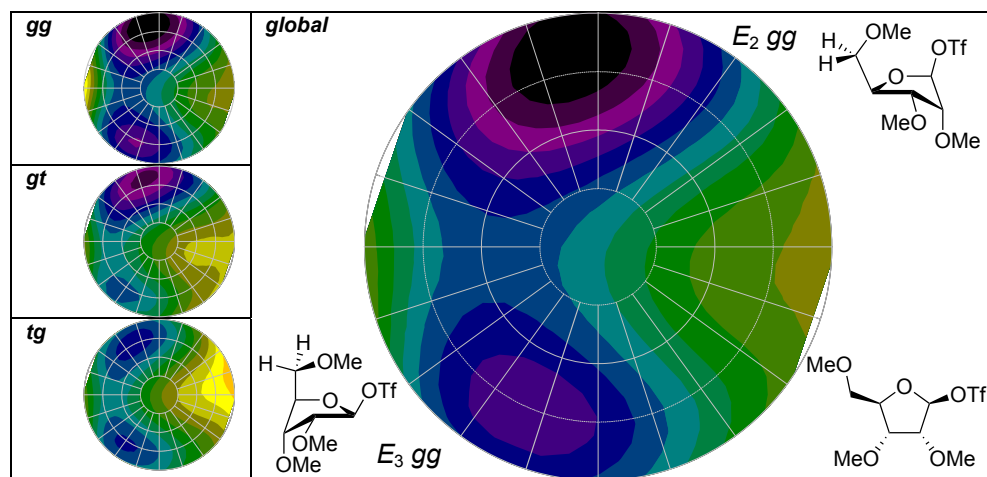
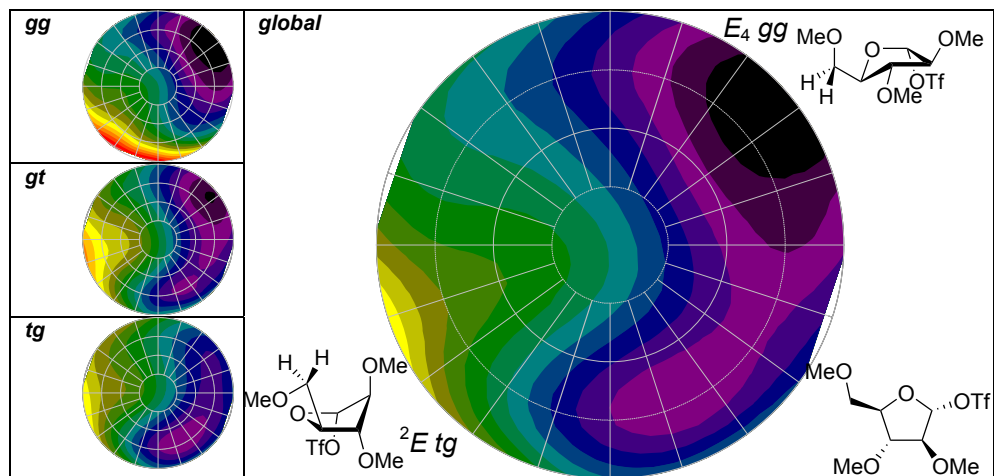


Figure A.1 2,3,5-Tri-O-benzyl-D-ribofuranosyl triflate ($\alpha : \beta = 1.0 : 0.0$ kcal/mol).

(α)



(β)

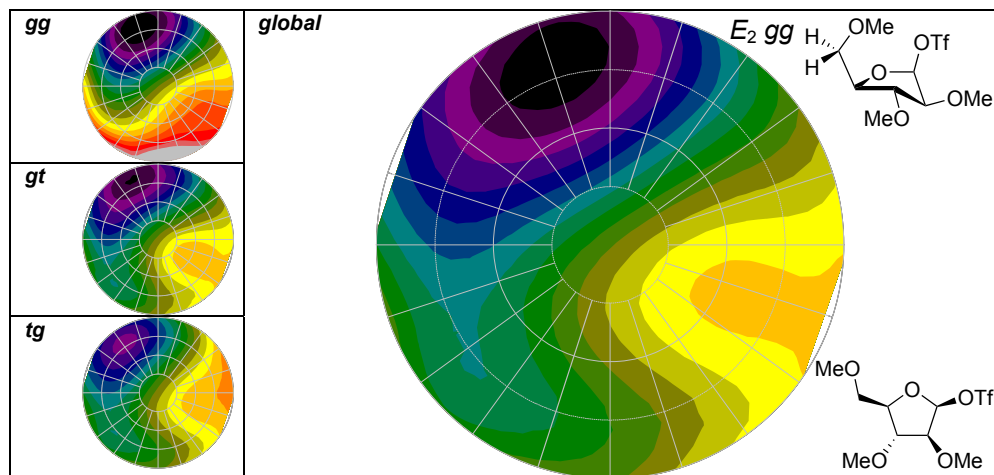
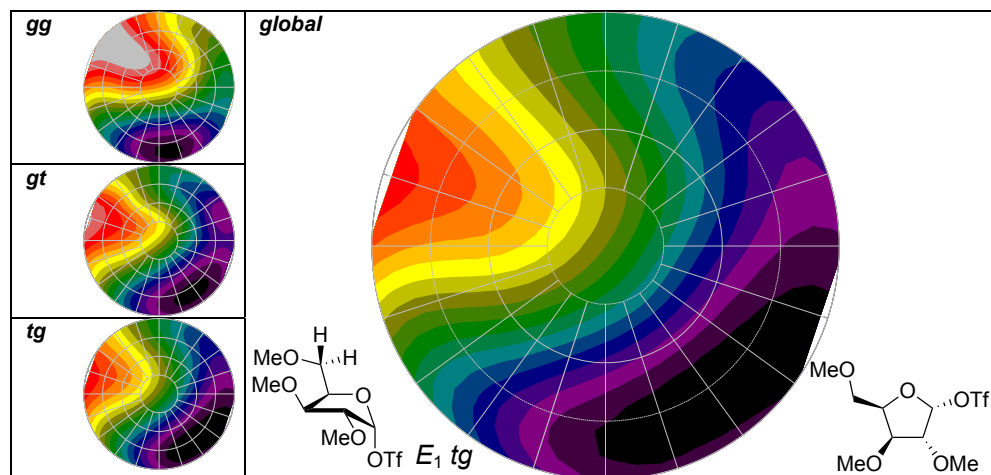


Figure A.2 2,3,5-Tri-O-benzyl-D-arabinofuranosyl triflate (α : β = 0.0 : 1.0 kcal/mol).

(α)



(β)

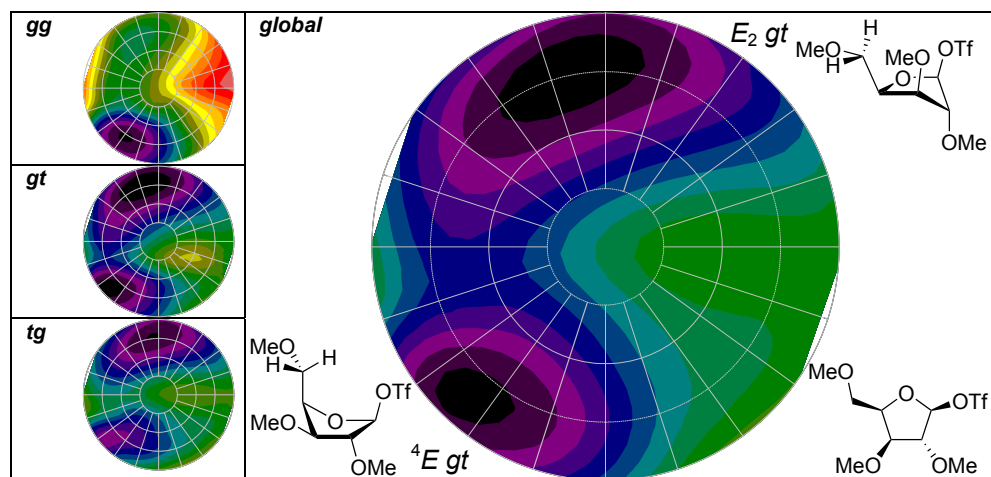
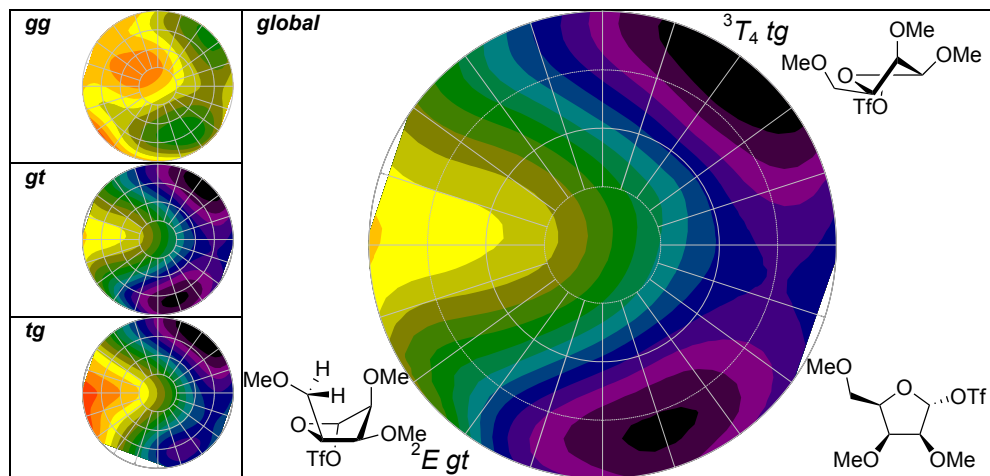


Figure A.3 2,3,5-Tri-O-benzyl-D-xylofuranosyl triflate (α : β = 0.6 : 0.0 kcal/mol).

(α)



(β)

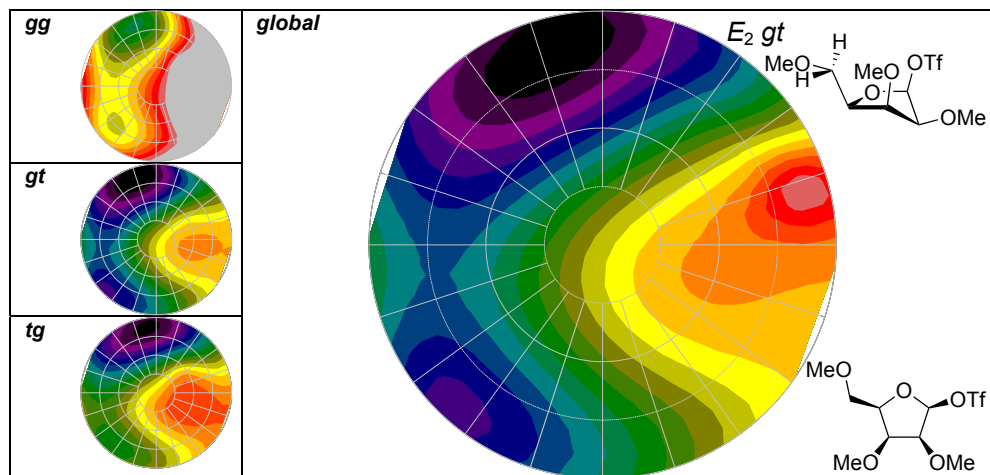


Figure A.4 2,3,5-Tri-O-benzyl-D-lyxofuranosyl triflate (α : β = 0.0 : 1.0 kcal/mol).

